



Departamento de Tecnología Electrónica

PhD Thesis

**ADVANCED DEVICES BASED ON  
FIBERS, INTEGRATED OPTICS AND  
LIQUID CRYSTALS FOR WDM  
NETWORKS**

Autor: Pedro Contreras Lallana

Tutor: Carmen Vázquez García

Leganés, Abril de 2011



# **Tesis Doctoral**

**TÍTULO :**

**ADVANCED DEVICES BASED ON FIBERS,  
INTEGRATED OPTICS AND LIQUID CRYSTALS FOR  
WDM NETWORKS**

**AUTOR :**

D. PEDRO CONTRERAS LALLANA

**TUTORA :**

DRA. CARMEN VÁZQUEZ GARCÍA

**DEPARTAMENTO :**

TECNOLOGÍA ELECTRÓNICA

**TRIBUNAL:**

**FIRMA**

PRESIDENTA : Dra. María Josefa Yzuel Giménez

VOCAL : Dr. Kevin Heggarty

VOCAL : Dr. Pedro Corredera Guillén

VOCAL : Dr. Salvador Elías Vargas Palma

SECRETARIO : Dr. José Manuel Sánchez Pena

**CALIFICACIÓN**

Leganés, de

de 2011



## AGRADECIMIENTOS

A pesar de ser el primer párrafo que aparece en este documento, como suele ser habitual, la sección de agradecimientos es la última parte de la Tesis que se escribe. Llegado este momento, en mi vida han sucedido un sinfín de situaciones, normalmente poco relacionadas con la investigación realizada, que no se llegan a plasmar dentro del documento pero que, al fin y al cabo forman parte de él.

Sírvase esta sección para expresar de alguna forma mi agradecimiento a todas las personas que directa o indirectamente me han ayudado a la realización de este trabajo. Lo más probable es que se me escape alguno, por ello, pido disculpas por adelantado antes de que me retiren el saludo.

En primer lugar, quiero dar las gracias a mis padres, que han realizado un esfuerzo importante, muchas veces poco reconocido, para que haya podido completar mi formación. También a mi hermano que me ha ayudado en los momentos más difíciles.

A Virginia, porque ha estado a mi lado, tanto en los buenos momentos como en los malos. Me ha servido de apoyo cuando más lo he necesitado, dando otro punto de vista a las dificultades.

A Ricardo, Alberto C., y Javier por compartir esos buenos ratos en la comida.

A la gente del B.16 y demás despachos... que grandes momentos hemos pasado: a Juan Carlos por compartir su positivismo, al Sánchez por dar su toque de realismo, a Pablo por hacernos reflexionar, al Barrios por alegrarnos la vida con sus historias, a Carlos por compartir sus inquietudes, a Dani resolvedor de problemas, a Julio puesto que ha sido uno de los orígenes de mi trabajo, al cubano eternamente joven.

Al grupo de colombianos y asimilados, Pedro D., Jesús P., Guillermo, Julio, Robinsón, Jesús R. y Jorge que nos aportan una visión diferente a nuestras costumbres.

A las nuevas incorporaciones, Alberto T., Fran y en especial Dimitrios que han aportado frescura a los cafés matutinos

A Carmen, la directora de este trabajo, porque me ha sabido guiar, no sin mucho esfuerzo, en la realización de este trabajo. También quiero mostrar mi agradecimiento a Pepe por habernos brindado la oportunidad de trabajar en este Grupo.

A Marimar y Oscar, porque son capaces de arreglar todos los papeles... para ayer, que siempre que nos acercamos a secretaría vamos con prisa.

También quiero hacer extensible mi agradecimiento al resto del personal del Departamento de Tecnología Electrónica, puesto que han servido como ejemplo y ayuda a todos los que nos hemos ido incorporando.

---

A los técnicos del laboratorio, Jesús P. Agustín, Cesar, Jesús A. porque tienen todo preparado cuando hay clase.

No me quiero olvidar de los becarios y contratados que están trabajando en el laboratorio del Grupo: Yolanda, Iván, Marta, Roberto, Agustín, Mercedes... y tantos que han pasado porque han conseguido mantener

También quiero recordar en estos momentos a todos aquellos que han pasado por la Charly, y que han buscado fortuna fuera de la universidad: Rodrigo, Angelito, Piña, María, Miguel Ángel, Manuel, Roca, César, Aurora...

A David Larrabeiti y Ricardo Romeral por la participación en Bone.

A Yolanda (madre), Paqui, Mari Carmen, Carmen, Ester y al resto de personal de la cafetería del Sabatini, porque gracias a sus cafés nos han mantenido despiertos.

A la gente de 300 y del equipo de liga interna, tanto los actuales como los pioneros en los partidos de los miércoles, puesto que gracias a ellos hemos conseguido mantener algo la forma... esférica.

I would also thanks to the Brest Telecom staff, Kevin, Bruno F., Bruno V., for making possible my research stay in Brest. I would appreciate Anne Catherine for helping me during my stay in France. I would also thank to the PhD student that work in the Optics Department.

I would also thanks to the La Sapienza personnel, Antonio, Domenico, Gianni, Rita, Romeo for their support during my research stay in Rome

Al personal del Grupo de Cristales Líquidos de la Universidad Politécnica de Madrid, José Manuel Otón, Xabi, Morten, Eva, Annia, Nourdine, Bea, David P... por su apoyo, y los buenos ratos pasados en los congresos.

A Joseba, Manuel López Amo, Pedro Corredera y tantos otros con los que hemos compartido buenos momentos.

También me gustaría dedicar unas líneas a mis amigos de la universidad, que a pesar de que cada vez nos vemos menos, todavía mantenemos el contacto y nos vemos muy de vez en cuando.

No me puedo olvidar en estos momentos de los amigos de Almenar de Soria, Pedro, David, Toño, Valen, Judith, Sandra... con los que he compartido muy gratos momentos. Así como tampoco quiero perder la oportunidad de agradecer a la Virgen de Lallana que algún favor habrá hecho, más que nada por eso de llevarla en el apellido.

Por último y no menos importante, quiero agradecer a mis compañeros de los diversos equipos de fútbol, II Milienio y Jackie Dani con los que me he podido desestresar en los momentos más complicados.

# Contents

---

<b>Contents .....</b>	<b>i</b>
<b>List of Figures.....</b>	<b>vii</b>
<b>List of Tables .....</b>	<b>xi</b>
<b>Glossary .....</b>	<b>xiii</b>
<b>Chapter I.....</b>	<b>1</b>
<b>INTRODUCTION .....</b>	<b>1</b>
<i>I.1.- Motivation and Objectives .....</i>	<i>3</i>
<i>I.2.- Contents of the Work.....</i>	<i>4</i>
<i>I.3.- Acknowledgements.....</i>	<i>6</i>
<b>Chapter II.....</b>	<b>7</b>
<b>SWITCHING TECHNOLOGIES IN OPTICAL NETWORKS.....</b>	<b>7</b>
<i>II.1.- Introduction .....</i>	<i>9</i>
<i>II.2.- Evolution of Optical Networks.....</i>	<i>9</i>
<i>II.3.- Types of Optical Networks.....</i>	<i>12</i>
II.3.a.- Backbone Networks .....	12
II.3.b.- Metropolitan Area Networks.....	13
II.3.c.- Access Networks.....	13

<i>II.4.- Applications of Polymer Optical Fibres .....</i>	<i>14</i>
II.4.a.- Polymer Optical Fibres in Automobile Networks .....	16
II.4.b.- Polymer Optical Fibre in Home and Office Networks.....	18
II.4.c.- Polymer Optical Fibre Sensors Networks .....	19
<i>II.5.- Parameters of Optical Switches.....</i>	<i>21</i>
II.5.a.- Switch Performance Parameters .....	22
II.5.b.- Network Requirements .....	23
II.5.c.- System Requirements .....	24
<i>II.6.- Type of Switches .....</i>	<i>24</i>
II.6.a.- Applications of Optical Switches.....	24
II.6.b.- Optical Switching Technologies .....	26
<i>II.7.- Comparison between Optical Switches .....</i>	<i>34</i>
<b>Chapter III.....</b>	<b>41</b>
<b>SWITCHES BASED ON LIQUID CRYSTALS.....</b>	<b>41</b>
<i>III.1.- Introduction to Liquid Crystal Switches.....</i>	<i>43</i>
III.1.a.- Basic Liquid Crystal Structures for Optical Switches.....	43
III.1.b.- Principle of Operation of Twisted Nematic Liquid Crystal Cells.....	44
III.1.c.- Optical Switching Based on Polarization Management.....	46
III.1.d.- Switches Based on Polymer Dispersed Liquid Crystal Cells.....	50
<i>III.2.- 3x1 Optical Multiplexer Based on Polarization Management .....</i>	<i>52</i>
III.2.a.- Device Structure .....	53
III.2.b.- Device Operation.....	53
III.2.c.- Optical Characterization .....	54
III.2.d.- Multiplexer Control Using a Computer.....	57
<i>III.3.- Multiplexer and Variable Optical Attenuator Based on Polymer Disperse Liquid Crystal Cells.....</i>	<i>59</i>
III.3.a.- Device Structure .....	60
III.3.b.- Device Operation.....	61
III.3.c.- Optical Characterization .....	61
<i>III.4.- Summary and Conclusions .....</i>	<i>66</i>
<b>Chapter IV .....</b>	<b>67</b>
<b>ADVANCED MULTIFUNCTIONAL OPTICAL SWITCH BASED ON LIQUID CRYSTALS .....</b>	<b>67</b>
<i>IV.1.- Introduction .....</i>	<i>69</i>
<i>IV.2.- Structure of the Switch.....</i>	<i>69</i>
<i>IV.3.- Device Operation .....</i>	<i>71</i>
<i>IV.4.- Functionalities .....</i>	<i>72</i>
<i>IV.5.- Bulk Optical Components Used in the Implementation.....</i>	<i>75</i>
IV.5.a.- Polarizing Beam Splitters.....	75
IV.5.b.- Twisted Nematic Liquid Crystal Cells: Design and Characterization .....	77
<i>IV.6.- Optical Characterization .....</i>	<i>85</i>
IV.6.a.- Preliminary Results .....	87
IV.6.b.- Device Characterization Using the Optical Test Bench .....	90
<i>IV.7.- Summary and Conclusions .....</i>	<i>95</i>

---

<b>Chapter V .....</b>	<b>97</b>
SWITCHES BASED ON INTEGRATED OPTICS .....	97
<i>V.1.- Introduction to Integrated Optic Switches .....</i>	99
<i>V.2.- Introduction to Ring Resonators.....</i>	100
<i>V.3.- Switches based on Ring Resonators and Liquid Crystals .....</i>	102
V.3.a.- Ring Resonator Theory .....	103
V.3.b.- Simulation Software and Waveguide Parameters .....	104
V.3.c.- Simple Ring Resonator Configuration .....	105
V.3.a.- Cross-Grid Configuration .....	107
V.3.a.- Compound Structure .....	109
<i>V.4.- Tap and Two Split Switch Based on Mach-Zehnder Interferometer.....</i>	111
V.4.a.- Proposed Structure of the Tap-and-Two Split Switch.....	112
V.4.b.- Theory.....	113
V.4.c.- Simulation of the Structure .....	115
<i>V.5.- Summary and Conclusions.....</i>	117
<b>Chapter VI.....</b>	<b>119</b>
OPTICAL CHARACTERIZATION BENCH.....	119
<i>VI.1.- Introduction .....</i>	121
<i>VI.2.- Requirements .....</i>	121
<i>VI.3.- Structure of the Optical Characterization Bench .....</i>	122
<i>VI.4.- Precision Movement System .....</i>	126
VI.4.a.- Motion Controller ESP 301 .....	126
VI.4.b.- Actuator CMA-25CCCL .....	127
<i>VI.5.- Software Developed.....</i>	127
<i>VI.6.- Test of the Optical Characterization Bench .....</i>	130
VI.6.a.- Set-up Used for the Test .....	130
VI.6.b.- Test using the 1mm Diameter Polymer Optical Fibre as Output Fibre.....	131
VI.6.c.- Test using the 62.5/125 $\mu$ m Multimode Glass Fibre as Output Fibre .....	132
<i>VI.7.- Summary and Conclusions .....</i>	133
<b>Chapter VII .....</b>	<b>135</b>
CONCLUSIONS AND FUTURE WORK.....	135
<i>VII.1.- Conclusions .....</i>	137
<i>VII.2.- Future Work .....</i>	140
<b>Chapter VIII.....</b>	<b>143</b>
RESUMEN DEL TRABAJO REALIZADO .....	143
<i>VIII.1.- Motivación y Objetivos .....</i>	145
VIII.1.a.- Objetivos.....	146
<i>VIII.2.- Tecnologías de Comunicación para Redes Ópticas .....</i>	147
VIII.2.a.- Tipos de Redes Ópticas .....	147
VIII.2.b.- Aplicaciones de la Fibra Óptica de Plástico.....	149
VIII.2.c.- Parámetros de los Comunicadores Ópticos.....	153
VIII.2.d.- Tipos de Comunicadores .....	154

---

VIII.2.a.- Comparación entre Conmutadores Ópticos.....	156
<i>VIII.3.- Conmutadores Basados en Cristal Líquido .....</i>	157
VIII.3.a.- Multiplexor 3x1 Basado en el Tratamiento de la Polarización .....	157
VIII.3.b.- Multiplexor y Atenuador Óptico Variable Basado en Células de Cristal Líquido Disperso en Polímero .....	159
<i>VIII.4.- Conmutador Óptico Multifunción Avanzado Basado en Cristal Líquido .....</i>	160
<i>VIII.5.- Conmutadores Basados en Óptica Integrada .....</i>	162
VIII.5.a.- Conmutadores y Filtros Sintonizables Basados en Anillos Resonantes y Cristal Líquido....	162
VIII.5.b.- Conmutador Óptico 2x2 Basado en un Interferómetro Mach -Zehnder.....	164
<i>VIII.6.- Banco de Caracterización Óptica.....</i>	166
<i>VIII.7.- Conclusiones y Trabajos Futuros .....</i>	167
VIII.7.a.- Líneas de Trabajo Futuras.....	171
<i>VIII.8.- Publicaciones Obtenidas .....</i>	172
<b>Appendix A .....</b>	<b>173</b>
<b>PUBLICATIONS RELATED TO THIS WORK.....</b>	<b>173</b>
A.1.- <i>Papers in International Journals and Books .....</i>	175
A.2.- <i>Contributions in International Conferences .....</i>	175
A.3.- <i>Contributions in National Conferences .....</i>	177
A.4.- <i>Research Stays.....</i>	177
A.5.- <i>Other Relevant Information .....</i>	178
<b>Appendix B .....</b>	<b>179</b>
<b>OPTICAL CHARACTERIZATION BENCH'S USER MANUAL.....</b>	<b>179</b>
B.1.- <i>Software for Controlling the Motion Controller.....</i>	181
B.1.a. Configuration of the Communication Ports.....	181
B.1.b. Data File.....	182
B.1.c. Parameters of the Actuators .....	182
B.1.d. Actuator Enabling .....	184
B.1.e. Single Movement of the Actuators.....	184
B.1.f. Return to Home .....	185
B.1.g. Stepped Movement of the Actuators .....	185
B.1.h. Voltage Measured with the Multimeter.....	186
B.2.- <i>Software for Controlling the Oscilloscope and the Wave Generator .....</i>	186
B.2.a. "Configuración" Tab.....	186
B.2.b. "Medidas" Tab.....	188
<b>Appendix C .....</b>	<b>191</b>
<b>SOFTWARE FOR THE SIMULATION OF MICRO RING-RESONATORS.....</b>	<b>191</b>
C.1.- <i>Introduction.....</i>	193
C.2.- <i>Starting with the Simulation Software .....</i>	193
C.3.- <i>Performing a Simulation .....</i>	196
C.4.- <i>Simulation Results .....</i>	198

<b>References.....</b>	<b>201</b>
<i>A - F:</i> .....	201
<i>G - L:</i> .....	207
<i>M - R:</i> .....	212
<i>S - Z:</i> .....	218



# List of Figures

---

<b>Chapter I.....</b>	<b>1</b>
INTRODUCTION .....	1
<b>Chapter II.....</b>	<b>7</b>
SWITCHING TECHNOLOGIES IN OPTICAL NETWORKS.....	7
Figure II-1 : Optical Fiber Ring Network.....	16
Figure II-2 : POF network within the Automobile.....	17
Figure II-3 : Structures of In-Home Networks: (a) Point-to-Point, (b) Tree, (c) Bus, (d) Star .....	18
Figure II-4 : Example of POF Network within the House .....	19
Figure II-5 : Scheme of a Multisensor System Based on POF [Vázquez-2004]......	20
Figure II-6 : Optical Switch Schematic for Parameter's Definition.....	22
Figure II-7 : Optical Switch Based on 2-D MEMS .....	27
Figure II-8 : Scheme of a 2x2 MZI based switch .....	28
Figure II-9 : MMI Coupler with Tunable Power Splitting Ratios.....	29
Figure II-10 : Basic Structure of a Ring Resonator.....	29
Figure II-11 : Electro-holographic Switch .....	32
<b>Chapter III .....</b>	<b>41</b>
SWITCHES BASED ON LIQUID CRYSTALS.....	41
Figure III-1 : Structure of a LC Cell .....	43
Figure III-2 : Representation of a TN_LC Cell Operation: (a) Crossed Polarizers, (b) Parallel Polarizers .....	45
Figure III-3 : Structure of the 1x2 LC Optical Switch.....	46
Figure III-4 : Block Diagram of Generic Polarization Management LC Switch .....	46
Figure III-5 : 2x2 Optical Switch Structure.....	47
Figure III-6 : 2x2 Operation Modes: (a) Crossed, (b) Direct, (c) Closed. ....	50
Figure III-7 : Internal Structure of a PDLC cell.....	50
Figure III-8 : Picture of the PDLC in two possible states, Opaque (a), Transparent (b) .....	51
Figure III-9 : Structure of the 3x1 Multiplexer based on Polarization Management.....	53
Figure III-10 : Set up used for the optical characterization. ....	54
Figure III-11 : Transmission of the Multiplexer's for each Input Port. ....	55
Figure III-12 : Excitation Wave Drived to the TN-LC and the Multiplexer Response. ....	56
Figure III-13 : Multiplexer Response for the Three Input Ports.....	57

<b>Figure III-14 :</b> Block Diagram of the 3x1 Multiplexer.....	58
<b>Figure III-15 :</b> Block Diagram of the Digital Stage.....	58
<b>Figure III-16 :</b> Schematic of the Proposed VMUX.....	60
<b>Figure III-17 :</b> Experimental Set Up Used for the VMUX Characterization.....	62
<b>Figure III-18 :</b> PDLC Response for Different Input Port Positions at two Wavelengths.....	63
<b>Figure III-19</b> Pictures of the VMUX in two States: <i>OFF</i> (a) and <i>ON</i> (b) at 650nm.....	63
<b>Figure III-20 :</b> Pictures of the VMUX in Two States: <i>OFF</i> (a) and <i>ON</i> (b) at 532nm.....	63
<b>Figure III-21 :</b> PDLC Response When 1kHz Sinusoidal Wave is Applied at 532nm (a) and 650nm (b)..	64
<b>Figure III-22 :</b> PDLC Response when 1kHz square wave is applied at 532nm (a) and 650nm (b).....	65
<b>Chapter IV .....</b>	<b>67</b>
<b>ADVANCED MULTIFUNCTIONAL OPTICAL SWITCH BASED ON LIQUID CRYSTALS .....</b>	
<b>Figure IV-1 :</b> Structure of the Advanced Multifunctional Optical Switch (AMOS). Output and Input Port Definition .....	70
<b>Figure IV-2 :</b> <i>OFF</i> state (a) and <i>ON</i> state (b), of the Advanced Multifunctional Optical Switch .....	71
<b>Figure IV-3 :</b> Operation as 3x1 Optical Multiplexer.....	72
<b>Figure IV-4 :</b> Overview of the Device Being Used as a 2x2 Optical Switch when it is <i>OFF</i> (a) and <i>ON</i> (b).....	74
<b>Figure IV-5 :</b> Overview of the device utilization as VOA (a), and VOPS (b) .....	74
<b>Figure IV-6 :</b> Transmission of Cell Type no 1, Between Crossed Polarizers and Parallel Polarizers when the LC is Switched (5Vrms) and when it is not Drovod (0V).....	81
<b>Figure IV-7 :</b> Transmission of Cell type 1 at Three Wavelengths, and Between Crossed and Parallel Polarizers.....	81
<b>Figure IV-8 :</b> Transmission of Cell Type no 2, Between Crossed Polarizers and Parallel Polarizers when the LC is Switched and when it is not Drovod.....	82
<b>Figure IV-9 :</b> Transmission of Cell type 2 at Three Wavelengths, and Between Crossed and Parallel Polarizers.....	83
<b>Figure IV-10 :</b> Transmission of Cell Type no 3, Between Crossed Polarizers and Parallel Polarizers when the LC is Switched and when it is not Drovod .....	83
<b>Figure IV-11 :</b> Transmission of Cell type 3 at Three Wavelengths, and Between Crossed and Parallel Polarizers.....	84
<b>Figure IV-12 :</b> Transmission of Cell Type no 4, Between Crossed Polarizers and Parallel Polarizers when the LC is Switched and when it is not Drovod .....	84
<b>Figure IV-13 :</b> Transmission of Cell type 4 at Three Wavelengths, and Between Crossed and Parallel Polarizers .....	85
<b>Figure IV-14 :</b> Picture of the implemented device for the first set of measurements <b>Error! Marcador no definido.</b>	
<b>Figure IV-15 :</b> Experimental Set up Used for the Preliminary Characterization. ....	88
<b>Figure IV-16 :</b> Transmission Obtained for Each Pixel of the Device, .....	89
<b>Figure IV-17 :</b> Pictures of two states of the implemented device: (a) <i>OFF</i> and (b) <i>ON</i> .....	89
<b>Figure IV-18 :</b> Picture of the Advanced Multifunction Optical Switch Built in the Optical Characterization Bench .....	91
<b>Figure IV-19 :</b> Transmission from <i>Input Port 2b</i> to Both Output Ports when the Voltage Applied to the TN-LC is Modified for the Three Types of Cells: (a) Type no 1, (b) Type no 3 and (c) Type no 4.....	92
<b>Figure IV-20 :</b> Response Times of the Advance Multifunctional Optical Switch Built with Cells Type no 1.....	94
<b>Figure IV-21 :</b> Response Times of the Advanced Multifunctional Optical Switch Built with Cells Type no 3.....	94
<b>Figure IV-22 :</b> Response Times of the Advanced Multifunctional Optical Switch Built with Cells Type no 4.....	94
<b>Chapter V .....</b>	<b>97</b>
<b>SWITCHES BASED ON INTEGRATED OPTICS .....</b>	
<b>Figure V-1 :</b> Basic Structure of a Ring Resonator.....	100
<b>Figure V-2 :</b> Ring Resonator structure as Optical Add/Drop Multiplexer.....	100
<b>Figure V-3 :</b> Ring Resonator Structure Built in Integrated Optics with LC in the Loop .....	102
<b>Figure V-4 :</b> Launch Parameters in the Commercial Software used in Simulations. ....	104
<b>Figure V-5 :</b> Different Frequency Responses of the $\mu$ RR obtained for Distinct Device Configurations. ....	105
<b>Figure V-6 :</b> $\mu$ RR with a single LC and $L_{coup}$ .....	106
<b>Figure V-7 :</b> Output Power in the Through Port (a), and at the Drop Port (b) versus Wavelength for Different $L_{coup}$ .....	107
<b>Figure V-8 :</b> Simulations of an Ideal Side-Coupled $\mu$ RR for Two Wavelengths with no LC, $L_{coup}=1\mu m$ .....	108
<b>Figure V-9 :</b> Simulations of Ideal Side-Coupled $\mu$ RRs with Two LC ON at $\lambda = 1.564\mu m$ : (a) Conventional, (b) Cross-Grid Configuration .....	108

<b>Figure V-10 :</b> Serial of Two μRR in a Cross-Grid Configuration: Structure (a), Individual Response (b) and Compose Response (c).....	109
<b>Figure V-11 :</b> Simulations of a Serial of two μRR in Cross-Grid Configuration for Three Wavelengths, and LC OFF.....	110
<b>Figure V-12 :</b> Serial Two μRR in a Cross-Grid Configuration for Different LC states. Compound μRR Response Versus Wavelength at Output 2 (a) and at Output 3 (b).....	110
<b>Figure V-13 :</b> Schematic of a Ta2S Switch Composed of a Fixed Splitter and an MZI .....	112
<b>Figure V-14 :</b> Output Power Response at Bar and Cross Outputs of MZI vs $\Delta n$ .....	112
<b>Figure V-15 :</b> Simulation Results for a MZI Optical Switch with Fixed Tap .....	114
<b>Figure V-16 :</b> Distribution of the optical power: in the MMI 3dB coupler (a), in the MZI at initial state (b) and when the MZI is Switched.....	115
<b>Chapter VI.....</b>	<b>119</b>
<b>OPTICAL CHARACTERIZATION BENCH.....</b>	<b>119</b>
<b>Figure VI-1 :</b> Structure Proposed for the Optical Characterization Bench.....	121
<b>Figure VI-2 :</b> Picture of the Three Axes Precision Linear Stage M-562-XYZ from Newport .....	122
<b>Figure VI-3 :</b> Picture of a 25mm Linear Translation Stage M-UMR8.25 from Newport.....	123
<b>Figure VI-4 :</b> Picture of the Rotation Stage M-RS65 from Newport.....	123
<b>Figure VI-5 :</b> Possible Implementation of the Input or Output Part .....	123
<b>Figure VI-6 :</b> Basic Structure of the Optical Characterization Bench .....	124
<b>Figure VI-7 :</b> Implementation of an Experiment in the Optical Characterization Bench .....	125
<b>Figure VI-8 :</b> Picture of the Oscilloscope TDS 1012 from Tektronix .....	125
<b>Figure VI-9 :</b> Picture of the Wave Generator A33120 from Agilent.....	125
<b>Figure VI-10 :</b> Picture of the Digital Multimetre 1906 from TTi .....	125
<b>Figure VI-11 :</b> Frontal panel of the motion controller ESP 301 from Newport.....	126
<b>Figure VI-12 :</b> Rear panel of the motion controller ESP 301 .....	126
<b>Figure VI-13 :</b> DC motor CMA-25CCCL from Newport .....	127
<b>Figure VI-14 :</b> Window for ordering a movement .....	128
<b>Figure VI-15 :</b> Configuration window for an actuador.....	128
<b>Figure VI-16 :</b> Window for configuring a split movement.....	128
<b>Figure VI-17 :</b> Window of the function for controlling the wave generator and the oscilloscope.....	129
<b>Figure VI-18 :</b> Set-up used for carrying out the test of the test .....	130
<b>Figure VI-19 :</b> Optical power coupled between the fibres in the horizontal axis for the POF.....	131
<b>Figure VI-20 :</b> Optical power coupled between the fibres in the vertical axis for the POF.....	131
<b>Figure VI-21 :</b> Optical power coupled between the fibres in the horizontal axis for the MMF.....	132
<b>Figure VI-22 :</b> Optical power coupled between the fibres in the vertical axis for the MMF.....	132
<b>Chapter VII .....</b>	<b>135</b>
<b>CONCLUSIONS AND FUTURE WORK .....</b>	<b>135</b>
<b>Chapter VIII.....</b>	<b>143</b>
<b>RESUMEN DEL TRABAJO REALIZADO .....</b>	<b>143</b>
<b>Appendix A.....</b>	<b>173</b>
<b>PUBLICATIONS RELATED TO THIS WORK.....</b>	<b>173</b>
<b>Appendix B .....</b>	<b>179</b>
<b>OPTICAL CHARACTERIZATION BENCH'S USER MANUAL .....</b>	<b>179</b>
<b>Figure B-1 :</b> Main Window of the Developed Software. ....	181
<b>Figure B-2 :</b> Configuration of the Communication Ports.....	182
<b>Figure B-3 :</b> Window Showing the Parameters of the Three Actuators.....	182
<b>Figure B-4 :</b> Window for Configuring the Parameters of Each Actuator.....	183
<b>Figure B-5 :</b> Button for enabling/disabling the actuators .....	184
<b>Figure B-6 :</b> Part of the Program's Window where Order the Movement to the Actuators .....	184
<b>Figure B-7 :</b> Part of the Program's Window where Order the Stepped Movement to the Actuators.....	185
<b>Figure B-8 :</b> Measured Obtained with the Multimeter .....	186
<b>Figure B-9 :</b> Information Displayed in the “Configuración” Tab.....	187
<b>Figure B-10 :</b> Detail of the Wave Generator Configuration Section .....	187
<b>Figure B-11 :</b> Detail of the Oscilloscope Configuration Section .....	188
<b>Figure B-12 :</b> Detail of the Additional Section.....	188
<b>Figure B-13 :</b> Detail of the “Medidas” Tab .....	189

<b>Appendix C .....</b>	<b>191</b>
<b>SOFTWARE FOR THE SIMULATION OF MICRO RING-RESONATORS.....</b>	<b>191</b>
<b>Figure C-1 : Start-up Window Displays the Global Parameters of the Simulation.....</b>	<b>193</b>
<b>Figure C-2 : Program Window with a Structure Drawn .....</b>	<b>194</b>
<b>Figure C-3 : Parameters of the Selected Waveguide .....</b>	<b>194</b>
<b>Figure C-4 : List of the Variables of a Schematic.....</b>	<b>195</b>
<b>Figure C-5 : Configuration of the Pathway.....</b>	<b>195</b>
<b>Figure C-6 : Window for Configuring Parameters of Monitors.....</b>	<b>196</b>
<b>Figure C-7 : Launch Parameters used in the Simulation.....</b>	<b>196</b>
<b>Figure C-8 : Window with the Simulation Parameters .....</b>	<b>197</b>
<b>Figure C-9 : Dialogue Box with the FDTD Output Options.....</b>	<b>197</b>
<b>Figure C-10 : Simulation Window.....</b>	<b>198</b>
<b>Figure C-11 : Results Obtained for Simulation Displayed in Winplot Window .....</b>	<b>198</b>
<b>Figure C-12 : Simulations Results Obtained for Simulation Displayed Using Matlab (a) and Winplot (b)</b>	<b>199</b>

# List of Tables

---

<b>Chapter I.....</b>	<b>1</b>
INTRODUCTION .....	1
<b>Chapter II.....</b>	<b>7</b>
SWITCHING TECHNOLOGIES IN OPTICAL NETWORKS.....	7
<b>Table II-1 :</b> Comparison between Different Switching Technologies.....	39
<b>Chapter III .....</b>	<b>41</b>
SWITCHES BASED ON LIQUID CRYSTALS.....	41
<b>Table III-1 :</b> Evolution of State of the Art and Performance of RotPol LC Switches. ....	49
<b>Table III-2 :</b> Transmission of the Multiplexer's for each Input Port. ....	56
<b>Table III-3 :</b> Response Times of the 3x1 Multiplexer. ....	57
<b>Chapter IV.....</b>	<b>67</b>
ADVANCED MULTIFUNCTIONAL OPTICAL SWITCH BASED ON LIQUID CRYSTALS.....	67
<b>Table IV-1 :</b> Summary of the Ports and TN-LC States for the 3x1 Multiplexer Functionality.	
OPa= <i>Output Port a</i> from Fig.IV.1 .....	73
<b>Table IV-2 :</b> Summary of the Ports and TN-LC States for the Dual 3x1 Multiplexer Functionality (see Fig.IV.1 for notation).....	73
<b>Table IV-3 :</b> Summary of the Ports and TN-LC states for the 2x2 Optical Switch (see Fig.IV.1 for notation).....	74
<b>Table IV-4 :</b> Summary of the Ports and TN-LC states for the VOA (see Fig.IV.1 for notation) .....	75
<b>Table IV-5 :</b> Summary of the Ports and TN-LC states for the Variable Optical Power Splitter (see Fig.IV.1 for notation).....	75
<b>Table IV-6 :</b> PBS Main Characteristics.....	76
<b>Table IV-7 :</b> Characteristics of the Manufactured Cells.....	79
<b>Table IV-8 :</b> Main Characteristics of the Cell Type no 1. ....	82
<b>Table IV-9 :</b> Main Characteristics of the Cell Type no 2. ....	82
<b>Table IV-10 :</b> Main Characteristics of the Cell Type no 3. ....	84
<b>Table IV-11 :</b> Main Characteristics of the Cell Type no 4. ....	85
<b>Table IV-12 :</b> Results Obtained for the Device Characterization when the Multimode 62.5/125 $\mu$ m Fiber is Used at the Input Ports. ....	91

<b>Table IV-13</b> : Response times of the Advanced Multifunctional Optical Switch. ....	93
<b>Chapter V</b> .....	<b>97</b>
SWITCHES BASED ON INTEGRATED OPTICS .....	97
<b>Table V-1</b> : μRR parameters, waveguide with LC on (LC-on) and off (LC-off) respectively. ....	105
<b>Table V-2</b> : FSR Obtained for Different LC Lengths from Figure V-5 (b). ....	106
<b>Chapter VI</b> .....	<b>119</b>
OPTICAL CHARACTERIZATION BENCH .....	119
<b>Table VI-1</b> : Characteristics of the CMA-25CCCL actuator from Newport .....	127
<b>Chapter VII</b> .....	<b>135</b>
CONCLUSIONS AND FUTURE WORK.....	135
<b>Chapter VIII</b> .....	<b>143</b>
RESUMEN DEL TRABAJO REALIZADO .....	143
<b>Appendix A</b> .....	<b>173</b>
PUBLICATIONS RELATED TO THIS WORK.....	173
<b>Appendix B</b> .....	<b>179</b>
OPTICAL CHARACTERIZATION BENCH'S USER MANUAL.....	179
<b>Appendix C</b> .....	<b>191</b>
SOFTWARE FOR THE SIMULATION OF MICRO RING-RESONATORS.....	191

# Glossary

---

<b>Acronym (Acrónimo)</b>	<b>English Term (Término en Inglés)</b>	<b>Spanish Term (Termino en Castellano)</b>
<b>ABS</b>	<b>Anti-Block System</b>	Sistema Antibloqueo
<b>AC</b>	<b>Alternate Current</b>	Corriente Alterna
<b>ADM</b>	<b>Add-Drop Multiplexer</b>	Multiplexor para Insertar/Extraer
<b>ADSL</b>	<b>Asymmetric Digital Subscriber Loop</b>	Bucle de Abonado Digital Asimétrico
<b>AMOS</b>	<b>Advanced Multifunctional Optical Switch</b>	Conmutador Óptico Multifunción Avanzado
<b>APS</b>	<b>Automatic Protection Systems</b>	Sistemas de Protección Automática
<b>BG</b>	<b>Bragg Gratings</b>	Redes de Bragg
<b>CATV</b>	<b>Community Antenna Television or Cable TV</b>	Televisión por Cable
<b>CCP</b>	<b>Customer Convenience Port</b>	Puerto de Conveniencia para el Usuario
<b>CWDM</b>	<b>Coarse Wavelength Division Multiplexing</b>	Multiplexación Vasta por División en Longitud de Onda
<b>D2B</b>	<b>Digital Domestic Bus</b>	Bus Doméstico Digital

---

<b>Acronym (Acrónimo)</b>	<b>English Term (Término en Inglés)</b>	<b>Spanish Term (Termino en Castellano)</b>
<b>DACS</b>	<b>Digital Acces Cross Connects Systems</b>	Sistema de Comutación Óptica para Acceso Digital
<b>DOS</b>	<b>Digital Optical Switch</b>	Comutador Óptico Digital
<b>DVD</b>	<b>Digital Video (Versatile) Disc</b>	Disco de Video Digital
<b>DWDM</b>	<b>Dense Wavelength Division Multiplexing</b>	Multiplexación Densa por División en Longitud de Onda
<b>ECU</b>	<b>Electronic Control Unit</b>	Unidad de Control Electrónico
<b>EDFA</b>	<b>Erbium-Doped Fibre Amplifier</b>	Amplificador de Fibra Dopada con Erbio
<b>EH</b>	<b>Electro-Holographic</b>	Electro-Holográfico
<b>EMI</b>	<b>Electromagnetic Interference</b>	Interferencia Electromagnética
<b>EMS</b>	<b>Engine Management System</b>	Sistema de Control del Motor
<b>FDDI</b>	<b>Fibre Distributed Data Interface</b>	Interfaz de Datos Distribuidos en Fibra
<b>FDTD</b>	<b>Finite Differences Time Domain</b>	Diferencias Finitas en el Dominio Temporal
<b>FSR</b>	<b>Free Spectral Range</b>	Rango Espectral Libre (Periodo)
<b>FTTB</b>	<b>Fibre to the Building</b>	Fibra hasta el Edificio
<b>FTTC</b>	<b>Fibre to the Curb (Cabinet)</b>	Fibra hasta el Bordillo (Cabina)
<b>FTTH</b>	<b>Fibre to the Home</b>	Fibra hasta el Hogar
<b>FTTx</b>	<b>Fibre to the X (Home, Building or Curb)</b>	Fibra hasta X (Hogar, Edificio o Cabina)
<b>FWHM</b>	<b>Full Width Half Maximum</b>	Ancho de Banda a Mitad de Potencia
<b>FWM</b>	<b>Four Wave Mixing</b>	Mezcla de Cuatro Ondas
<b>GI</b>	<b>Graded Index</b>	Índice Gradual
<b>GI-POF</b>	<b>Graded Index Polymer Optical Fibre</b>	Fibra Óptica de Plástico de Índice Gradual
<b>GMPLS</b>	<b>Generalized Multi-Protocol Label Switching</b>	Comutación Multi-Protocolo Generalizado mediante Etiquetas
<b>GPIB</b>	<b>General Purpose for Instrumentation Bus</b>	Bus para Instrumentación de Propósito General
<b>GPS</b>	<b>Global Positioning System</b>	Sistema de Posicionamiento Global

<b>Acronym (Acrónimo)</b>	<b>English Term (Término en Inglés)</b>	<b>Spanish Term (Termino en Castellano)</b>
<b>HCC</b>	<b>Home Communication Controller</b>	Controlador de Comunicación en el Hogar
<b>HFC</b>	<b>Hybrid Fibre Coax</b>	Híbrido Fibra-Coaxial
<b>IDB</b>	<b>Intelligent Data Bus</b>	Bus de Datos Inteligente
<b>IEEE</b>	<b>Institute of Electrical and Electronic Engineers</b>	Instituto de Ingenieros Eléctricos y Electrónicos
<b>IL</b>	<b>Insertion Loss</b>	Pérdidas de Inserción
<b>ISDN</b>	<b>Integrated Services Digital Network</b>	Red Digital de Servicios Integrados
<b>ISO</b>	<b>International Organization for Standardization</b>	Organización Internacional para la Estandarización
<b>ITO</b>	<b>Indium Tin Oxide</b>	Óxido de Indio Estaño
<b>KLTN</b>	<b>Potassium Lithium Tantalate Niobate</b>	Niobato Tantalo de Litio Potasio
<b>LAN</b>	<b>Local Area Network</b>	Red de Área Local
<b>LASER</b>	<b>Light Amplified by Stimulate Emission of Radiation</b>	Luz Amplificada por Emisión Estimulada de Radiación
<b>LC</b>	<b>Liquid Crystal</b>	Cristal Líquido
<b>LC-SLM</b>	<b>Liquid Crystal Spatial Light Modulator</b>	Modulador Espacial de Luz de Cristal Líquido
<b>LCOS</b>	<b>Liquid Crystal On Silicon</b>	Cristal Líquido sobre Silicio
<b>LED</b>	<b>Light Emitting Diode</b>	Diodo Emisor de Luz
<b>LiNbO<sub>3</sub></b>	<b>Lithium Niobate</b>	Niobato de Litio
<b>MAN</b>	<b>Metropolitan Area Networks</b>	Redes de Área Metropolitana
<b>MC-OXC</b>	<b>Multicast-Capable Optical Cross Connect</b>	Matriz de Conmutación Óptica Capaz de Transmisión Múltiple
<b>MEMS</b>	<b>Micro-Electromechanical Systems</b>	Sistemas Micro-Electromecánicos
<b>MMF</b>	<b>MultiMode Fibre</b>	Fibra Óptica Multimodo
<b>MMI</b>	<b>Multi Mode Interference</b>	Interferencia Multimodo
<b>MOST</b>	<b>Media Oriented System Transport</b>	Sistemas de Transporte Orientado al Medio
<b>MP2MP</b>	<b>Multipoint to Multipoint</b>	Multipunto a Multipunto

<b>Acronym (Acrónimo)</b>	<b>English Term (Término en Inglés)</b>	<b>Spanish Term (Termino en Castellano)</b>
<b>MZI</b>	<b>Mach-Zehnder Interferometer</b>	Interferómetro Mach-Zehnder
<b>NA</b>	<b>Numerical Aperture</b>	Apertura Numérica
<b>NW</b>	<b>Normally White</b>	Normalmente Blanco
<b>OADM</b>	<b>Optical Add/Drop Multiplexer</b>	Multiplexor Óptico de Inserción/Extracción
<b>OBS</b>	<b>Optical Burst Switching</b>	Comutación Óptica de Ráfagas
<b>O/E/O</b>	<b>Optical/Electrical/Optical</b>	Óptico/Eléctrico/Óptico
<b>OPS</b>	<b>Optical Packet Switching</b>	Comutación Óptica de Paquetes
<b>OSI</b>	<b>Open System Interconnection</b>	Sistema de Interconexión Abierto
<b>OSM</b>	<b>Optical Spectral Monitoring</b>	Monitorización del Espectro Óptico
<b>OXC</b>	<b>Optical Cross-Connects</b>	Matriz de Comutación Óptica
<b>P2MP</b>	<b>Point to Multi-point</b>	Punto a Multi-punto
<b>P2P</b>	<b>Point to Point</b>	Punto a Punto
<b>PBS</b>	<b>Polarizing Beam Splitters</b>	Divisores Polarizadores de Haz
<b>PF</b>	<b>Perfluorinated</b>	Perfluorinada
<b>PDL</b>	<b>Polarization Dependence Loss</b>	Pérdidas Dependientes a la Polarización
<b>PLC</b>	<b>Planar Lightwave Circuits</b>	Circuitos Ópticos Planares
<b>PLZ</b>		
<b>PMMA</b>	<b>Polymethyl-Methacrylate</b>	Polimetil-metacrilato
<b>PMD</b>	<b>Polarization Mode Dispersion</b>	Dispersión del Modo de Polarización
<b>POF</b>	<b>Polymer Optical Fibre</b>	Fibra Óptica de Plástico
<b>PON</b>	<b>Passive Optical Networks</b>	Redes Ópticas Pasivas
<b>PolRot</b>	<b>Polarization Rotation</b>	Rotación de la Polarización
<b>PSTN</b>	<b>Public Switched Telephone Network</b>	Red Telefónica Comutada

<b>Acronym</b> (Acrónimo)	<b>English Term</b> (Término en Inglés)	<b>Spanish Term</b> (Termino en Castellano)
<b>ROADM</b>	<b>Reconfigurable Optical Add/Drop Multiplexer</b>	Multiplexor Óptico de Inserción/Extracción Reconfigurable
<b>RoF</b>	<b>Radio over Fibre</b>	Radio sobre Fibra
<b>RR</b>	<b>Ring Resonator</b>	Anillo Resonante
<b>SaD</b>	<b>Split and Delivery</b>	Divide y Entrega
<b>SDH</b>	<b>Synchronous Digital Hierarchy</b>	Jerarquía Digital Síncrona
<b>SI</b>	<b>Step Index</b>	Salto de Índice
<b>SLM</b>	<b>Spatial Light Modulator</b>	Modulador Espacial de Luz
<b>SOA</b>	<b>Semiconductors Optical Amplifier</b>	Amplificador Óptico de Semiconductor
<b>SOI</b>	<b>Silicon Over Insulator</b>	Silicio Sobre Aislante
<b>SONET</b>	<b>Synchronous Optical Network</b>	Red Óptica Síncrona
<b>SOS</b>	<b>Silica on Silicon</b>	Dióxido de Silicio (Sílice) Sobre Silicio
<b>DSPM</b>	<b>Self Phase Modulation</b>	Auto-Modulación de Fase
<b>SSFLC</b>	<b>Surface Stabilized Ferroelectric Liquid Crystal</b>	Cristal Líquido Ferroeléctrico Estabilizado en Superficie
<b>Ta2S</b>	<b>Tap and two Split</b>	Monitorizar y Divide en Dos
<b>TaC</b>	<b>Tap-and-Continue</b>	Monitorizar y Continúa
<b>TDM</b>	<b>Time Division Multiplexing</b>	Multiplexación por División Temporal
<b>TeO<sub>2</sub></b>	<b>Peratellurite</b>	Dióxido de Telutio (Peratelurita)
<b>TFT</b>	<b>Thin Film Transistor</b>	Transistor de Película Delgada
<b>TIR</b>	<b>Total Internal Reflection</b>	Reflexión Interna Total
<b>TN-LC</b>	<b>Twisted Nematic Liquid Crystal</b>	Cristal Líquido Nemático Torsionado
<b>TNE</b>	<b>Transient Nematic Effect</b>	Efecto Nemático Transitorio
<b>TOSW</b>	<b>Thermo-Optic Switch</b>	Comutador Termoóptico
<b>TPA</b>	<b>Two-Photon Absorption</b>	Absorción de Dos Fotones

<b>Acronym</b> (Acrónimo)	<b>English Term</b> (Término en Inglés)	<b>Spanish Term</b> (Termino en Castellano)
<b>UTP</b>	<b>Untwisted Pair</b>	Par Trenzado
<b>VLSI</b>	<b>Very Large Scale Integration</b>	Escala de Integración Muy Elevada
<b>VMUX</b>	<b>Variable Optical Attenuator - Multiplexer</b>	Atenuador Óptico Variable - Multiplexor
<b>VOA</b>	<b>Variable Optical Attenuator</b>	Atenuador Óptico Variable
<b>WDM</b>	<b>Wavelength Division Multiplexing</b>	Multiplexación por División en Longitud de Onda
<b>WGM</b>	<b>Whispering Gallery Modes</b>	Modos de Galería con Eco
<b>WGP</b>	<b>Wire Grid Polarizers</b>	Polarizadores por Malla de Conductor
<b>XPM</b>	<b>Cross-Phase Modulation</b>	Modulación de Fase Cruzada
<b>μRR</b>	<b>Micro-Ring Resonator</b>	Micro-Anillo Resonante

# **Chapter I**

## **Introduction**

---



### I.1.- Motivation and Objectives

The increment of bandwidth required for new services offered to users make necessary the use of optical fibres in data transmission. Glass optical fibres are widely used in long distance communications, and there are many devices implemented for using in these networks, but these technologies are sometimes expensive for their used in local loops.

Different systems implemented over the established technology are used for increasing local loops bandwidth, but more services are demanded at home. Those applications require more bandwidth than the offered by the usual twisted copper pair.

Multimode fibres (both silica and polymer) with larger core diameters and numerical aperture, allows for large tolerance on axial misalignments, which results in cheaper connectors as well as associated equipment, but with a bandwidth penalty with regards to their singlemode counterparts, mainly due to the introduction of modal dispersion. On the other hand, polymer optical fibre (POF) offers several advantages over conventional multimode optical fibre over short distances (ranging from 100m to 1000m) such as the even potential lower cost associated with its easiness of installation, splicing and connecting. This is due to the fact that POF is more flexible and ductile, making it easier to handle. Consequently, POF termination can be realized faster and cheaper than in the case of multimode silica fibre. Therefore, the number of applications that use POF is quickly increasing. POF is being used in video transmission in medical equipment, or in multimedia applications for civil aviation and high range cars, in-home and access networks, wireless LAN backbone or office LAN, and in intrinsic optical sensor networks among others.

Even greater channel capacity can be available using a specific type of POF, perfluorinated Graded-Index POF (PF GIPOF), having low attenuation and large bandwidth from 650nm to 1300nm. Link lengths for in-building/home scenarios are short (less than 1 km), and thus the loss per unit length is of less importance. Transmission of 10Gbps data over 100m and transmission of 1.25Gbps Ethernet over 1 km have been experimentally demonstrated with PF GIPOF. On the other hand, combiners and multiplexers are basic elements in POF networks using Wavelength Division Multiplexing (WDM) and there are not that many already developed. It is important to have low losses devices and reconfiguration can be an additional feature in those networks. On the other hand, reconfigurable optical networks in critical applications demand devices able to have different functionalities, including switching. This work has focused in the development of different optical switches for a wide range of optical networks.

Different switching technologies are available. Liquid crystals are widely used as displays, but they are also employed in telecommunications. Other common technology used in data routing is integrated optics. In this case, light propagates by means of a waveguide and the modification of its parameters makes possible switching operation. Micro-Electromechanical Mechanisms, MEMs, based in small

mobile mirrors that can change the direction of the incident light when required are an important optical switching technology.

The objective of the present work is the proposal of several optical switches using different technologies depending on the final application. Some of these structures have been experimentally tested whereas others have been simulated.

Most of the presented switches use liquid crystals, having different functionalities and broadband operation range, so allowing wavelength division multiplexing. To these respect it has been developed an optical multiplexer/combiner and an advanced multifunctional optical switch (AMOS), both implemented with Nematic Liquid Crystal technology.

It has also been developed a multiplexer/combiner based on Polymer Dispersed Liquid Crystals.

The third kind of switches proposed are micro ring-resonators combined with liquid crystals. Micro ring resonators consist of a circular waveguide attached to one or two straight waveguides acting like input and output ports. Light that passes through the structure can be filtered according to the ring resonator characteristics: ring length, coupling ratio, losses... The use of liquid crystal makes possible the tuning of the ring resonator filtering properties.

The last proposed switch is made of a passive splitter and a Mach-Zehnder Interferometer. This kind of devices makes use of integrated optics and interference for switching purposes. The variation of the optical properties influencing the two light beam interference can be done in different ways: thermally, electrically...

Finally, an automated optical characterization bench has been implemented in order to make easy the measurements. It is composed by a three axis translation stage with three actuators, several linear translation stages that allows the user to modify the bench structure for adapting it to his experiment, and different machinery for mounting the optics.

## I.2.- Contents of the Work

Once the motivation and objectives for developing this research work have been introduced, it is necessary to expose the structure followed for presenting the work.

In Chapter II, an introduction of switching in optical networks is given. Different concepts and parameters needed for understanding the developed work are introduced. Applications of Polymer Optical Fibre are introduced in a second part of this Chapter. An overview about the main characteristics and technologies used in optical switches is also presented. Finally, a comparison between different optical switches technologies is given.

Chapter III offers an overview of switches based on Liquid Crystals. After a brief introduction of this kind of switches, it is described a novel optical multiplexer based on polarization management and implemented with Nematic Liquid Crystal cells.

Next part of the chapter is dedicated to explain a multiplexer and variable optical attenuator based on Polymer Dispersed Liquid Crystal. Finally, a summary and some conclusions about the implemented switches are given.

In Chapter IV, description of an advanced multifunctional optical switch based on Liquid Crystals is given. The proposed device is able for operating as a 3x1 optical multiplexer/combiner (OM/OC), optical dual 3x1 multiplexer/combiner (ODM/ODC), a 2x2 optical switch (OS), a Variable Optical Attenuator (VOA) and a Variable Optical Power Splitter (VOPS). A complete characterization of the implemented device, using bulk components, is given. Finally, a summary and some conclusions about the main results are given.

Chapter V refers to switches based on integrated optics. After a brief introduction of this kind of switches, an overview about Ring Resonators is given. Section III proposes different structures of switches based on micro ring resonators combined with liquid crystals. Next, an optical switch based on an integrated Mach-Zehnder Interferometer capable of taping a part of the input power for the local node is described. Finally, a summary and some conclusions about the described switches are given.

In Chapter VI, the implementation of the optical characterization bench is explained. The proposed system is versatile and allows the user to define which axis can be automated. An overview of the structure of the optical characterization bench is given. Next, the precision movement system, in charge of making the automated movements is presented. Finally, some measurements and a summary of the bench's characteristics are listed.

The main conclusions of this work and future research tasks are in Chapter VII.

Chapter VIII presents the summary of the work written in Spanish.

A list of the publication, contributions and other relevant information is in Appendix A.

The user manual of the optical characterization bench is in Appendix B.

Appendix C contains a detailed description of the software used for simulations of the micro ring resonators.

Finally, the list of references used in the present work is given.

### I.3.- Acknowledgements

The present research work has been supported by the following Spanish projects: TIC2003-038783 (DISFOTON), TEC2006-13273-C03-03-MIC (FOTOCOMIN) and TEC2009-14718-C03-03-MCI (DEDOS) of the Spanish Interministerial Commission on Science and Technology (CICYT), FACTOTEM-CM: S-005/ESP/000417, and FACTOTEM-II-CM: S2009/ESP-1781 and FENIS-CCG06-UC3M/TIC-619 of Comunidad Autónoma de Madrid.

Additional financial support has been obtained from European Thematic Network SAMPA: Synclinic and Anticlinic Mesophases for Photonic Applications (HPRN-CT-2002-00202), carried out during the V Framework Program of the European Union, COST Action 299 FIDES: Optical Fibres Dedicated to Society, and from the European Network of Excellence: ePhoton/ONe+ (FP6-IST-027497), both carried out during the VI Framework Program of the European Union, and BONE: Building the Future Optical Network in Europe (FP7-ICT-216863) carried out during the VII Framework Program of the European Union.

Some of the results obtained in chapter III were obtained during the research stays in the Optic Department of Telecom Bretagne of Brest (France) in July 2007 and from October to November 2008, where the manufacture and characterization of nematic liquid crystal cells were done. Mobility actions of University Carlos III of Madrid in 2007 and 2008 are acknowledged for funding these research stays in Brest (France).

Some of the results obtained in chapter V were obtained during the research stay in the Electronic Engineering Department of La Sapienza University of Rome (Italy), from October 2005 to January 2006, where the first micro ring-resonators were designed and simulated. I would like to thank to the SAMPA program for funding this mobility action.

I would appreciate Juan José Cañadas Rufo and Antonio José Martín del Toro for the work developed in their Bachelor Project, José Joaquín Ferrer de la Cruz for the labour done during his Master Thesis. Some of the results obtained are related to their activity. I would be grateful with Mercedes Chaparro de la Peña for the work executed for partially controlling the Optical Test Bench. Finally, I would also like to thank to Diego Rivero for the information obtained from his work.

I would also acknowledge to the Liquid Cristal Group form the Polytechnic University of Madrid (CLIQ) for the samples and suggestions given. And I would also like to thank to the staff of the Displays and Photonics Application Group (GDAF) group for their support.

## **Chapter II**

# **Switching Technologies in Optical Networks**

---

*In this chapter, an overview of the switching technologies used in Optical Networks is presented. The first part introduces the optical networks. There are different types of networks depending on the technology. Backbone and Metropolitan Area Networks are deployed using glass fibres with low attenuation and dispersion where wavelength multiplexing allows the use of the same fibres for transmitting at the same time different types of information.*

*Polymer Optical Fibres can be used in short range networks where their bandwidth and attenuation allows data transmission at low cost compared with conventional fibres. An overview of Polymer Optical Fibre applications is given in section two.*

*Last sections of this chapter, introduces the technologies used for switching in Optical Networks. The main parameters used in optical switching are listed. Then a description of the technologies is given. Finally, a comparison between the optical switching technologies is reported.*



## II.1.- Introduction

Development of optical communication systems has allowed the implementation of new services offered to users. Bandwidth requirement of these telecommunications applications has increased in the last years, and users demand more services that also require transmission of large amount of data. These new functions are available thanks to the use of optical fibres as transmission media and the introduction of optical devices that perform some functions previously implemented by electronics circuits.

Related to optical fibres, a method for increasing the data rate transmitted is by using Wavelength Division Multiplexing (WDM). This technique consists on guiding several wavelengths through the same fibre; each wavelength carries their own information without mixing with adjacent channels, thus the transmission bandwidth is increased. Wavelengths are separated at the reception stage and there is a photodiode obtaining the information sent in each channel.

In this way, the present work proposes optical devices, based on different technologies, for being used in WDM networks. The first part of this chapter focuses in the description of basic concepts about optical networks. The latest part introduces main characteristics of the different optical switching technologies.

## II.2.- Evolution of Optical Networks

The huge expansion experimented in last decades by optical networks relied in the development, among other devices, of optical fibre technology. The birth of the Laser (Light Amplified by Stimulate Emission of Radiation) starts a new era in telecommunications. However, it was not successful until the invention of optical fibres, so as the key technology that enables broadband Internet services, its inventor Charles K. Kao was honoured with 2009 Nobel Prize.

The original idea of transmitting images from inaccessible places to the eye was the beginning of optical fibres. The first approach consisted in align many transparent fibres parallel to each other in a bundle, so that each fibre would transmit one pixel of the image from the one end to the other end. In the first attempts, the image quality was not so good because the fibres scratched each other and light leaked between them [DeCusatis-2008].

Brian O'Brien solves that problem trapping light inside the fibre by covering it with a transparent cladding, making it a tiny optical waveguide. That invention was the origin of practical endoscopes for medical imaging. Most transparent glasses available had an attenuation of one decibel per meter, so it was not suitable for optical communications.

Antoni Karbowiak tried to obtain an optical waveguide similar to the microwave dielectric waveguide, which were solid plastic rods that guides microwaves along

their exterior. He looked for an optical waveguide that propagates only a single mode, for avoiding the problems of propagation of multiple modes as it happened in the millimetre waves. This constraint required bare fibres only 0.1 to 0.2 $\mu\text{m}$  in diameter, too small for practical use.

Finally, Charles K. Kao realized that an optical waveguide with a thin cladding of transparent material with a lower refractive index would confine the light within the fibre. Furthermore, if the difference between the refraction index of the core and cladding was small, the core diameter could be increased to several micrometres and still transmit only a single mode. That large core allows the implementation of practical applications.

In 1966, C. K. Kao and George Hockham estimated a single mode fibre optic communication system with a transmission capacity of a Gigahertz, more than was available in coaxial cable or radio systems. The problem was making a glass fibre as clear as they needed [Kao-1966].

In 1970, a team of scientist directed by Robert Maurer managed to reduce attenuation below 20dB/km, near 7dB/km by using fused silica [Kapron-1970]. At the same time, the first semiconductor diode laser that could operate continuously at room temperature was demonstrated.

Different systems were tested, and the first primitive fibre-optic links started to be used. Mostly, it was used in transmitting data from measurements instruments, in difficult environments where interference or voltage differentials made electronic transmission impossible. It was neither cheap nor easy technology, that used short links.

Due to the problems of coupling light into a small core of few microns, Bell laboratories shifted to multimode fibres with cores of 50 or 62.5 $\mu\text{m}$  and graded refractive index to increase bandwidth. It could be good enough for 10 to 20km links, using an 850nm gallium arsenide laser, which was the most mature technology.

New family of semiconductor diode based on InGaAsP that emitted from 1.3 to 1.6 $\mu\text{m}$  was developed at Lincoln Labs. In addition, another key advance was developed at Nippon Telegraph and Telephone in Japan, two new transmission windows in glass fibres, at 1.3 and 1.5 $\mu\text{m}$  were proposed [Hecht-2004].

These two new windows presented better transmission characteristics than the 850nm window. Their lower attenuation allowed transmissions over longer distances. In addition, the new fibres had much higher bandwidth at 1.3 $\mu\text{m}$ , but only in single mode fibres. This technology was the seed for implementing submarine fibre optic cables. Finally, the first transatlantic fibre cable was laid at the end of 1988.

Since the earliest 1980s, telecommunication systems were developed by exploiting the zero material dispersion characteristics of silica fibre, which occurs at 1.28 $\mu\text{m}$  wavelength [Pal-2006, Payne-1975], in close proximity to its second low-loss wavelength window, which is centred at 1.3 $\mu\text{m}$  [Yamada-1981]. Monomode fibres and injection lasers allowed transmission of data rates from 565Mbps to 2.5Gbps in longer distances than 100km.

In the computer industry, the first standardized Local Area Network (LAN) operating at 100Mbps was the Fibre Distributed Data Interface (FDDI). Introduced in the mid-1980s, the original FDDI standard used multimode graded index fibre with 62.5 or 85 $\mu$ m cores and signal transmission using 1.3 $\mu$ m Light Emitting Diodes (LED); which cost less than diode lasers and could transmit signals up to 2km between nodes. Each node regenerated the signal and the entire network could expand up to 200km of cable [Hecht-2006].

In 1987, David Payne, from the University of Southampton in England, developed the Erbium-Doped Fibre Amplifiers (EDFA), whose operation wavelength coincided with the 1.5 $\mu$ m transmission window [Miya-1979, Mears-1987]. In addition, Emmanuel Desurvire, from Bell Labs, demonstrated that two 1Gbps signals at separated wavelengths could be amplified simultaneously using an EDFA without appreciable crosstalk [Desurvire-1989].

Data traffic grew fast thanks to the dramatic expansion of Internet. Handling that traffic would require expanding the capacity of the global telecommunications networks. In 1995 and 1996, Ciena, Lucent and Pirelli introduced the first commercialized Wavelength Division Multiplexing (WDM) systems. WDM would transmit several wavelengths simultaneously using the same fibres, which increases the fibre's bandwidth, although it required installation of different fibres than previous installed.

Development of the AllWave and the Monomode fibre SMF-28e that was devoid of the OH-loss peak, centred at 1.38 $\mu$ m, extended the low loss wavelength window in silica fibre from 1.28 $\mu$ m to 1.65 $\mu$ m.

Optical switching technologies started to be taken into account in long haul optical networks. The first Cross-Connect Digital Access and Cross-Connect System II (DACS-II) was introduced in 1981. It handled DS-1 lines (1.5Mbps) and cross-connect traffic at data rates DS-0 (64kbps). In 1988, the second DACS-IV-2000 (wideband cross-connect) and the third DACS III-2000 were presented. The third one achieved transmission rates that includes OC-48 (2.5Gbps) and up to 2048 cross-connects channels at DS-3 (45Mbps) data rate.

In the 1990s decade, development of Synchronous Optical Networking (SONET) systems caused the infrastructure improvement, providing scalability in the switching, allowing the implementation of protection schemes such as the Automatic Protection Systems (APS) or Rings Based Restoration. During the same decade, point-to-point Dense Wavelength Division Multiplexing (DWDM) systems were deployed. The WaveStarTm Bandwidth Manager (1988) was capable of handling up to OC-192 (~10Gbps) communications, and 4608 STT-1 (51.84Mbps) channels. [Kaminow-2008 a, Kaminow-2008b] The use of WDM networks made necessary the use of Optical Add/Drop Multiplexers (OADM) for making available intermediate accesses in optical networks.

## II.3.- Types of Optical Networks

Previous section presents the origin and evolution of optical networks that are used for telecommunication systems. Those networks can be classified attending to the type of information they transmit: voice, video and data. Public Switched Telephone Network (PSTN) traditionally handled Voice. Video is usually broadcasted from a station to the users. It can be transmitted in free-air, or using a cable network or Community Antenna Television (CATV), usually known as Cable TV. Finally, data refers to transmission done between computers. However, the integration of technologies and services means that the transmission of different information is carried out by using the same transmission media. Other classification of data networks is attending to their area of influence. In that sense, there are Backbone Networks, Metropolitan Area Networks (MAN) or Access Networks.

### **II.3.a.- Backbone Networks**

These kinds of networks refer to the core networks that perform data transmission at long distances. These networks interconnect regional offices that concentrate data from many users allowing a continuous traffic demand. Final users' data are gotten by Access Networks, that are collected by means of Metropolitan Area Networks. Finally, MANs are linked thanks to Backbone Networks.

Backbone Networks can extends worldwide, terrestrial and subsea networks, or in a shorter range, international, national or regional area. In these networks, monomode fibre in combination with WDM is used in order to achieve the required bandwidth in long distances.

One of the objectives of Backbone Networks is their adaptation to the amount of traffic demanded in each time, which makes that the core resources are shared between users. Cross-Connects are used for managing the bandwidth of this kind of networks. Thus, their requirements come from those used in switching devices of general transport data networks.

Bandwidth demanded for data transmission is increased and the fact that the basic operation of backbone networks is traffic directing causes the introduction of optical technology for handling the network resources. Switching in the optical domain is faster and needs fewer resources than doing it in the electrical domain. Only those channels directed to an electrical device or those requiring IP routing are converted to electrical domain.

Evolution of optical cross connects (OXC) comes from the evolution of the optical networks, more users demands more services that require more bandwidth. This causes the need of improving bandwidth handling in backbone networks and consequently in switching devices like OXC.

The use of optical switching devices in optical networks is a more efficient solution and allows data transmission at higher rates in longer distances. It is used for routing in wavelength-routed WDM networks, network management for protection and restoration applications and multicasting systems.

Wavelength-routed WDM networks allow optical switching only by directing each individual wavelength to a destination. By using OXC, each channel can be reconfigured for transmitting information to other point.

Protection and restoration networks consist in configuring an alternative optical path for transmitting the information when the main route has a failure. The new connection can be related to a single link or a complete connection, end-to-end. Failure management is carried out dynamically; when the nodes adjacent to the failure are noticed is known as link restoration, on the other hand, when the end nodes are warned about the failure is denoted as path restoration. In those situations, the OXC are reconfigured for building the new optical path.

Multicasting refers to the possibility of a network for transmitting multiple copies of the same information to several points in the network. This characteristic is used for applications such as data distribution, videoconference, online games, e-learning... Switching devices capable of allowing multicast are necessary in order to minimize the amount of network resources required. The main benefits of OXC are their independence of the data rate transmitted and the information codification.

### **II.3.b.- Metropolitan Area Networks**

Metropolitan Area Networks are in charge of joining Access Networks with Backbone Networks. Despite that SONET and Synchronous Digital Hierarchy (SDH) have been used for implementing these networks, clients diversity, protocols and granularities make necessary the use of CWDM and DWDM that allows scalability, more bandwidth...

All the advantages of OXC commented in the Backbone section apply to MAN. In this type of networks, it is common the use of Add-Drop Multiplexer (ADM) that allows the extraction or not of different wavelengths from an optical fibre. In addition, Traffic Grooming technique is used; several low speed traffics are packed in a high-speed one, reducing the number of switching devices.

### **II.3.c.- Access Networks**

Access Networks connect users with the service providers. In telephone system, it is known as local loop and it is based on twisted pair. This technology is used for transmitting voice at low frequency, so low bandwidth is obtained. Integrated Services Digital Network (ISDN) and Asymmetric Digital Subscriber Loop (ADSL) increases the bandwidth offered to users using the same transmission media.

New services and applications demanded by users require more bandwidth, thus, a change in the transmission media to optical fibre technology is a solution, but requires a great inversion. Different scenarios are possible depending on the available budget.

Access networks based on optical fibres are classified depending on the limit where the fibre is deployed, thus three types are considered, Fibre to the Home (FTTH),

Fibre to the Building (FTTB) or Fibre to the Curb (FTTC). All these setups usually are grouped as FTTx. Other possibility is the known as Hybrid Fibre Coax (HFC) that consists in a system that comprises both technologies.

Different topologies are used in this kind of networks: point-to-point (P2P) topologies and passive optical networks (PON). The first one is the traditional scheme; a dedicated wire is used for connecting user with the central office. It is a simple architecture, but it implies a dedicated fibre for each customer.

An alternative topology is based on a star topology, where a switch is used for multiplexing data from different customers to the central office. This scheme reduces the amount of fibre necessary but implies the use of additional power [Ilyas-2003].

Other possibility is the use of PONs. This technology substitutes the switch placed in the neighbourhood by a passive optical device such as a splitter/combiner, either ring and tree topologies are possible. PON minimizes the amount of deployed fibre and the number of transceivers and reduces the power consumption required.

The main advantages of this technology are their reliability, their easy maintenance; they do not require power supply for the network and they are also transparent to bit rates and modulation formats. Structure of the network is simple; all the complexity is in the central office instead of distributing it along the network. These networks make use of Coarse WDM (CWDM) technology that combines different wavelengths in a single optical fibre, WDM, at low cost.

CWDM combines wavelength channels separated 20nm (determined by UIT-T G.694.2), which reduces system restrictions allowing the use of cheaper devices. Such as optical sources that do not need temperature control or low cost passive optical multiplexer and demultiplexers. Besides, this technology offers scalable bandwidth; several, even all the channels can be replaced by Dense WDM (DWDM) wavelengths increasing the bandwidth. This technique is known as DWDM over CWDM.

## II.4.- Applications of Polymer Optical Fibres

Other type of fibres used in optical networks is Polymer Optical Fibre (POF). This kind of fibre has a core and cladding made of polymer. Their diameter is typically wider than the diameter of glass fibres. In addition, POF is flexible, lightweight and enables easy and safe handling. Due to the POF's large diameter, high accuracy positioning is not required for connections so installing costs are reduced. Furthermore, like occurs with other optical fibres, they are immune against electromagnetic interferences (EMI).

The first POF was demonstrated by DuPont in the mid-1960s. Named “*Crofom*”, it had a step index (SI) polymethylmethacrylate (PMMA) core. Incomplete purification of the source materials made high attenuation values about 1000dB/km. During the 1970s loss were reduced nearly to the theoretical limit that is approximately 125dB/km at a wavelength of 650nm. Mitsubishi Rayon commercialized SI POF for

the first time, called “*Eska*” in 1975. Later, in the 1980s other manufacturers, Asahi Chemical and Toray, also started POF commercialization.

The first Graded Index (GI) POF, with PMMA core, was introduced by Keio University in 1976 [Ohtsuka-1976]. Its refractive index profile was near parabolic and exhibited attenuation near 1000dB/km. Attenuation was reduced by doping the structure with low molecular weight compounds [Koike-1991]. Then, the refractive index profile of the GI-POF was formed by the radial concentration distribution of the dopant [Ishigure-1994].

Very low attenuation in the 1300nm wavelength range was obtained in Perfluorinated (PF) GI-POF by substituting fluorine for all hydrogen bonding in polymer molecules. The first PF- GI-POF fibre was presented in 1994 [Koike-1994], Asahi Glass., Ltd commercialized an amorphous PF-GI-POF with the trade name of “*Lucina*”.

During the 1990s many researches attempted to employ POF for high speed communications [Bates-1992]. However, the high bandwidth characteristics of GI-POF was verified in 1990 [Ohtsuka-1990], a 17.3GHz communication at 670nm wavelength over 15m length. The first transmission of a 2.5Gbps using GI-POF over 100m, was reported in 1994. 11Gbps over 100m was achieved in 1999. A 1-Gbps campus LAN using PF GI-POF was deployed at Keiko University in 2000. GI POF has been used in Tokyo in houses complexes, hospitals, medical conferences halls, and so on [Kaminow-2008a].

Despite the quick development of glass optical fibres, POF has not been used in optical networks until the 1990s decade. PMMA exhibits attenuation about 100dB/km. SI-POF has a bandwidth in the order of 10Mbps/km, therefore, it is appropriated for communications in distances shorter than 100m, showing a bandwidth near 100Mbps. On the other hand, PF-GI-POF has attenuation reduced to 10dB/km, furthermore, its bandwidth can reach 10.7Gbps over 220m [Lee-2007, Montero-2011]. This distance complies with the novel IEEE 10GBASE-LRM standard [IEEE-2006], which is developed for the support of 10GbE installed fibres. Based on all these experiments it is clearly demonstrated that PF GIPOF could cover broadband fields, from the areas of very short-reach networks to the access networks.

For the reasons given above, POF is used in short-distance transmission systems. In those applications, copper has not been replaced by glass optical fibres due to their cost and the reduced bandwidth required. POF is suitable for substituting copper wires due to their intrinsic characteristics:

- Immune against EMI
- Safety, there is not explosion risk under flammable atmospheres.
- Large bandwidth for short distances, less than one hundred meters.
- Lightweight.
- Easy and economical processing.
- Easy in handling and connecting which reduces installation costs.
- Low radius of curvature.
- Safe in handling, it is suitable to consumer use.

Thus, POF has been used in different areas such as automotive, avionics, home networks, medical equipment or sensor applications. Some examples are:

- In the entertainment system in cars: Digital Domestic Bus (D2B), Media Oriented System Transport (MOST) or IDB 1394 systems.
- In home networks.
- As sensors along or integrated in sensor networks.
- For control networks, such as Byteflight.
- In automation: Hke Profmet, Sercos or Fast Ethernet.
- As Back Plane Interconnect, that consists on substituting massive copper wires links by optical fibres.
- In illumination

Applications related to the present work are described in more detail in the following sections.

#### II.4.a.- Polymer Optical Fibres in Automobile Networks

The amount of multimedia applications in automobiles has increased in last years, radio turner, DVD (Digital Video Disc) player, Video displays, GPS (Global Positioning System), Mobile... In 1998, the first application in data communication used in vehicles and based on POF, it is Digital Domestic Bus (D2B), and was developed by DaimlerChrysler. It allowed data rates up to 5.6Mbps.

Next generation of optical busses was the Media Oriented System Transport (MOST) system. It was developed under the participation of several car manufacturers, such Audi, BMW, DaimlerChrysler... Its bit rate was about 25Mbps, enough for DVD data transmission [Muyshondt-2005, Schönfeld-2000, Kibler-2004, Baierl-2001]. Most architecture is based on a unidirectional ring, and every device works as a repeater.

The drawback of the architecture was the loss of operation when a component fails. To improve the system availability, a bypass switch can be used as possible solution for connecting/disconnecting new devices to the MOST network. Thus, the bypass switch is closed when an Electronic Control Unit (ECU) shuts down (see Figure II-1). A possible implementation of a Plug and Play Connector and By-Pass Switch is proposed in [Lallana-2007].

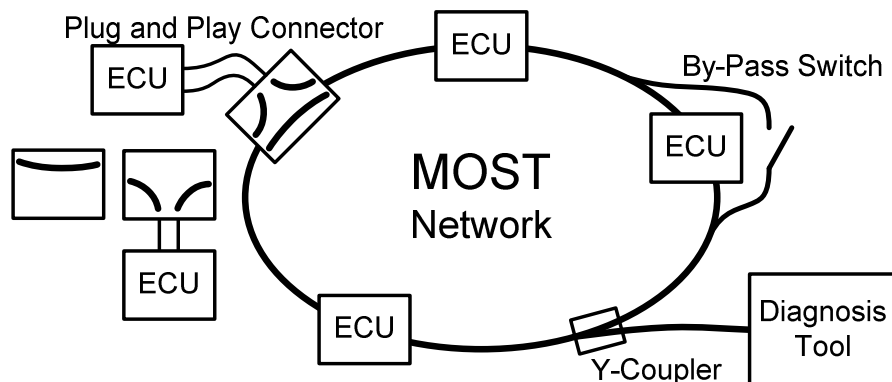


Figure II-1: Optical Fibre Ring Network

MOST has separated the communication devices into different networks according to the bandwidth required:

- Power Train: ABS (Anti-Block System), EMS (Engine Management System), Suspension, Gear Box.
- Body Electronics: Instrument Cluster, Air-Conditioning, Anti-Theft, Window Control, Mirror Adjust, Seat Adjust.
- Chassis Systems: Steer-by-wire, Brake-by-wire.
- Surround Sensing: Access to Diagnosis Data, Electronic Logbook, Electronic User Manual.
- Infotainment: Navigation, Telephone, Audio/Video Internet, Multimedia.

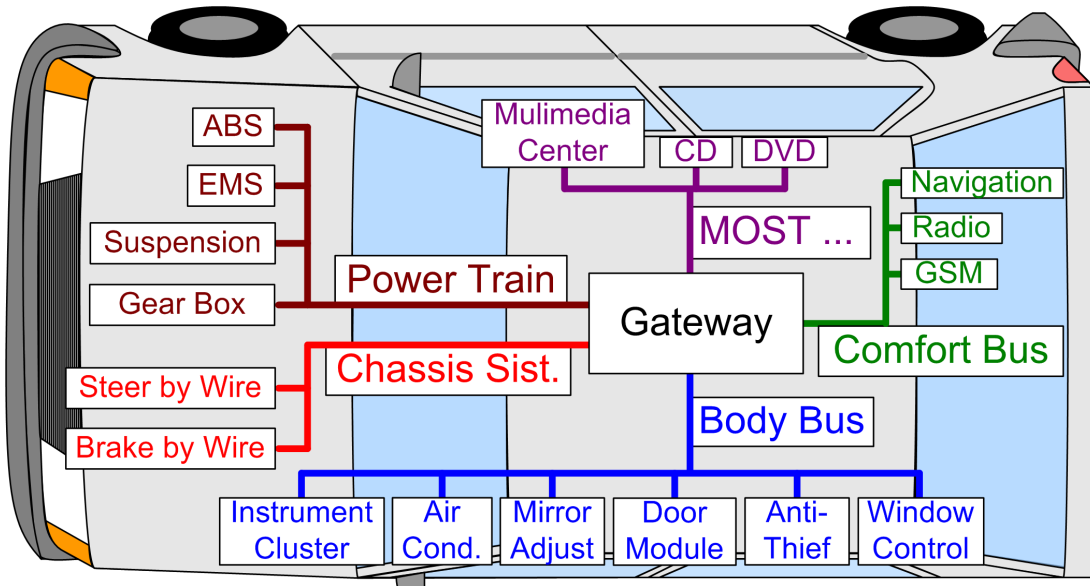


Figure II-2: POF network within the Automobile

Each network satisfies the ISO/OSI seven layers model. The total length of fibre used in the car has been less than 30m. A schematic of the different networks used in a car is shown in Figure II-2.

Another system developed by BMW has been Byteflight. It connects airbag systems with other control components in the Intelligent Safety Integration System. The connectors and fibres used correspond to the MOST standard. However, the data transmission is bidirectional on one fibre. Its data rate is about 10Mbps.

The possibility of using Standard IEEE 1394, known as Firewire, in automobiles has been demonstrated by some carmakers. This standard has been widespread in home applications and the desire of transmitting uncompressed video data has produced their deployment in vehicles. In addition, it has the possibility to connect external devices to the vehicle system via Customer Convenience Port (CCP). The standard that comprises the greater requirements in vehicles is the Intelligent Data Bus (IDB) 1394. Transmission media for the described system was symmetrical twisted copper cables, as well as POF was used for longer links. The maximum transmission lengths were 10-18m.

## II.4.b.- Polymer Optical Fibre in Home and Office Networks

Office Networks is deployed using Untwisted Pair (UTP) Cat5e and Cat6 cables and multimode silica fibre. Cat5e allowed a data rate of 100Mbps over a distance of 100m, while Cat6 has a bandwidth of 600Mbps over the same distance. However, UTP is affected by electromagnetic interference (EMI). In addition, the use of wireless technologies made ease network installation.

Optical fibres are used for achieving higher transmission data rates. Despite POF has worst attenuation than silica fibres, it offers some advantages such as its ease of connection and installation, allowing lower curvature radius and reduced cost.

The structure of the networks deployed in houses is based in the technology used for office networks. It is an extension of broadband access networks. A Home Communication Controller (HCC) is in charge of collecting the information from different services provided to the user, and distribute the data to the entire house using the in-home network.

Different topologies are possible for the network. The most straightforward is the point-to-point (P2P) architecture (Figure II-3 (a)), which uses a single fibre for connection the HCC to each wall outlet in a room. Alternative of P2P technology is the point-to-multipoint (P2MP) architecture. In the tree structure (Figure II-3 (b)), each riser fibre connects each floor with the HCC, signal is distributed for different fibres to all the rooms in the floor. Instead of that, in the bus architecture (Figure II-3 (c)) the same fibre is used for distributing the signal along the floor.

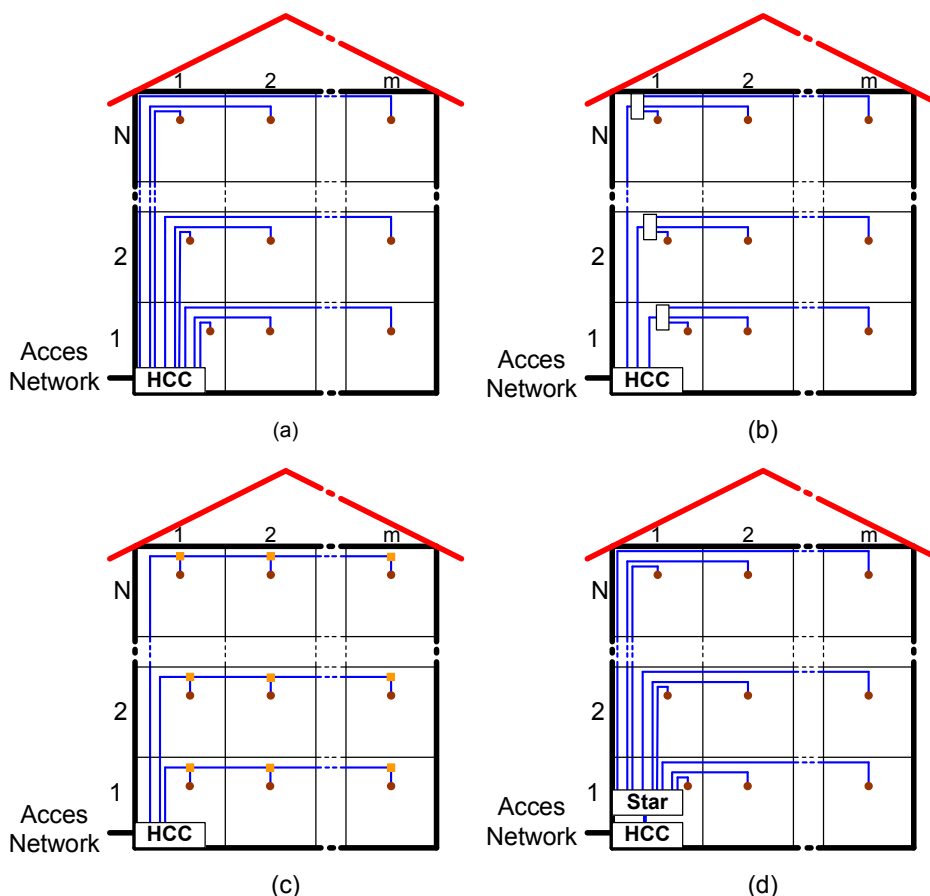


Figure II-3: Structures of In-Home Networks: (a) Point-to-Point, (b) Tree, (c) Bus, (d) Star

Finally, a multipoint-to-multipoint (MP2MP) architecture is composed like a star-shaped network (Figure II-3 (d)), where each wall outlet is connected by a single fibre to a star coupler placed near the HCC. This scheme allows the communication between different rooms without the intervention of the HCC.

The architectures may be implemented in two flavours: all optical or opaque. In the first scheme, no conversion to the electrical domain is required, while in the second type, opto-electric-optical (O/E/O) conversion is performed where it is required.

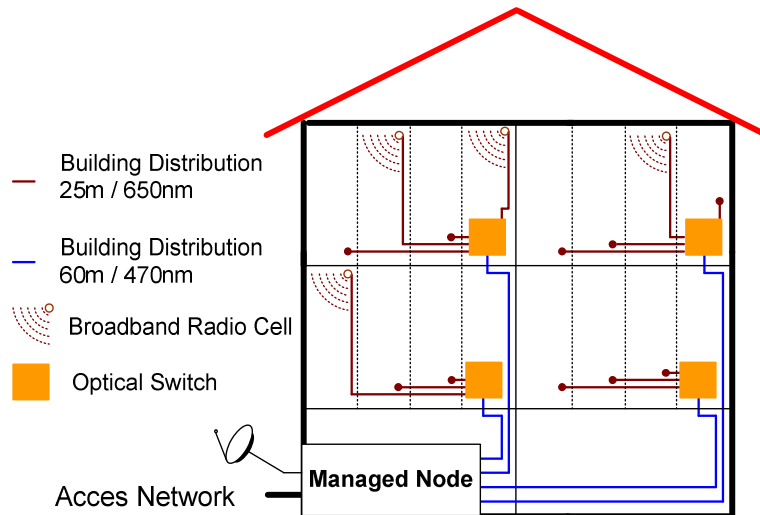


Figure II-4: Example of POF Network within the House

A possible example of the network using POF is shown in Figure II-4. The building network is based on 470nm duplex POF transceivers. Apartments are equipped with 650nm simplex transceivers. Wireless systems are installed in the rooms, being each room a pico-cell. As those signals reach the room through optical fibres they are called Radio over Fibre (RoF) systems.

In Chapter IV an advanced optical switch based on Liquid Crystal [Lallana-2011] for being used in POF networks is described; being able to work in multimode Radio over Fibre (RoF) systems or as part of the HCC described below.

#### II.4.c.- Polymer Optical Fibre Sensors Networks

POF is also used in sensor networks; it can be used both as the transmission media, and as the sensor. POF networks makes possible the implementation of remote sensing points, the measurement is transmitted by this kind of fibre to a remote point for their evaluation

In many sensor applications, the distance between the sensor and the evaluation system is relatively short and the measurement does not require high bandwidth. In addition, optical fibre is safety in nature allowing their use in flammable atmospheres, avoiding explosion risks. In [Vázquez-2004] a level sensor for being used in oil tanks is presented.

POF in combination with switching devices permit spreading the number of measuring points. In [Vázquez-2003] a 1x2 optical switch allows the implementation of a network with two measuring points that can be asked in different time intervals. The same scheme can be used for implementing a safety system where an additional sensor is used when the main one fails. A scheme with more sensor heads by using a multiplexer is presented in Figure II-5.

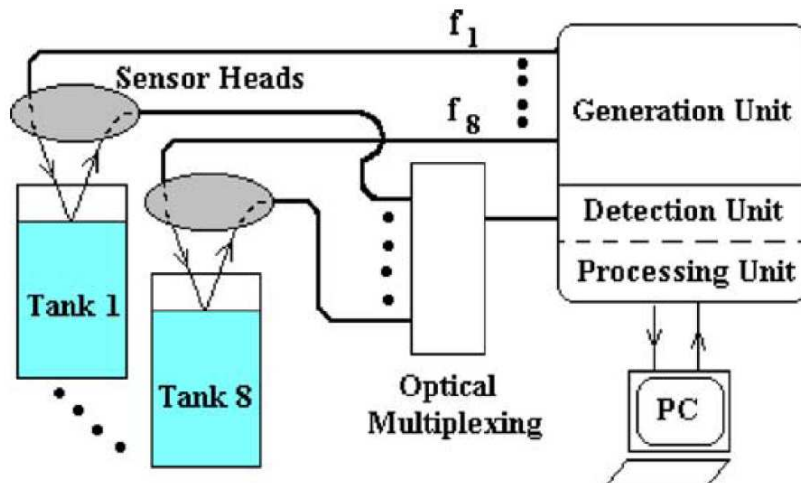


Figure II-5: Scheme of a Multisensor System Based on POF [Vázquez-2004].

Furthermore, like occurs with glass fibres, POF is also used as the sensor. A general overview of Fibre optic sensors using POF is given in [Kalymnios-2004, Poisel-2005]. POF based sensors can be classified in different groups [Ziemann-2008], some examples are given below.

- **Transmission and Reflection Sensors**

This kind of sensor is based on the coupling properties of POF. The principle can be used with other fibres, but POF has the advantage of having a large cross-sectional area and numerical aperture. The structure consists of a fibre that guide light to the measuring point, light that is coupled out and coupled back in again, either into the same fibre or into another. They are extrinsic fibre-optic sensors. The magnitude to be measured modifies the returning optical power, so the corresponding process can be detected.

An example of this technique is presented in [Vázquez-2004], where the tank level is measured by the light reflected in the liquid surface (see Figure II-5). In [Zubia-2007] a sensor for determining wind speed in a wind generator is presented, it is based on the reflection obtained of the hollow slotted cylinder attached to the rotor's vanes of an anemometer.

This type of systems is suitable for measuring distances, pressure or deformation.

- **Sensor with Fibre as Sensitive Elements**

This type of sensor exploit the influence of different parameter when light propagates along an optical fibre. They are intrinsic fibre-optic sensor. The most usual is the increase of attenuation when the fibre is bent.

[Durana-2009] reports an elongation POF sensor for monitoring the deflection of an aircraft flap subjected to different types of loading conditions. Two fibres are placed in the flag surface; one was fixed on the top while the other is stuck to the bottom one. When one of the measuring fibres is elongated under stress, the other is compressed, and then light transmitted by the elongated fibre covers a longer distance and the phase difference between both optical signals changes.

- **Sensor with Surface-Modified Fibres**

In many applications, the sensitivity obtained with a normal fibre is insufficient. Then, the sensitivity improves by making modifications in the fibre. Such modification can be mechanical damage to the cladding, changes in the refractive index or a coating with chemically active materials.

A sensor developed by Siemens- VDO used for detecting collision with pedestrians is presented in [Miedreich-2004, Djordjevich-2003], that is based on a POF with certain zones of the cladding damaged used for measuring the deflection. Another sensor used in automobile industry is an evanescent field sensor for jam protection in car windows [Kodl-2003, Poisel-2005], that is based on a POF without optical cladding. [Lomera-2007] proposes a sensor for measuring liquid fluid levels that also uses a surface effect. In [Montero-2009] a self-referencing intensity based sensor for liquid detection is proposed. It is based on bending losses of a partially polished POF coupler.

- **Sensor for Chemical Materials**

The presence of chemical materials can be detected by using a POF with the sensitive material, which modify light transmission along the fibre, correspondingly to the desired element.

## II.5.- Parameters of Optical Switches

Once an overview of the optical network and an introduction about POF applications have been given, it is time to introduce the optical switches used in optical networks. Before starting with the optical switching explanation, the parameters used in the description of optical switches are introduced in [Papadimitrou-2003, Chua-2010, Rivero-2008]. Parameters definitions are based on Figure II-6 nomenclature. Only one active input (with incoming light) is considered for describing these characteristics.

Switches characteristics have to be taken into account during optical network design in order to fulfil transmission requirements. These factors affect to the system operation causing a system failure if the restrictions are not properly calculated.

The description of the parameters is in three sections, depending on their application range. In the first part, there are the parameters related to the switch performance. In a second subsection, the parameters related to network requirements are introduced. Finally, system requirements considerations are presented.

### II.5.a.- Switch Performance Parameters

Among the different parameters that describe optical switches behaviour, the main characteristics are:

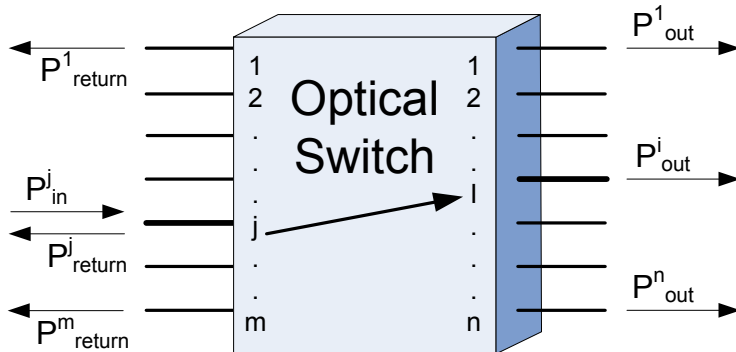


Figure II-6: Optical Switch Schematic for Parameter's Definition.

- **Insertion Loss**

Insertion Loss refers to the fraction of the input signal power that is lost when light is transmitted through the switch towards one of its outputs. It consists of coupling loss, waveguide propagation loss, and excess loss. It is measured in decibels (dB) and must be as small as possible and its value should be uniform over all the input-output connections

$$IL = -10 \cdot \log \left( \frac{P_{out}^i}{P_{in}^j} \right) > 0 \quad [II-1]$$

- **Excess Loss**

Excess Loss is the ratio of the total power at all output ports to the input power.

$$EL = -10 \cdot \log \left( \frac{\sum_{k=1}^n P_{out}^k}{P_{in}^j} \right) > 0 \quad [II-2]$$

- **Crosstalk**

Crosstalk is the ratio of the power leaked to the not selected output to the input power. It is used to measure the signal interference between channels. This ratio should be low.

$$CT = 10 \cdot \log \left( \frac{P_{out}^n}{P_{in}^j} \right) < 0 \quad [II-3]$$

- **Extinction Ratio (ON – OFF switches)**

Extinction Ratio is the ratio of the output power in the on-state to the output power in the off-state. This ratio should be as large as possible.

- **Return Loss**

Return Loss refers to the ratio of the optical power returned to the input port to the input power.

$$IL = -10 \cdot \log \left( \frac{P_{out}^j}{P_{in}^j} \right) > 0 \quad [II-4]$$

- **Directivity**

Directivity is the ratio of the power returned to any other input to the input power.

$$IL = -10 \cdot \log \left( \frac{P_{return}^m}{P_{return}^j} \right) > 0 \quad [II-5]$$

- **Switching Time**

Switching time is the time elapsed from the switching command to the moment the signal in the correspondent output is stable (90% of the final value when it is a rising transition and 10% in the falling one).

- **Polarization Dependence Loss (PDL)**

Polarization Dependence Loss is the peak-to-peak difference in transmission for light with orthogonal states of polarization. Optical switches must have low PDL (typ. < 0.5dB).

- **Other switch performance parameters**

The *Polarization Mode Dispersion* (PMD) specifies the dispersion produced in the information transmitted because distinct polarization states travel at different speeds when they pass through the switch. The *bit rate* gives the amount of bits per second that the switch can manage; *wavelength dependence* of the different parameters quantifies similarities in their operation wavelength range and *symmetry* implies the difference between switching times in *on-off* and *off-on* transitions.

## II.5.b.- Network Requirements

*Multicast* indicates the capability of the switch for routing input data to several outputs simultaneously. Switch *dimensions* refers to the amount of input/output ports of the device, *scalability* is the ability to obtain switches with a greater number of

ports from a basic low-port count structure, and *non-blocking* means the flexibility to route or reroute any input port to any unused output port.

### **II.5.c.- System Requirements**

Other parameters to be taken into account when designing a system are: scalability/reliability that measures the switch lifetime, port to port repeatability that alludes to the length equality of the different optical paths in the switching matrix, power consumption that refers to the electrical power required for switch operation or cost.

## **II.6.- Type of Switches**

The main advantage of optical switching is that allows optical routing without converting the transmitted information to the electrical domain. The elimination of the two required conversions (optical to electrical and electrical to optical) improves the system characteristics: reduces the network equipment, increases switching speeds and decreases operating power [Papadimitrou-2003, Ma-2003 and Rivero-2008].

Up to now, limitations in optical technology, have limited management task of optical switches in data transmission, such as data processing or buffering in the optical domain. Three approaches have been proposed for the migration of the switching functions from electronics to optics. Optical Packet Switching (OPS) offers almost arbitrary granularity comparable to currently applied electrical packet switching and require faster switches, in the nanosecond range [Liua-2006]. Generalized Multi-Protocol Label Switching (GMPLS) provides bandwidth at a granularity of a wavelength and Optical Burst Switching (OBS) that lies between them [Papadimitrou-2003].

### **II.6.a.- Applications of Optical Switches**

Optical switches are widely used in the next network applications. Their use depends on the type of network in which the switch is employed.

#### **• Optical Cross-Connects (OXC)**

This kind of switches performs the interconnection of different network nodes using a dedicated wavelength, creating a lightpath. In this way, OXCs allow the transmission of information point-to-point [Ramaswami-2002]. Switches used inside OXCs reconfigure them to support new lightpaths.

All optical cross connects switch data without any conversion to electrical domain, they are independent of the protocol and the data rate used. On the other hand, they are not able for implementing managing functions and they do not allow signal

regeneration. Although the determination of the minimum response time required for wavelength division multiplexing (WDM) transport network restoration or flexible bandwidth allocation depends on several network management and service-related issues, it is widely agreed that the switching time of an OXC should not exceed a few tens of milliseconds [MacDonald-2000].

- **Protection Switches**

This application allows data transmission even when a network-level failure occurs. Optical protection functions usually require optical switches with smaller amount of ports, 1x2 or 2x2.

Optical switches developed for these applications have to be reliable, since these switches are single points of failure in the network. In addition, switching speed is not a critical requirement because different task are necessary to determine the failure, and these processes take longer than the optical switch.

- **Optical Add/Drop Multiplexer (OADM)**

These multiplexers allow the insertion (add) and/or the extraction (drop) of optical channels (wavelengths) to or from the optical transmission stream. Using OADMs, channels in a multi-wavelength signal can be added or dropped without any electronic processing. If they can be reconfigured, they are named ROADM. They can be used as building blocks for optical cross-connects (OXC).

- **Optical Signal Monitoring**

These switches tap a portion of a Wavelength Division Multiplexing (WDM) signal, and supervise each optical channel characteristics. They are also referred to as Optical Spectral Monitoring (OSM).

They use a small power portion of the optical signal transmitted; separate the obtained light in individual wavelengths and control their accuracy, optical power levels and optical crosstalk.

Switches used in this application should have low insertion loss and good uniformity [Dugan-2001]

- **Network Provisioning**

This application refers to reconfigurable switches that allow establishing new data routes or modifying established ones. A network switch should carry out reconfiguration request over time intervals of about few minutes.

The requirements of the response time and the number of ports for the optical switching applications are shown in Figure II-7 [Fernsemer-2001].

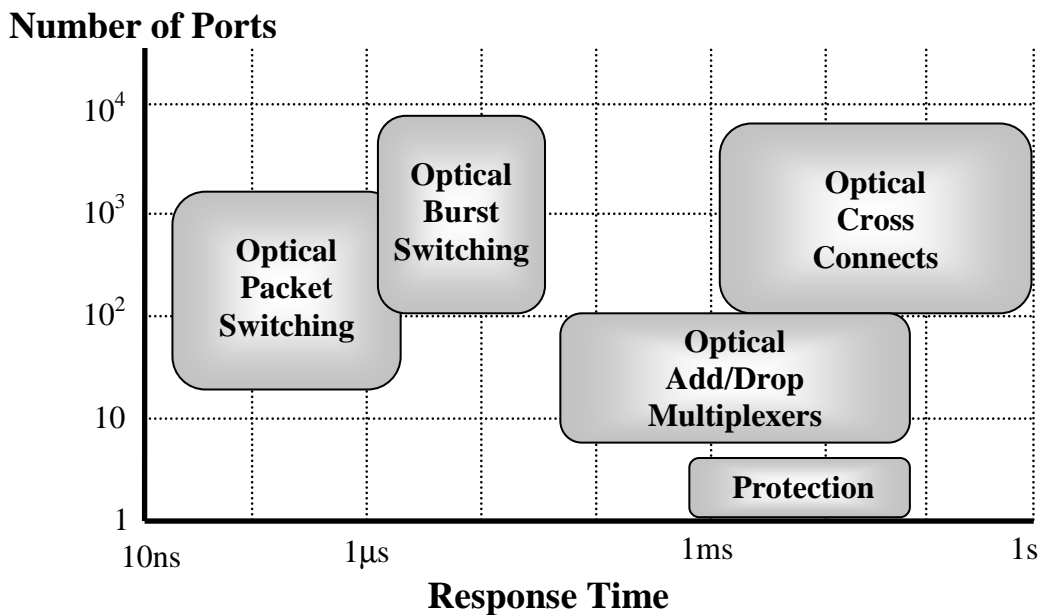


Figure II-7: Requirements of Optical Switching Applications

## II.6.b.- Optical Switching Technologies

According to the technology used in the implementation of the optical switch and the principle used for switching, they can be classified in the following types:

- **Opto-mechanical Switches**

In this type of devices, the switching function is carried out by some mechanical means. Prisms, mirrors and directional couplers are used to perform switching.

This technology was the first commercially available. They exhibit low insertion losses, low PDL, low crosstalk and low fabrication cost. Their switching speeds are in the order of milliseconds. Opto-mechanical switches are used in fibre protection and low port count wavelength add/drop applications.

- **Micro-Electromechanical Systems (MEMS)**

Although this technology can be considered as a subsection of the previous technology, it is presented separately because it has been widely developed, having a great interest in telecommunication applications.

It consists of small mobile refractive surfaces mirrors that route incident light beams according to their destination. Two typical dispositions are possible for implementing OXC using MEMS: two dimensions (2-D MEMS) and three dimensions (3-D MEMS) [Dobbelare-2002]. In the first type, the micro-mirrors are distributed in a cross-bar configuration in a single plane (see Figure II-8). These switches have  $N$  input and  $N$  output ports and  $N^2$  mirrors. Collimated optical beams propagate parallel to the surface where the micro-mirrors are placed. Active micro-mirrors are moved to the light path reflecting the optical signal at 90°, from the incident beam, towards the

active output. Switches based on 2-D MEMS are digital, since there are two possible mirror position. Reconfigurable OADMs can be also implemented using this kind of MEMS.

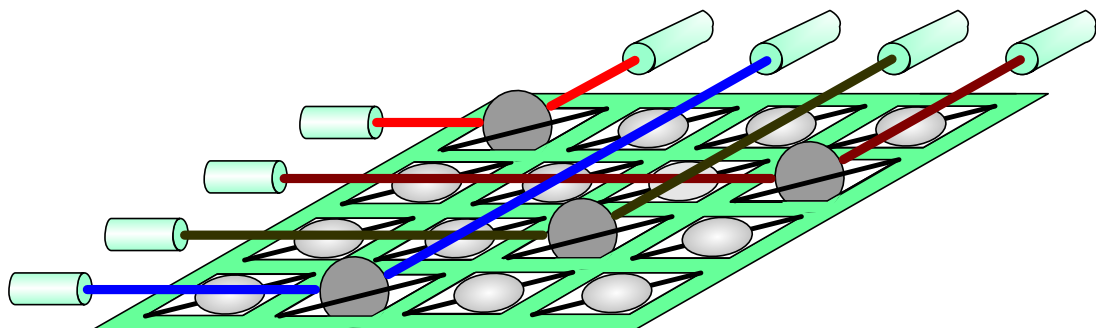


Figure II-8: Optical Switch Based on 2-D MEMS

2-D MEMS are not scalable over 32 inputs and 32 outputs due to the exponential growing in the amount of mirrors and possible routes. In addition, when the switch has more inputs, light travels more length when passes through the switch.

For larger switches, 3-D MEMS are the solution. They are formed by two 2-D matrix of mirrors placed in front of the input ports and output ports respectively; there is a dedicated movable mirror for each input port and for each output port. A pair of mirrors moves in order to direct the input light to the desired output port. Mirrors operate in analogue mode, and are able to move in two axes [Ramaswami-2002].

By using 3-D MEMS, very large port count OXC switches, with more than 1000 inputs and outputs, are possible. A drawback of this kind of switches is the complexity required for the feedback system required for maintaining mirrors' positions.

Mirror movement is obtained by different methods. The needed forces that move optical parts in the switch may be electrostatic, electromagnetic or thermal, but electrostatic actuation is the preferred method thanks to their easy manufacture and integration, and because it allows low power consumption. A batch fabrication process allows high volume of production of low cost devices, where many switches can be manufactured on a single silicon wafer.

Switches based on MEMS technology have low loss, short switching time, low power consumption, low crosstalk and polarization effects, and they are independent of wavelength and bit rate. Apart from OXC applications, switches bases on this technology are used in OADM, optical service monitoring or optical protection switching. Their main drawbacks are the mirror fabrication, the opto-mechanical packaging, the mirror control algorithm and implementation.

### • Thermo-optic Switches

The operation of these devices consists on the variation of the refraction index due to temperature modification of the material. There are two switches groups: Thermo-Optic Switches (TOSW) where the thermo-optic effect is applied to an optical waveguide, and the others that are based on the thermo-optic effects of materials.

TOSW are composed by two basic types, Interferometric Switches and Digital Optical Switches (DOS) [Bregni-2001]. They are usually integrated optical devices composed by two interacting waveguide arms where light propagates through it [Sakuma-2001]. The phase error between light travelling for both arms determines the amount of light at output port. By heating one of the arms the refraction index is modified and the light transmission changes.

Interferometric switches are usually based on the Mach-Zehnder Interferometer (MZI) (see Figure II-9). The MZI is comprised of two 3dB couplers joint by two waveguides. Input signal splits in the first coupler and recombines in the second one. If the two waveguides that connect both couplers are identical, both optical beams are in phase and the recombined signal that comes from *In 1* has a maximum in *Out 2* and a minimum in *Out 1*.

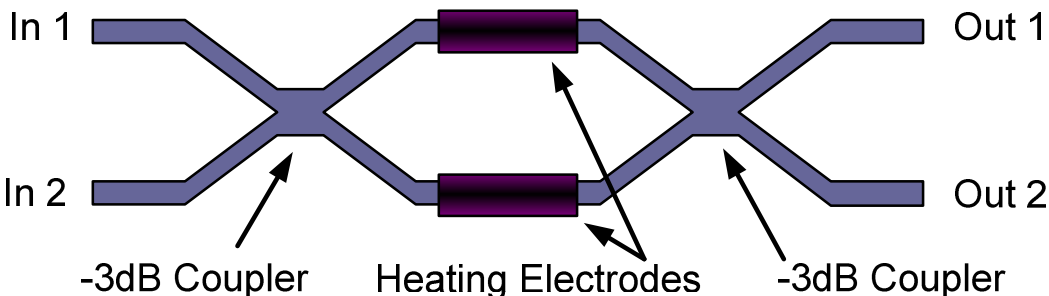


Figure II-9: Scheme of a 2x2 MZI based Switch

If a modification of the refraction index of one of this waveguides is induced, one optical beam is delayed respect to the other one. When the two optical paths are in phase opposition, the recombined signal has a maximum in *Out 1* and a minimum in *Out 2*. Then, the switch output is selected by modifying the refractive index difference between both waveguides,  $\Delta n$ . The refractive index variation of the waveguide is usually controlled by using the thermo-optic effect.

More detail information about this kind of switches is given in Chapter V, where a Tap and Two Split Switch for being used in Multicast-Capable Optical Cross Connects (MC-OXC) architecture based on Mach Zehnder Interferometer MZI is proposed [Fernández-2009].

A generalized version of a MZI is based on the Multimode Interference (MMI). A MMI coupler consists of a wider waveguide, which is the MMI zone, where smaller input/output waveguides are attached.

According to [Soldano-1995] the self-imaging principle is produced in a MMI waveguide, and can be stated as follows: *Self-imaging is a property of multimode waveguides by which an input field profile is reproduced in single or multiple images at periodic intervals along the propagation direction of the waveguide*. Consistent with this, an NxN coupler can be implemented by using a MMI zone with the adequate length and placing the input/output waveguides in the proper positions.

Compact MMI couplers with tunable power splitting ratios are presented in [Leuthold-2001]. This idea exploits the self-imaging principle fulfilled in an MMI waveguide. Output self-image depends on the previous self-images formed in the

waveguide, consequently, if the previous self-images are modified, the output self-image changes. This can be accomplished by inducing a refraction index variation around some selected spots within the MMI where the self-images occur. An example of this structure is shown in Figure II-10.

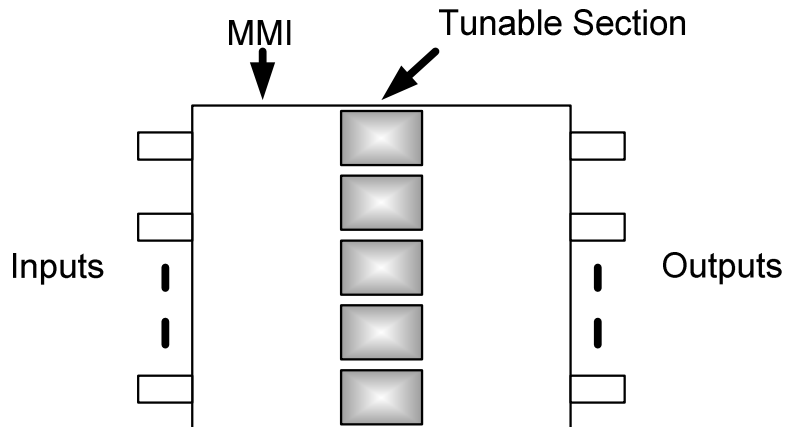


Figure II-10: MMI Coupler with Tunable Power Splitting Ratios

Other interferometric switches are based on Ring Resonators that are made of a closed circular waveguide coupled to one or more input/output waveguides (see Figure II-11). One part of the input light couples to the loop, and travels back along the ring. Light in the loop interferes with the input light, and depending on the light wavelength, constructive or destructive interference is possible.

Resonant frequencies correspond with destructive interferences, which depend on the optical delay time. The optical delay time corresponds with the time taken by light when it is propagated along the loop. Thus, depending on the light wavelength that passes through the device, it is transmitted, or filtered if it matches up with the resonant frequency of the RR.

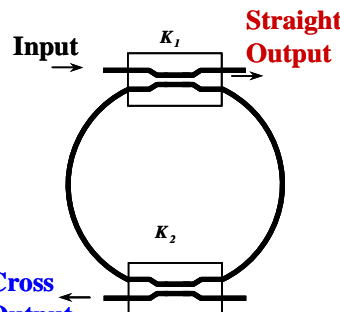


Figure II-11: Basic Structure of a Ring Resonator

Resonant frequencies of a RR can be modified by changing the optical delay time. It is done by modifying the refractive index of the loop, usually by means of the thermo-optic effect or current injection.

Other different technologies are used for carrying out the variation of the loop's refraction index: applying a voltage [Maune-2003], magneto-optic [Tanushi-2005], even by modifying the refraction index of the cladding. The inclusion of a Liquid

Crystal waveguide inside the loop for modifying its behaviour is proposed in [Vázquez-2007]. This technique is further described in Chapter V.

An all-optical switch can be implemented by applying other beam in the same wavelength range. Light is absorbed by silicon by the Two-Photon Absorption (TPA) effect, thus free carriers are created in the material. Consequently, the refraction index is changed and this modifies the resonant frequencies. This process happens in the tens of picoseconds [Almeida-2004].

On the other hand, examples of switches bases on the thermo-optic effect on material are Bubble type Switches, Thermocapillarity or Coated Microsphere Resonators.

Bubble Switches [Fouquet-1998] have been developed by Agilent. It consists on delivering light from one waveguide to a crossing waveguide in silica Planar Lightwave Circuit (PLC) using Total Internal Reflection (TIR) of the interface between a waveguide and a thermally generated bubble. Bubbles are created and sustained in an organic fluid index matched to silica PLC by heaters that are deposited on an attached silicon substrate. No bubbles are formed in the fluid when it is not heated, thus light can be transmitted along the input waveguide without any reflection. Insertion Loss near 8dB and response times about 10ms are achieved using this technology [Uebbing-2006].

Thermo-capillarity Optical Switches has the operation principle [Sakata-2001, Rivero-2008, Makihara-2000] that consists of a crossing waveguide substrate that has a groove at each crossing point with a pair of micro-heaters. The groove is partially filled with the refractive index matching liquid and it is sealed by an upper lid.

Optical switching is based on the liquid movement produced by the surface tension in the liquid caused by heating (thermo-capillarity). When the liquid is present at the crossing point, the light is transmitted through the groove. On contrast, when the liquid moves away from the crossing point, the signal is reflected to the crossing waveguide thanks to the TIR produced on the groove wall. These switches have switching time better than 50ms.

Coated Microsphere Resonators Switches [Tapalian-2002] are a special type of spherical resonator cavities. Microspheres are a three-dimensional Whispering Gallery Modes (WGM), typically 50-500 $\mu\text{m}$  in diameter, which can be fabricated by melting an optical fibre edge. The process creates a smooth surface, which contributes to low optical WGM propagation losses. The spherical curvature perpendicular to the optical path in microspheres focuses the WGMs, reduces the mode volume, and thus increases the cavity quality factor,  $Q$ .

WGMs propagate by TIR around the sphere equator, remaining confined in a thin layer beneath the surface in switches based on this technology. The WGM frequencies are sensitive to the shape and near-field environment of the microsphere. For optical switching, this sensitivity is exploited by coating the microsphere with a conjugated polymer film. The resonator mode frequencies are shift when the polymer coating film is pumped. As the pump light is absorbed by the coated microsphere, its temperature increases and the resonant frequency is modified. These switches are easy manufacture and have switching timer in the order of 100ms.

- **Electro-optic Switches**

These kind of switches perform switching by using electro-optic effects, which usually offers better response times compared with other technologies. The main technologies are based on Lithium Niobate ( $\text{LiNbO}_3$ ), Semiconductors Optical Amplifiers (SOA), Liquid Crystals (LC), Electro-holographic (EH) and Brag Gratings electronically switching.

Lithium Niobate ( $\text{LiNbO}_3$ ) switches are based on the large electro-optic coefficient of this material, its refractive index is sensible to electric fields [Krähenbül-2002, Ma-2003]. One of its applications is the 2x2 directional coupler based on interference. Its coupling ratio is modified by changing the refractive index of the material in the coupling area [Potasek-2002].

Switching time is limited by the capacitance of the electrode configuration, but times less than nanoseconds are achieved with this technology. Polarization independence is possible but higher voltage is needed, which limits the switching time. On contrast, the main drawbacks of this kind of switches are their high insertion loss and crosstalk.

Semiconductor Optical Amplifier (SOA) based switches are optical devices controlled by current [Nashimoto-2001]. These devices are used for many purposes in optical networks. SOAs can be used as optical gates that are turned OFF/ON by controlling its bias current [Sakuma-2001]. When the bias voltage is reduced, no population inversion is achieved, and the device absorbs the input signals. On the other hand, when bias voltage is present, the device amplifies the input signal. High extinction ratio is obtained thanks to the combination of amplification with absorption.

Other types of semiconductor switches are base on MZI or MMI couplers that are presented in section II-6.b. In [Ramos-2009] it is introduced an active MZI built using a combination of a MZI structure with SOAs.

Liquid Crystal (LC) switches are based on the electro-optic properties of some organic materials, which have intermediate characteristics between crystalline solids and amorphous liquids. They are anisotropic in some properties as dielectric constant or refractive index, like solids, and simultaneously they are fluids. Consequently, their optical properties can be controlled by applying voltage. The electro-optic coefficient in LC is higher than in  $\text{LiNbO}_3$ , which makes them one of the most efficient electro-optics materials.

LC switches control the polarization state of the incident light by driving voltage to the LC. The polarization change, in combination with polarization selective beam splitters allows optical space switching. An optical 3x1 multiplexer using this technique is presented in [Lallana-2006]. A more complex structure that allows the implementation of several functionalities is proposed in [Lallana-2011]. Section III.1 explains operation of some LC switches in more detail.

A special case of NLC is a polymer dispersed liquid crystal (PDLC). This type of Liquid Crystals is used for implementing Variable Optical Attenuators (VOA) [Ramanitra-2003, Chanclou-2005, Jurado-2005]. A combination of a 3x1 Optical

Multiplexer that can perform independent variable attenuation over each individual input port is proposed in [Lallana-2008]. PDLC behaviour is presented in more detail in Chapter III.

Electro-holographic (EH) switches are based on control of the reconstruction process of volume holograms by externally applying an electric field [Agranat-1999]. This technique uses a prefixed hologram stored in a LC Spatial Light Modulator (LC-SLM) for directing the input light beam to the selected output port.

The device consists of a Potassium Lithium Tantalate Niobate (KLTN) crystal in which a volume electro-holographic grating is prestored. When voltage is not driven to the crystal, the incident beam is transmitted. If an electric beam is applied to the crystal, the incoming beam incident at  $45^\circ$  to the input plane is diffracted and is emerged from the crystal at  $45^\circ$  to the output plane. In addition, lower voltage values induce that less optical power is reflected.

The structure of an electro-holographic switching matrix is shown in Figure II-12. The switches are arranged in a crossbar configuration. The WDM signal is propagated along the lower row and it is split in single wavelength channels by a set of passive filters. Each component propagates along one of the columns of the crossbar. The desired components are directed to the desired output by activating the appropriate EH switch.

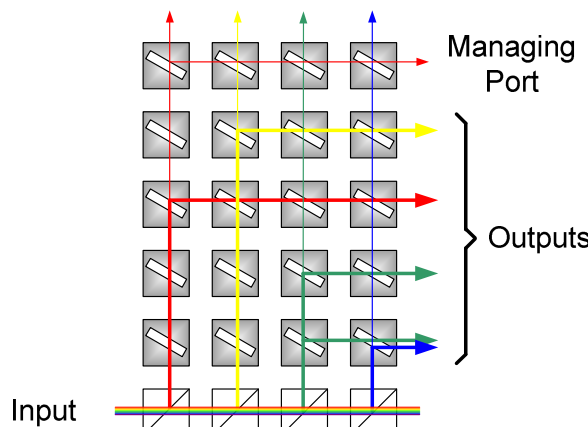


Figure II-12: Electro-holographic Switch

Multicast and any combination of the input wavelengths in an output port are possible. Besides, residual power of each channel can be used for monitoring wavelengths and dynamic power management is feasible.

A  $1 \times N$  electro-holographic switch based in an electrically addressed Spatial Light Modulator (SLM) is presented in [Fracasso-2003]. It operates at 1550nm, using Ferroelectric Liquid Crystal (FLC) modulators providing fast switching times.

Electronically switchable waveguide Bragg Gratings, which are based on holographic polymerized polymer/liquid crystal composites, are a mixture between LC and EH.

- **Acousto-optic Switches**

Acousto-optic Switches are based on the acousto-optic effect of some materials, where the refractive index of an optical medium is modulated by acoustic waves, such as the peratellurite ( $\text{TeO}_2$ ) [Sapriel-2002] or  $\text{LiNbO}_3$  [d'Alessandro-1993]. An acoustic wave or elastic wave travelling in a medium induces a periodical strain in the medium that alters the polarizability of the material and, consequently, its refractive index.

The refractive index modulation caused in the material induces a dynamic phase grating that can diffract light. If the material is isotropic, the diffraction due to acousto-optic effect results in beam deflection. In anisotropic materials, this deflection comes along with variation in light polarization.

The principle of polarization insensitive acousto-optic switch is as follows. The input signal is split in two polarized beams by means of a Polarizing Beam Splitter (PBS). These two components are directed to two parallel waveguides TE mode (S-Polarized light) goes to the lower waveguide while the TM mode (P-Polarized light) travels along the upper waveguide.

A surface acoustic wave is created and propagated in the same direction as the lightwaves. Thanks to the acousto-optic effect in the material, the equivalent of a moving grating is formed and can be phase-matched to an optical wave at the selected wavelength. A phase matched signal changes its polarization state, while a non-matched signals maintains its polarization state. Finally, the PBS placed at the end of the switch joints the obtained signals in the suitable output depending on the switch state.

Then, if the optical waves are phased matched to the acoustic wave, their polarization states are switched, in the upper waveguide a S-polarized beam is obtained and a P-polarized is gotten in the lower waveguide. The last PBS directs both polarized lights to the upper output port. On contrast, for the unmatched phase optical waves, both polarizations remains, and the light beams are guided to the lower output.

If the incoming signal is multiwavelength, it is possible to switch several different wavelengths simultaneously, as it is feasible to induce various acoustic waves in the material with distinct frequencies at the same time.

- **Opto-optical Switches**

Opto-optical switches are based on the intensity-dependent nonlinear effect in optical waveguides, such as two-photon absorption, Lightwave self action that induces the Self Phase Modulation (SPM) phenomenon and the Kerr effect that causes the Four Wave Mixing (FWM) and the Cross Phase Modulation (XPM) [Ma-2003].

There are two main types of opto-optical switches: optical fibre-based switches [Potasek-2002] and Semiconductor-based Switches. Semiconductor-based all optical waveguide are low consumption, ultrafast (less than picoseconds), high crosstalk, operating at room temperature and polarization independent.

## II.7.- Comparison between Optical Switches

Good switches should have low insertion loss, low crosstalk, and low switching voltage/consumption. Table II-1 summarizes most important parameters of the different switching technologies that are presented before.

### • **Opto-mechanical Switches**

Opto-mechanical switches are the first devices developed for optical switching. For this reason, in general, they exhibit lower switching speeds, but they are also more expanded than other technologies.

Equally than other electromechanical devices, they have high crosstalk, low insertion loss and PDL. On the other hand, their switching speeds are in the order of milliseconds and present high power consumption.

### • **Micro-Electromechanical Systems (MEMS)**

MEMS have low insertion loss, low crosstalk, are wavelength and polarization independent. They are used in large OXC that operates in backbones, but introduces more complexity in terms of controlling in the electrical part of the device, which make them less attractive for other applications as OADMs or small-scale switches.

In general, free space switches exhibit switching time near 1ms, which make them suitable for protection and restoration in the optical layer where no frequent state changes happens. Planar waveguides switches based on Silica on Silicon (SOS) have the advantage of integrated optics and the mechanical actuation, while those based on Silicon Over Insulator (SOI) have very high switching speed, on the order of 1ns.

In general, MEMS require high excitation voltages and high power consumption. They have good stability, but lower than other technologies due to the use of mobile parts. In addition, free space MEMS cannot perform the drop-and-continue function, which is important for implementing multicast capabilities.

### • **Thermo-optic Switches**

The principal advantage of this kind of switches is their polarization insensitivity and their switching speed. They have low crosstalk and relatively medium-high extinction ratio values. Nevertheless, interferometer based switches are strongly wavelength dependent. Their temperature dependence makes necessary their control for managing properly the device's operation.

### • **Electro-optic Switches**

In general, the main characteristic of the devices based in this technology is their switching speed. SOA and MMI switches have switching speeds in the order of nanoseconds, even hundreds of picoseconds. Devices based in these two technologies have also low insertion losses in comparison with switches based on LiNbO<sub>3</sub> and LC that exhibit higher insertion loss but also higher crosstalk.

Electro-optic switches are stable and reliable. These characteristics in conjunction with their switching speeds make these switches suitable for being used in Optical Packet Switching, Optical Burst Switching or Fast Demultiplex/Multiplex of Ultra High Capacity optical signal. On contrast, fastest switches present higher excitation voltages.

- **Acousto-optic Switches**

This kind of devices has good switching speeds, in the order of hundreds of nanoseconds. These switches can also operate with multiple wavelengths, which make them suitable for being used in frequency selective switches for WDM networks.

Their relatively low crosstalk and some time dependent intermodulation effects limit their use in WDM networks to 2nm wavelength spacing systems. In addition, due to their switching speeds, these switches allow the implementation of multicast, and require low power consumption. On contrast, they are very expensive.

- **Opto-optical Switches**

The main advantages of the Opto-optical switches, apart from their fast switching speeds (in the order of picoseconds), is their transparency with network protocols, bitrates and the amount of channels they can manage. In addition, they reduce their cost and their power consumption because there are not any electrical to optical conversion.

Switch	$\lambda$ (nm)	Dimensions	Cross-Talk (dB)	Insertion loss (dB)	PDL (dB)	Turn-on/ D. time	Control Voltage	Application	Cost
<b>MEMs (Free Space)</b>									
[Dobbelaere-2002] Mirror/gap-closing electrostatic actuator	1550	8 x8 16 x 16 (Up to 512 x 512)	$\leq -50$	< 1.7 $\leq 3.1$	0.25	7ms	$\leq 50V$	High Capaciy Backbone Networks or OXC	Low
[Peter-2002] Micro- optical fiber switch for a large number of interconnects using a deformable mirror	1550	1 x N	$\leq -30$	2 ~ 3	Low	Sub- millisecond	< 190V	OXC	Low
<b>MEMs (Waveguide)</b>									
[Chen-2010] MEMs Multifunction Optical Device	1550	1x2	-39	2.5	0.7	9ms	139.3V	Small scale Switch or OADM	Low
[Ollier-2002] SOI technology by LETI	1250 ~ 1650	1 x 2 1 x 8	$\leq -42$ $\leq -52$	< 1.5 $< 2$	< 0.5 $< 0.3$	1 ms	< 70V	Small scale Switch or OADM	Low
<b>Thermo-optic Switch</b>									
[Han-2009] 10-Channel Polymer Thermo-Optic Digital Optical Switch	1530 - 1560	1 x 10	< -45	1.35	0.1	5ms	50mW	ROADM	
[Mizuno-2005] MZI Thermo Óptic Switch	1450 - 1610	2 x 2	-30	1.6	0.1			For practical large- scale switch	
[Okuno-2003] Optical Switches Using Silica- based PLC Technology		1 x 128	-63	2.6		1 – 3 ms	3.5W	Medium scale matrix	
[Sakata-2001] Thermo- capillarity optical Switch	1500 - 1600	16 x 16 N x N	-59 $\leq -30$	5.6 4 (shorter path) - 10 (longer path)			13W 0.15W (2 x 2)	Large scale matrix	Promising Commercialization

Switch	$\lambda$ (nm)	Dimensions	Cross-Talk (dB)	Insertion loss (dB)	PDL (dB)	Turn-on/ D. time	Control Voltage	Application	Cost
[Tapalian-2002] Thermo-optical switch using coated microsphere resonators	1500	1 x 2	Very High $Q > 10^8$	Exceptionally Low	Low	100ms	405 nm Laser ( $10^4$ mW/cm $^2$ )	Promising for ultradense WDM channel networks	
[Uebbing-2006] Heat and Fluid Flow in an Optical Switch Bubble	1260-1360 1480-1580	---	-55	8.5	0.2	10ms	25dBm	Large scale matrix	Low
<b>Electro-optic Switch</b>									
[Krähenbühl-2002] Ti : LiNbO <sub>3</sub> DOS	1520 - 1570	1 x 2	> 45	4	Independent	5ns	18V	Moderated sized switch matrix switch	Low
[Nashimoto-2001] PLZ DOS	Good	1 x 2 1 x 8	$\leq -22$ $\leq -40$	5	Independent	20ns	10V	Small scale switch or OADM	Low
[Gallep-2002] SOA-based switch		1 x 4 1 x 8	$\leq -12$	0	< 1	200ps	200mA	Small scale switch or OADM	Not Commercialized
[Zheng-2011] Polymer on silicon MZI based Electro-Optic Switch	1550	2x2	-30	6.7			1.375V	Small scale switch or OADM	
<b>Electro-Optic Based on Liquid Crystals</b>									
[Riza-1998a] EH Optical Switch (1x2)	1300 and 1500	1 x 2 (Up to 240 x 240)	Avoided by Management and Monitoring	0.5 per switch operation	Very Low	< 10ns	300W (240 x240)	OXC	Not disclosed
[Lallana-2006] Optical Multiplexer based on LC	650-850	3x1	-24	4		5 – 20ms	3Vrms	Protection	



Switch	$\lambda$ (nm)	Dimensions	Cross-Talk (dB)	Insertion loss (dB)	PDL (dB)	Turn-on/ D. time	Control Voltage	Application	Cost
[Yang-2008a] NLC Bidirectional 2x2 Switch	808 FLC	2x2	-36.22	2.5		60.6μs 35 μs	±15 ±5V		
[Lallana-2011] Advanced Multifunctional Optical Switch	532-850	2 x (3x1)	-15	~15		~10 - 100ms	5Vrms	Protection and Restoration	
[Chanciou-2005] Optical Fibered VOA Using Phase Shifting PDLC	1550	1 x 1	-34	<1	0.18		20Vrms	VOA	
[Lallana-2008] Multiplexer and VOA based on PDLC	530-650	3x1	-31	1.6		2.6 – 12.4ms	20Vrms	VOA	
[Fracasso-2003] EH LC Wavelength Selective Optical Switch	1550	1 x 14	-33	10	0.6	~10μs			
[Domash-1997] Electronically Switchable waveguide Bragg gratings switch	1400 - 1600	2 x 2	-32 (ER)	< 1	Very Low	10 ~ 15ns	50mW	OADM	Potentially Low
<b>Acousto-Optic Switch</b>									
[Quintard-2009] 2x2 Acousto-Optic Optical Switch	1550	2 x 2	-50	17	0.5	200 ns	200mW	Wavelength selective switch	Vey high
<b>Opto-Optical Switch</b>									
[Porzi-2010] All-Optical Low Power 2x2 Cross/ Bar Switch with SOA	1540	2x2	-18	2.3			(Optical Control) 3dBm	OXC	

Table II-1: Comparison between Different Switching Technologies.



# **Chapter III**

## **Switches Based on Liquid Crystals**

---

*In this chapter, the description of switches based on Liquid Crystal and some novel devices are presented.*

*An introduction about switches based on Liquid Crystal and the basic structure for optical switches is described. The principle of operation of Nematic Liquid Crystal cells and Polymer Dispersed Liquid Cristal technology is also presented.*

*Polarization management switching using liquid crystal is described and 3x1 Multiplexer based on polarization management is proposed. Implementation and characterization of the device are given in last part of the section.*

*The structure of an optical multiplexer and Variable Optical Attenuation based on Polymer Dispersed Liquid Crystal is given in the last part of this chapter. Implementation and characterization of the device are also presented.*



### III.1.- Introduction to Liquid Crystal Switches

Some basics aspects about switches based on Liquid Crystal are reported in this section [Li-2010]. In last decades, a large amount of applications used Liquid Crystals (LCs), most of them related to displays. LCs are organic compounds that possess characteristics intermediates between crystalline solids and amorphous liquids. They are anisotropic in some properties as: dielectric constant or refractive index, like solids, and simultaneously they are fluids. For this reason, their optical properties can be controlled by means of low electric fields.

Due to the LCs nature, they are filled into cells in order to implement LC based devices. Cell structure is shown in Figure III-1. A cell consists of a thin layer of material sandwiched between two glass substrates. The thickness of the LC layer is kept uniform by using small spacers made of plastic microspheres or glass fibre. Transparent electrodes, usually Indium Tin Oxide (ITO), are placed inside the substrates in order to apply an electric field to the LC molecules and controlling light transmission through the LC cell. Rubbed alignment films are needed to force the LC molecular orientation on the substrates [Takatoh-2005].

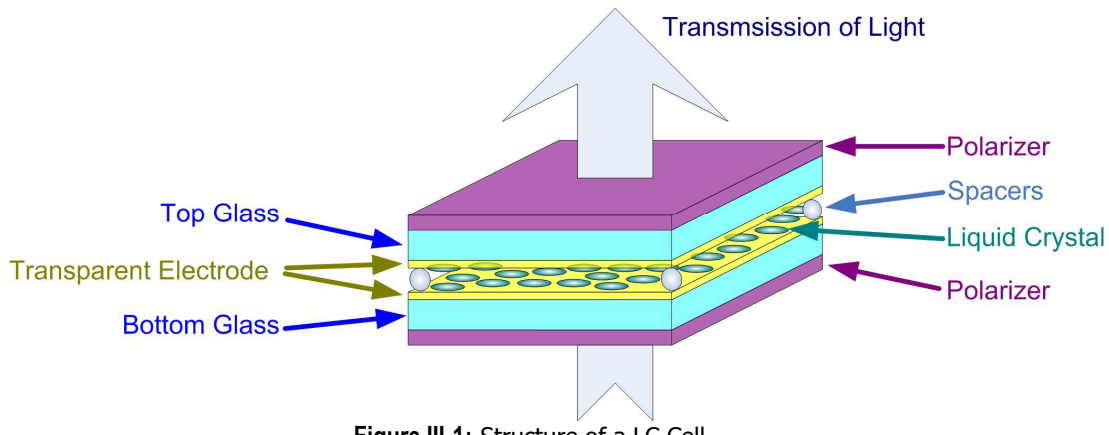


Figure III-1: Structure of a LC Cell

#### III.1.a.- Basic Liquid Crystal Structures for Optical Switches

In last years, LC cells are being used in optical switching in telecommunications networks [Hardy-1999, Cornwell-2000]. Different structures based on LCs have been proposed in literature: twisted Nematic (TN) cells, Surface Stabilized Ferroelectric Liquid Crystals (SSFLC) or LC Spatial Light Modulators (SLM). The first ones are described in section III-2.

SSFLC cells are the most widely used devices based on FLC. In these devices, the FLC layer between both glass substrates is very thin, 1 or 2  $\mu\text{m}$ , thus the natural helical structure is unwrapped [Clark-1980]. In this kind of cells, the bistable bookshelf layer is the molecular orientation most used, in order to prevent the natural helix formation, it is necessary to stabilize the macroscopic spontaneous polarization vector by the surface.

The electro-optic effect is a rotation on the smectic cone driven by coupling between the polarization and the electric field. When a voltage is applied, the molecular orientation changes and the device remains in the same state until an opposite voltage is driven, thus, this structure has memory effect or bistability.

When a SSLC device is placed between crossed polarisers, with one of them parallel to the molecular axis of one of the two stable states, a very low transmission is obtained for one of these states. Optical transmission for the other state is optimum for a given wavelength, and decreases abruptly for others. Response times of a few microseconds can be achieved with low switching voltages and low power consumption.

A LC-SLM is a device that modulates in one or two dimensions an optical beam in amplitude, phase or polarization, using the birefringence properties of the LC. Most of the LC-SLMs are driven electrically, but optically addressed analogue light valves are also proposed [Moddel-1989].

Most widespread LC-SLMs are transmissive panels that consist of a LC layer aligned between two glass substrates and make use of the Thin Film Transistor (TFT) technology for controlling the voltage applied to each pixel. Such displays are used for laptop computers, Televisions...

More compact LC-SLMs can be obtained with Liquid Crystal On Silicon (LCOS) geometry [Underwood-1987, Lelah-2001]. The device structure is a LC layer sandwiched between a reflective silicon backplane and a transmissive counter-electrode. Very dense column/row circuits and pixel/mirror arrays can be built through a Very Large Scale Integration (VLSI) process, so very compact devices with high resolution are possible. Such devices can be used in high-definition rear-projection televisions, portable video projectors, wavefront control, adaptive optics, beam steering for tweezers [Hossak-2003], optical switching matrices or wavelength selective switches [Baxter, 2006]. In that case, it is necessary to adapt the LCOS characteristics to the optical fibre transmission constraints [Hegarty-2003].

Another optical switches based on LC are those devices built in integrated optics that use LC properties for changing their optical properties. In this sense, optical switches based on micro ring resonators and LC are presented in this work in Chapter V.

### **III.1.b.- Principle of Operation of Twisted Nematic Liquid Crystal Cells**

Nematic Liquid Crystals with positive dielectric anisotropy, for which the dielectric constant is greater in the long molecular axis than that in the other direction, are used in TN-LC cells. Homogeneous planar alignment, the LC molecular axis is parallel to the glass substrate plane, and perpendicular rubbing directions in both alignment layers are used. Therefore, the LC molecules perform a 90° twist through the thickness of the LC cell (PolRot cell). When a linearly polarized light that passes through a TN-LC cell its polarization state is modified and finally the light goes out at 90° of the incoming direction. This circumstance occurs while Mauguin condition is satisfied [Li-2010]:

$$d \cdot \Delta n >> \frac{\lambda}{2}$$

[III-1]

where  $d$  is the cell thickness,  $\Delta n$  is the LC birefringence, defined as the difference between the LC extraordinary and ordinary refractive indexes ( $n_e - n_o$ ), and  $\lambda$  is the light wavelength.

If voltage greater than the Threshold Voltage,  $V_{th}$ , is applied to the cell, LC molecules reorients. When voltage is greater enough, the LC molecules are aligned parallel to the electric field, that is, their molecular axis is perpendicular to the glass substrate plane, and the polarization rotation disappears. The voltage driven to the cell for obtaining a complete molecular reorientation is known as Switching Voltage,  $V_{sw}$ . Thus, light transmission is controlled by the voltage applied to the TN-LC cell, lower voltages induce less polarization shifts. Taking into account the TN-LC behaviour, explained before, light passing through a TN-LC cell placed between polarisers can be controlled electrically.

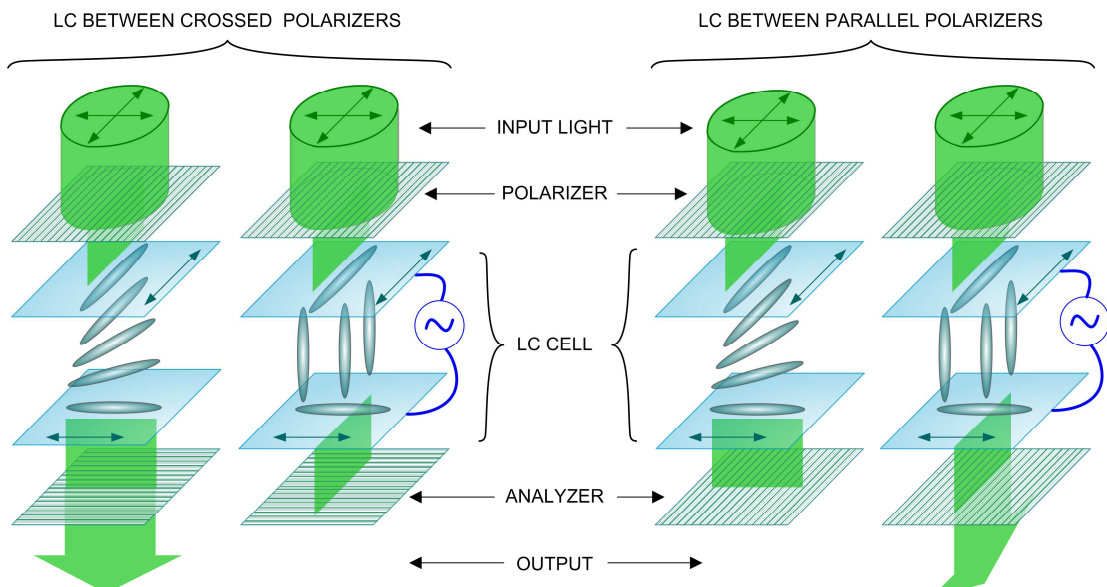


Figure III-2: Representation of a TN\_LC Cell Operation: (a) Crossed Polarizers, (b) Parallel Polarizers

In most displays applications, two crossed polarisers are placed on the outside of the glass substrates, with the transmissive axis of each polariser parallel to the rubbing direction of each alignment layer. When no voltage is applied, OFF state, the incident light is transmitted, so this operation mode is also known as Normally White (NW). In ON state, the output polariser blocks the light and the device appears dark.

On the other hand, the TN-LC cell can also be placed between parallel polarisers. In this situation, optical transmission behaves in the opposite way. In OFF state, light is blocked by the output polariser and the device appears dark, while in ON state light can pass through the device.

### III.1.c.- Optical Switching Based on Polarization Management

The polarization rotation (PolRot) is the first configuration used in LC switches [Wagner-1980] because the basic principles were widely used in the TN-LC displays for years. This switch is based on the change of polarization state of the incident light as result of applying an electric field over the TN-LC cell.

A combination of TN-LC with spatial polarization selective calcite crystals or Polarization Beam Splitters (PBS) allows optical space switching. Other optional elements in this kind of switches are: mirrors, half wave plates, quarter wave plates, half angle prisms, right-angle prisms, beam displacement prisms, total internal reflection prisms, birefringent crystals. Most of these devices are based on free space optics bulk elements, using lenses for coupling light in optical fibres.

A simple example of a TN-LC switch based on polarization management is the 1x2 LC switch structure shown in Figure III-3. A PBS, a polariser and a TN-LC cell composed the switch. The principle of operation described in [MacAdams-1990; Vázquez-2003], depending on the voltage applied to the cell, the input light is guided to output port 2 or 3.

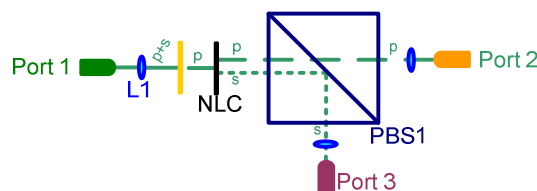


Figure III-3: Structure of the 1x2 LC Optical Switch

In this device, 50% (3dB) of the incoming light power is filtered in the input polariser. Losses reduction is possible if the optical switch can manage over the two polarizations.

In order to make the device polarization insensitive and to minimize losses, the polarization diversity method is used; by treating each polarization mode in parallel. The input signal is decomposed into its TE (S-Polarized light) and TM (P-Polarized light) components, which are managed separately and recombined at the switch output. It is also important that the optical paths followed by each polarized light when passes through the device are as similar as possible in order to reduce Polarization Dependence Losses (PDL) (see Figure III-4).

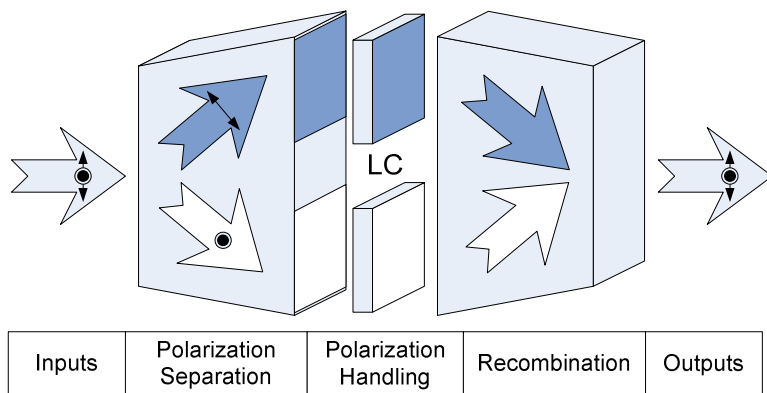


Figure III-4: Block Diagram of Generic Polarization Management LC Switch

Different configurations based on the principles described above have been proposed in literature for implementing optical switches. Most of them are based on free space optics bulk elements and only a few of them use fibre-optics devices [Sumriddetchkajorn -2000].

Better response times are obtained with FLC cells, near 35 $\mu$ s [Riza-1999; Yang-2008a], while TN-LC cells exhibit higher response times, tens of milliseconds. A reduced response time can be obtained using TN-LC and the Transient Nematic Effect (TNE), 60 $\mu$ s is reported in [Yang-2008b].

On the other hand, TN-LC cells can operate in a wider wavelength range because its cell thickness at first of second minimum can be optimised for a multiband operation fulfilling Mauguin's regime in order to obtain the polarization switch. On contrast, the FLC thickness,  $d$ , determines the wavelength in which the polarization shift is 90°. A TN-LC device with a uniform response in the C-band (1530-1560nm) is described in [Sumriddetchkajorn-2000]. Evolution of state of the art of polarization management switches, showing their characteristics are given in Table III-1.

Switches that use the polarization diversity method are more complex but exhibit low Insertion Losses, 1.4dB [McAdams-1990b]. In [Vázquez-2005b] a 2x2 optical switch based on TN-LC is presented. The structure, shown in Figure III-5, is polarization independent because both polarizations are guided through the device. The structure is composed by Polarizing Beam Splitters (PBS1-PBS4), TN-LC cells (NLC1-NLC4), quarter wave plates (Plate 1- Plate 4), and mirrors (Mirrors 1 – Mirror 3).

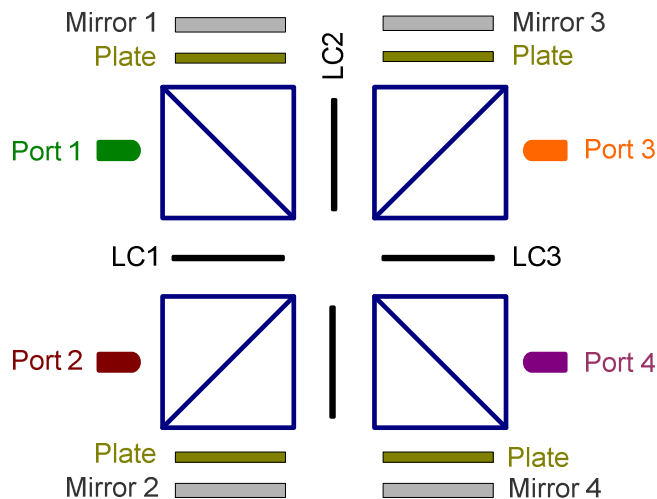


Figure III-5: 2x2 Optical Switch Structure.

<i>Contribution</i>	<i>LC cell</i>	$\lambda$ (nm)	<i>Type</i>	<i>Fibre</i>	<i>Cross Talk</i> (dB)	<i>Insertion loss</i> (dB)	<i>PDL</i> (dB)	<i>Turn-on/D. time</i>	<i>Control Voltage</i>	<i>Elements</i>
[Wagner-1980]	TN-LC	633	1X2	MM, 50 $\mu$ m	-20	0.4 <sup>1</sup>			2.5V	2PBS, 2AP, 1LLC
[Soref-1981]	TN-LC	632.8	<u>1</u> 2X2	MM	-27 (29.1)	2.5		50/150ms	5V	4PBS 2LLC, 7 AP
[Soref-1982]	TN-LC	633	2x2	No Fibre	-32	3			6V	2 LC 2 HWP 3 Calcites
[McAdams-1990a]	NLC - FLC		2x2		-20	1.4		250 $\mu$ s	15Vrms	2 NLC pasivso, 2 SS-FLC, 2 M, 4 HIEP
[McAdams-1990b]	FLC	633	1x4		21.6	3.5		50 $\mu$ s		4 FLC, 4 PBS
[Grimes-1991]	FLC	820 (670)	6X6	POF +MM 62,5		11.1	Pol. Depend	150 $\mu$ s		6FLC, 6 GL
[Noguchi-1991]	LCLM	670	128X128	SM	-21.2 average	7.9 reduced loss				PBS, Patterns BRs
[Fujii-1993]	TN-LC	1300	2X2 1X2	SM	-43.3 -37	2.2	0.2 dB			2 PBS, 2 AP, 5 LC, 2 BR
[Sakano-1995]	LCLM	670	256x256		-17	13.8				LCLM 1 QWP, 1M
[Riza-1998a]	FLC	1300	2x2	SM	-34.13	6.94	0.5	35.3 $\mu$ s		4PBS, 2M, 4LC,2AP, 2HWP,2QWP, 1LB
[Noguchi-1998]	NLC-SLM	1550	64x64		-25.9	9.47	0.21			2x2 switch based
[Riza-1999]	FLC	1550	2x2	SM	-40	6.76 [1.8 structure loss]	Pol. Depend.	35.3 $\mu$ s		1PBS,2LC, 2P,1M,1HWP, 1QWP,1AP
[Sumriddetchkajorn-2000]	Fiber Loop Mirror	1550 (1540 - 1590)	2x2	SMF DSF	-31.2	2.22	0.08	ms- $\mu$ s		2 Circulators, 2x2 Coupler,2 WDM, 1 PPS

<i>Contribution</i>	<i>LC cell</i>	$\lambda$ (nm)	<i>Type</i>	<i>Fibre</i>	<i>Cross Talk</i> (dB)	<i>Insertion loss</i> (dB)	<i>PDL</i> (dB)	<i>Turn-on/D. time</i>	<i>Control Voltage</i>	<i>Elements</i>
[Cao-2002]		1550			-19.32	2.1		0.8ms		
[Vázquez-2003]	TN-LC	650-850	1x2	POF	-22	7		ms	8V	1PBS, 1LC, 1P
[Riza-2005]	TN-LC				-20 Sim.	2 Sim				2FO-Circulator 2 PBS, 2 LC, 2 TIR, 2 BDP
[Vázquez-2005b]	TN-LC		2x2 (+1)	POF	-30	5		ms		4 PBS, 4 LC, 4 M, 4 QWP, 4 L
[Lallana-2006]	TN-LC	650-850	3x1	POF	-24	4		5 - 20ms	3Vrms	2 PBS, 6 LC, 1 P, 1+3 L
[Yang-2008a]	NLC FLC	808	2x2		-36.22	2.5		60.6μs 35 μs	±15transient ±5V hold	4 PBS, 2 HWP, 4 QWP, 4 M
[Yang-2008b]	---	---	---	---	---	---		---	---	9 PBS, 12 PSLM, 6 QWP, 6 M
[Lallana-2011]	TN-LC	532-850	2x(3x1)	POF	-15	~15		~10- ~100ms	5Vrms	3 PBS, 6 LC, 2+6 L

<sup>1</sup>neglecting reflections, expected up to 1.2dB with MM fibres and GRIN-rod lenses

**Table III-1:** Evolution of State of the Art and Performance of RotPol LC Switches.

AP:	right-Angle Prism	LB:	Leakage Block	PMF:	Polarization Maintaining Fibre
BDP:	Beam Displacing Prism	LCLM:	Liquid Crystal Light Modulators	PPS:	Programmable Phase Shifter
BR:	Birrefringent Crystal	LLC:	Large LC cells	QWP:	Quarter Wave Plate
FLC:	Ferroelectric Liquid Crystal	M:	Mirror	SM:	SingleMode
GL:	GRIN Lens	MM:	MultiMode	TIR:	Total Internal Reflection Prism
HWP:	Half Wave Plate	NLC:	Nematic Liquid Crystal	TN-LC:	Twist Nematic Liquid Crystal
HIEP:	High Index Equilateral Prism	P:	Polarizer	SS-FLC:	Surface Stabilized Ferroelectric
L:	Lens	PBS:	Polarizing Beam Splitter	Liquid Crystal	

Optical switching is obtained by applying voltage to the suitable pair of TN-LC cells, thus three operation modes (shown in Figure III-6) are possible:

- Direct Mode: NLC2 and NLC4 ON; Port 1 → Port 3 & Port 2 → Port 4.
- Crossed Mode: No voltage is applied; Port 1 → Port 4 & Port 2 → Port 3.
- Closed Mode: NLC1 and NLC3 ON; Port 1 → Port 2 & Port 3 → Port 4.

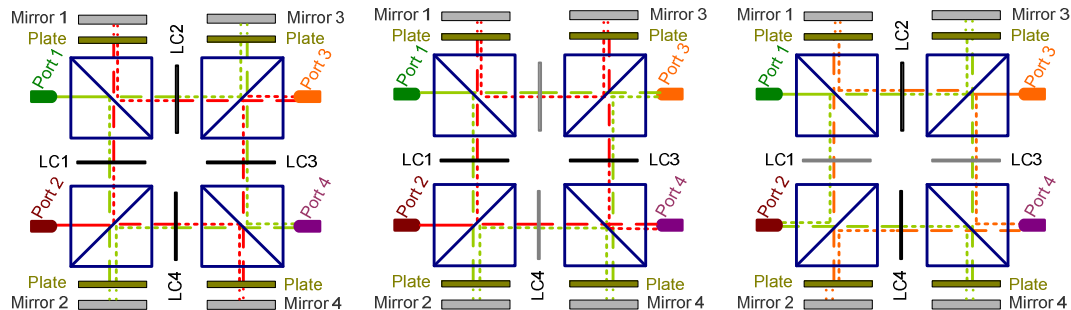


Figure III-6: 2x2 Operation Modes: (a) Crossed, (b) Direct, (c) Closed.

When a TN-LC is activated, grey coloured in the figure, and polarization state passes through the cell. On the other hand, when a TN-LC is inactive, white in the figure, the polarization state of light is rotated.

### III.1.d.- Switches Based on Polymer Dispersed Liquid Crystal Cells

The Polymer Dispersed Liquid Crystal (PDLC) consists of a polymer matrix with lots of LC droplets distributed along the polymer matrix. The Nematic LC is uniformly aligned inside each droplet, but the nematic directors of each droplet is randomly aligned and polarization independent and differs from one droplet to others. The PDLC mixture is sandwiched between two transparent substrates with electrodes onto their surfaces [Pena-2003]. The structure of a PDLC is shown in Figure III-7.

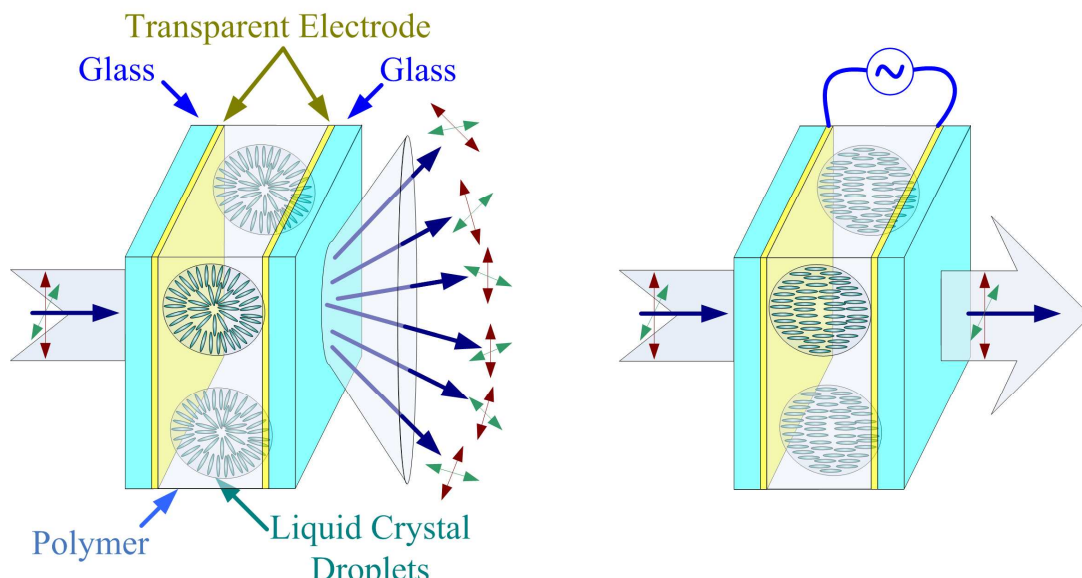
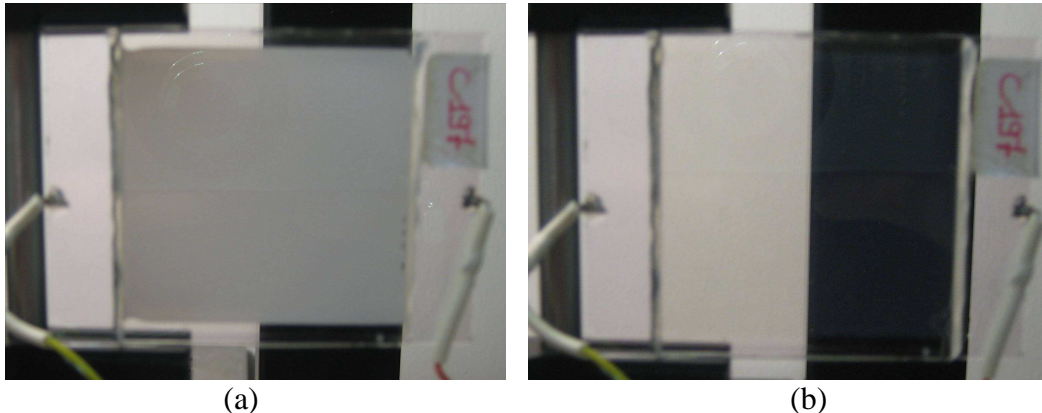


Figure III-7: Internal Structure of a PDLC cell.

Without voltage, the structure strongly scatters light. In this case, the PDLC cell appears white (see Figure III-8 (a)). When voltage is applied, the nematic molecules align parallel to the electric field, and the structure becomes transparent because the refractive index of the polymer is close to the ordinary LC refractive index,  $n_o$  (see Figure III-8 (b)).



**Figure III-8:** Picture of the PDLC in Two Possible States, Opaque (a), Transparent (b)

No polarizers are required for this opaque/transparent switching. Therefore, transmission in the transparent state can be very high, allowing its use in optical switches. Electrically controllable intermediate transmission levels are available as well [Pena2002].

The contrast adaption to wavelength is performed by adjusting the LC droplet size by next equation:

$$\Delta n \cdot a / \lambda = 0.3 \quad [\text{III-2}]$$

where  $a$  is the droplet radius,  $\lambda$  the light wavelength and  $\Delta n$  corresponds to the LC birefringence, as it is defined in section III.1.b [Bosc-1996]. During the UV polymerisation of the monomer, a higher power leads to smaller radius droplets.

PDLC has been mainly reported in the implementation of Variable Optical Attenuators (VOA) [Chanciou-2003, Chanciou-2005, Du-2004, Hirabayashi-2001, Ramanitra-2003, Zubia-2002]. A VOA is a device with one input and one output that can modify its transmission reducing the optical power at its output. Most of these structures operate at 1500nm. An optical VOA based on a 2x2 coupler implemented with POF and PDLC [Zubia-2002] operates at 650nm.

Some of these devices are used for adjusting the optical power that reach to the reception stage in optical networks for equalization of signals travelling different light paths. As an example, optical fibre amplifiers have different amplification levels for each wavelength. This situation complicates reception in WDM networks. VOA can be used for equalizing the optical power in the receivers, adjusting the losses for each wavelength.

There are other different ways to implement a VOA [Adamopoulos-2004, Losert-2004]. Some of them are based on MEMs technology [Lee-2004, Syms-2004]. An interesting VOA, with response times in the millisecond order, small size and based

on transparent electro-optics ceramics is proposed in [Jiang-]. A PDLC is used for refracting a polarized beam for guiding it towards a delay line [Riza-1998b, Madamopoulos-1998]

### III.2.- 3x1 Optical Multiplexer Based on Polarization Management

From the operation of a TN-LC, a 2x2 optical switch based on polarization management has been described in section III.1.c. In this point, a novel structure of a 3x1 optical multiplexer based on TN-LC is presented.

The proposed scheme of the 3x1 optical multiplexer (MUX) can manage both polarizations by using the polarization diversity method, so the structure is more complex but fewer losses are anticipated because both light polarizations are managed. In addition, low voltage, low power consumption and wide operation wavelength range are expected thanks to the use of TN-LC cells for the device implementation.

This structure is suitable for being used in POF and GI-POF networks. POF are being used in a growing amount of applications because, in short distances, they offer high bandwidth at low cost. In-home or automobile applications are some of the niches where they are being used.

Few control elements have been developed for these networks, so, it could be interesting to propose optical switches for being used in POF and GI-POF networks in order to give more flexibility to these networks. Multiplexers allow the implementation of Wavelength Division Multiplexing (WDM) over a transmission fibre because they can combine different wavelengths in a single fibre. Different information from diverse sources can be transmitted using distinct wavelengths. Due to the light transmission through optical fibres, the information is maintained when is propagated.

POF networks operate in the visible wavelengths region (450nm, 550nm and 650nm), while GI-POF offer low attenuation from the visible range until 1300nm. The scheme of the multiplexer presented in this section can be used in several wavelength ranges; it only depends on the bulk elements that form the device. The implementation of the multiplexer has been optimized for operating in the visible wavelength range.

In this section, it is first described the MUX structure and operation. The characterization of the implemented optical multiplexer is presented after. Finally, an overview about control electronic and software developed for controlling the multiplexer using a computer is introduced.

### III.2.a.- Device Structure

The device structure is shown in Figure III-9. PBSs, TN-LC cells, polarisers and lenses compose the MUX. There are three input ports, P-1, P-2 and P-3 and a single output port P-4. The device's ports can be made of both, POF and GI-POF.

The input PBS, *PBS1*, splits the incoming light from each input port in two orthogonal independent linear polarized beams. TN-LC cells with three pixels handle each obtained ray. Switching is obtained by applying voltage to the proper TN-LC pixels.

A PBS, *PBS2* and polarisers *P-p*, are placed after each TN-LC for acting like analysers.

Finally, the output lens focuses light in the output port. Additionally, in each input port is placed a lens in order to collimate light from the fibre.

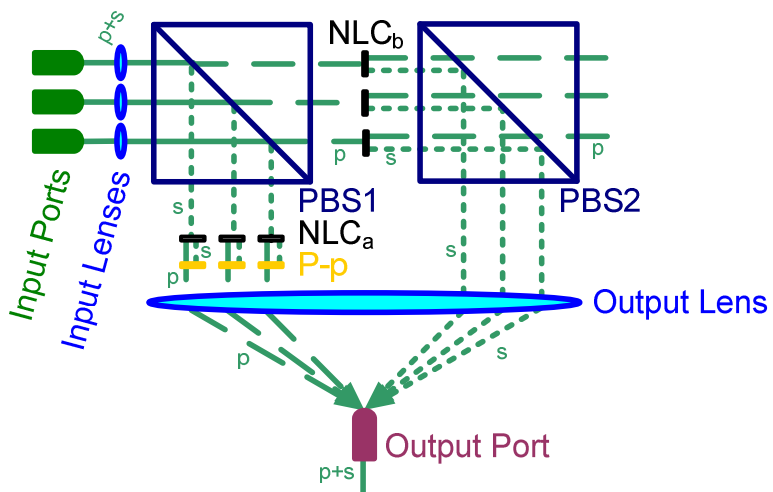


Figure III-9: Structure of the 3x1 Multiplexer based on Polarization Management.

### III.2.b.- Device Operation

For each input port, there are two possible configurable states, *OFF* and *ON*. In *ON* state, no voltage is applied to the TN-LC cell, the light from the input port is guided to the *Output Port*. Light beam from the input ports is split by *PBS1* in two orthogonal polarized beams, P-Polarized light is transmitted while S-Polarized light is reflected at 45°.

The polarized beam that passes through the PBS is shifted by the TN-LC named *NLC<sub>b</sub>* and the resulting ray, that is S-Polarized, is reflected at 45° by *PBS2* towards the output lens. On the other hand, the polarized beam that is reflected by *PBS1* is modified by *NLC<sub>a</sub>*. The obtained P-Polarized beam is transmitted through the *P-p* polariser towards the output lens. Both rays are focused in the output port thanks to the *Output Lens*.

In *OFF* state, the TN-LC are switched by applying voltage to them, the light of the input port are not guided to the *Output Port*. As it has been described before, the input light is split by *PBS1*, P-Polarized beam is transmitted while S-Polarized is reflected a 45°. In one optical path, the transmitted beam passes through *NLC<sub>b</sub>* remaining P-Polarized. The obtained P-Polarized beam is also transmitted by *PBS2*. On the other optical route, the S-Polarized beam that has been reflected by *PBS1* passes through *NLC<sub>a</sub>* maintaining its polarization state. The resulting S-Polarized ray is filtered by the “P-p” polariser. As a result, any beam from the input port can be focused in the output port.

Each pixel of the TN-LC cell can be switched independently of the others, so the proposed multiplexer is reconfigurable. The same signal should be applied to the suitable pair of pixels in order to perform the switching.

### III.2.c.- Optical Characterization

Two different types of characterization have been carried out: static and dynamic. Only measurements at one wavelength have been done. A description of the set up used in both types of characterizations and the different measurements performed are presented in next sub-sections.

- Set up

Figure III-10 shows the experimental set up used for doing the measurements. Each port has been measured independently of the other in order to avoid interchannel noise.

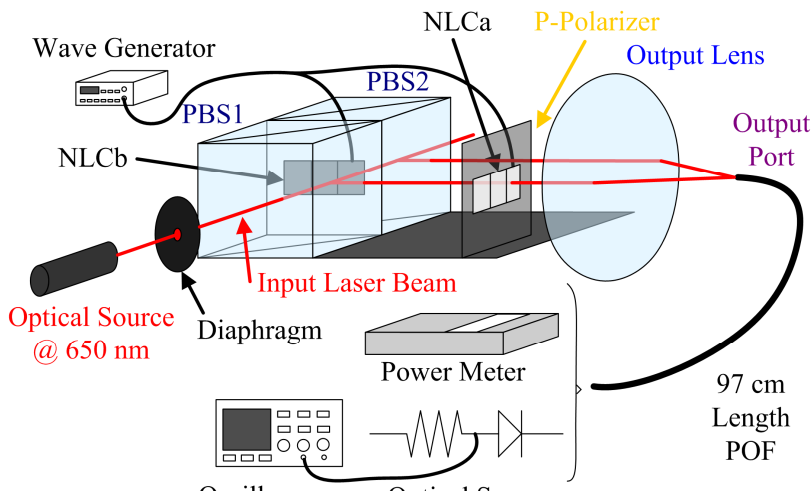


Figure III-10: Set up Used for the Optical Characterization.

The proposed device has been implemented with PBS from Melles Griot 03 PBB 013, the TN-LC cells have been fabricated in the *CLIQ Group of the Universidad Politécnica de Madrid* and a 50mm lens is used as *Output Lens*. A visible laser diode at 650nm (620nm – 680nm) and 5.0mW from Power Technology Inc. has been used as optical source. An iris diaphragm has been used at the laser’s output for limiting the beam’s spot and avoiding light propagation outside of the TN-LC pixel. No input

lenses have been used because the used laser diode includes the collimation optics. A 97 cm length POF connects multiplexer's output with the measure instrument.

Two different measurements systems have been utilized depending on the characterization type. A 557B Rifocs commercial optical power meter has been employed for the static measurements, while an Infineon SFH 350V phototransistor with a  $100\Omega$  and a Tektronix digital oscilloscope has been used for the dynamic characterization.

### • Static Measurements

This section refers to the measurements made when the excitation of the liquid crystal is maintained during a long period. An 8kHz frequency square which amplitude was modified from 0V to 4V, has been applied to the pair of liquid crystal cells that form an optical path. In this way, switching voltage of the TN-LC cells, insertion losses and crosstalk, as it is defined in section II.2.b., can be obtained. A 557B Rifocs commercial optical power meter has been employed for making measurements.

The transmission obtained for the three ports is shown in Figure III-11. The three curves have a similar behaviour, input ports are *ON* from 0V to  $1V_{rms}$ , and they can be considered as *OFF* for amplitudes higher than  $3V_{rms}$ .

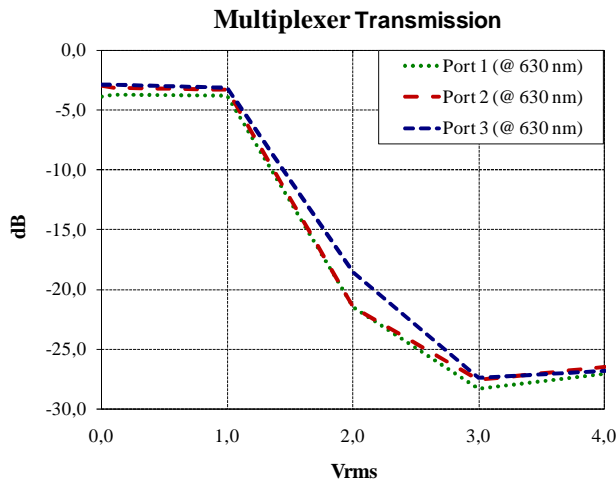


Figure III-11: Transmission of the Multiplexer's for each Input Port.

Maximum transmission is obtained for low voltages. When voltage driven to the TN-LC is increased, LC molecules start to reorient and the polarization state of the incident linear polarized light is rotated less than  $90^\circ$ , thus more light power is transmitted in PBS2 and filtered by the *P-p* polariser, so less light can reach to the *Output Port*.

The measured optical power after the diaphragm is  $-6.9\text{dBm}$ . Insertion losses of the multiplexer have been less than  $4\text{dB}$ , Extinction Ratio, as it is defined in section II.5, is more than  $23\text{dB}$ . Table III-2 summarises losses and isolation obtained for each port.

Port	Insertion (dB)	Crosstalk (dB)
P1	3.9	23.2
P2	3.0	23.5
P3	2.9	23.9

Table III-2: Transmission of the Multiplexer's for each Input Port.

### • Dynamic Measurements

This section refers to measurements made when the excitation of the liquid crystal is switched on/off repeatedly. An 8kHz frequency and 3V amplitude square wave have been driven during 50ms, multiplexer *OFF* state, and 0V have been applied for other 50ms, in other words, a square envelope of 10Hz is used for modulating the 8kHz square wave. The described wave has been applied to the proper pair of pixels that form each optical path. An Infineon SFH 350V phototransistor with a  $100\Omega$  and a Tektronix digital oscilloscope has been used for the dynamic characterization.

A capture of the oscilloscope is shown in Figure III-12. The upper part of the picture displays the excitation signal applied to the TN-LC pixels, while the transmission of the multiplexer's *Input Port 2* is shown in the lower section.

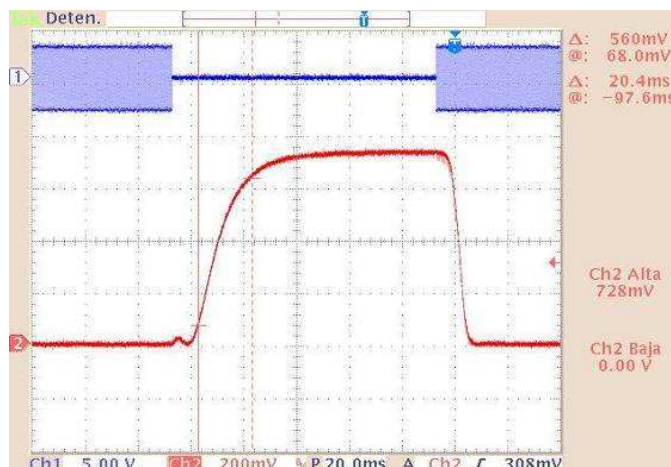


Figure III-12: Excitation Wave Driven to the TN-LC and the Multiplexer Response.

According to section III.2.b, each input of the multiplexer is *OFF* when voltage is applied to the TN-LC, while the input is *ON* when no voltage is applied. Thus, the multiplexer switching from *OFF* to *ON* states is shown in the left part of the figure. The voltage applied to the TN-LC cells is stopped, so this transition corresponds to the LC relaxation time. Rising time,  $t_{rise}$ , about 20.4ms has been obtained, in addition, a delay in switching on the multiplexer,  $t_{on}$ , defined as the time interval since the voltage is switched off until optical path is active, have been less than 30.5ms.

Multiplexer switching from *ON* to *OFF* states is presented in the right part of the picture. Fall time,  $t_{fall}$ , about 5.2ms have been obtained, and the delay in switching off the multiplexer,  $t_{off}$ , defined as the time interval since the voltage is applied until the optical path is inactive have been near 12ms.

Same excitation has been applied to the three ports of the multiplexer and similar measurements have been obtained. The results can be observed in Figure III-13. These measurements are in accordance with liquid crystal properties, because it is common that relaxation times are greater than molecular orientation times.

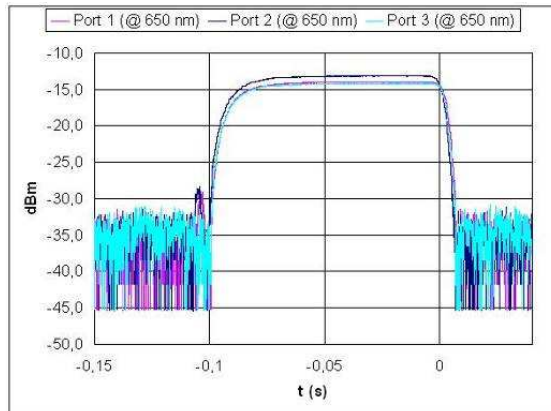


Figure III-13: Multiplexer Response for the Three Input Ports.

A summary of the obtained characterization for the three inputs of the multiplexer is shown in Table III-3.

Port	$t_{on}$ (ms)	$t_{rise}$ (ms)	$t_{off}$ (ms)	$t_{fall}$ (ms)
P1	29.2	20.0	12.0	5.2
P2	30.4	20.4	12.0	4.8
P3	28.8	14.8	10.8	4.8

Table III-3: Response Times of the 3x1 Multiplexer.

The novel structure proposed for the optical 3x1 multiplexer is based on polarization management. The device has been implemented with TN-LC cells that are able of working in a wide wavelength range, and need low excitation voltages and have low consumption.

The device has been characterized. Insertion losses less than 4dB and crosstalk better than 23 dB at 650nm have been measured. In addition, 30ms and 15ms setup and rise times have been obtained.

### III.2.d.- Multiplexer Control Using a Computer

Additional control electronic and software has been implemented for controlling multiplexer state using a computer. Six output signals are generated for exciting TN-LC cells. A serial communication is provided for modifying the multiplexer state remotely. Additional feedback information is possible thanks to four optical sensors. In this way, if a 10/90 optical coupler is used in each port of the multiplexer, their optical power can be measured, and proper operation of the multiplexer could be checked.

Figure III.14 shows the block diagram of the entire multiplexer. The designed electronic is divided in three different stages: digital control, analogue adaptation and

feedback stages. Digital stage is the principal part of the design and generates the signals needed for controlling the rest of the system. Analogue adapt stage modifies signals voltage for the TN-LC cell requirements. Feedback stage converts optical power coming from each multiplexer port to digital values, serving as entries for the digital part.

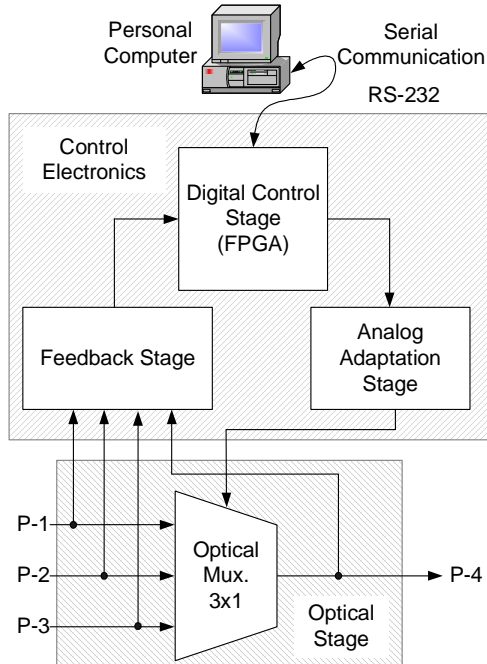


Figure III-14: Block Diagram of the 3x1 Multiplexer.

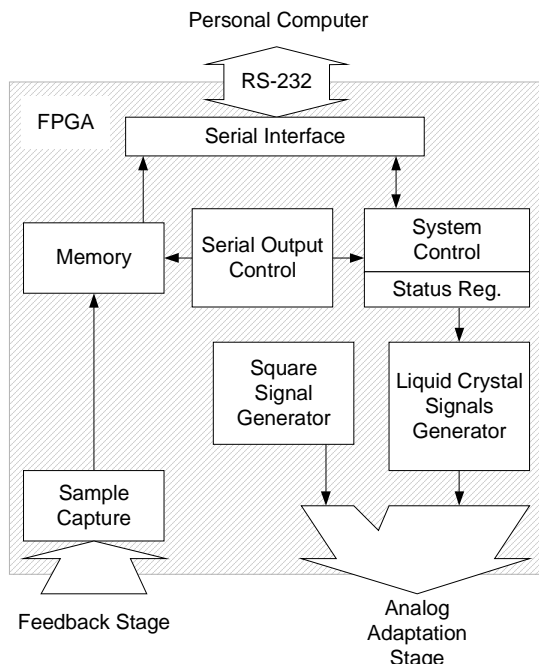


Figure III-15: Block Diagram of the Digital Stage.

Digital part is implemented in a programmable integrated circuit, a FPGA (Field Programmable Gate Array) [Cañas-2006]. In these devices, a hardware description of the electronics is programmed, multiple configurations are allowed, thus, the improving and debugging of the designs is easy.

Scheme of the digital stage is shown in Figure III.15. The state register stores the multiplexer operation mode. An 8kHz square wave is generated by the square wave generator and six different signals are used for controlling TN-LC cells. Not excitation is applied to those cells that belong to an active input port, *ON* state of the multiplexer, while the square wave is applied to the liquid crystals that form an inactive multiplexer input, *OFF* state.

Analogue adapt stage is in charge of applying 8kHz square wave to the corresponding TN-LC cells depending on the output provided by the digital part. A voltage conversion is carried out; in this way, the continuous component of the square wave is eliminated, because it could damage the TN-LC cell, and its amplitude is adjusted to the adequate value for exciting the cells. 3 Volts amplitude is enough for the switching of the used TN-LC cells, but the implemented design allows modifying this value.

In the feedback stage, a four channel, parallel, analogue to digital converter transforms the optical sensor measurements in a digital eight bits bus. Digital stage continuously request samples to the converter and stores them in an inner memory.

Control of the multiplexer is done by means of a computer using RS-232 serial communication. A serial interface and an additional serial output control are available for allowing data transfer. A subsequent electronics adapt voltage values to the protocol specifications. By this way, multiplexer operation mode can be switched and the user can ask for the optical power measurements and check the proper operation of the device.

In this way, an application has been programmed for allowing the control of the multiplexer using a computer. Users can select which input ports are active or inactive. Due to the device's implementation, there are no restrictions about how many optical paths are active at the same time; even the three ports can be active at the same time.

The program is sending and requesting information continuously to the device. In this way, every modification of the configuration can be sent and checked immediately. Additionally, the user can select which optical measurements are displayed in the program window.

### III.3.- Multiplexer and Variable Optical Attenuator Based on Polymer Disperse Liquid Crystal Cells

Other novel structure for implementing an optical multiplexer is the one described below. The proposed scheme is based on Polymer Disperse Liquid Crystal (PDLC) cell. It is the active element of the switch and controls with the voltage applied to it light transmission through the device. This configuration is simpler than the one proposed in section III.2., but higher voltages are needed for switching PDLC cells.

The proposed multiplexer is also designed for being used in POF and GI-POF networks, so, same considerations previously reported about the wavelength operation range has to be taken into account.

As it is introduced in section III.1.d, PDLC has been reported in the implementation of Variable Optical Attenuators (VOA) [Chanclou-2003, Chanclou-2005, Du-2004, Hirabayashi-2001, Ramanitra-2003, Zubia-2002]. A VOA is a device with one input and one output that can modify its transmission reducing the optical power at its output. Most of these structures operate at 1500nm. An optical VOA based on a 2x2 coupler implemented with POF and PDLC [Zubia-2002] operates at 650nm.

There are other different ways to implement a VOA [Adamopoulos-2004, Losert-2004]. Some of them are based on MEMs technology [Lee-2004, Syms-2004]. An interesting VOA, with response times in the millisecond order, small size and based on transparent electro-optics ceramics is proposed in [Jiang-]. A PDLC is used for refracting a polarized beam for guiding it towards a delay line [Riza-1998b, Madamopoulos-1998]

VOAs are used for adjusting the optical power that reach to the reception stage in optical networks for equalization of signals travelling different light paths. As an example, optical fibre amplifiers have different amplification levels for each

wavelength. This situation complicates reception in WDM networks. VOA can be used for equalizing the optical power in the receivers, adjusting the losses for each wavelength.

In addition, variable light transmission is achieved with PDLCs, thus, the novel proposed design acts as a combination of a Multiplexer and a Variable Optical Attenuator (VOA). An Nx1 Multiplexer is a system capable of joining N optical inputs in a single output. On the other hand, a VOA is a device with one input and one output that can modify its transmission reducing the optical power at its output.

The VOA-Nx1 Multiplexer (VMUX) is capable of attenuating each input port independently of the others, even switching it off, and combining the resulting light into a single output fibre.

In this section, the description of the structure and operation is first detailed, while the characterization of the implemented optical multiplexer is presented at the end.

### III.3.a.- Device Structure

The structure of the proposed switch is composed by a PDLC cell with as many pixels as input ports, each pixel controls light coming from each input port, and a single lens for focusing all the inputs in the output port. Collimation lenses are provided in order to collimate light that comes from each optical fibre. The proposed structure is shown in Figure III-16.

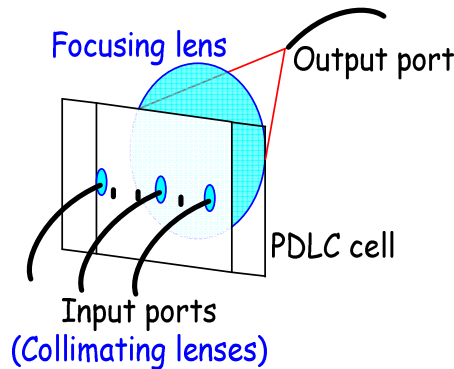


Figure III-16: Schematic of the Proposed VMUX.

PDLC are polarization independent, they do not need polarisers neither PBS for optical switching, like occurs with TN-LC, for this reason, fewer elements are needed and less insertion losses are expected. Furthermore, it is supposed that PDL will be also smaller.

In addition, the structure is fully reconfigurable, their input ports are wavelength independent and they work in the same way for all the wavelengths and independently of the other inputs. For this reason, apart of WDM over a fibre, it can also implement Time Division Multiplexing (TDM), even a mixture of both. Furthermore, variable attenuation of each input port is available.

### III.3.b.- Device Operation

As mentioned in section III.1.d., PDLC consists of a matrix of polymer material where microdroplets with molecules of nematic liquid crystal are dispersed. Droplets radius is comparable to the incident light wavelength. This mixture is sandwiched between transparent substrates covered with a transparent conductor that allows applying an electric field to the mixture.

In *OFF* state, when no voltage is applied to the PDLC cell, the LC molecules are uniformly aligned inside each droplet, but the nematic director of each droplet is randomly aligned and differs from the others. In this scenario, the structure presents an inhomogeneous refraction index than causes to the incoming light to be strongly scattered. The output rays are not parallel to the incoming light and the beam is not transmitted. Figure III-7 (a) shows the diffusing state.

In *ON* state, when a voltage is applied to the electrodes that cover the PDLC cell, LC molecules are aligned parallel to the electric field, that is, the molecular axis is perpendicular to the substrate plane. Thus, the nematic directors of all the droplets are parallel. In this situation, the polymer matrix and the microdroplets exhibit almost the same refraction index in the light propagation direction, because the polymer matrix is designed for having the ordinary LC refraction index. This causes the input light optical beams passes parallel and are transmitted through the cell. PDLC clear state is shown in Figure III-7 (b).

The output lens is capable of focusing all the parallel rays that are transmitted into the output port.

In summary, the PDLC can act as optical switch, light can pass through the device when an AC voltage is applied to the cell, and incoming light is not able to pass through the PDLC when no voltage is applied. Intermediate voltages can allow its behavior as a VOA. Furthermore, a PDLC with as many pixels as multiplexer inputs can be used as the switching element of the VMUX.

### III.3.c.- Optical Characterization

Switching voltage, insertion losses, isolation and response times, as defined in section II.2.b, are measured for several positions of the optical sources at two different wavelengths: 530nm and 650nm. There are two types of tests : static and dynamic measurements. The first one corresponds to the PDLC transmission characterization when its excitation is maintained during a long period. The second group of measurements evaluates PDLC response times when it switched. A description of the set up used in both types of characterizations is presented in next point.

- **Set up**

A diagram of the set up used for characterizing the VMUX is shown in Figure III-17. The device have been formed by the PDLC sample, composed by a mixture that uses 80% by weight of TL205 LC with 20% of PN393 monomer (from Merck), a 40mm diameter focusing lens and the output fibre (200cm length POF). PDLC transmission

has been measured for several positions of the optical sources respect to the center of the focusing lens, “ $r$ ”, in order to check the PDLC capability for being used as VMUX. For all the situations the optical sources have been placed close to the PDLC sample,  $d < 1\text{mm}$ .

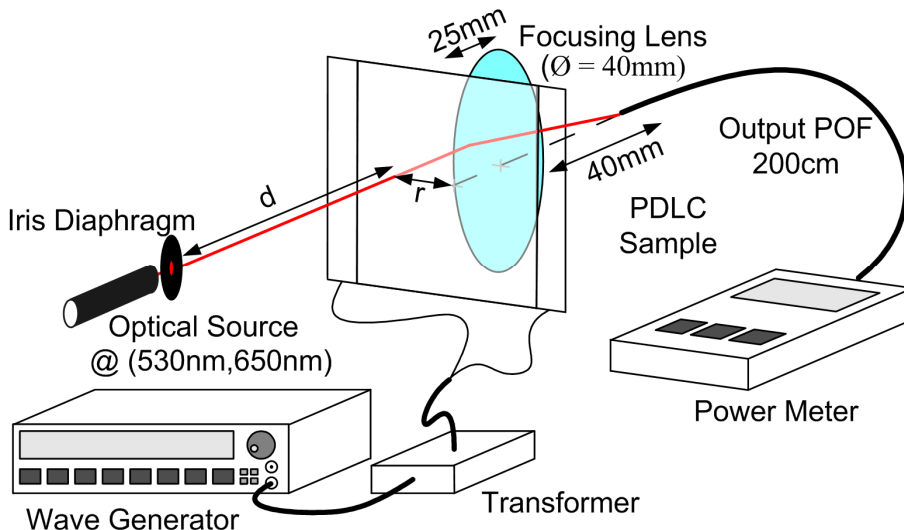


Figure III-17: Experimental Set Up Used for the VMUX Characterization.

Two visible laser diodes: one at 532nm and 0.99mW from Hero and the other at 650nm and 5mW from Power Technology Inc have been used in the test. An iris diaphragm has limited the laser beam spot. A Hewlett Packard wave generator has been employed for generating PDLC excitation. Different measurement systems have been employed for static and dynamic characterization.

- **Static Measurements**

This section refers to the measurements done when the excitation of the liquid crystal cells is maintained during a long period. PDLC transmission has been measured for different amplitudes of a 50Hz sinusoidal wave. A 2.4:1 transformer has been utilized for adapting voltage level drove to the PDLC sample. In this way, the switching voltage, insertion losses and attenuation could be determined. A 557B Rifocs commercial optical power meter has been employed for making measurements.

PDLC response at both wavelengths, when the optical source has been placed in front of the centre of the focusing lens,  $r = 0$ , and when the optical source has been placed in one side,  $r = 15\text{mm}$  from the centre of the lens, is shown in Figure III-18.

Complete switching has been obtained for drive voltages of 20Vrms in all the situations. Insertion losses have been less than 1.6dB at 532nm and 1dB at 650nm. Crosstalk, as defined in section II.5.b, have been near 39.5dB at 532nm and 31dB at 650nm. Gray scales have been achieved approximately from 10Vrms to 20Vrms, transmission can be configured modifying the voltage applied to the PDLC. Despite that not significant attenuation differences versus “ $r$ ” have been obtained when 650nm laser have been used, PDLC responses have been a bit different at 532nm.

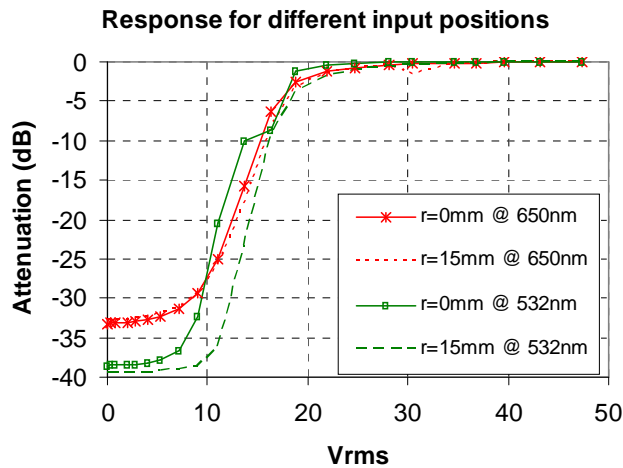


Figure III-18: PDLC Response for Different Input Port Positions at two Wavelengths.

Figure III-19 shows the VMUX states when the 650nm wavelength optical source is used. *OFF* state is shown in Figure III-19 (a) and *ON* state is presented in Figure III-19 (a). In Figure III-20, the VMUX states when the 532nm wavelength optical source is used are illustrated. *OFF* state is shown in Figure III-20 (a) and *ON* state is presented in Figure III-20 (a).

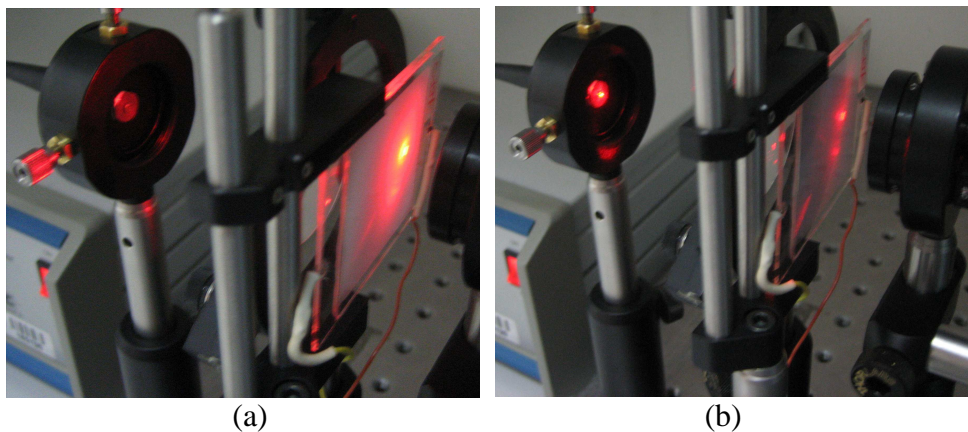


Figure III-19 Pictures of the VMUX in two States: *OFF*(a) and *ON*(b) at 650nm.

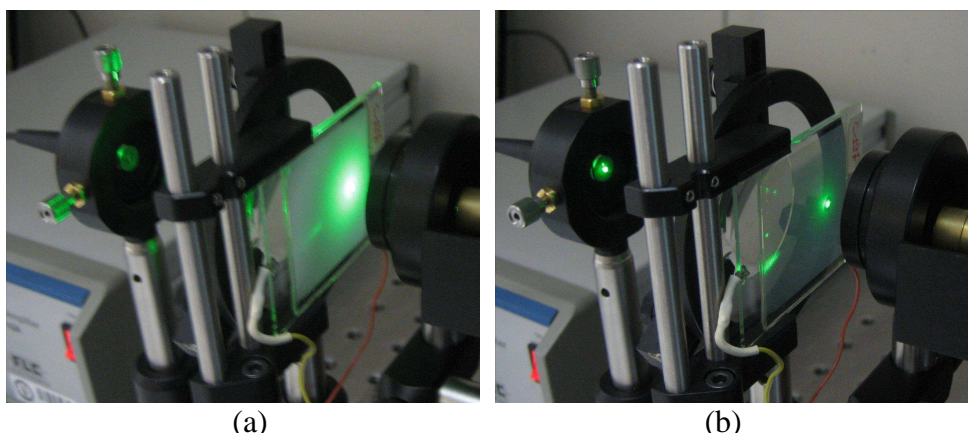
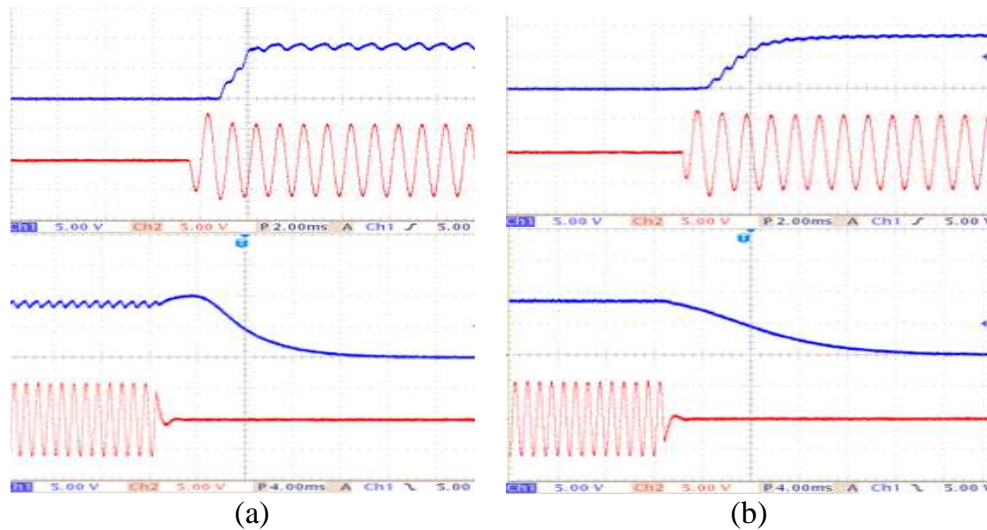


Figure III-20: Pictures of the VMUX in Two States: *OFF*(a) and *ON*(b) at 532nm

- **Dynamic Measurements**

This section refers to measurements when the PDLC is switching on/off repeatedly. A digital Tektronix oscilloscope and a SFH 350V photodiode with a resistor compose the main elements of the setup used to determine PDLC response times. Two sets of measurements have been done. In the first one, a 2.4:1 transformer have been used to drive voltage to the PDLC, whereas in the second group of tests, a x10 wide bandwidth amplifier from FLC Electronics has been utilized.

Figure III-21 shows PDLC response times for the first set of measurements. In this case, due to the transformer limitations, a 1kHz sinusoidal wave have been applied to the cell. A 40Vrms, 1kHz sinusoidal wave has been applied for 0.5s and 0V has been drove to the PDLC during 0.5s, in other words, an envelope of 1Hz has been used for modulating the 40Vrms, 1kHz sinusoidal wave. In both figures, a 10 factor has to be applied to the measurements done with channel 2 (PDLC driving voltage) due to the probe was in x10 position. Figure III-21 (a) describes PDLC response at 532nm, the rise time is in the upper part of the figure and decay time is in the lower section. Excitation signal is depicted below the obtained transmission response. Figure III-21 (b) represents the same situation when the 650nm optical source is used.



**Figure III-21:** PDLC Response when 1kHz Sinusoidal Wave is Applied at 532nm (a) and 650nm (b).

Figure III-22 shows PDLC response times for the second set of measurements when a x10 wide bandwidth amplifier has been used. A 1kHz square wave has been applied to the sample in order to keep the same conditions than the previous measurements. These figures maintain similar layout than the previous ones, upper part of each illustration represents rise time at the corresponding wavelength, whereas lower section represents decay time. In this case, the excitation signal is shown over the PDLC response. Figure III-22 (a) represents PDLC response at 532nm, rise time can be observed in the upper part of the figure and decay time can be seen in the lower section. Figure III-22 (b) represents the same situation when the 650nm optical source is used.

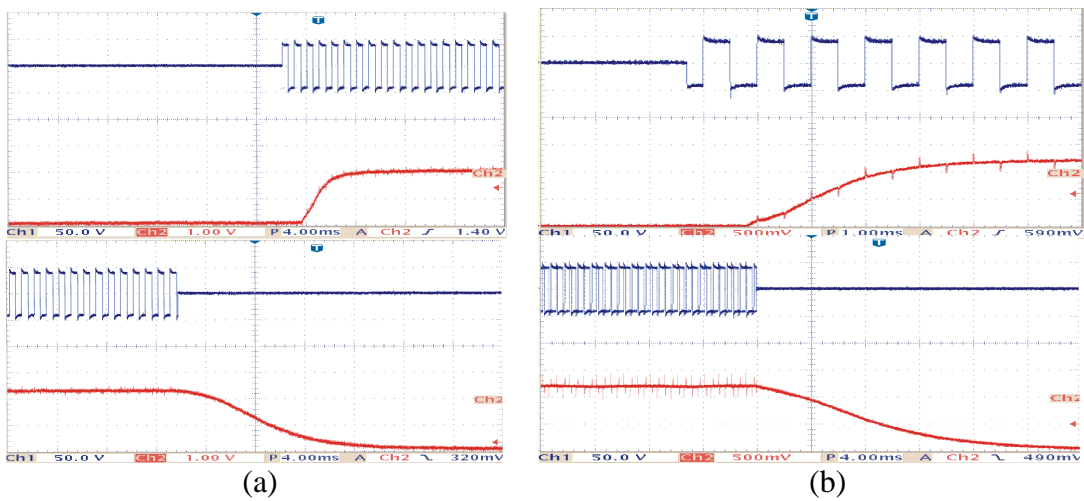


Figure III-22: PDLC Response when 1kHz Square Wave is Applied at 532nm (a) and 650nm (b)

For both wavelengths, there are similar results in the two set of characterizations. Rise time less than 2.6ms and decay time better than 12.4ms have been measured. Difference between rise and decay times is in concordance with nematic liquid crystal properties where it is known that relaxation times are greater than excitation times.

A ripple in the PDLC transmission can be observed mainly when a 1kHz sinusoidal have been applied. It seems that the PDLC is able to follow excitation. Ripple have been less for square wave voltages; it can be suppressed by using a higher frequency (typically 100 kHz).

The novel structure proposed for the VMUX, VOA and multiplexer, is formed by a PDLC cell and a lens that focuses the transmitted light in the output port. The device is projected for being used in POF and GI-POF networks.

VMUX used a PDLC cell without any pixel. The input has been placed in different positions of the PDLC cell in order to check the device operation.

The scheme has been characterized, both static and dynamically. Complete switching has been obtained for drive voltages of 20Vrms in all the situations. Insertion losses have been less than 1.6dB at 532nm and 1dB at 650nm. Extinction Ratio, see section II.5, has been near 39.5dB at 532nm and 31dB at 650nm. Gray scales have been achieved approximately from 10Vrms to 20Vrms.

Related to dynamic characterization, the PDLC cells have worked better when a 1kHz frequency square wave has been applied. In this case, rise time less than 2.6ms and decay time better than 12.4ms have been measured.

### III.4.- Summary and Conclusions

In this chapter, an overview about switches based on LC cells has been presented. The study has been focused in two kinds of switches, those based on polarization management with TN-LC cells and those based on PDLC cells.

Two novel structures for implementing a multiplexer have been proposed. Both structures are planned for operating in POF and GI-POF networks.

A polarization independent 3x1 Multiplexer implemented with TN-LC has been measured at a single wavelength. Insertion losses less than 4dB and crosstalk better than 23 dB at 650nm have been measured. In addition, 30ms and 15ms setup and rise times have been obtained.

The structure of an optical multiplexer and VOA (VMUX) based on PDLC have been proposed in the last part of this chapter. A PDLC cell without any pixel has been used in the implementation. The input has been placed in different positions of the PDLC cell in order to check the device operation.

Static and dynamic characterization have been carried out. Complete switching has been obtained for drive voltages of 20Vrms in all the situations. Insertion losses have been less than 1.6dB at 532nm and 1dB at 650nm. Attenuation, relationship between the situations when transmission is high and low, has been near 39.5dB at 532nm and 31dB at 650nm. Grey scale have been achieved approximately from 10Vrms to 20Vrms. Rise time less than 2.6ms and decay time better than 12.4ms have been measured when a 1kHz frequency square wave has been applied.

## **Chapter IV**

# **Advanced Multifunctional Optical Switch Based on Liquid Crystals**

---

*In this chapter, an Advanced Multifunctional Optical Switch based on Liquid Crystals is presented.*

*The proposed structure can work as 3x1 Optical Multiplexer/Combiner, dual 3x1 Optical Multiplexer/Combiner, 2x2 Optical Switch, Variable Optical Attenuator or Variable Optical Power Splitter. A single device can have all these functionalities without any hardware modification, only by selecting the proper ports of the device.*

*The structure of the proposed switch is in the first section. In the second part, switch operation is explained. The third part of this chapter describes the functionalities that the proposed device can do.*

*This switch has been implemented and characterized. The results obtained for the device are presented in last section.*



#### IV.1.- Introduction

The device proposed in section III.3 is a multiplexer based on Polymer Dispersed Liquid Crystal (PDLC) capable of performing variable attenuation over each individual input port. That is, it groups two functions in the same device, so fewer components are required in the optical network and low losses are induced.

It is important to have low losses and reconfiguration can be an additional feature in optical networks, especially in passive optical network where there is not additional amplification. Ideal combiners made up of cascading 2x2 directional couplers have high insertion losses, of at least 6 dB for a three input/one output port device. Reconfigurable optical networks in critical applications demand devices able to have different functionalities [Chen-2008, Vazquez-2008], including switching.

As already reported, it is useful the integration of different functionalities in the same device, in this way cost and losses reductions can be achieved. There have been several integrating proposals: a compact optical cross-connect add-drop switch based on NLC [Patel-1995], a scalable holographic optical switch based on FLC [Crossland-2000], a smart value-added module, or a tap coupler, that allows different tap ratios [Riza-2007], or an integration of an optical switch with optical splitting and attenuating functions [Chen-2008] with a non-liquid crystal technology. Most of the proposals given above operate in the 1550nm wavelength range with a maximum bandwidth of 60nm; usually integrate just 2 functionalities and are not suitable for being used in broadband POF networks.

#### IV.2.- Structure of the Switch

In Chapter III an introduction about LC switches are given, focusing in two different technologies based on LC. In one hand, a 3x1 multiplexer based on TN-LC and polarization management is introduced in section III.2. On the other hand, an optical multiplexer and VOA, VMUX, implemented with PDLC cells is presented in section III.3.

In this chapter, an improvement of the 3x1 multiplexer structure is proposed. It is also based on polarization management, whose operation principles are described in section III.1.c. The new structure has analogue characteristics to the previous one, so, low voltage, low power consumption and wide operation wavelength range are expected.

The optical scheme of the new Advanced Multifunctional Optical Switch (AMOS) is shown in Figure IV-1. The *P-p* polariser, placed after the TN-LC named *NLC<sub>a</sub>* in the the 3x1 multiplexer scheme, (see Figure III.9) is substituted by a PBS, *PBS<sub>2</sub>*, in order to make use of the remaining optical power that is not guided to the original output port, *Output Port 1*. An additional lens, *Output Lens 2*, is placed perpendicularly to the existent one, *Output Lens 1*, for focusing the obtained light in the additional port, *Output Port 2*.

The added output makes the structure more flexible, because different functionalities can be performed using the same structure, by only selecting the proper ports for each function.

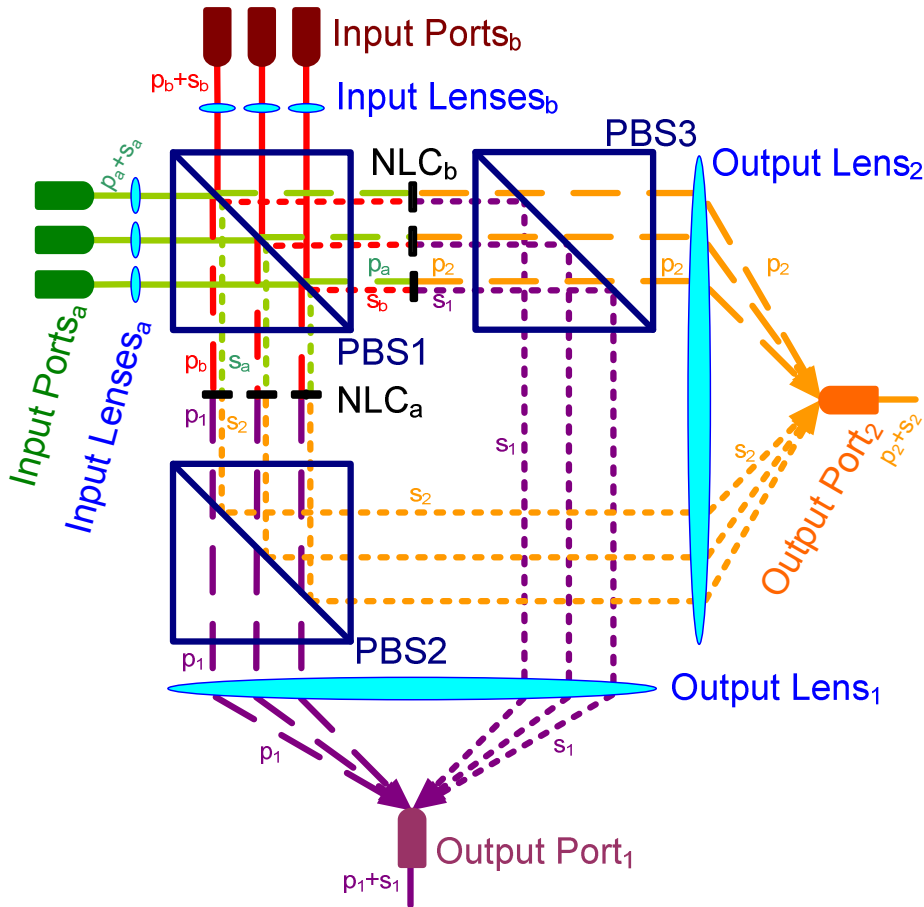


**Figure IV-1:** Structure of the Advanced Multifunctional Optical Switch (AMOS).  
Output and Input Port Definition

The proposed structure is also planned for being used in POF and GI-POF networks. POF networks operate in the visible wavelengths region (450nm, 550nm and 650nm), while GI-POF offer low attenuation from the visible range until 1300nm. The scheme of the multiplexer presented in this section can be used in several wavelength ranges, it only depends on the bulk elements that form the device. Different TN-LC cells have been designed and manufactured, for achieving to the required operation wavelength.

Summarizing, the novel structure proposed for the Advanced Multifunctional Optical Switch is composed by PBS, TN-LC cells and lenses. Three pairs of inputs are provided for multiplexing operation. Both, Polymer Optical Fibre (POF) and Graded-Index POF (GI-POF) can be used as input ports and output ports.

As it is commented in the 3x1 multiplexer description, the proposed device is capable of treating both linear polarizations, then, less losses are expected. The input PBS,  $PBS_1$ , splits the incoming light from each input port in two orthogonal independent linear polarized beams. P-polarized light is transmitted, while S-polarized light is reflected at  $45^\circ$ .

Each of the obtained beams is handled by one TN-LC cell. Both cells are controlled with the same square wave. Switching is obtained by applying voltage to the TN-LC cells. Two PBS,  $PBS_2$  and  $PBS_3$ , are placed after each TN-LC cell for acting like analyzers. These two PBS are similar to  $PBS_1$  and they work in the same way, S-Polarized light is reflected at  $45^\circ$ , while P-Polarized light is transmitted. The two output lenses, *Output Lens 1* and *Output Lens 2*, focus the beams in the output ports, *Output Port 1* and *Output Port 2* respectively. Additionally, in each input port is placed a lens in order to collimate light from the fibre.

#### IV.3.- Device Operation

The TN-LC cells are the active element of the proposed device. They are capable of working in a wide wavelength range. This kind of cells modifies their optical behaviour depending on the voltage applied to them, as it is explained in section III.1.b.

In *OFF* state, when no voltage is applied to the TN-LC cell, the light beam from one port of *Input Ports a* is guided to *Output Port 1* and consequently, the matched port of *Input Port b* is directed to *Output Port 2*. Figure IV-2 (a) shows the propagation when the device is in *OFF* state. Light beam from *Input Port a* is split by  $PBS_1$  in two polarized beams, P-Polarized light is transmitted while S-Polarized light is reflected at  $45^\circ$ .

On one hand, the polarized light that passes through  $PBS_1$  is shifted by the TN-LC cell named  $NLC_b$ , and the resulting ray, which is S-Polarized, is reflected  $45^\circ$  by  $PBS_3$  towards *Output Lens 1*. On the other hand, the beam that is reflected  $45^\circ$  by  $PBS_1$  is modified by  $NLC_a$ , the P-polarized ray obtained passes through  $PBS_2$  and is able to reach to *Output Lens 1*. Finally, both beams are focused in *Output Port 1* by *Output Lens 1*. Light can be coupled to the output fibre thanks to the high numerical aperture of POFs. In a similar way, *Input Port b* is guided to *Output Port 2*.

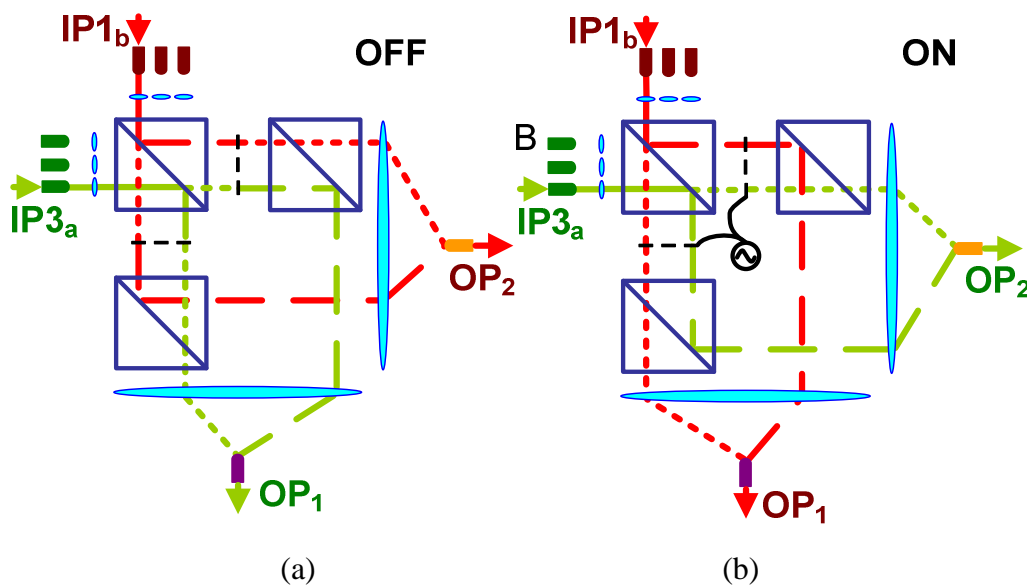


Figure IV-2: *OFF* state (a) and *ON* state (b), of the Advanced Multifunctional Optical Switch

In *ON* state, shown in Figure IV-2 (b), when the TN-LC are switched thanks to the voltage applied, the *Input Port a* is coupled to *Output Port 2* and the corresponding *Input Port b* is guided to *Output 1*. As it is commented before, the light from *Input Port a* is split by *PBS1*, P-Polarized light is transmitted while S-Polarized is reflected at 45°.

In one optical path, the beam that passes through *PBS1* passes through *NLCb* remaining P-Polarized. The obtained ray is transmitted in *PBS3* and is able to reach to *Output Lens 2*. On the other optical route, the S-Polarized beam is reflected by *PBS1*, passes through *NLCa* and is reflected at 45° by *PBS2* towards *Output Lens 2*. Finally, both beams are focused in *Output 2* by this lens. In a similar way, *Input Port b* is directed to *Output Port 1*, which is the opposite of the *OFF* state.

Each pixel of the TN-LC cell can be switched independently of the others, so the proposed device can also work as a multiplexer. An optical path can be switched by applying voltage, or not, to the suitable pair of pixels.

#### IV.4.- Functionalities

Different optical functionalities can be implemented with the same device, only by selecting the suitable device ports and using a set of electrical control signals.

- **3x1 Optical Multiplexer/Combiner (OM/OC).**

As it is stated in section III.2, by using only three inputs and one of the outputs, the device can be used as an optical 3x1 multiplexer if a different wavelength is launched in each input. On the other hand, optical power at each input can be also combined at the output port. A summary of the ports used and control signals are presented in Table IV-1 using notation from Fig.IV.1 Figure IV-3 shows the operation of the device as 3x1 multiplexer.

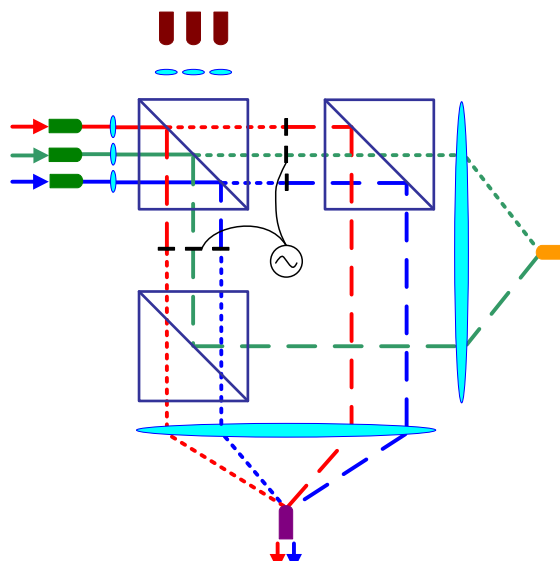


Figure IV-3: Operation as 3x1 Optical Multiplexer

Input Port	TN-LC states	Output Port	Mux State
IP1a	OFF	OP1	ON
	ON	---	OFF
IP2a	OFF	OP1	ON
	ON	---	OFF
IP3a	OFF	OP1	ON
	ON	---	OFF

**Table IV-1:** Summary of the Ports and TN-LC States for the 3x1 Multiplexer Functionality.  
OPa=Output Port a from Fig.IV.1

The device inputs are wavelength independent because they work in the same way for different wavelengths. Time Division Multiplexing (TDM) can also be implemented by means of this device, even a mixture of a TDM and a WDM, i. e, different fibres involving WDM can be temporally multiplexed into a single fibre. Any combination of each input port that carries a different wavelength: 530nm, 650nm and 850nm, is possible in the output fibre at the same time.

POF can transmit two wavelengths with relatively low losses, thus, in automobile applications two distinct services can use the same transmission media for communicating. For example, 530nm wavelength can be used for sending information related to multimedia applications, integrated webcams instead of mirrors... and 650nm wavelength can be used for interchange data related to safety systems [Chen-2008].

- **Dual 3x1 Optical Multiplexer/Combiner (DOM/DOC)**

As it is described in section IV.1, the same device can operate as two complementary 3x1 Multiplexers. Inputs to the device are grouped in pairs, when the *Input Port a* is guided to *Output Port a*, the other input of this pair, *Input Port b*, is coupled to *Output Port b*. On the other hand, when the multiplexer is switched, *Input Port a* is directed to *Output Port b* and the matched *Input Port b* is propagated to *Output Port a*.

A summary of the ports used and the control signals are presented in Table IV-2.

Input Ports	TN-LC states	Output Port 1	Output Port 2	Dual Mux State
IP1a & IP1b	OFF	IP1a	IP1b	BAR
	ON	IP1b	IP1a	CROSSED
IP2a & IP2 b	OFF	IP2a	IP1b	BAR
	ON	IP2b	IP1a	CROSSED
IP3a & IP3b	OFF	IP3a	IP1b	BAR
	ON	IP3b	IP1a	CROSSED

**Table IV-2:** Summary of the Ports and TN-LC States for the Dual 3x1 Multiplexer Functionality  
(see Fig.IV.1 for notation).

- **2x2 Optical Switch (OS)**

The proposed device can work as a 2x2 switch by using only one pair of inputs, *Input Port 2a* and *Input Port 2b*, instead of the three available in the previous

application. An overview of the device working as a 2x2 switch is illustrated in Figure IV-4.

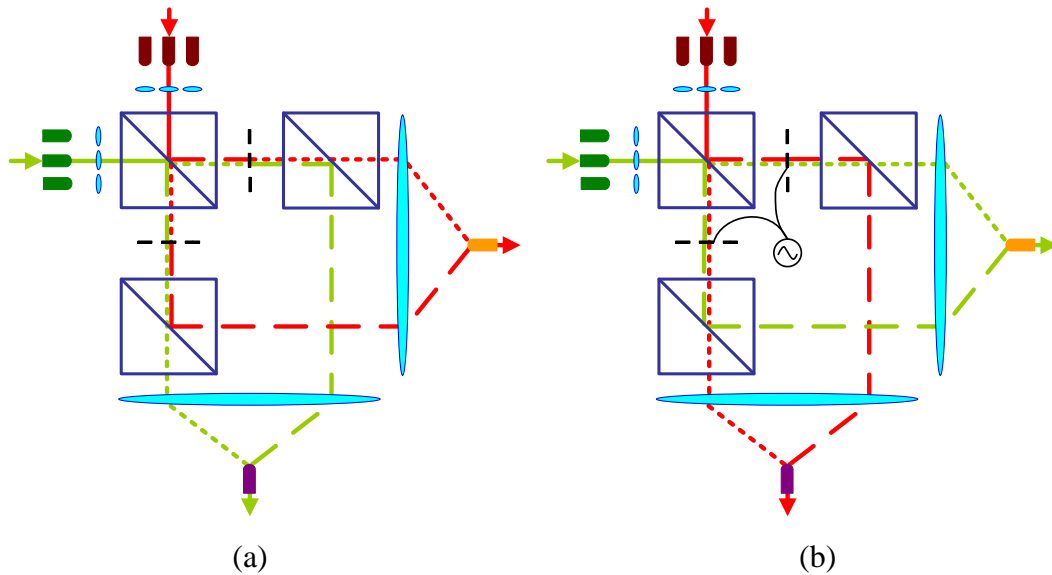


**Figure IV-4:** Overview of the Device Being Used as a 2x2 Optical Switch when it is OFF (a) and ON (b)

A summary of the ports used and control signals are presented in Table IV-3.

Input Ports	TN-LC states	Output Port a	Output Port b	2x2 Switch State
IP2 a & IP2b	OFF	$P2a$	$P2b$	CROSSED
	ON	$P2b$	$P2a$	BAR

**Table IV-3:** Summary of the Ports and TN-LC States for the 2x2 Optical Switch (see Fig.IV.1 for notation).

- **Variable Optical Attenuator (VOA)**

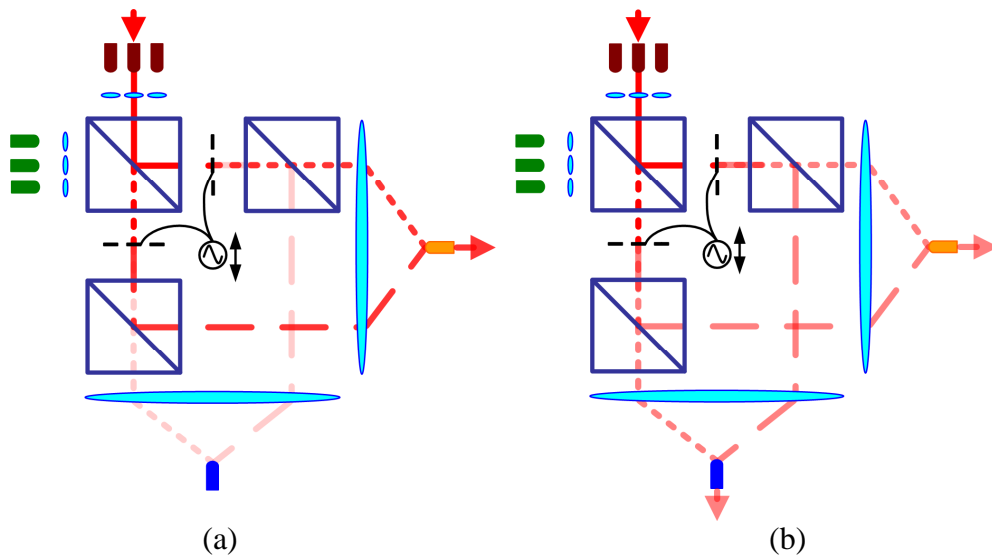


**Figure IV-5:** Overview of the Device Utilization as VOA (a), and VOPS (b).

By using only one of the input ports of the device and only one of its outputs, for any input, the proposed structure can also be used as a Variable Optical Attenuator because the TN-LC are able for achieving intermediate transmission levels, gray scale, by applying lower voltage to the cells. This situation is depicted in Figure IV-5 (a).

A summary of the ports used and control signals are presented in Table IV-4.

Input Port	TN-LC states	Output Port 2	VOA State
IP2b	Low Voltage	High Optical Power of IP2b	Transmitted
	High Voltage	Low Optical Power of IP2b	Attenuated

Table IV-4: Summary of the Ports and TN-LC States for the VOA (see Fig.IV.1 for notation)

- **Variable Optical Power Splitter (VOPS)**

In the same way, by applying different voltage levels to the liquid crystal cells, and using both outputs, as it is shown in Figure IV-5 (b), the proposed device can also operate as Variable Optical Power Splitters (VOPS) because the remaining light that is not guided to the desired output appears in the other output.

All the functionalities described above can be implemented in the same device by only selecting the proper ports without any hardware modification.

A summary of the ports used and control signals are presented in Table IV-5.

Input Port	TN-LC states	Output Port 2	Output Port b
IP2b	Low Voltage	High Optical Power of IP2ba	Low Optical Power of P2a
	High Voltage	Low Optical Power of IP2b	High Optical Power of P2a

Table IV-5: Summary of the Ports and TN-LC states for the Variable Optical Power Splitter (see Fig.IV.1 for notation).

## IV.5.- Bulk Optical Components Used in the Implementation

One of the most important properties of the Advanced Multifunction Switch is that it has to operate in a wide wavelength range. Different optical components make up the proposed optical switch, and for this reason, these components have to be able to work in the desired wavelengths. Characterization of each element has been carried out in order to determine which the most suitable ones for the device implementation are.

### **IV.5.a.- Polarizing Beam Splitters**

A comparison between different Polarizing Beam Splitters (PBS) has been carried out for obtaining their optical properties. Four types of PBS have been tested:

- Cube PBS of Melles Griot 03 PBB 003 (450nm – 650nm)
- Cube PBS of Melles Griot 03 PBB 013 (650nm – 850nm)
- Wire Grid PBS of Moxtec with antireflection coating (450nm – 650nm): PPBS202C
- Wire Grid PBS of Moxtec without antireflection coating: PPBS202A

Insertion Losses and Extinction Ratio of the PBS, as it is defined in Section II.5, for both outputs at different wavelengths are measured and results are shown in Table IV-6. Tx refers to the transmitted X-polarized optical power, while Rx denotes the reflected X-Polarized optical power.

Polarizer	Characteristics	550nm	630nm	850nm	1300nm
PBB 003	IL Tp (dB)	0.7	0.5	0.8	1.0
	ER Tp/Ts (dB)	27.1	27.2	0.6	0.1
	IL Rs (dB)	0.2	0.3	12.1	13.8
	ER Rs/Rp (dB)	24.1	18.8	26.8	1.0
PBB 013	IL Tp (dB)	1.4	0.6	0.4	0.2
	ER Tp/Ts (dB)	3.3	25.7	14.2	0.7
	IL Rs (dB)	3.65	0.2	0.2	7.4
	ER Rs/Rp (dB)	19.8	24.8	16.8	6.95
WGPPBS02A	IL Tp (dB)	1.8	0.4	1.7	0.2
	ER Tp/Ts (dB)	27.5	33.6	14.7	8.6
	IL Rs (dB)	0.7	0.1	0.6	0.8
	ER Rs/Rp (dB)	19.7	18.4	17.1	10.1
WGPPBS02C	IL Tp (dB)	1.1	0.3	1.3	0.2
	ER Tp/Ts (dB)	25.7	29.7	14.4	8.5
	IL Rs (dB)	0.4	0.15	0.6	1.1
	ER Rs/Rp (dB)	18.95	22.9	11.5	9.1

Table IV-6: Measurements of PBS Main Parameters.

Three Wire Grid (WG) PBS PBS02A from Moxtek have been used for the implementation of the advanced multifunctional optical switch because they can operate in a wider wavelength range.

From measurements (see Table IV-6), it can be seen that each PBS has low losses and high extinction ratios within specified wavelength range. As an example, PBB003 has losses from 0.5dB to 0.7dB, and ER of 27dB at 630nm and 550nm respectively. In terms of wavelength range operation, a better performance is obtained with WG PBS, having losses below 1dB and ER higher than 10dB in a 600nm wavelength range from 550 to 1300nm.

#### IV.5.b.- Twisted Nematic Liquid Crystal Cells: Design and Characterization

Special TN-LC cells were fabricated during a research stay in Telecom Bretagne, Brest (France) under supervision of Mr. B. Vinouze. Telecom Bretagne has a 100-class clean room that allows the development of the required processes involved in TN-LC cells manufacture: Glass substrate treatment and cleaning, LC cell assembly and filling using vacuum. An adjacent room has the necessary equipment for cutting glass substrates and making optical characterization.

Four different types of TN-LC cells, in order to obtain the expected wavelength range of operation; were designed and manufactured. Specifications proposed for the device are a contrast more than 20dB or 30dB for the following wavelength ranges:

- 800nm to 1300nm range.
- 400nm to 800nm range.
- 600nm to 1300nm range.

Three LC mixtures were available for the cell design. Only two of them were considered as suitable for fulfilling the parameters required:

- Ref A is a not conventional LC mixture, with a very high birefringence, as defined in section III.1.b., 0.38 at 633nm.
- Ref B is a LC mixture used in telecommunication applications, with a high birefringence, 0.224 at 633nm.
- Ref C is a LC mixture used usually in display applications, with a low birefringence, 0.105 at 633nm.

The optimization of the TN-LC has been made by using the Gooch and Tarry transmission law [Gooch-1975]. This calculation gives the transmission through the TN-LC cell when it is placed between crossed polarizers versus the LC thickness without voltage applied to the cell (see Figure IV-6).

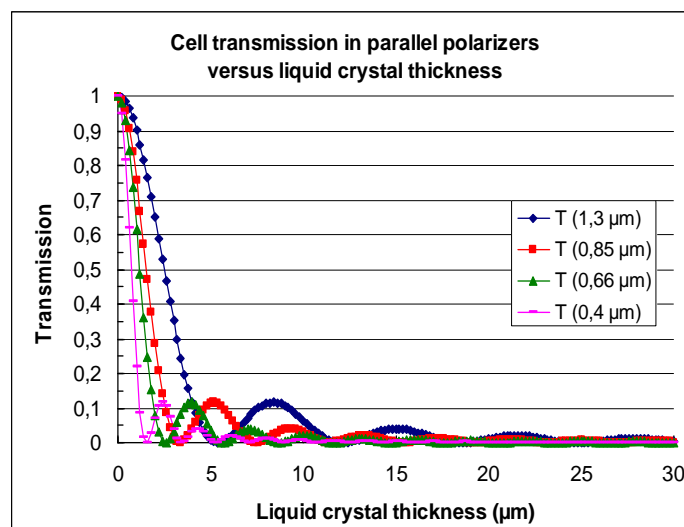
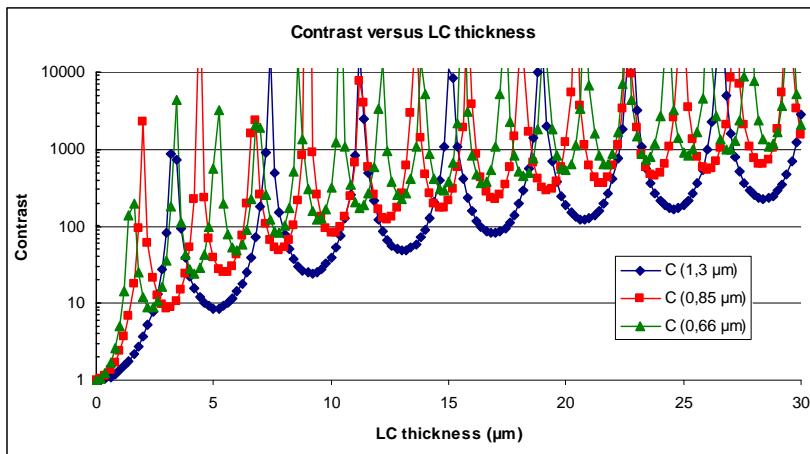


Figure IV-6: Simulation of Transmission for a TN\_LC Cell at Different Wavelengths



**Figure IV-7:** Contrast Simulation of TN\_LC Cell Filled with Mixture Ref A for 660nm, 850nm and 1300nm.

The shape of the transmission curve is a damped sinusoid whose minima depend on the cell thickness and the wavelength. Figure VI-7 shows in log scale the contrast, that is the inverse of the transmission, at different wavelengths when the TN-LC Cell is filled with mixture Ref A.

A detail of the transmission curves in the 7μm cell thickness is show in Figure IV-8.

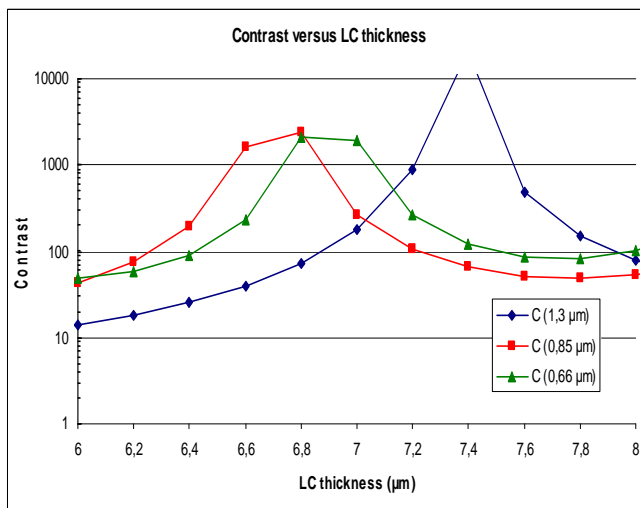


**Figure IV-8:** Detail of the Contrast Simulation of TN\_LC Cell Filled with Mixture Ref A for 660nm, 850nm and 1300nm.

Summarizing the obtained results for the simulations, the optimum cell thickness for a 20dB contrast is given in Table IV-7 while the optimum cell thickness for a 30dB contrast is presented in Table IV-8.

Wavelength Range (nm)	Optimal Thickness (μm)			Thickness Tolerance (μm)		
	Ref A	Ref B	Ref C	Ref A	Ref B	Ref C
<b>850-1300</b>	7.05	11.8	26.0	±0.3	±1.0	±2.0
<b>400-850</b>	6.8	11.2	25.3	±0.8	±1.4	±3.4
<b>660-1300</b>	7.05	11.8	26.0	±0.3	±1.0	±2.0

**Table IV-7:** TN-LC Cell Thickness for 20dB Contrast.

Wavelength Range (nm)	Optimal Thickness ( $\mu\text{m}$ )			Thickness Tolerance ( $\mu\text{m}$ )		
	Ref A	Ref B	Ref C	Ref A	Ref B	Ref C
850-1300	11.2	18.9	41.6	$\pm 1.4$	$\pm 0.1$	$\pm 0.4$
400-850	15.75	23.3	50.4	$\pm 0.5$	$\pm 0.5$	$\pm 1.2$
660-1300	22.65	38.0	>70	$\pm 0.7$	$\pm 0.4$	---

Table IV-8: TN-LC Cell Thickness for 30dB Contrast.

As result of the simulations done, the last mixture was discarded because it is not suitable for this application. As it was expected, higher the LC birefringence lower the cell thickness. The four configurations proposed, using the first two mixtures, are shown in Table IV-9.

Cell Type	Wavelength Range	Cell Thickness	LC Mixture	Expected Extinction Ratio
no 1	400nm – 1300nm	7 $\mu\text{m}$	Ref A	20dB
no 2	400nm – 1300nm	11 $\mu\text{m}$	Ref B	20 dB
no 3	850nm – 1300nm	11 $\mu\text{m}$	Ref A	30dB
no 4	400nm – 850nm	15 $\mu\text{m}$	Ref A	30dB

Table IV-9: Characteristics of the Manufactured Cells.

The TN-LC cells have been manufactured according to the parameters defined from simulations. The first step has been the fabrication of the mask. The pattern with the pixels that make up each cell has been transferred to a chrome mask. Figure IV-9 shows the schematic with the pixels distributions that have been patterned to the chromium mask.

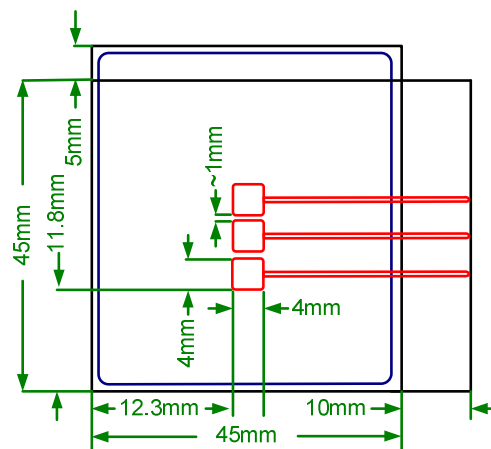


Figure IV-9: Pixel Distribution of the Fabricated Cells.

In order to fabricate the chrome mask, the pattern has been printed in a transparent film. It has been transferred to the photoresist layer that previously covers the chrome mask using an ultraviolet light. The photoresist has been removed from the zones exposed to the light by using a developer. The remaining photoresist, which has the shape of the pattern to be transferred to the chrome mask, has been cured by heating it in an oven. The exposed chrome has been attacked, and finally the remaining photoresist has been cleaned.

Once the chrome mask has been manufactured, it has been used for transferring the pixel pattern to the electrode layer that covers the glass substrate. Only one glass substrate of each TN-LC cell has been treated, the other glass substrate is the counter electrode, and it is not necessary to pattern it.

A thin layer of Indium Tin Oxide (ITO) is used as electrode. The pixels pattern has been transferred to the ITO by means of a photolithographic process similar to the method described for the chrome mask.

The molecular orientation inside the TN-LC cells is obtained by means of the alignment layers. These layers consist of a polyamide rubbed in the desired directions. In the case of a TN-LC cell, the rubbing in both substrates is perpendicular in order to obtain the molecules helix. First, the polyamide has been deposited by spin coating, then the polyamide layer has been cured in an oven, and finally the polyamide deposited in both substrates have been rubbed in perpendicular directions.

The spacers that are in charge of maintain the cell thickness are deposited by sputtering. The glue used for making up the cell structure has been applied to one substrate by serigraphy. After the cell assembly, the glue has been cured in the oven. Then, the cell is ready for being filled in.

The fabricated cells have been filled in with the LC mixture by the vacuum process. The LC is injected inside the cell by capillarity and pressure differences. Once the vacuum has been created in the vacuum chamber, the liquid crystal mixture has been placed together the orifice left in the assembled cell for filling it in.

Once the cell has been filled in, the orifice for filing it in is sealed in order to prevent leaks of LC and its spoilt. Metallic pins are placed in the electrodes edges for applying voltage to the LC. The pins are fixed using glue and silver paste. Finally, the wires are soldering to the metallic pins.

The manufactured cells have been characterized in order to check their behaviour. Three different set of measurements has been carried out for obtaining the TN-LC response.

Spectral response of the TN-LC cells has been obtained using an AvaSpec-128 Fibre Optic Spectrometer from Avantes, whose wavelength operation range is from 360nm to 850nm. Transmission between crossed polarisers and parallel polarisers has been measured for two states of the cells, when no voltage is applied to the cell and when a 5Vrms, 10kHz square wave has been droved to it.

Transmission of the TN-LC cells at three wavelengths when the excitation voltage is modified has been carried out using three different optical sources: A 1mW laser diode at 532nm form Hero, a 5.0nmW laser diode at 650nm from Power Technology Inc and an 850nm LED from Ratioplast Optoelectronic. Square waves with of frequencies, from 100Hz to 20kHz, have been droved to the TN-LC cells for obtaining the cell's response. In the following experiments, a 10kHz frequency square wave has been used for characterizing the TN-LC cells.

Dynamic response of the TN-LC cells two wavelengths, 532nm and 650, has been obtained using an Infineon SFH 350V phototransistor with a resistor. The obtained voltage has been measured with an oscilloscope.

The results obtained for each type of TN-LC cell are presented below:

- **Cell type no 1: 6.8 $\mu$ m thick cell filled with Ref A mixture**

Figure IV-10 shows transmission of the cell when it is placed between crossed polarisers and parallel polarisers when the cell is switched on and when no voltage is applied to it.

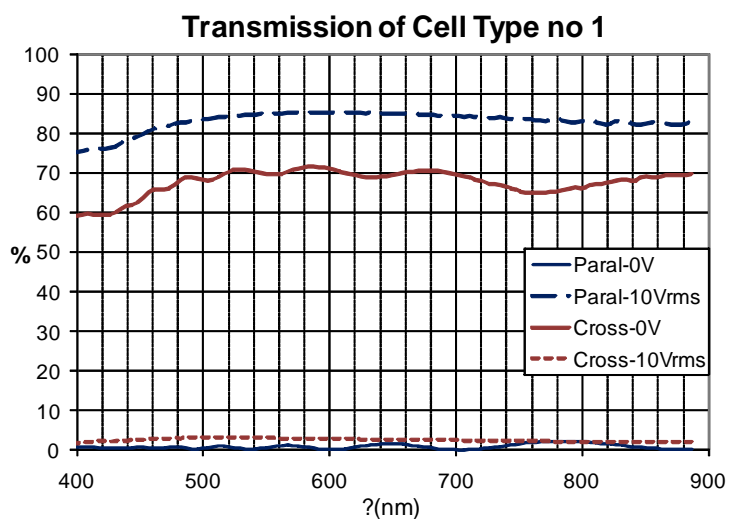


Figure IV-10: Transmission of Cell Type no 1, Between Crossed Polarizers and Parallel Polarizers when the LC is Switched (5Vrms) and when it is not Drovod (0V)

Figure IV-11 shows the transmission of the Cell type no 1 between crossed polarisers and parallel polarisers at three wavelengths, when the voltage applied to the cell is modified.

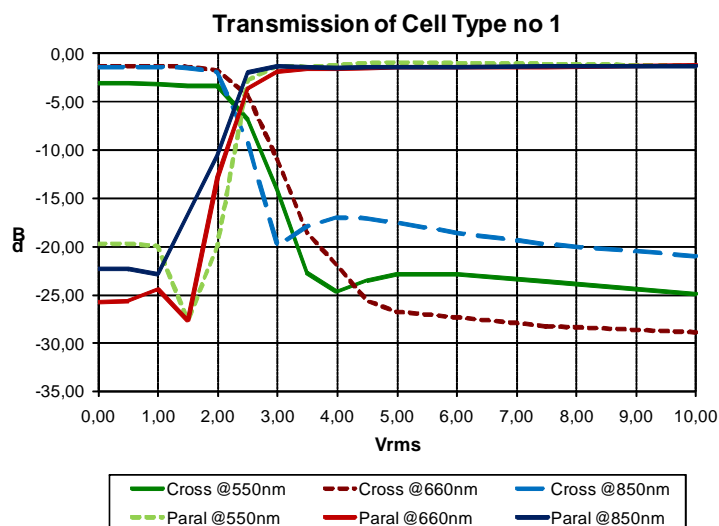


Figure IV-11: Transmission of Cell type 1 at Three Wavelengths, and Between Crossed and Parallel Polarizers

Table IV-10 summarizes main characteristics of cells type no1.

Characteristics	550nm		660nm		850nm	
	Cross P	Par P	Cross P	Par P	Cross P	Par P
<b>Insertion Losses (dB)</b>	3.1	1.0	1.3	1.2	1.3	1.3
<b>Crosstalk (dB)</b>	-21.8	-26.75	-27.6	-26.45	-19.7	-21.5
<b>Rise Time (ms)</b>	44.6	3.2	42.4	2.4	---	---
<b>Fall Time (ms)</b>	4.0	46.0	4.8	52.6	---	---

Table IV-10: Main Characteristics of the Cell Type no 1.

At low voltage, higher transmission is obtained when the TN-LC cell is placed between cross polarizers, while higher transmission is achieved when the cell is placed between parallel polarizers for higher voltages.

- **Cell type no 2: 11.8µm thick cell filled with Ref B mixture**

Figure IV-12 shows transmission of the cell when it is placed between crossed polarisers and parallel polarisers when the cell is switched on and when no voltage is applied to it.

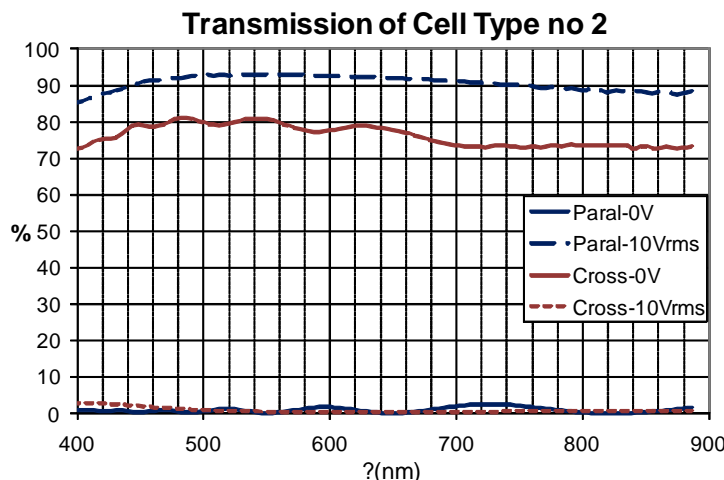


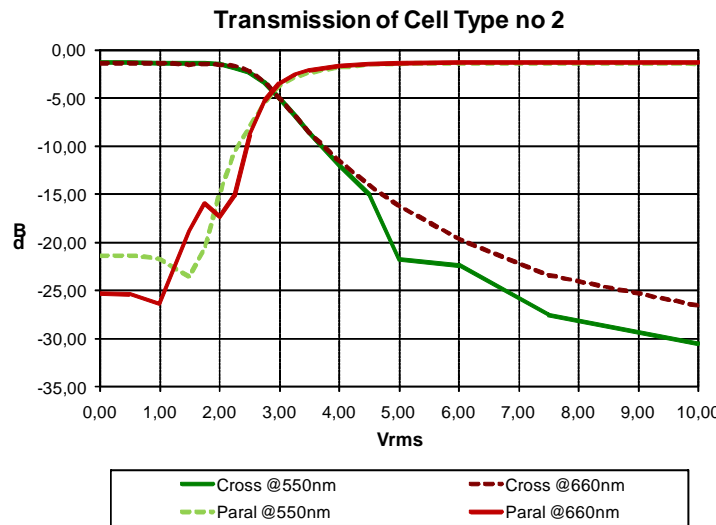
Figure IV-12: Transmission of Cell Type no 2, Between Crossed Polarizers and Parallel Polarizers when the LC is Switched and when it is Drovved

Table IV-11 summarizes main characteristics of cells type no 2.

Characteristics	550nm		660nm		850nm	
	Cross P	Par P	Cross P	Par P	Cross P	Par P
<b>Insertion Losses (dB)</b>	1.3	1.4	1.4	1.25	---	---
<b>Crosstalk (dB)</b>	-29.2	-22.4	-25.4	-25.2	-17.4	-16.9

Table IV-11: Main Characteristics of the Cell Type no 2.

Figure IV-13 shows the transmission of the Cell type no 2 between crossed polarisers and parallel polarisers at three wavelengths, when the voltage applied to the cell is modified.

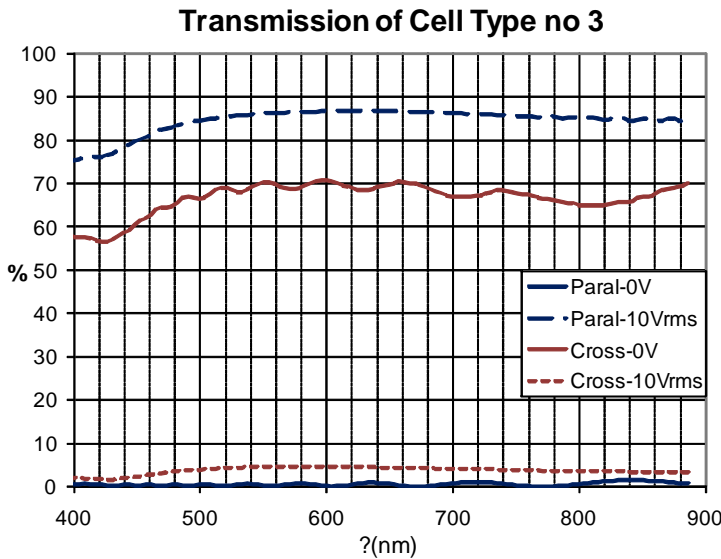


**Figure IV-13:** Transmission of Cell type 2 at Three Wavelengths, and Between Crossed and Parallel Polarizers

Cell type no 2 has not been used in the implementation of the prototype because only one cell of this type was fabricated.

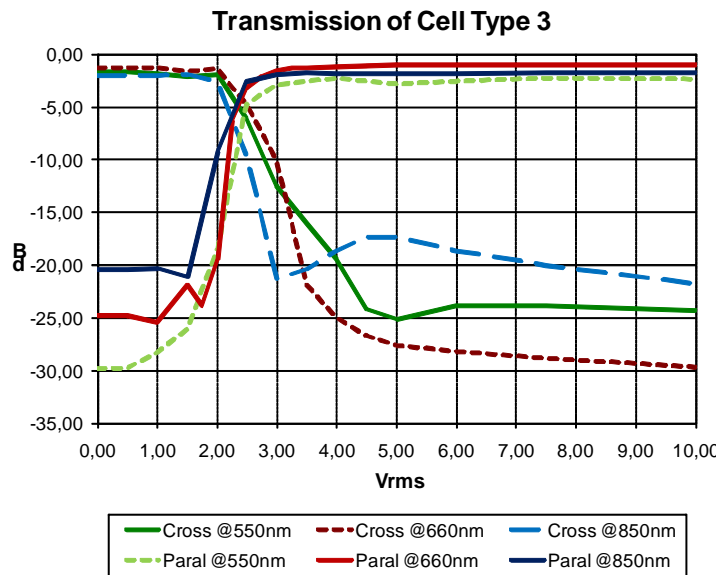
- **Cell type no 3: 11.2 $\mu$ m thick cell filled with Ref A mixture**

Figure IV-14 shows transmission of the cell when it is placed between crossed polarisers and parallel polarisers when the cell is switched on and when no voltage is applied to it.



**Figure IV-14:** Transmission of Cell Type no 3, Between Crossed Polarizers and Parallel Polarizers when the LC is Switched and when it is not Drovèd

Figure IV-15 shows the transmission of the Cell type no 3 between crossed polarisers and parallel polarisers at three wavelengths, when the voltage applied to the cell is modified.



**Figure IV-15:** Transmission of Cell type 3 at Three Wavelengths, and Between Crossed and Parallel Polarizers

Table IV-12 summarizes main characteristics of cells type no 3.

Characteristics	550nm		660nm		850nm	
	Cross P	Par P	Cross P	Par P	Cross P	Par P
<b>Insertion Losses (dB)</b>	1.7	2.3	1.3	1.4	2.0	1.75
<b>Crosstalk (dB)</b>	-23.5	-27.5	-28.4	-32.0	-19.4	-19.4
<b>Rise Time</b>	44.6	6.1	42.4	4.1	---	---
<b>Fall Time</b>	4.0	66.4	4.8	115.0	---	---

**Table IV-12:** Main Characteristics of the Cell Type no 3.

This type of cell is optimized for operating in the 850-1300nm wavelength range. Contrary to expected, more contrast have been obtained at 550nm and 630nm.

- **Cell type no 4: 15.7µm thick cell filled with Ref A mixture**

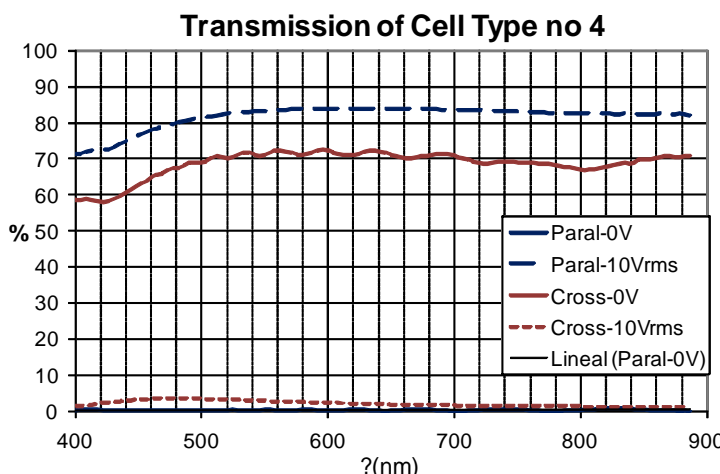


**Figure IV-16:** Transmission of Cell Type no 4, Between Crossed Polarizers and Parallel Polarizers when the LC is Switched and when it is not Drove

Figure IV-16 shows transmission of the cell when it is placed between crossed polarisers and parallel polarisers when the cell is switched on and when no voltage is applied to it.

Figure IV-17 shows the transmission of the Cell type no 4 between crossed polarisers and parallel polarisers at three wavelengths, when the voltage applied to the cell is modified.

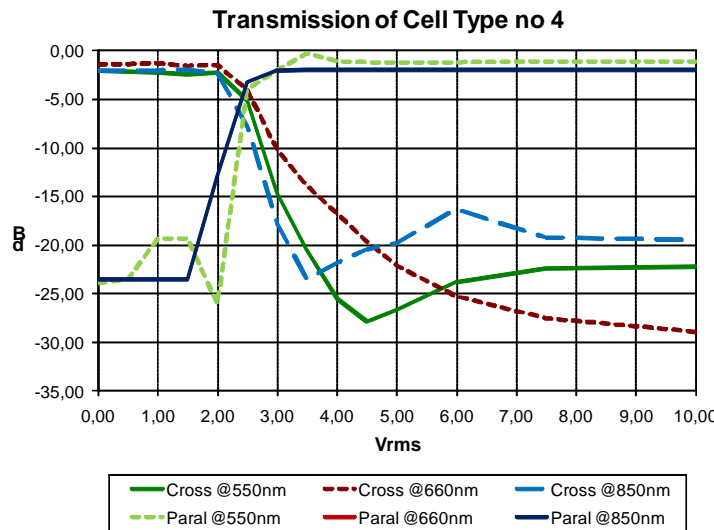


Figure IV-17: Transmission of Cell type 4 at Three Wavelengths, and Between Crossed and Parallel Polarizers

Table IV-13 summarizes main characteristics of cells type no 4.

Characteristics	550nm		630nm		850nm	
	Cross P	Par P	Cross P	Par P	Cross P	Par P
<b>Insertion Losses (dB)</b>	2.1	0.3	1.3	1.3	2.0	2.0
<b>Crosstalk (dB)</b>	-25.9	-25.9	-27.7	-24.0	-21.5	-21.6
<b>Rise Time</b>	119.0	13.0	122.2	7.5	---	---
<b>Fall Time</b>	10.6	120.0	17.0	140.0	---	---

Table IV-13: Main Characteristics of the Cell Type no 4.

#### IV.6.- Light Coupling and Scalability

The last stages that make up the optical switch are in charge of focusing the light from both optical paths in both output ports, and it is formed by the two *Output Lenses* and the *Output Ports*. The proposed optical switch is designed for operating in multimode optical fibres, especially in Polymer Optical Fiber (POF) and Graded Index POF (GI-POF).

One of the main characteristics of step index POF is its large core, 980 $\mu$ m, and high Numerical Aperture, near 0.5. These two properties allow an easy light coupling into the output port of the device, reducing losses. Thanks to this, only by using a single

focusing lens, most of the guided optical power that arrives to the output port can be coupled to the output fibre. Therefore, there is a compromised between the output lenses parameters and the optical fibre.

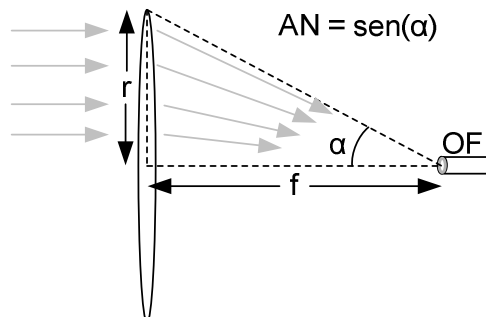


**Figure IV-18:** Relation between Numerical Aperture of the Output Fiber and the Output Lens Characteristics

According to the schematic presented in Figure IV-18, the relationship between the radius ( $r$ ) and the focal length ( $f$ ) of the Output Lens and the Numerical Aperture (NA) of the output fibre is given by equation [IV-1]:

$$NA = \sin(\alpha) > \arctan\left(\frac{r}{f}\right) \quad [\text{IV-1}]$$

Where  $\alpha$  is the angle of acceptance.

The Output Lenses used in the implementation of the proposed device have 50mm diameter and 75mm focal length; so ideally, light beams would arrive to the focal point with fewer angles than 18.5°. On the other hand, as POF has 0.5 NA, the beams that arrive to the fibre with fewer angles than 30° should be couple properly and therefore transmitted along the fibre.

If the beams that arrive to the output fibre are not collimated properly, the light is not focused in the focal point, and the spot of the output light to be coupled into the fibre increases. Thus, if the input collimated beams have divergence, it is propagated to the output port and the output beam spot is enlarged. For this reason, it could be interesting to use a fibre lens in the output port in order to collect the light that is not properly focused.

On the other hand, in order to calculate the maximum number of input ports, it depends mainly on the output lens size and the divergence of the collimated beam that comes from each port. In this way, the NA of POF makes the non-ideal collimated beam have more divergence, than other fibers. An estimation of 4° has been measured from the implemented set up. In that case, pixel size should be enlarged for covering the whole beam spot.

Following the consideration given above, the pixel size should be about 9mm width for POF applications, and 4mm for GI-POF because last one exhibits fewer NA, and this reduces the beam divergence. The pitch in both cases is considered to be 1mm. According to that, the pixels distributions for POF and GI-POF applications in the output lens is shown in Figure IV-19.

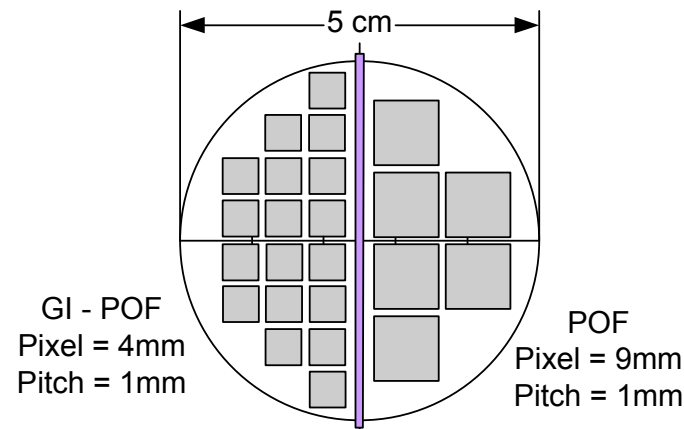


**Figure IV-19:** Pixel Distribution for GI-POF and POF applications in the Output Lens

Taking into account the restrictions given before, the amount of input port could be 6 for POF applications and 18 for GI-POF networks in the current design. New designs using other lens and pixels can accommodate other number of maximum ports.

#### IV.7.- Optical Characterization

Preliminary results of de advanced multifunctional optical switch were obtained at two wavelengths. Deeper characterization of the advanced multifunctional optical switch has been carried out in the optical test bench that is described in Chapter VI.

##### IV.7.a.- Preliminary Results

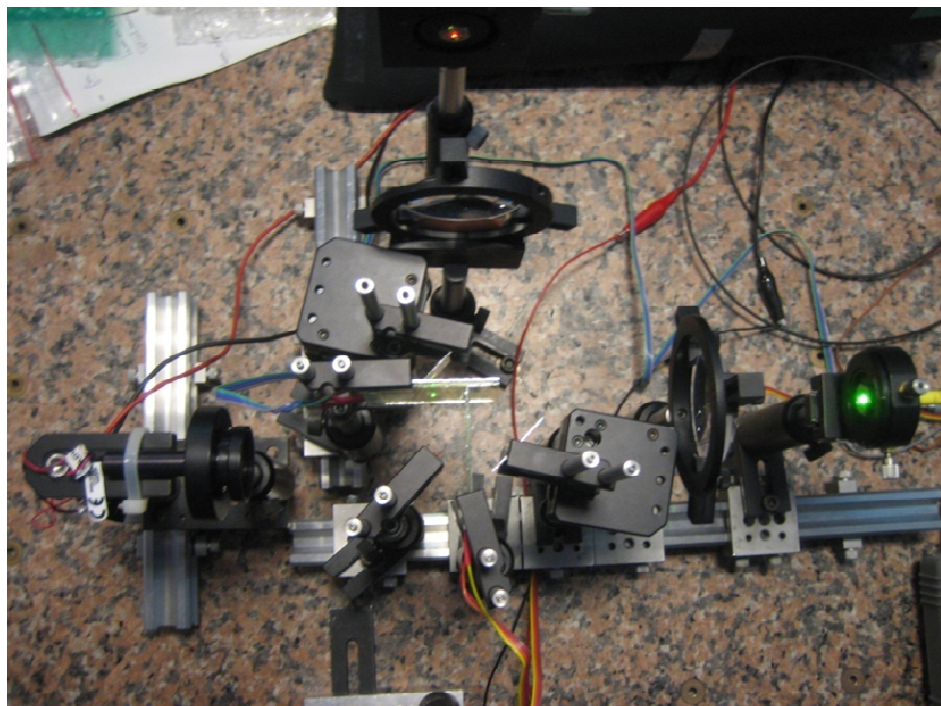


**Figure IV-20:** Picture of the Implemented Device for the First Set of Measurements

Figure IV-20 presents a picture of the implemented device. Three uncoated wire grid polarizing beam splitters PBS02A from Moxtek, two 11 $\mu$ m thick nematic liquid crystal cells optimized for working in the 850nm – 1300nm wavelength range and two 50mm diameter plane-convex lenses with 75mm focal length have been used in the implementation of the device. The use of uncoated PBS and NLC allows their operation in a wide wavelength range, although higher losses and reflections are expected. By the way, only two wavelengths characterization was made.

A schematic of the experimental set up used for making the measurements is shown in Figure IV-21. Each port has been measured independently of the others. Two visible laser diodes have been used for doing the characterization. One laser diode at 650nm and 5.0mW from Power Technology Inc has been placed at the *Input Port a* of the device, and a laser diode at 532nm and 1mW from Hero has been applied to the *Input Port b*. Not input lenses have been employed because the laser diodes include collimation optics.

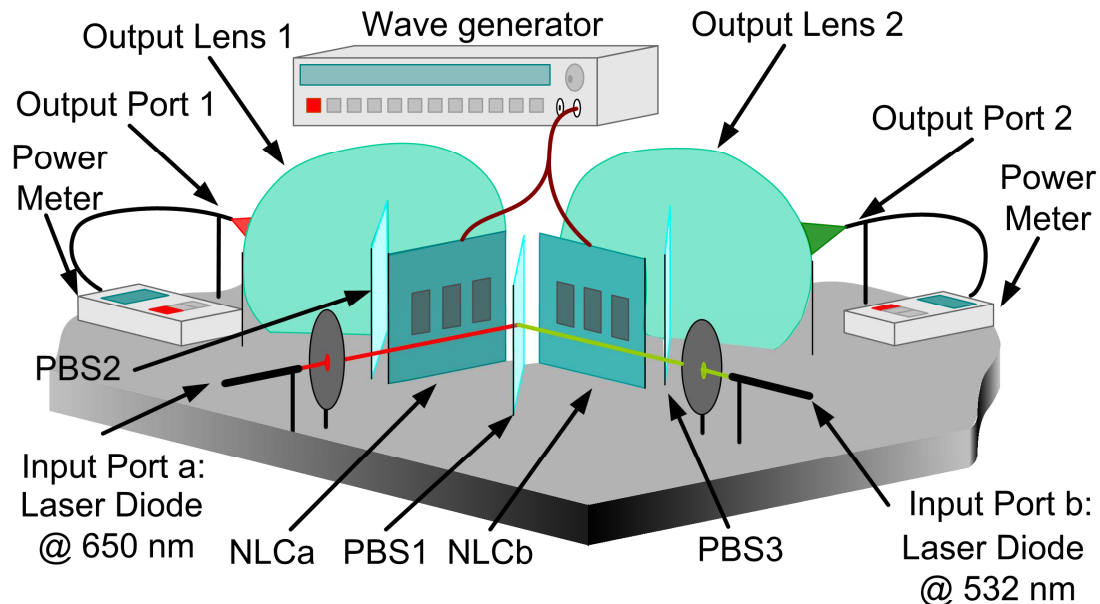


Figure IV-21: Experimental Set up Used for the Preliminary Characterization.

POF has been used in both output ports. A 557 Rifocs commercial optical power meter has been used for obtaining the measures. A Hewlett Packard wave generator has been used for applying voltage to the liquid crystal cells. A 10kHz frequency square wave with different voltage levels has been applied to the suitable pair of pixels in order to characterize the device transmission at both wavelengths.

Measurements have been taken in two different steps for each pixel of the proposed device. In a first stage, light from the laser diode at 650nm has been measured in both outputs. In the second stage, light from the laser diode at 532nm has also been measured in both outputs. Figure IV-22 shows the transmission obtained for all the three pixels at both wavelengths.

When no voltage is applied to the liquid crystal cells, *OFF* state, *Input Port a* is guided to *Output Port 1* and *Input Port b* is directed to *Output Port 2*. In the experimental set up used, when the laser diode at 650nm (*Input Port a*) has been

used high optical power of light has been measured in *Output Port 1*, and very low optical power is measured in *Output Port 2*.

Similar situation happens with the light from the 532nm laser diode (*Input Port b*), more transmission is obtained in *Output Port 2* that in *Output Port 1* (see Figure IV-23 (a)).

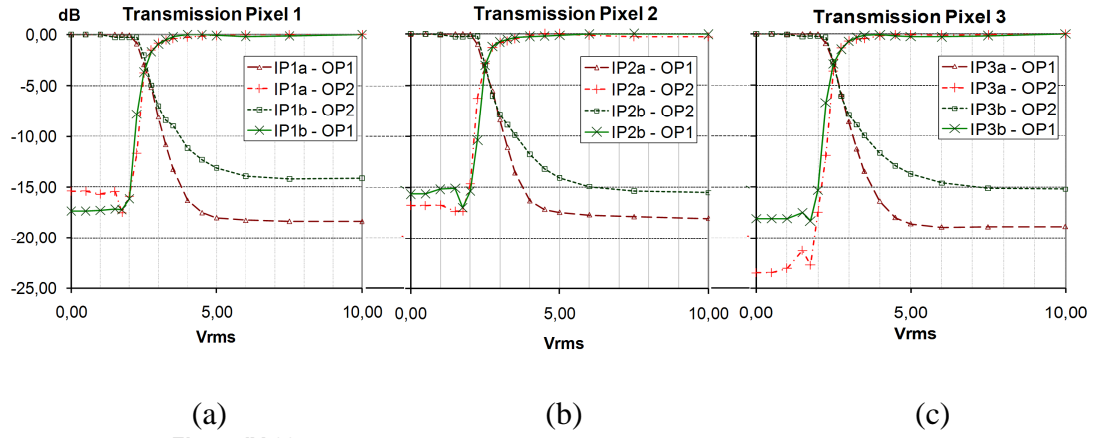


Figure IV-22: Transmission Obtained for Each Pixel of the Device,

The optical transmission of the device is modified when the voltage applied to both TN-LC cells is increased. Finally, when the cells are completely switched, the device is in *ON* state: light from *Input Port a* is guided to *Output Port 2* and light from *Input b* is directed to *Output Port 1*. In the experimental set up used, there is more optical power from the 650 nm laser diode (*Input a*) in *Output Port 2b*. And vice versa, more transmission from the 532 nm laser diode (*Input b*) is measured in *Output Port 1* (see Figure IV-23 (b)).

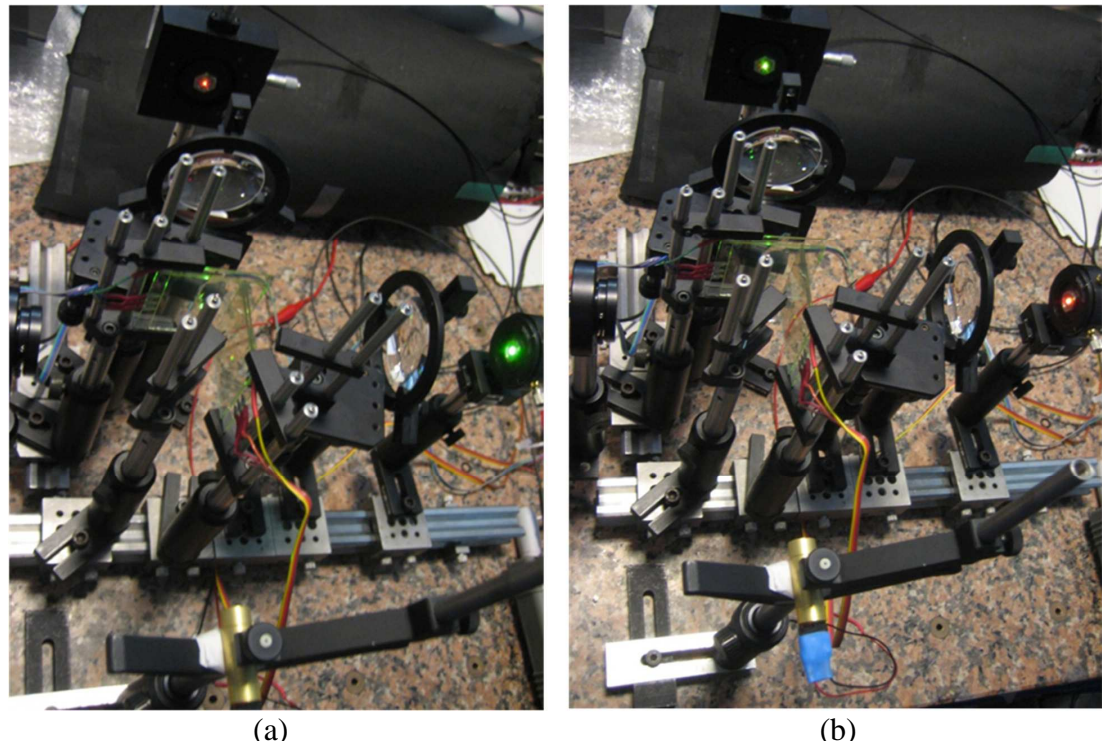


Figure IV-23: Pictures of Two States of the Implemented Device: (a) OFF and (b) ON.

From the experimental results, Figure IV-22, crosstalk, as it is defined in section II.2.b, higher than 14dB at 532nm and better than 17dB at 650nm have been obtained with the sample used.

Variable optical transmission or attenuation can be obtained by applying intermediate voltage levels to the TN-LC cells, ranging from 2 to 6Vrms,  $V_{th} < V < V_{sw}$ ; lower voltages induce less polarization shifts. Input light is split and directed to both outputs with a variable ratio depending on the applied voltage, and consequently on the manipulation of the stage of light polarization by the LC. In this situation, the proposed device is operating between *OFF* and *ON* states when implementing this mode.

#### IV.7.b.- Device Characterization Using the Optical Test Bench

The proposed Advanced Multifunctional Optical Switch has been characterized using the optical test bench described in Chapter VI. Remote control of the optical test bench is possible and automated measurement can be carried out. The optical device has been built in a separate aluminium base plate for allowing its removal from the Optical Characterization Test Bench when required.

The proposed device has been characterized with the three types of TN-LC available: Cell type no 1, no 3 and no 4. The same implementation has been used for all the possibilities and only the TN-LC has been interchanged. In both set of measurements, only the central pixel of each TN-LC cell has been characterized.

Two set of measurements have been carried out for characterizing the optical device. In the first one, multimode silica 62.5/125 $\mu$ m fibre has been used at the input ports. GRIN lenses have been placed at the fibre output for collimating light. Two multimode 99:1 couplers have allowed measuring the insertion losses and crosstalk, as it is defined in Chapter II.5, in both input ports.

Response times of the optical switch have been measured in the second set of measurements. As optical source, three laser diodes at different wavelengths have been placed at the input ports. Optical power at the device's outputs have been measured by means of an amplified photodetector connected to an oscilloscope

- **Optical Characterization of the Switch using Multimode Silica 62.5/125 $\mu$ m Fibre as Input Port**

An optical source from Ratioplast Optoelectronic with two interchangeable LEDs at different wavelengths, 660nm and 850nm, has been used for characterizing the Advanced Multifunctional Optical Switch. Light is guided by means of a 99:1 multimode fibre coupler from the optical source to the optical switch's inputs. The 1% branch serves for estimating the optical power in the switch.

Two GRIN lenses have been used for collimating the light that exits from the optical fibre. The obtained beam is directed to the optical device. In this experiment, POF has not been used because due to its high Numerical Aperture (NA) the collimated beam has a large divergence, making more difficult the characterization of the

device. Figure IV-24 shows a picture of the Advanced Functional Optical Switch implemented in the Optical Characterization Bench.

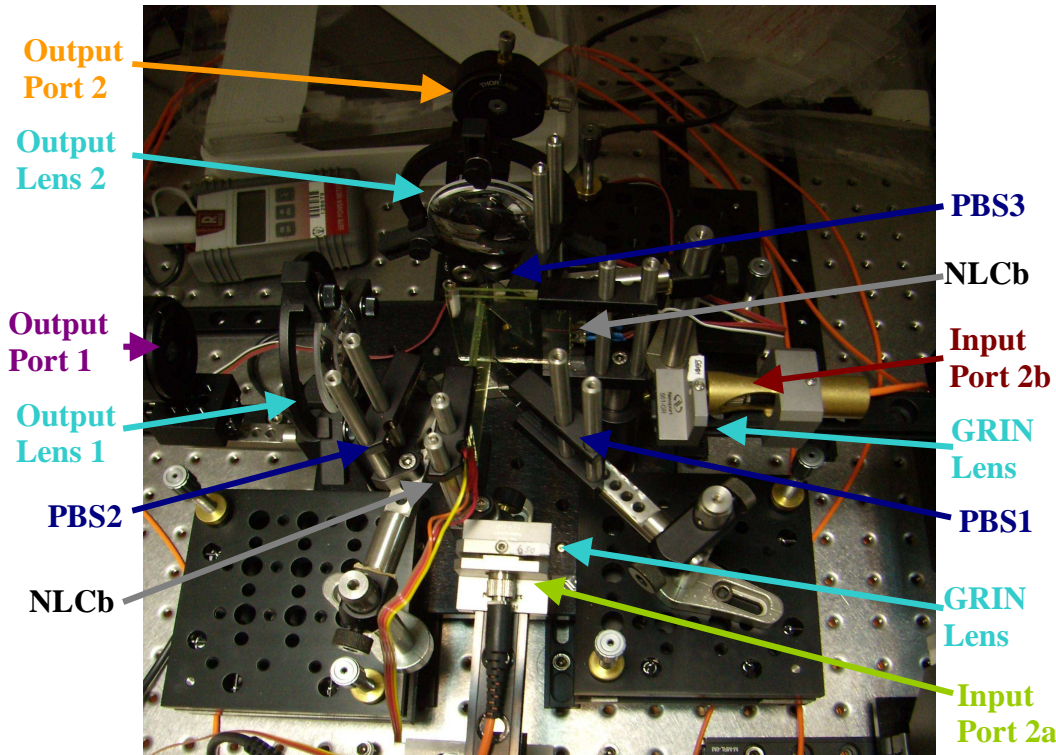


Figure IV-24: Picture of the Advanced Multifunction Optical Switch  
Built in the Optical Characterization Bench

The Optical Characterization Bench has been programmed for measuring output light when the amplitude of a 10kHz frequency square wave is modified from 0.200Vpp to 10Vpp in steps of 0.2V.

Cells Type no 1	(400nm – 1300nm)	Insertion Losses (dB) (Fibre – Fibre)		Crosstalk (dB)	
		660nm	850nm	660nm	850nm
Input Port a	Output Port 1	13.1	12.0	-15.9	-18.8
Input Port a	Output Port 2	14.2	12.25	-14.2	-18.2
Input Port b	Output Port 1	15.15	11.25	-17.6	-14.8
Input Port b	Output Port 2	15.55	10.9	-16.0	-13.6
Cells Type no 3					
Input Port a	Output Port 1	12.8	11.9	-23.7	-18.4
Input Port a	Output Port 2	13.5	11.9	-18.4	-18.5
Input Port b	Output Port 1	13.2	11.1	-23.7	-16.1
Input Port b	Output Port 2	15.3	10.8	-14.9	-16.1
Cells Type no 4					
Input Port a	Output Port 1	12.9	12.0	-21.9	-17.1
Input Port a	Output Port 2	14.1	12.3	-20.8	-19.3
Input Port b	Output Port 1	15.1	11.3	-5.0	-16.0
Input Port b	Output Port 2	15.2	10.8	-19.1	-15.7

Table IV-14: Results Obtained for the Device Characterization when the Multimode 62.5/125µm Fibre is Used at the Input Ports.

A 20cm stretch of POF has been used for guiding light from the output port to an amplified photodiode PDA100A from Thorlabs. The obtained voltage has been measured using a TDS1200 oscilloscope from Tektronix.

The experimental results obtained in this set of measurements are summarized in Table IV-14.

From measurements, it can be seen that best overall performance is achieved in AMOS using cell type n°1. In this case, AMOS has a 900nm wavelength range operation with losses around 13dB, and crosstalk better than -15dB.

Anyhow, insertion losses higher than expected have been obtained. This can be produced by the divergence of the light that comes from the input port making that the output beam is not focused well in the output fibre.

This issue can be improved by using a fibre lens in the output ports in order to collect more light. Insertion losses smaller than 5dB can be estimated from the insertion losses measured of the bulk elements.

Figure IV-25 shows the optical transmissions from *Input Port 2b* to both Output Ports when the voltage applied to the TN-LC is modified for the three types of cells. It can be seen a voltage adjustable around 15dB range

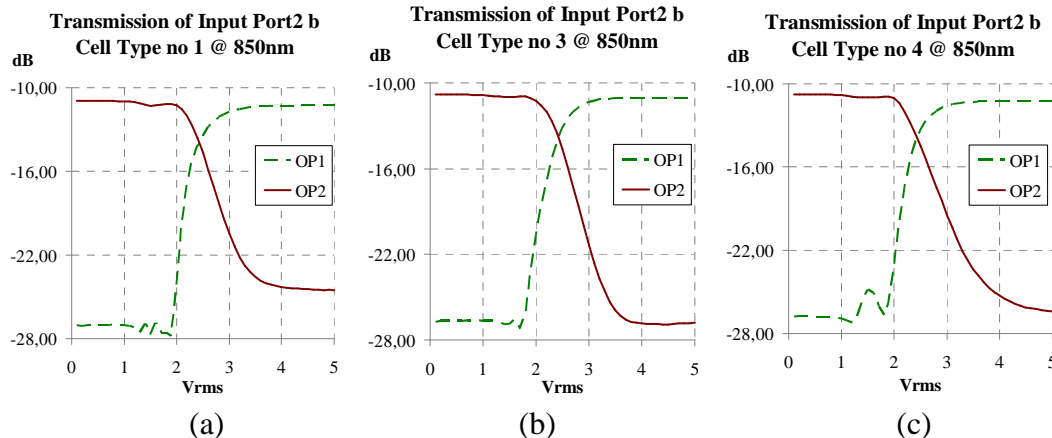


**Figure IV-25:** Transmission from *Input Port 2b* to Both Output Ports when the Voltage Applied to the TN-LC is Modified for the Three Types of Cells: (a) Type no 1, (b) Type no 3 and (c) Type no 4.

The proposed device allows variable optical power transmission from the input port to the output ports. According to Figure IV-25, this variation can be achieved approximately from 2Vrms to 3Vrms.

In this way, Variable Optical Power Splitter (VOPS) is considered when both outputs, *Output Port 1* and *Output Port 2*, are used. Variable splitting ratios can be achieved by adjusting the voltage driven to the TN-LC cells. Moreover, Variable Optical Attenuator is obtained when only one output is used.

- **Dynamic Characterization of the Switch using Laser Diodes at the Input Ports**

Dynamic optical characterization of the proposed device has been carried out using three Lasers at different wavelengths: a 532nm and 1mW Laser module from Hero, a 650nm and 5mW Laser module from Power Technology Inc. and an 850nm and 10mW from Thorlabs.

The output part of the experiments is similar to the used in the previous characterization; a 20cm stretch of POF has been used for guiding light from the output port to the amplified photodetector PDA100A from Thorlabs. A TDS1200 digital oscilloscope from Tektronix has been used for measuring the voltage.

A wave generator 33120A from Agilent has been used for driving the excitation voltage to the TN-LC cells. A 5Vrms and 10kHz square wave has been applied to the TN-LC cells for 0.5s and 0V has been applied for 0.5s.

All the three types of cells have been characterized, but only one input port has been measured. Figure IV-26, Figure IV-27 and Figure IV-28 show the response times obtained in the characterization for the different types of cells used, and Table IV-15 summarizes the obtained results.

<b>Input Port 2b</b>	<b>Rise Time</b>			<b>Fall Time</b>		
	<b>532nm</b>	<b>650nm</b>	<b>850nm</b>	<b>532nm</b>	<b>650nm</b>	<b>850nm</b>
<b>Cells Type no 1</b>						
<b>Output Port 1</b>	10.1	8.6	8.4	33.2	39.8	42.4
<b>Output Port 2</b>	38.8	39.4	40.0	20.5	24.3	17.3
<b>Cells Type no 3</b>						
<b>Output Port 1</b>	24.4	21.0	14.4	73.9	73.8	94.8
<b>Output Port 2</b>	70.6	76.3	101.6	59.8	23.0	15.2
<b>Cells Type no 4</b>						
<b>Output Port 1</b>	39.8	27.4	28.8	119.4	118.4	125.0
<b>Output Port 2</b>	117.0	118.3	116.0	38.6	29.4	31.8

Table IV-15: Response times of the Advanced Multifunctional Optical Switch.

Response times from tens to hundreds of milliseconds have been obtained. Larger times are related to Liquid Crystal's relaxation times while larger times correspond with LC's excitation times. It is usual that relaxation times are larger than excitation times in this type of cells.

The response times represented in Figure IV-26, Figure IV-27 and Figure IV-28 correspond to the configuration of the device when the light goes from *Input Port b* to *Output Port 1*. According to the device response, higher transmission is obtained when the TN-LC cells are switched on. So, the represented rise time of the optical switch, left part of the presented figures, are related to LC's excitation time.

On the other hand, right part of the figures show the fall time of the optical switch for the configuration used in the measurements. Larger times are obtained because the presented responses are related to LC's relaxation times that are usually larger than excitation times. As it is expected, larger response times are obtained for wider TN-LC cells.

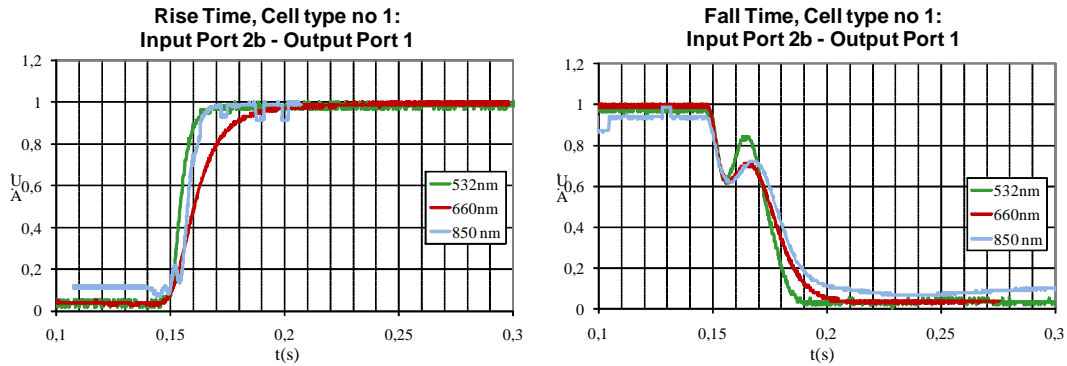


Figure IV-26: Response Times of the Advance Multifunctional Optical Switch Built with Cells Type no 1

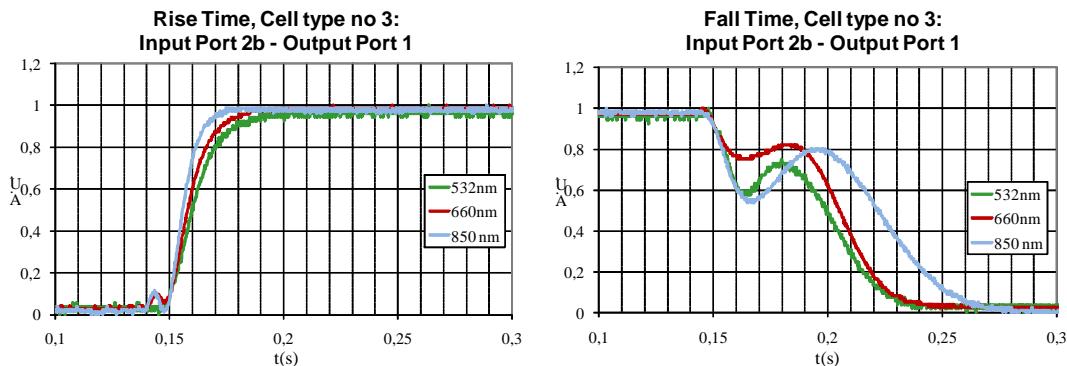


Figure IV-27: Response Times of the Advanced Multifunctional Optical Switch Built with Cells Type no 3

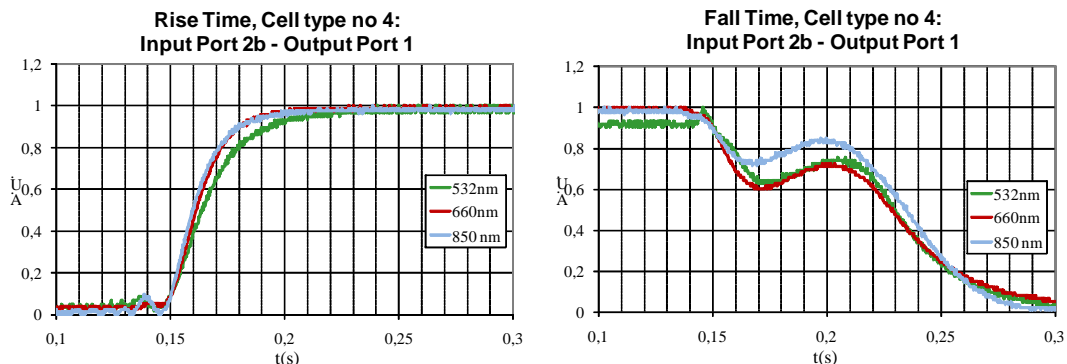


Figure IV-28: Response Times of the Advanced Multifunctional Optical Switch Built with Cells Type no 4

Higher response times are obtained when the AMOS is measured respect to the TN\_LC. Rise times obtained in that case are higher than those measured for the single LC characterization. This is due to the fact that more liquid crystal has to be switched. On the other hand, fall time does not differ much from the TN-LC characterization. This thing is due to the fact that fall time is related to the viscosity of the material and it does not depend on the voltage applied.

In addition, as it is expected, the response times of wider TN-LC cells are higher than those obtained for thinner cells. This is caused because the response times are proportional to the cell thickness.

According to the response times measured, the proposed device is suitable for being used in applications where switching speed is not fundamental

#### **IV.8.- Summary and Conclusions**

In this chapter, a novel structure of an Advanced Multifunctional Optical Switch has been presented. The scheme is based on TN-LC polarization management with TN-LC cells.

The proposed device is suitable for being used in Multimode Optical Fibre Networks, where the output light can be easily coupled to the output port due to the fibre high numerical aperture. In the specific case of POF, those networks operate in the visible wavelengths range, 532nm and 650nm. In addition, Graded-Index POF is able for operating up to 1300nm. Due to this, the proposed device is designed for working properly in a wide wavelength range. In the measurements it has been tested its operation in a 300nm range.

Twisted Nematic Liquid Crystal (TN-LC) cells are able of perform light switching in a wide wavelength range, and for this reason they are the candidate used for acting like active element in the proposed device.

The proposed scheme is scalable. The main restrictions come from the output lens, which is in charge of focusing all the output light in the output port. The angle of the focused beams should be smaller than the acceptance angle of the output fibre. The lens used in the implementation is 50mm diameter and has a focal length of 75mm, this makes to the output lens fulfil the requirements of the numerical aperture of the output POF

On the other hand, the divergence of the input beams cause that the output light is not focused properly into the output fibre. More light can be collected if a fibre lens is used in the output port. Due to the numerical aperture of POF, collimation in this kind of fibres makes greater divergences. In that case, the pixel size should be enlarged for covering the beam spot that comes from the input port.

Taking into account these restrictions, using the same lenses in the output ports, up to 6 input ports could be implemented in POF applications, and up to 18 for GI-POF applications.

Due to the large operation wavelength range, up to four different types of TN-LC cells have been designed and fabricated for testing purposes. Characterization of the manufactured TN-LC cells has been carried out in order to check that they work properly in the operation range.

The proposed device has been characterized at different wavelengths in order to obtain the most relevant parameters. High insertion losses have been obtained, this can be due to the divergence of the input light, and can be in part corrected by using fibre lenses in the output ports.

The obtained crosstalk, is usually better than 15dB for 650nm and 850nm. Transmission through the device can be modified by applying less voltage to the TN-LC, so, variable attenuation can be achieved.

The response times has also been characterized. The proposed device is suitable for being used in applications where switching speed is not fundamental. Larger response times are obtained for the whole optical device than when only one LC cell has been characterized. A reason can be that the optical paths followed for each polarization are slightly different and makes the pulse wider. In addition, more liquid crystal has to be switched in order to commute the device.

Larger times are related to Liquid Crystal relaxation times. It is usual that relaxation times are larger than excitation times in this type of cells. In addition, larger times are obtained for wider cells, because the equivalent capacitor is higher in this case.

From measurements carried out, it can be seen that best overall performance is achieved in AMOS using cell types 1. In this case, AMOS has a 900nm wavelength range operation with losses around 13dB, crosstalk better than -15dB, rise times in the order of tens of milliseconds, and fall times shorter than 43ms.

Finally, the proposed device can perform different functionalities without hardware changes, only by selecting the proper input and output ports and control electronics. Thus the device can act as an 3x1 Optical Multiplexer/Combiner, Dual 3x1 Optical Multiplexer or 2x2 Optical Switch. Moreover, by applying a variable voltage to the TN-LC cells, a Variable Optical Attenuator and a Variable Optical Power Splitter can be performed with the same device, and variable splitting or attenuation ratios are possible.

Comparing the proposed AMOS with the optical multiplexer presented in section III.2, better contrast is obtained for the optical multiplexer. This can be due to the use of cube Polarizing Beam Splitters (PBS) with Antirefringent Coating that exhibit more extinction ratio but in a reduced wavelength range. In addition, shorter response times are obtained for the multiplexer proposed in section III.2.

# **Chapter V**

## **Switches Based on Integrated Optics**

---

*In this chapter, the description of optical switches and tuneable filters based on Integrated Optics is presented. In the first section of the chapter, an introduction about integrated optics switches is given. In the second part, there is an overview about Ring Resonator structure. Section three is about switches based on Ring Resonator with Liquid Crystal placed inside of the ring in order to modify its behaviour. A more complex structure based also in micro Ring Resonators and Liquid Crystals is anticipated for being employed as a scalable 1x3 Wavelength Selective optical switch. Simulations of the proposed structures are also presented.*

*In the last section of this chapter, a Tap and Two Split optical switch for being used as multicast capable optical cross connect node architecture is proposed. The structure for implementing the proposed switch is made of a Multimode Interference splitter and couplers as part of a Mach-Zehnder Interferometer. Finally, the results obtained in the simulations of the proposed structure are given.*



## V.1.- Introduction to Integrated Optic Switches

Previous chapters were focused on switches made of bulk components and free air propagation. LC is used as active element in all the described devices, TN-LC is utilized for implementing the 3x1 multiplexer presented in section III.4 and the advanced multifunction optical switch described in chapter IV, while the VMUX employs PDLC.

In this chapter, three switches based on integrated optics are proposed. Among the integrated technologies available, two of these technologies are proposed for implementing the described devices. In the two first switches, Ring Resonators (RR) in combination with LC is used. The other switch is based on Multi Mode Interference (MMI) splitters and Mach-Zehnder Interferometer (MZI).

Integrated Optics allows implementing miniaturized devices with high functionality on a common substrate, which also reduces fabrication costs [Chen-2006]. In addition, Planar Lightwave Circuits (PLCs) have low loss and allows the implementation of practical integrated devices such as modulators [Martin-1975, Baehr-2005, Liu-2004 a, Liu-2007, Thomson-2010], switches [Keil-1996, Suzuki-2004], filters [Bogaerts-2010, Goh-1998], multiplexers [Neyer-1984, Doer-2005] or sensors [Ksendzov-2005, Rogozinski-2005]

Different materials have been used for implementing PLC devices, such as Lithium Niobate [Neyer-1984, Sizhuo-1999, Higuma-2001, Tan-2008], III-V semiconductor compounds [Deri-1991], polymers [Eldada-2000, Viens-1999, Noh-2006, Wu-2006], glass [Bell-1991, Duport-1994, Ramaswamy-1988, d'Alessandro-2008] or LC [Yujie-2009, Whinnery-1977].

Integrated optics based on silicon [Soref-1986, Kawachi-1990] exhibit high index contrast between the core and common claddings allowing light concentration and guiding, thus, waveguides and devices are compact and lower waveguide radii are possible. In addition, silicon technology allows the use of established CMOS fabrication techniques to define integrated circuits [Layadi-1998].

Switching in integrated optics is obtained by modifying the refraction index of the waveguide core or the refraction index of the cladding. There are different techniques for obtaining the desired effect. Thermo-optic by heating a zone of the device, Electro-optic when a current is used, Acusto-optic by using an acoustic or elastic wave travelling that produces periodical strain in the device, all-optical switching [Almeida-2004], or using mobile parts.

## V.2.- Introduction to Ring Resonators

A Ring Resonator (RR) is an optical device composed basically by a  $2 \times 2$  coupler where one of its outputs is connected to one of its inputs forming a ring, as shown in Figure V-1. The coupling ratio of the coupler,  $\kappa$ , controls the amount of the input optical power that is coupled to the ring. Light that travels along the ring comes back to the second coupler input and interacts with the input light, which enters to the coupler through its first input. Depending on the light wavelength, constructive or destructive interference are possible, so the response of the RR is a succession of maxima and minima optical power that repeat periodically in function of wavelength.

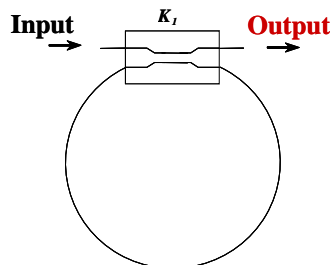


Figure V-1: Basic Structure of a Ring Resonator

The periodicity or separation between resonant frequencies, known as Free Spectral Range (FSR), depends on the optical time delay, which corresponds with the time taken by light when it is propagated along the ring resonator.

An additional coupler placed in the middle of the RR (see Figure V-2) allows obtaining the complementary response of the RR. Those wavelengths that present maxima in the *Straight Output* correspond with minima in the *Cross Output*. This structure is used for implementing Optical Add/Drop Multiplexers (OADM).

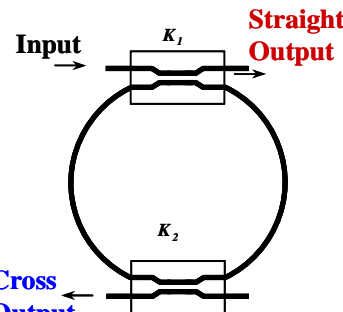


Figure V-2: Ring Resonator structure as Optical Add/Drop Multiplexer

OADM are useful in Passive Optical Networks (PON) where WDM is performed, and as part of optical cross-connects in long haul networks. Data are transmitted at different wavelengths, depending on the information or the destination; the selected wavelength is obtained in the desired points by using a RR centred at that wavelength. Such wavelength is extracted in the *Cross Output* while the rest of the information is transmitted through the *Straight Port* at the remaining wavelengths.

Additionally, new data can be transmitted from this point at selected wavelength using the *Add Port* that is symmetric to the *Cross Output* in Figure V-2.

RR have also been used as routers in Self-Routing Frequency Division Multiple Access (SR-FDMA) networks [Tsao-1995, Vázquez-2000], and as filters in DWDM (Dense Wavelength Division Multiplexing) systems with carriers spacing of 50 GHz, or less [Little-2004]. Non-linear optical applications, such as all-optical switches [Heebner-1999], also use ring resonators. The resonant frequencies of filters based on RR devices have already been shifted by changing the equivalent loop length by carrier injection [Djordjev-2002a], or local heating [Little-2004]. The optical response of this kind of filters can be improved by using second order structures [Vargas-2010].

Other applications of RR are their use as sensor: for chemical vapor sensor [Sun-2004] or protein detection [Ksendzov-2005]. In addition, the RR structure can also be used for self-referencing intensity based sensors [Vázquez-2005a]. By using this technique, it is possible to cancel the measurement errors due to fluctuations of the optical power that are not related to the magnitude to be measured, such as the lifetime of the optical power source...

More recently microring resonators ( $\mu$ RR) tuning has been achieved by liquid flowing in the microchannel which constitutes the upper cladding of the resonator waveguides [Levy-2006]; and 3nm shift by all optical control using 980nm light pulses is reported in [Beaugeois-2007]. Thermally tuneable switches based on ring resonators are reported in [Djordjev-2002b] and absorption is used for controlling the switch in [Geuzebroek-2002, Little-1998a]. Ultra compact micro ring resonators with quality factor ( $Q$ , defined as the ratio between resonance frequency and 3-dB bandwidth) up to 250, and a free spectral range (FSR) of 24 nm are reported in [Little-1998b] as fundamental building blocks in more complex optical processing circuits. New tuning capabilities, by coupling coefficient changes in compound Sagnac embedded in ring resonators as reported in [Vázquez-2005c]

Thermally changing the RR refractive index, by introducing a heater close to the resonator, may induce problems related to power dissipation when many resonators have to be integrated in a DWDM multiplexing system. This effect is reduced in ring resonators fabricated from silicon-on-insulator (SOI) wafers with an electrical tuning, by incorporating nematic liquid crystals as the waveguide side cladding; achieving a tuning range of 0.22 nm [Maune-2003]. The high refractive index contrast available in SOI allows compact micro ring resonators with low loss and high- $Q$ .

Some developments in RR filters was focused on achieving flattop drop-port responses with a sharp rolloff (-30 dB at closely spaced adjacent channels), low or a wide FSR. Equally important for add-drop applications is a high-extinction, boxlike notch response across the channel band in the through port to avoid so-called coherent cross talk between drop and add data, as obtained in [Popovic-2006]. Vertically coupled  $\mu$ RRs and cross-grid topology have also been demonstrated, a review of the different achievements can be seen in [Kokubun-2005].

### V.3.- Switches based on Ring Resonators and Liquid Crystals

RR structure for integrated optics is preferable made of a circular waveguide, or a disk, evanescently side-coupled to a pair of waveguides (see Figure V-3). Power is transferred between waveguides via the resonances of the ring.

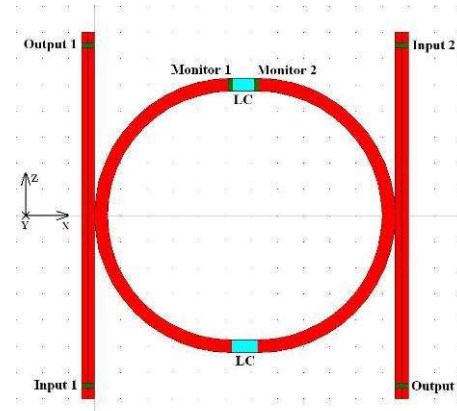


**Figure V-3:** Ring Resonator Structure Built in Integrated Optics with LC in the Loop

A previously stated, the RR can be implemented using different materials such as InGaAsP/InP [Levy-2006], GaAs/AlGaAs, SOI [Kokubun-2005, Koonath-2006, Little-1998 b, Maune-2003], polymeric materials [Maalouf-2006]. In that respect, compact devices such as 1x3 add/drop port microring resonators on silicon have been fabricated [Koonath-2006]. Lithographic precision is rarely sufficient to achieve critical coupling (a condition in which null output field amplitude is achieved at specific wavelengths, see next section) in fabricated high  $Q$  resonators; and some form of trimming is usually necessary. On the other hand, active devices such as switches need a control parameter to reconfigure the state of the device.

As it is presented in section III.1, LC technology has been used as a control element in switching fabrics, even it has been demonstrated electrical tuning in ring resonators fabricated from silicon-on-insulator wafers by incorporating nematic liquid crystals as the waveguide side cladding, but achieving a limited tuning range of 0.22nm [Maune-2003]. Channel waveguides made of SiO<sub>2</sub>/Si grooves filled with liquid crystals are presented in [d'Alessandro-2006 a, Donisi-2010]. A new RR structure with liquid crystals (LC) inside the loop, in the waveguide core, as the control element can be seen in Figure V-3. More recently, tunable couplers based on tuning LC properties inside waveguide regions have been reported within photonic crystal structures [Yasuda-2005, Liu-2004b].

In next section, an overview of the theory applied to Ring Resonators is presented, in order to help understanding the expected behaviour of the  $\mu$ RR, although commercial software based on Finite Differences Time Domain FDTD have been used in the simulations.

### V.3.a.- Ring Resonator Theory

As previously reported, a RR is made of a circular waveguide coupled to a waveguide. In a first approximation, the parameters used in describing directional couplers formed by placing two waveguides in close proximity from coupled mode equations and identical waveguides are the coupling coefficient,  $\kappa$ ; and the distance of coupling,  $l$ . The relation of those parameters to power coupling ratio  $K$  is given by [Madsen-1999, Vargas-2003, Montalvo-2008].

$$(\cos \kappa \cdot l)^2 = K \quad [\text{V-1}]$$

The following 2x2 transfer matrix describes the relationships between input and output fields of the coupling region:

$$\begin{bmatrix} E_3 \\ E_4 \end{bmatrix} = (1-g)^{\frac{l}{2}} \begin{bmatrix} \sqrt{K} & j\sqrt{1-K} \\ j\sqrt{1-K} & \sqrt{K} \end{bmatrix} \begin{bmatrix} E_1 \\ E_2 \end{bmatrix} \quad [\text{V-2}]$$

where  $(1-g)$  are the power coupler excess loss in the evanescent field region.

The RR transfer function at the straight or through port (see Figure V-2), considering previous description of the evanescent field region, is given by:

$$\left| \frac{E_3}{E_1} \right|^2 = (1-g) \left[ \frac{K - 2\sqrt{K}H^* \cos(\beta L_t) + (H^*)^2}{1 - 2\sqrt{K}H \cos(\beta L_t) + (1-K)(H^*)^2} \right] \quad [\text{V-3}]$$

Where  $H^*$  is overall loop loss, and it is:

$$H^* = 10^{-\frac{\alpha_1 L_1 + \alpha_2 L_2}{20}} \sqrt{(1-g)ATN} \quad [\text{V-4}]$$

where  $ATN$  represents any losses inside the loop apart from material absorption loss, such as scattering losses in an interface between two different materials or radiation losses in waveguide bends;  $\alpha_1$  and  $\alpha_2$ ,  $L_1$  and  $L_2$  are attenuation coefficients and lengths of SiN and LC sections respectively.  $L_t$  is total loop length, being  $L_t = 2 \cdot \pi \cdot R + 2 \cdot L_2$  and  $\beta$  is the fundamental mode propagation coefficient in the waveguide.

Resonance frequencies are obtained when  $\cos(\beta L_t) = 1$ , and the FSR is the inverse of the optical delay time ( $\text{FSR}=1/\tau$ ), which is given by:

$$\tau = \frac{n_1 \cdot 2 \cdot \pi \cdot R + n_2 \cdot 2 \cdot L_2}{c} \quad [\text{V-5}]$$

being  $c$  the speed of light,  $n_1$ , and  $n_2$  the effective refractive index of SiN and LC sections respectively.

Critical coupling, or condition that makes the through port output field equal to zero, is given by:

$$K = (H^*)^2 \quad [V-6]$$

The quality factor of the resonator is given by:

$$Q = \frac{f_0}{FWHM} \cong \frac{f_0}{FSR} \mathfrak{J} \quad [V-7]$$

where  $f_0$  is the fundamental resonance frequency, and  $FWHM$  is the Full Width Half Maximum and  $\mathfrak{J}$  is the *Finesse*, which is given by:

$$\mathfrak{J} = \frac{FSR}{FWHM} \quad [V-8]$$

### V.3.b.- Simulation Software and Waveguide Parameters

Once the introduction of the equations that governs RR behaviour is presented, it is time to introduce the software and the waveguide parameters used for testing the design. Apart from commercial *FullWAVE* software (by R-Soft), in some cases output data are afterwards treated with MATLAB.

Some of the results and simulations have been partially obtained during the research stay in La Sapieza, University of Rome under the supervision of Prof. Antonio d'Alessandro, and supported by PhD student Domenico Dionisi. Some of the results are summarized in [Vázquez-2007].

The type of input field is selected through the drop down box shown in Figure V-4. For 2D simulations, this input field is a normal mode of a slab waveguide with characteristics matching those of the input waveguide. TE input mode is considered in all the simulations, which is defined to be primarily along Y,  $E_y(x,z)$ .

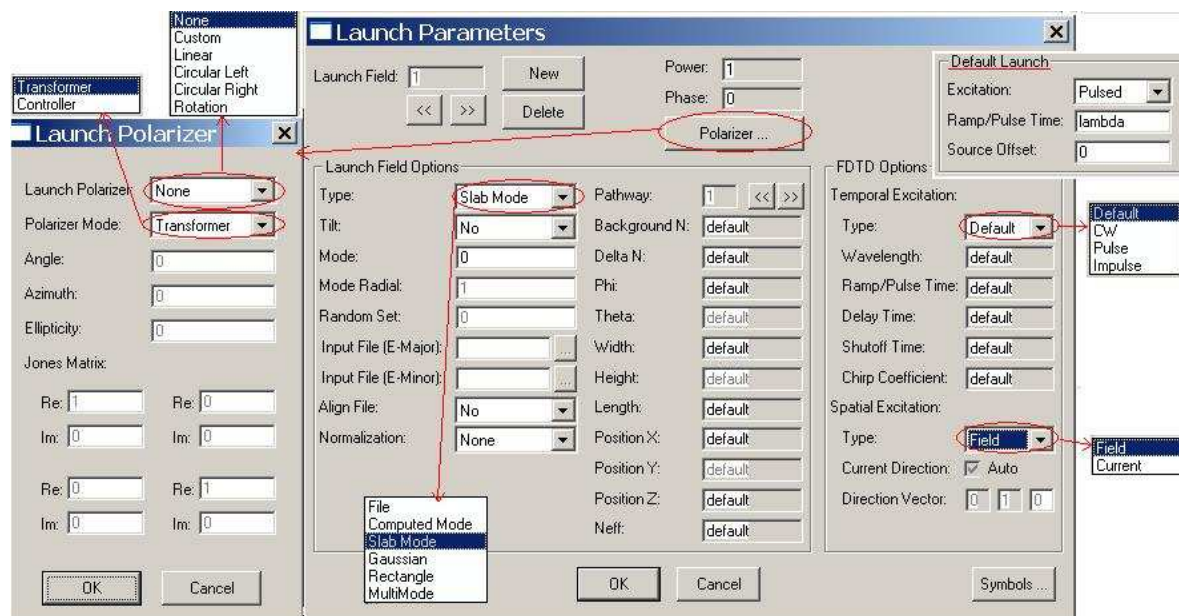


Figure V-4: Launch Parameters in the Commercial Software used in Simulations.

Impulse excitation is used for obtaining the response in the wavelength domain. For checking RR behaviour at a single wavelength, CW excitation is employed.

The high refractive index contrast available in silicon-on insulator SOI is used in the simulations, expecting compact micro ring resonators with low loss and high- $Q$ . The waveguides of  $\mu$ RR prototypes have the parameters described in Table V-1. LC effective refractive index are closed to those reported in [Maune-2003] for a NLC E7 mixture. Ideal waveguides in terms of attenuation coefficient are considered, that is,  $\alpha=0\text{dB/cm}$ . In this device the LC refractive index can be changed by applying an external electric field (electrooptic effect), which induces a molecular reorientation. In fact, it is assumed that when no electric field is applied (LC-off), TE light senses the LC extraordinary refractive index (1.75) and when the electric field is applied (LC-on), the LC molecules are reoriented such that TE light senses the LC ordinary refractive index (1.5).

	Core (LC-on)	Core (LC-off)	Core (SiN)	Cladding (SiO <sub>2</sub> )
Refractive Index @ 1550nm	1.5	1.75	2.01	1.45
Wavelength			1.5 $\mu\text{m}$	

Table V-1:  $\mu$ RR parameters, waveguide with LC on (LC-on) and off (LC-off) respectively.

### V.3.c.- Simple Ring Resonator Configuration

As previously reported there is a great interest in developing compact tuneable  $\mu$ RR to be used as part of complex photonic circuits. In this respect, SOI and LC offer a good opportunity, which up to now is only explored in a single configuration and with a limited tuning range of 0.22nm.

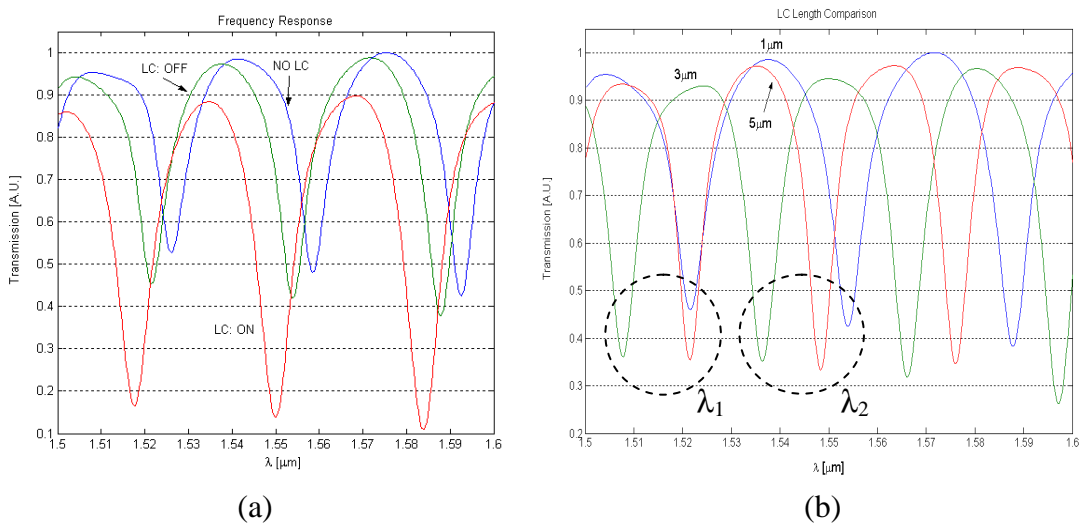


Figure V-5: Different Frequency Responses of the  $\mu$ RR obtained for Distinct Device Configurations.

In this section, a  $\mu$ RR with LC in the waveguide core in part of the loop length, which is technologically possible as reported in [d'Alessandro-2006b] is analyzed. The influence of LC inside the loop in OFF and ON state, for a LC length of 1  $\mu\text{m}$ ,

and the particular case of having no LC can be seen in Figure V-5 (a). For this specific design a tuning range of 10nm is achieved, this value can be increased up to half the FSR (13nm), so tuning from peak to null wavelengths, for a LC length of 5 $\mu\text{m}$ . It has also been shown the dependence of  $\mu\text{RR}$  FSR on the different lengths of the LC section in the loop (see Figure V-5 (b)).  $\mu\text{RR}$  waveguide parameters are those reported in Table V-I, and with radius R of 5 $\mu\text{m}$ .

Figure V-5 (b) shows the transfer functions for different lengths of the LC waveguide, the FSR of each one depends on the total loop length, calculations are reported on Table V-2.  $\lambda_i$  for  $i=1,2$  are the first two resonance frequencies from 1.5 to 1.6 $\mu\text{m}$ .

LC Length	$\lambda_1$ ( $\mu\text{m}$ )	$\lambda_2$ ( $\mu\text{m}$ )	$\Delta\lambda$ (nm)	FSR (THz)
1 $\mu\text{m}$	1.522	1.554	32	4.05
3 $\mu\text{m}$	1.508	1.536	28	3.62
5 $\mu\text{m}$	1.522	1.548	26	3.31

Table V-2: FSR Obtained for Different LC Lengths from Figure V-5 (b).

- **Critical Coupling Optimization and Compact Design**

The analysis of filter's transmission for different gaps between the waveguide and the resonator can be used for analysing the critical coupling and it is basic for achieving high  $Q$  values, as it has been measured in [Morand-2006].

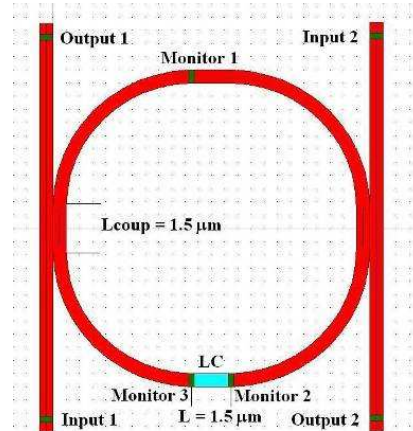
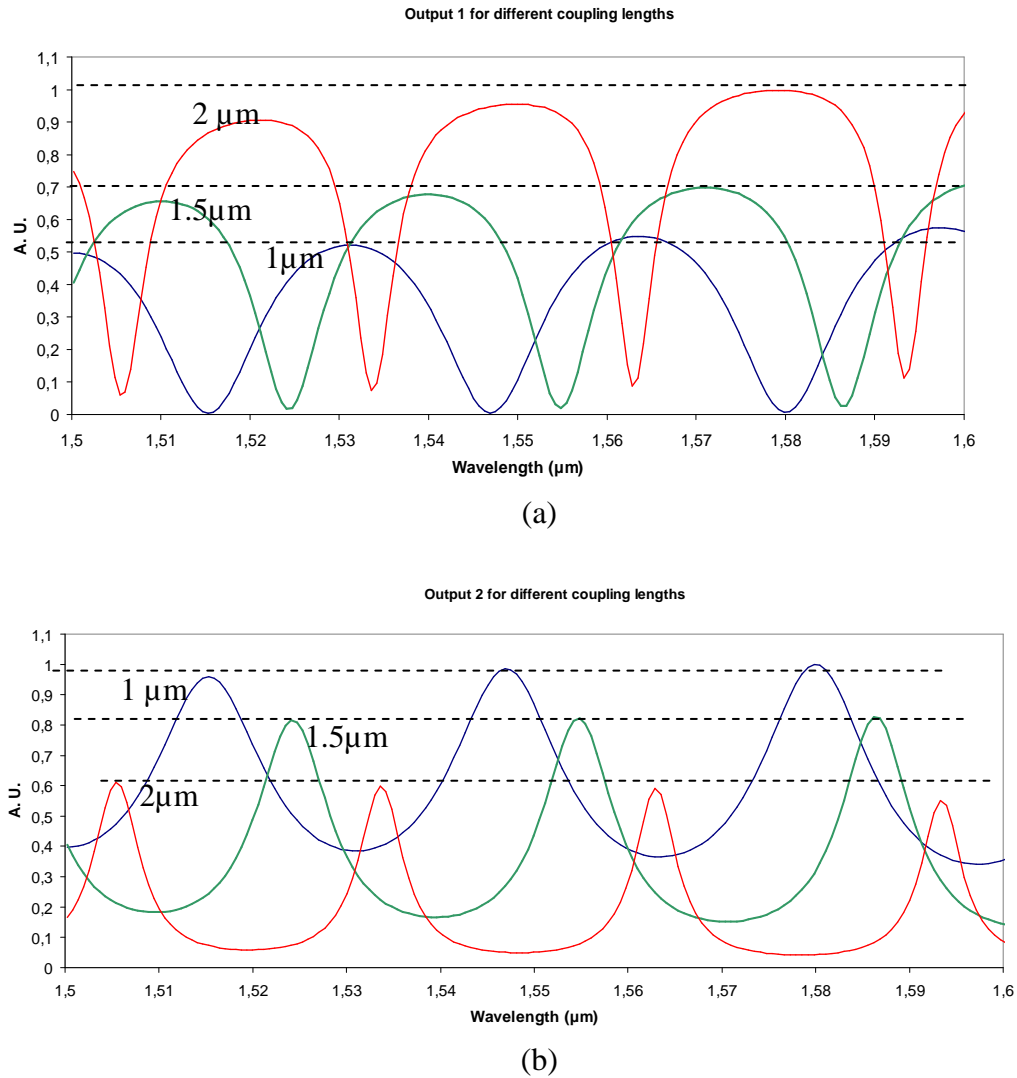


Figure V-6:  $\mu\text{RR}$  with a single LC and  $L_{coup}$

This influence is shown in Equation V-1 where it is observed that critical coupling depends on the coupling strength between the waveguide and the ring resonator. A specific straight waveguide of length,  $L_{coup}$ , with no Gap between both waveguides are included in the evanescent coupling length for improving crosstalk and insertion losses (see Figure V-6). Some simulations with different straight coupling lengths,  $L_{coup}$ , have been developed. Additionally only one LC is placed in the loop length after the drop channel to avoid optical power loss related to Fresnel reflections in the interface of two materials and related to refractive index changes. Results are shown in Figure V-7 for both outputs, in all simulations, the loop length in  $L_{coup}$  has also been increased. Analyzing the through port response at Figure V-7 (a), a higher

crosstalk is achieved by using  $L_{coup}=1.8\mu\text{m}$ , but considering also the drop port, Figure V-7(b), a better design length is around  $1.5\mu\text{m}$ .



**Figure V-7:** Output Power in the Through Port (a), and at the Drop Port (b) versus Wavelength for Different  $L_{coup}$

### V.3.a.- Cross-Grid Configuration

On the other hand, for achieving compact designs, cross-grid configurations with vertically coupled  $\mu\text{RR}$  have been proposed [Kolubun-2005]. Therefore, in this section, a planar  $\mu\text{RR}$  in a cross-grid configuration is designed. The structure has an input and three outputs. Optical behaviour in each output port depends on the LC state.

Numerical simulations of the instantaneous electric field intensity pattern in an ideal side-coupled for two wavelengths with no LC, and a coupling length,  $L_{coup}$ , of  $1\mu\text{m}$ . is shown in Figure V-8. In cross-grid configuration, output 1 is minimum for  $\lambda = 1.548\mu\text{m}$  (Figure V-8 (a)), and it is maximum for  $\lambda = 1.565\mu\text{m}$  (Figure V-8 (b)). In

the same way, in the conventional configuration, output 1 is minimum for  $\lambda = 1.548\mu\text{m}$  (Figure V-8 (c)) and output 1 is maximum for  $\lambda = 1.565\mu\text{m}$  (Figure V-8 (d)).

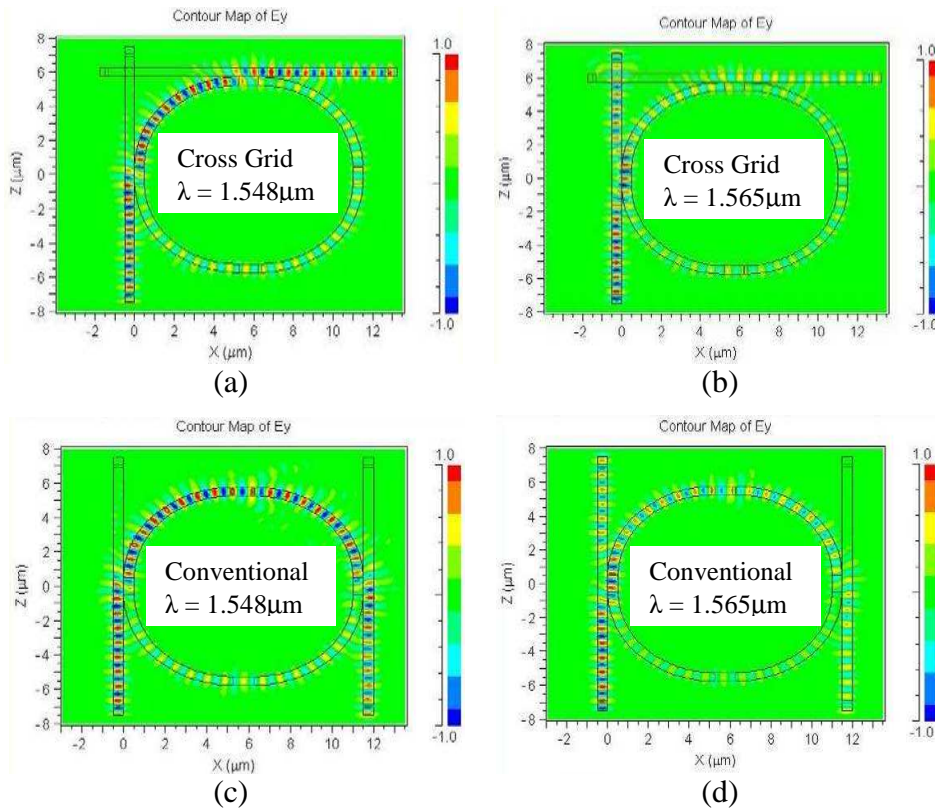


**Figure V-8:** Simulations of an Ideal Side-Coupled  $\mu\text{RR}$  for Two Wavelengths with no LC,  $L_{\text{coup}}=1\mu\text{m}$

Two wavelengths with complementary response have been chosen, a channel wavelength of  $1.548\mu\text{m}$  that is dropped in both configurations and a channel wavelength of  $1.565\mu\text{m}$  that goes through in both configurations but with some losses. Equivalent behaviour has been obtained in both configurations.

Simulations of the different structures at  $1.564\mu\text{m}$  wavelength with two strengths of LC, in ON state, placed in the loop length are shown in Figure V-9. Lower losses have been obtained for the structure when the LC is placed after the drop port. For this device, changing LC from ON to OFF state, a 7 nm detuning is achieved

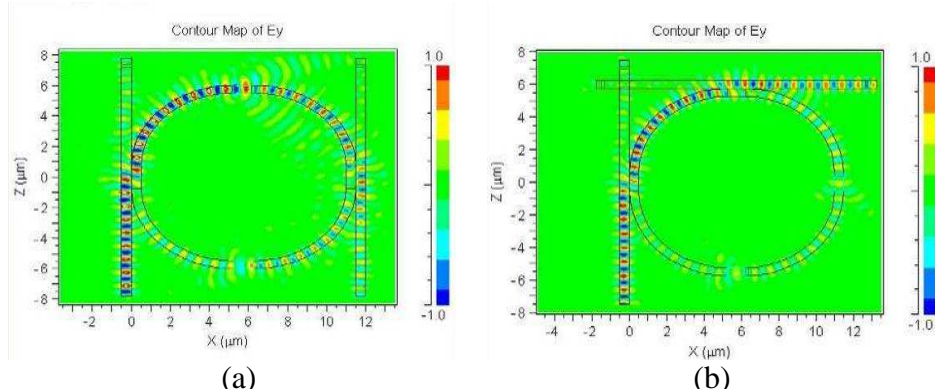


**Figure V-9:** Simulations of Ideal Side-Coupled  $\mu\text{RRs}$  with Two LC ON at  $\lambda = 1.564\mu\text{m}$ :  
 (a) Conventional, (b) Cross-Grid Configuration

### V.3.a.- Compound Structure

Different compound structures can be developed, for obtaining switches that are more complicated. A serial of two  $\mu$ RR in a cross-grid configuration is proposed. It has been tested as a reconfigurable three-channel demultiplexer (see Figure V-10). The through (output 1) and drop (output 2) port response versus wavelength for each individual  $\mu$ RR are shown in Figure V-10 (b), they are identified by LC length labels as: LC1 (2 $\mu$ m) and LC2 (1.9 $\mu$ m) and in all cases LCs are OFF. Three outputs power channels versus wavelength in the compound configuration are presented in Figure V-10 (c), where there are marked those wavelengths that have a maximum output power only at a single output channel: 1)  $\lambda_1=1.595\mu\text{m}$ ; 2)  $\lambda_2 = 1.554\mu\text{m}$ ; 3)  $\lambda_3 = 1.541\mu\text{m}$  (c).

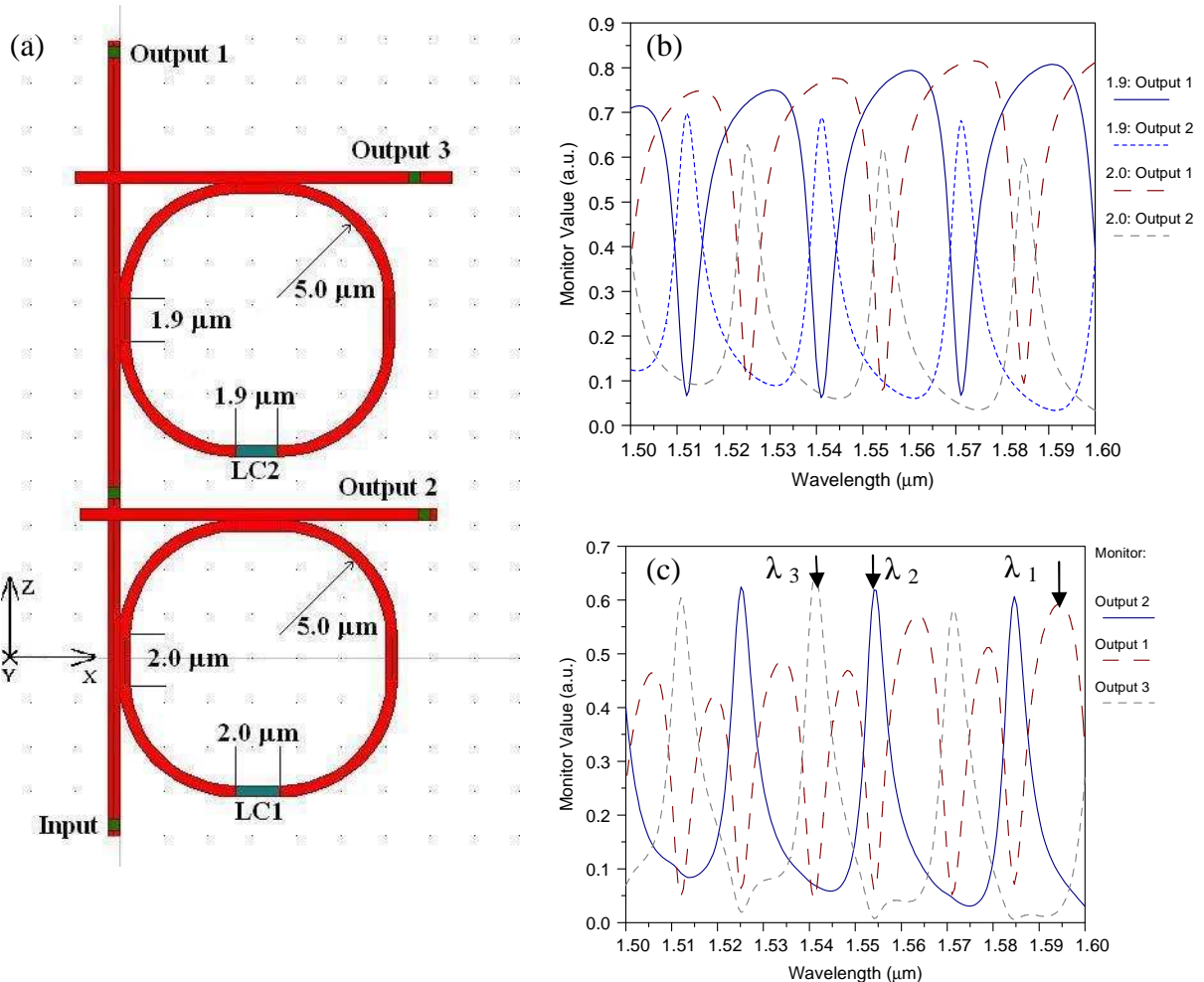


**Figure V-10:** Serial of Two  $\mu$ RR in a Cross-Grid Configuration: Structure (a), Individual Response (b) and Compose Response (c)

Instantaneous electric field intensity patterns in the serial  $\mu$ RR configuration, shown in Figure V-10 (a), have been numerically simulated for the selected input channel wavelengths that are marked in Figure V-10 (c). Those simulations are presented in Figure V-11 for all LC in OFF state.

Maximum at *Output 1* and minimum at *Output 2* and *Output 3* are obtained at  $1.541\mu\text{m}$  wavelength (see Figure V-11 (a)). Maximum at *Output 2* and minimum at *Output 1* and *Output 3* is obtained for  $1.554\mu\text{m}$  wavelength (see Figure V-11 (b)). Maximum at *Output 3* and minimum at *Output 1* and *Output 2* are obtained at  $1.595\mu\text{m}$  wavelength (see Figure V-11 (c)). The maximum crosstalk is achieved for wavelength  $\lambda = 1.554\mu\text{m}$  demultiplexed at *Output 2*. In all these simulations, LC is in OFF state.

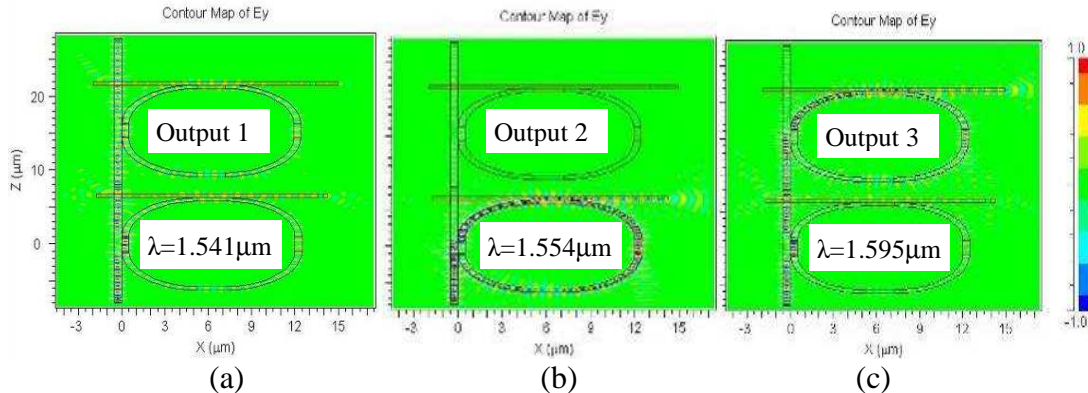


**Figure V-11:** Simulations of a Serial of two  $\mu$ RR in Cross-Grid Configuration for Three Wavelengths, and LC OFF.

It seems that for avoiding possible coupling between ring resonators at closed LC sections, they should be a bit more apart from each other, this will be optimize in future designs. In addition, as previously reported by other authors the through channel, or wavelength demultiplexed at output port 1 has high losses because there is a multiplication of the transfer function of both RR with the corresponding accumulative loss penalties.

Finally, simulations of serial two  $\mu$ RR cross-grid configuration output powers versus wavelength for different LC ON and OFF conditions have been developed. Results are shown on Figure V-12, *Output 2* corresponds to Figure V-12 (a) while *Output 3* is in Figure V-12 (b).

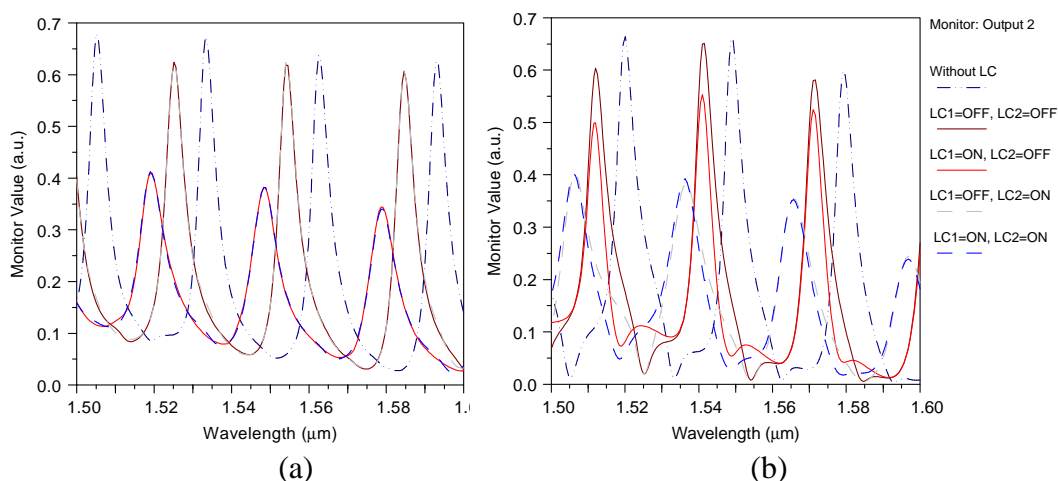


**Figure V-12:** Serial Two  $\mu$ RR in a Cross-Grid Configuration for Different LC states. Compound  $\mu$ RR Response Versus Wavelength at Output 2 (a) and at Output 3 (b).

If a specific channel, for instance a TE field at  $\lambda = 1.541\mu\text{m}$ , is launched; it can be seen that maximum output power is on port 3. By changing the LC state, the output power at a specific wavelength in each output is shifted.

Depending on the output considered, the state of a specific LC does not affect to the frequency response. On the other hand, related to the *Output 3*, tuning range of about 5nm in the different conditions and loss increasing is observed, as previously reported. In addition, losses increase in all channels when both LC are ON.

#### V.4.- Tap and Two Split Switch Based on Mach-Zehnder Interferometer

In this section, a specific switch for being used in Multicast-Capable Optical Cross Connect (MC-OXC) architecture is developed [Fernández-2009].

Multicast is a way for providing communication from point-to-multipoint, one source sends information to multiple destinations [Zhou-2005]. Optical multicast refers to performing multicast directly on optical layers in the network.

Optical multicast can be developed over WDM networks where a dynamically configurable photonic switch, or Optical Cross-Connect (OXC) is placed in each node. OXCs have the capability to switch connection based on wavelengths carrying data. When the OXC is able for light splitting is referred as MC-OXC.

For a point-to-point request, the *lightpath* concept is used. It corresponds to an all optical channel form the starting point to the receiver. In order to implement optical multicast, the *lightpath* concept was generalized in [Sahasrabuddhe-1999] to that of *light-tree*, that refers to the point-to-multipoint all-optical wavelength channel.

The key element of *light-tree routing* is the MC-OXC. Different architectures have been proposed, Split and Delivery (SaD) [Ali-2000 a, Hu-1998] or Tap-and-Continue (TaC) [Ali-2000b]. Tap and two split (Ta2S) is a compromise because has some advantages in comparison with the previous architectures; it is power efficiency and is easier to perform than any  $n$  split.

Therefore, a device with a single input signal and two output signals, able to switch to any of the outputs (0:100 or 100:0), or to share the optical power to both outputs (50:50) is necessary. The optical switch has also to be able to tap a fixed value of the incoming signal. This novel device is named *Tap-and-2-Split switch (Ta2S switch)* that we have designed for the first time with existing photonic devices.

#### V.4.a.- Proposed Structure of the Tap-and-Two Split Switch

According to the requirements presented, the Ta2S switch has three outputs. TAP is used for providing 6% of the input power to the local node (see Figure V-13). The remaining optical power can be switched from an output to the other, or even 50% in each one. These outputs, named  $P_{BAR}$  and  $P_{CROSS}$ , allow connecting this node with two adjacent nodes. In this way, continue or splitting functionalities are possible.

The 2-split operation is a good choice because only splitting in two is a good compromise between the amount of the used resources and power efficiency. In addition, it is easier to perform splitting in two than multiple splitting, in terms of, component used, losses or manufacturing complexity. In this way, the use of optical amplification is reduced.

The given fixed tap value comes from analyzing the optical transmission along an  $n$ -nodes branch. The signal has to transverse  $m$  nodes performing tap-and-2-splitting until it cannot be detected by the following node. The number of reachable nodes is optimized by using a fixed 6% tap.

The proposed switch, as a novel contribution of this PhD work, has been designed in integrated optics in order to obtain a more compact device. The structure is comprised by a 94:6 MultiMode Interference (MMI) splitter for implementing TAP operation, followed by a reconfigurable Mach-Zehnder Interferometer (MZI) switch [Tarek-2006] that perform the continue or split functionalities. A schematic of the novel device is shown in Figure V-13.

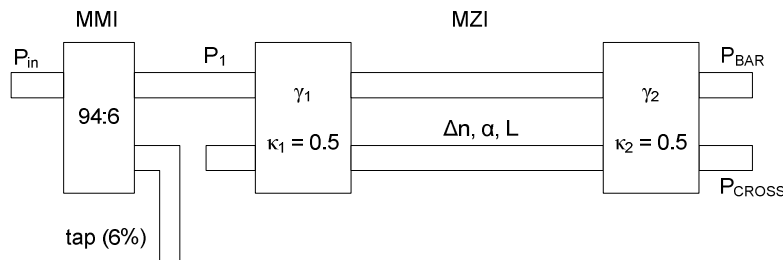


Figure V-13: Schematic of a Ta2S Switch Composed of a Fixed Splitter and an MZI.

The MZI is formed by two 3dB MMI couplers, with coupling ratios  $\kappa_1 = \kappa_2 = 0.5$  and excess losses  $\gamma_1$  and  $\gamma_2$ , joint by two waveguides of length  $L$  and attenuation  $\alpha$ . The switch output is selected by modifying the refractive index difference between both waveguides,  $\Delta n$ .

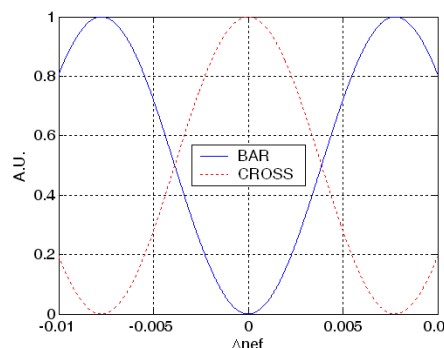


Figure V-14: Output Power Response at Bar and Cross Outputs of MZI vs  $\Delta n$ .

Thus, when  $\Delta n = 0$ , at initial setup, all the optical input power is guided to the  $P_{CROSS}$  output port, having both Mach-Zehnder arms equal length  $L$ . When the refractive index difference is induced, either by applying current or by thermo-optic effect, the optical power at both output ports changes. Output power variations,  $P_{BAR}$  and  $P_{CROSS}$ , with the refractive index difference changes between the waveguides are shown in Figure V-14. Outputs are symmetrical, a maximum in cross output coincides with a minimum in bar output, and the optical power at each port can be adjusted modifying  $\Delta n$ .

A compact solution can be realized using MMI splitter for the tap [Feng-2007] and 3dB MMI couplers [Vázquez-1995] in the MZI. The MMI operation is based on the property of self-image of the light propagation in planar waveguides [Heaton-1999, Soldano-1995]. A MMI coupler consists of two inputs and two outputs attached to a wider section waveguide whose length determines the coupling ratio.

In next section, there is an overview of the theory applied to the switch based on a MZI, in order to help understanding the expected behaviour of the switch, although commercial software based on FDTD have been used in the simulations.

#### V.4.b.- Theory

The structure of the switch is made of three MMIs, joint by waveguides. Proposed MMI couplers have their input and output waveguides placed at a third part of the MMI width in order to obtain a shorter device, and its length is given by:

$$L_{MMI}(3dB) = \frac{1}{2} L_\pi = \frac{1}{2} \frac{4 \cdot W_e^2 \cdot n}{3 \cdot \lambda_0} \quad [V-9]$$

Where  $L_\pi$  is the beat length,  $W_e$  is the MMI width,  $\lambda_0$  is the vacuum wavelength and  $n$  is the effective refractive index of the waveguide [Feng-2007, Vázquez-1995].

The overall behaviour of the proposed Ta2S is governed by the next expressions. Equation V-10 presents the optical power in the  $P_{BAR}$ , while Equation V-11 corresponds to  $P_{CROSS}$ .

$$\left| \frac{P_{BAR}}{P_{IN}} \right| = \Gamma \cdot \left[ \frac{(1 - \kappa_1) \cdot (1 - \kappa_2) \cdot e^{-2 \cdot \Delta\alpha \cdot L} + \kappa_1 \cdot \kappa_2}{-2 \cdot \sqrt{(1 - \kappa_1) \cdot (1 - \kappa_2) \cdot \kappa_1 \cdot \kappa_2} \cdot e^{-\Delta\alpha \cdot L} \cos(\Delta\beta \cdot L)} \right] \quad [V-10]$$

$$\left| \frac{P_{CROSS}}{P_{IN}} \right| = \Gamma \cdot \left[ \frac{(1 - \kappa_1) \cdot (1 - \kappa_2) \cdot e^{-2 \cdot \Delta\alpha \cdot L} + \kappa_1 \cdot \kappa_2}{+2 \cdot \sqrt{(1 - \kappa_1) \cdot (1 - \kappa_2) \cdot \kappa_1 \cdot \kappa_2} \cdot e^{-\Delta\alpha \cdot L} \cos(\Delta\beta \cdot L)} \right] \quad [V-11]$$

$$\Gamma = (1 - Tap) \cdot (1 - \gamma_{Tap}) \cdot (1 - \gamma_1) \cdot (1 - \gamma_2) \cdot e^{-2 \cdot \alpha \cdot L} \quad [V-12]$$

$$\Delta\beta = \frac{2 \cdot \pi}{\lambda_0} \cdot \Delta n \quad [V-13]$$

Being  $P_{IN}$ ,  $P_{BAR}$  and  $P_{CROSS}$  optical powers at the input, bar and cross output respectively.  $Tap$  is the optical portion of the power needed for the tap operation.  $\gamma_{tap}$ ,  $\gamma_1$  and  $\gamma_2$ , are the excess losses of each MMI coupler;  $\kappa_1$  and  $\kappa_2$  are the coupling ratios.  $L$  is the waveguide length,  $\alpha$  is the attenuation of the waveguide in Neppers/m.  $\Delta\alpha$  is the attenuation increment due to the variation of the refraction index in Neppers/m.  $\Delta\beta$  is the change of the propagation constant due to refractive index change ( $\Delta n$ ), and  $\lambda_0$  is the vacuum wavelength.

When the refractive index is modified, an increment of the attenuation loss is expected. The increment of attenuation simulated is accorded to the equation given in [Leuthold-2001] for free-carrier-absorption when current injection is used to change the refractive index.

The necessary  $\Delta n$  for optical switching is obtained by solving Equation V-10, when bar output is 1, considering that there are no losses when the MMI is switched.

$$\Delta n = \frac{\lambda_0}{2 \cdot L} \quad [\text{V-14}]$$

The obtained refraction index variation necessary for switching a 100  $\mu\text{m}$  length waveguide MZI has been  $\Delta n = -7.75 \cdot 10^{-3}$ . Simulations have been made with a 6% *tap*, 0.1 dB extinction losses for each MMI, coupling ratios  $\kappa_1 = \kappa_2 = 0.5$ , 100  $\mu\text{m}$  waveguide length ( $L$ ), and 1.55  $\mu\text{m}$  vacuum wavelength.

A description of the Ta2S switch has been done using Matlab in order to probe the equations presented. These simulations have been carried out because it is important to know the losses induced by the optical switch, because it has to be taken into account for estimating the overall losses along the light tree, that determine the election of one or another lightpath.

Output powers of the Ta2S switch as a function of refractive index variations at ideal (lossless) and real case are shown in Figure V-15 (a). Excess losses, as it is defined in Section II.5, about 0.7dB and 0.55dB have been obtained for bar and cross outputs, respectively, when they have been active. Insertion losses have been about 3.7dB when switch have been in (50:50) configuration. A fabrication tolerance error of 0.1% in both MMI coupling ratios,  $\kappa_1$  and  $\kappa_2$ , have also been considered in simulations. A detail of the bar output in active state is shown in Figure V-15 (b).

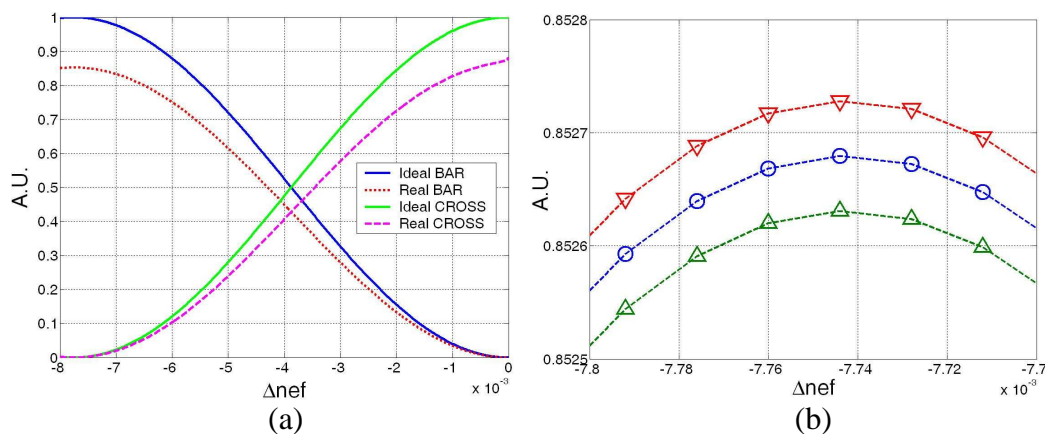
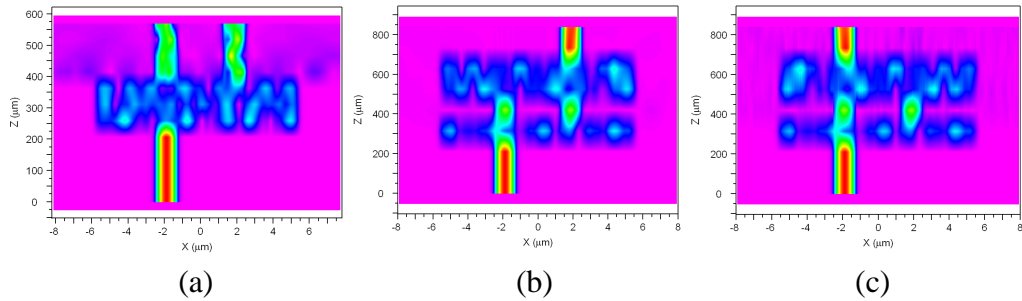


Figure V-15: Simulation Results for a MZI Optical Switch with Fixed Tap

#### V.4.c.- Simulation of the Structure

Finally, simulations using the Beam Propagation Method (BPM) at  $\lambda_0 = 1550\text{nm}$  have also been carried out in order to show the operation principle. The effective refraction index of the ridge waveguides has been 3. The waveguides have been  $1.3\mu\text{m}$  wide, and the 3dB MMI couplers have been  $11.3\mu\text{m}$  wide and  $170\mu\text{m}$  long. A detail of the optical power distribution in the 3dB MMI, is shown in Figure V-16 (a). Two simulations of the MZI with  $100\mu\text{m}$  long waveguides between the two couplers, have been carried out. Figure V-16 (b) shows the initial state while Figure V-16 (c) corresponds to simulation when  $\Delta n=-0.00775$ . The output for both cases has changed.



**Figure V-16:** Distribution of the optical power: in the MMI 3dB coupler (a), in the MZI at initial state (b) and when the MZI is Switched

The Ta2S can also be realized using a tuneable splitter [Leuthold-2001], a  $2\times 2$  MMI with symmetric splitting ratios. The insertion losses for the different states of the Ta2S optical switch are given by the following equation:

$$PL_{Ta2S} = PL_{tap} + \begin{cases} PL_{cross} \\ PL_{bar} \\ PL_{2-split} \end{cases} \quad [V-15]$$

Where  $PL_{tap}$  corresponds with the insertion losses due to the tap operation,  $PL_{cross}$  and  $PL_{bar}$  are losses in cross or bar states and  $PL_{2-split}$  is the excess loss when performing 2-splitting, and corresponds with the given values.

Once the insertion losses of the Ta2S optical switch are given, the expression for losses in the complete node is given by:

$$IL = PL_{ta2S} + 10 \log(m) + (\log_2 P + 1) \cdot PL_{sw2x1/2x2} \quad [V-16]$$

Being,  $IL_{Ta2S}$  the insertion losses obtained before,  $P$  the number of output ports,  $m$  is the split factor, 1 or 2,  $PL_{sw2x1/2x2}$  is the power loss due to the  $1\times 2$  or  $2\times 2$  switching element.

A comparison of the 2-STCM, based on the Ta2S optical switch, with other technologies for different number of ports is given in Figure V-17. It shows the power loss of a single optical signal when a tap/drop and continue action is preformed. The insertion losses of the 2-STCM remain low when the number of ports increases.

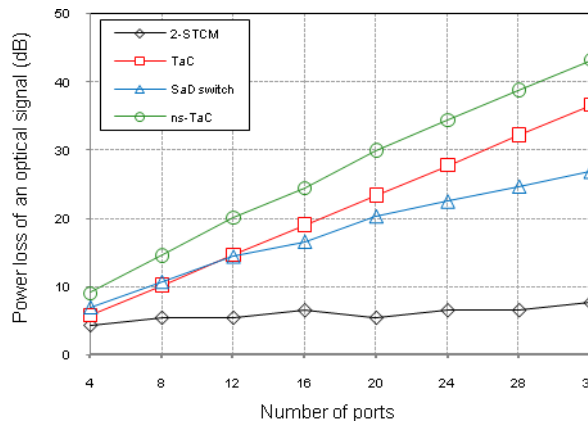


Figure V-17: Comparison Between Different Architecture Modules

Related to the overall behaviour of the architecture based on the proposed optical switch, the average optical power that arrives at each node is one of the most important parameters in the evaluation of these architectures. A comparison of the ratio of the average incoming power to each node per kilometre is shown in Figure V-18.

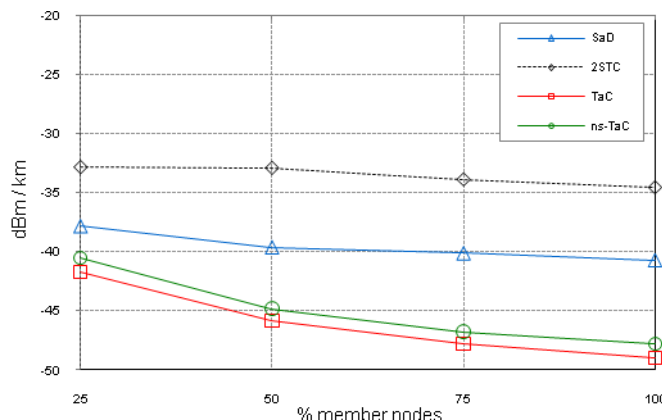


Figure V-18: Ratio of Average Incoming Power per Kilometer (dBm/km) for Different Architecture Modules

Higher optical power is received in the 2STC architecture, built with the proposed optical switch, Ta2S. This is due to the combination of the optical switch proposed that has less losses than other alternatives, the use of the 6% tap for the local node and the advantage of only splitting in two, if it is necessary, the incoming optical power that reduces the power losses when light propagates through the node.

Usefulness of the device in terms of optimizing the selection of the final light path in terms of reconfigurable routing in long haul networks have been studied by members of Prof. D. Larrabeiti researching group of Telematics Department at UC3M.

Further information, about software simulation tool can be seen in Appendix C.

### V.5.- Summary and Conclusions

In this chapter, an overview about switches based on integrated optics has been presented. The study has been focused in two kinds of switches, those based on RR and LC and those based on a MZI.

For the first technology, RR in combination with LC, different designs are proposed. Simulations of the basic structure with distinct parameters: different RR lengths, coupling ratio or waveguides stretches with LC inside the loop, are carried out in order to test the variation of the RR response.

All the parameters modified have changed the FSR of the structure. RR tuning has been possible by changing the state of the LC present in the waveguide. LC switch can be obtained by applying voltage to it.

Availability of RR with LC inside the loop in cross-grid has also been probed. Its behaviour is similar to the basic structure when same parameters are used. Cross-grid scheme allows implementing compound structures. Thus, a reconfigurable three-channel demultiplexer comprised by two serial RR is proposed. Reconfiguration has been done by modifying electrically the LC state.

Last section of the chapter has been focused in implementing a Tap and two Split Ta2S switch for being used in a multicast capable optical cross connect node architecture that features both tap-and-continue and tap-and-binary-split functionalities. By using this type of optical switch, the power efficiency of the light tree is increased, and less uses of optical amplifier is required.

An optical switch based on integrated optics has been designed for implementing the required functionalities. It is comprised by a 94:6 MMI splitter in combination with a reconfigurable MZI switch.

Simulation of the Ta2S switch has been done. Matlab has been used for simulating the behaviour of the switch described by the equations given in section V.4.b. These simulations have been carried out because it is important to know the losses induced by the optical switch, because it has to be taken into account for estimating the overall losses along the light tree, that determine the election of one or another lightpath.

The obtained refraction index variation necessary for switching a  $100\mu\text{m}$  length waveguide MZI has been  $\Delta n = -7.75 \cdot 10^{-3}$ . Simulations have been made with a 6% *tap*, 0.1 dB extinction losses for each MMI, coupling ratios  $\kappa_1 = \kappa_2 = 0.5$ ,  $100\mu\text{m}$  waveguide length ( $L$ ), and  $1.55 \mu\text{m}$  vacuum wavelength. BPM software has been utilized in order to probe the results obtained in Matlab.



# Chapter VI

## Optical Characterization Bench

---

*This chapter describes the implementation of an optical bench that can be used for characterizing different optical devices. After a brief introduction, the requirements of the optical characterization bench are indicated. The proposed structure of the bench is presented in section three.*

*Section four introduces the precision movement system. It is composed by a universal controller that can manage up to three axes, and the actuators in charge of doing the movement. The application programmed in LabView that allows the control of the system using a computer is presented in section five.*

*Measurements carried out for testing the behaviour of the system is given in section six, while measurements within the framework of this PhD work where reported on section IV. Finally, the summary and main conclusions are given in the last point of the present chapter.*



## VI.1.- Introduction

Previous chapters describe different novel structures proposed for different optical devices. Those presented in Chapter III and IV have been partially characterized with the optical bench reported in this chapter.

Additionally to the optical characterization of the implemented schemes, the bulk elements that make up these devices need also being tested in order to determine its contribution to the overall behaviour. This issue reaches in a great amount of measurements to be done. For this reason, it is convenient to develop an automated measure system for characterizing all the components.

The automated characterization system should allow characterizing a huge variety of components, thus, it should be reconfigurable. Distinct optical sources and sensors should be used in order to make different types of characterizations. Therefore, the Optical Characterization Bench is implemented for making easy the measurement acquisition.

The proposed system is able of obtaining measurements automatically. Additionally, an automated position system makes possible the acquisition of different measurements when the input or the device under test, are in different positions.

In this chapter, the description of the Optical Characterization Bench is given, in order to show just the potential and work done in setting up the bench.

## VI.2.- Requirements

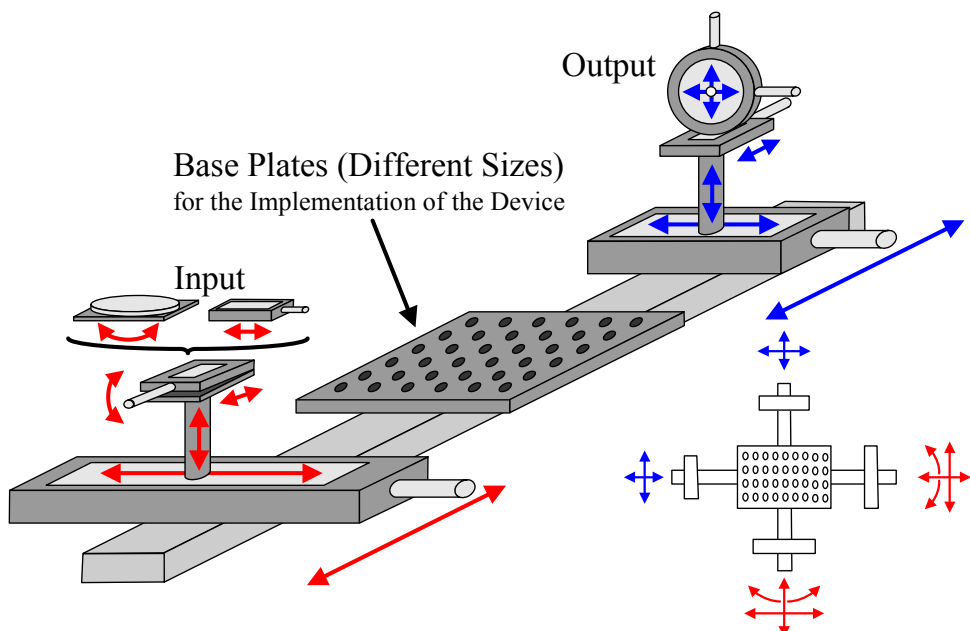


**Figure VI-1:** Structure Proposed for the Optical Characterization Bench.

The proposed system should be used in a wide variety of applications, so the main requirement is its flexibility. Figure VI-1 shows the structure proposed for the Optical Characterization Bench.

The Optical Characterization Bench is divided in three sections: input, device under test and output. The device under test should be placed in a separate base in order to allow its retirement without dismantle the experiment when required. Different bases sizes should be necessary for implementing devices with distinct lengths.

Both input and output parts should allow their movement in different axes. In this way, characterization of a sample when the input comes from distinct positions can be done. Depending on the application or device under test, some of the allowed movements should be manual, and some others could be automated. Additional inputs and outputs should be provided for the characterization of some devices.

The movement range can vary from microns, when the optical bench is used for coupling light in singlemode optical fibres, to several centimetres when an optical device is characterized. Related to the elements used in the input ports, it is possible the use of different types of optical fibre (singlemode and multimode silica and polymer one) with different kinds of connectors, but it is also possible the use of laser modules at different wavelengths. In the output ports, in addition to the optical fibres, some photodiodes or optical powerometers can also be used in the devices' characterization. For this reason, it is necessary to have different elements that makes possible the use of the listed elements in the proposed Optical Characterization Bench.

### VI.3.- Structure of the Optical Characterization Bench

The Optical Characterization Bench is basically formed by a three axes precision linear stage, translation stages, breadboards and rails. In addition, automation of three axes is carried out by using actuators handled by a motion controller.



**Figure VI-2:** Picture of the Three Axes Precision Linear Stage M-562-XYZ from Newport

The three axes precision linear stage is placed at the input of the Optical Characterization Bench. It has a 13mm travel in all its axes M-562-XYZ from Newport, and additionally a tilt mount with a rail is placed at its top. Different items are available for being mounted in the rail; fibre and lenses holders can be used for implementing and aligning the input part of the system. Figure V-2 shows a picture of the three axes precision linear stage.

Four 25mm linear travel translation stages M-UMR8.25 from Newport (see Figure VI-3) and two 50mm linear travel stages M-UMR8.51 from Newport can be combined using angle brackets and other mounting elements allow the implementation of other inputs or outputs. In addition, a rotation stage M-RS65 from Newport (see Figure VI-4) makes possible performing angular displacements. Figure VI-5 introduces a possible implementation of the input or output systems.



Figure VI-3: Picture of a 25mm Linear Translation Stage M-UMR8.25 from Newport



Figure VI-4: Picture of the Rotation Stage M-RS65 from Newport



Figure VI-5: Possible Implementation of the Input or Output Part

Three motorized actuators can be used for automating three axes of the system. Manual actuators can be used with the rest of the other translation stages. The automated axes can be used in different places depending on de applications, or the measurements to be done. A precision movement system, capable of controlling three actuators can be used for automating the desired axes of the input or of the output.

Figure VI-6 shows the picture of the proposed Optical Characterization Bench. Rail system makes easy the implementation of the experiment. The three axes precision linear stage is placed in one of the inputs, as it is depicted in the lower part of Figure VI-6. The device under test can be built in a separate aluminium plate that can be removed from the Optical Characterization Bench without disassembling. Two possible structures made with the linear translation stages are illustrated in right part and upper part of the same figure.

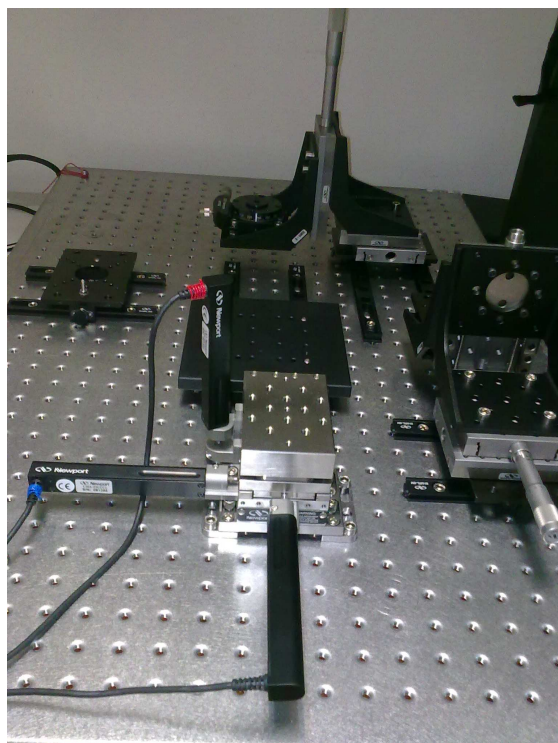


Figure VI-6: Basic Structure of the Optical Characterization Bench.

An experiment implemented in the Optical Characterization Bench is shown in Figure VI-7. It has two inputs and two outputs. One input is placed at the bottom of the picture and is composed by a multimode optical fibre and a GRIN lens. The other input is located on the right and is formed by an 850nm Laser. The two outputs are formed by polymer optical fibre and are located in front of each input, one is at the top of the figure and the other is located on its left. Finally, the device under test is in the centre of the picture.

The Optical Characterization Bench is complemented by different optical sources and detectors. In addition, an oscilloscope TDS 1012 from Tektronix (Figure VI-8), a wave generator 33120A from Agilent (Figure VI-9) and a digital multimeter 1906 from TTi (Figure VI-10) are connected to a computer by means of the General Purpose Interconnect Bus (GPIB).

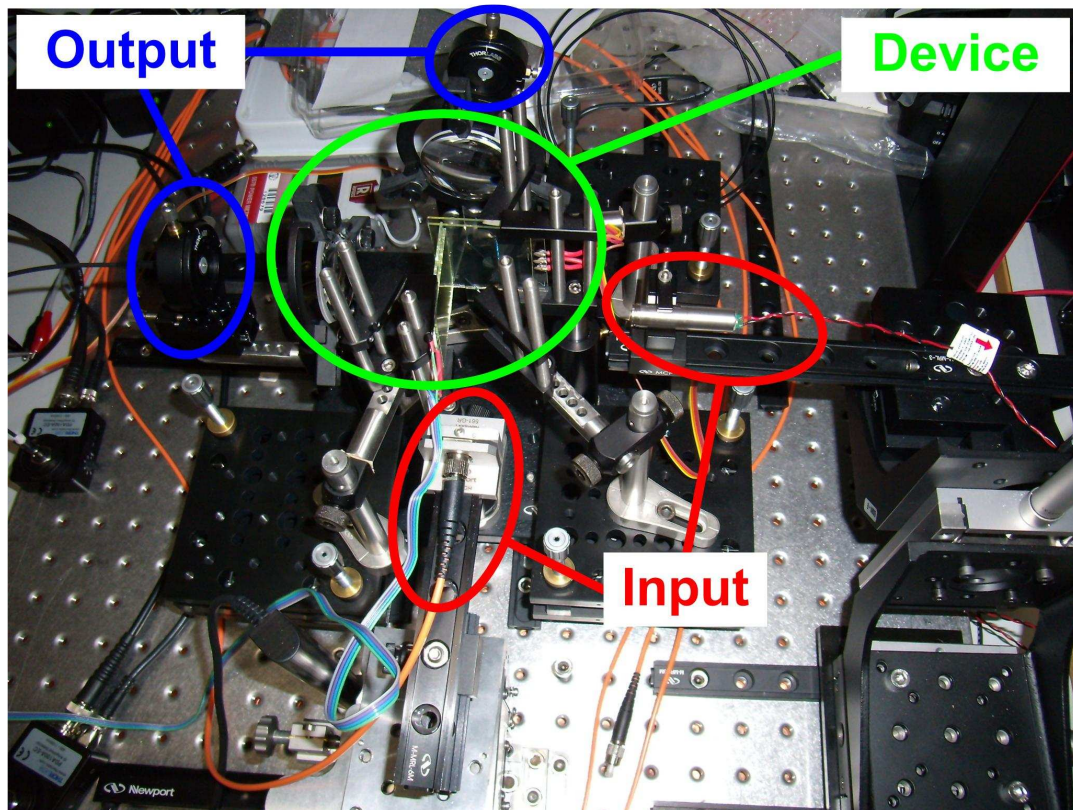


Figure VI-7: Implementation of an Experiment in the Optical Characterization Bench



Figure VI-8: Picture of the Oscilloscope TDS 1012 from Tektronix



Figure VI-9: Picture of the Wave Generator A33120 from Agilent



Figure VI-10: Picture of the Digital Multimeter 1906 from TTI.

## VI.4.- Precision Movement System

The precision movement system is made of a three axes movement controller EPS 301 and three automated actuators CMA25CCCL, all from Newport. The actuators control the desired movement for automating the characterization of the device under test.

### VI.4.a.- Motion Controller ESP 301

The motion controller is capable of handling up to three axes. It can control any combination of stepper motors and DC motors up to 3A current in each axis. It can be controlled by means of a GPIB, USB, RS-232 interfaces, or by using the frontal panel. Figure VI-11 shows the picture of the frontal panel of the motion controller. It is provided with button for controlling the actuators in stand-alone mode. Figure VI-12 shows the rear panel with the available connections (The GPIB bus does not appear in the photo).

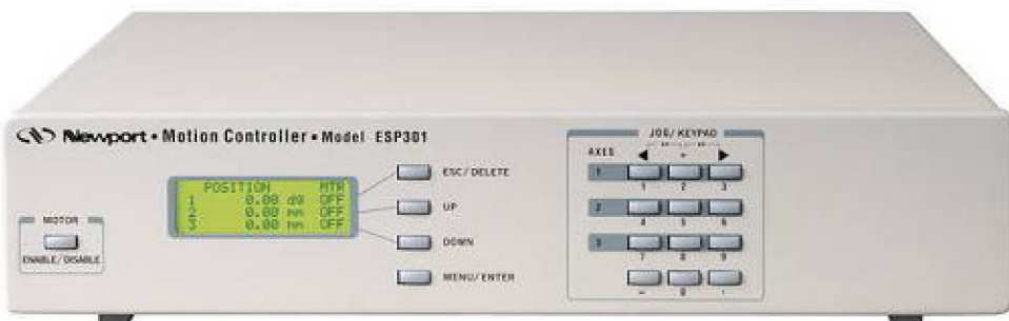


Figure VI-11: Frontal panel of the motion controller ESP 301 from Newport



Figure VI-12: Rear panel of the motion controller ESP 301

The motion controller allows several positioning modes. Speed and acceleration are configurable. Different types of movements are possible, synchronized or not, linear and circular or some axes can implement master-slave movements.

#### VI.4.b.- Actuator CMA-25CCCL

This actuator is a 25mm travel DC motor with an encoder that provides feedback to the motion controller. It allows incremental movement shorter than  $1\mu\text{m}$  and loads up to 90N. Figure VI-13 shows a picture of the actuator. The main characteristics of this actuator are shown in Table VI-1.



Figure VI-13: DC motor CMA-25CCCL from Newport

Characteristics	
<i>Movement Range</i>	25mm
<i>Minimum Incremental Movement</i>	$0.2\mu\text{m}$
<i>Maximum Speed</i>	$0.44\text{mm/sec}$
<i>Maximum Axial Load (+Cx)</i>	90N
<i>Bidirectional Repeatability</i>	$3\mu\text{m}$
<i>Retract Movement</i>	<i>less than <math>15\mu\text{m}</math></i>
<i>Feedback</i>	40 pts/rev rotator encoder
<i>Motor Type</i>	Servo motor DC UE10CC

Table VI-1: Characteristics of the CMA-25CCCL actuator from Newport

#### VI.5.- Software Developed

A software programmed in LabView has been implemented for making easy the control of the Optical Characterization Bench [Ferrer-2010]. It can move each actuator in order to place each axis properly. It also allows the modification of the configuration of each actuator; additionally it can split a movement in different steps in order to capture measurements in each single position. In addition, control of the wave generator is implemented for exciting, the device under test if it is necessary.

The main windows used in the program are presented in the next figures. Figure VI-14 shows a capture of the window for ordering a movement. Relative and absolute movements are possible. A position for each axis can be configured; incremental movement can be also applied to the desired actuators.

Figure VI-15 presents the window for configuring the parameters for the movement of each motor: speed and acceleration. In addition, it is also possible configuring limits for the movement of each axis. Different windows are available for configuring each actuator.

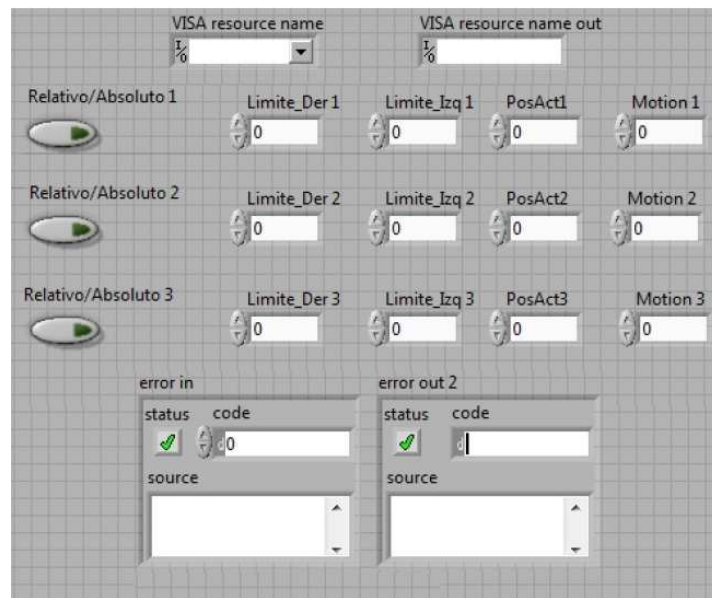


Figure VI-14: Window for ordering a movement



Figure VI-15: Configuration window for an actuator.

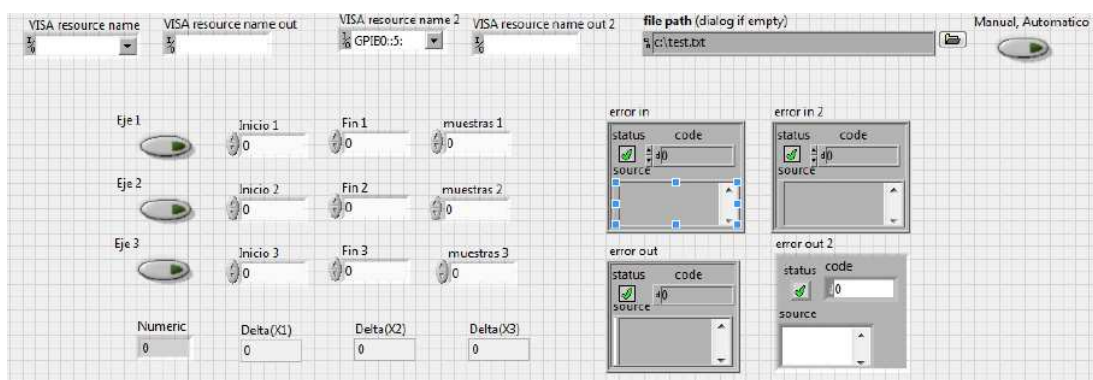
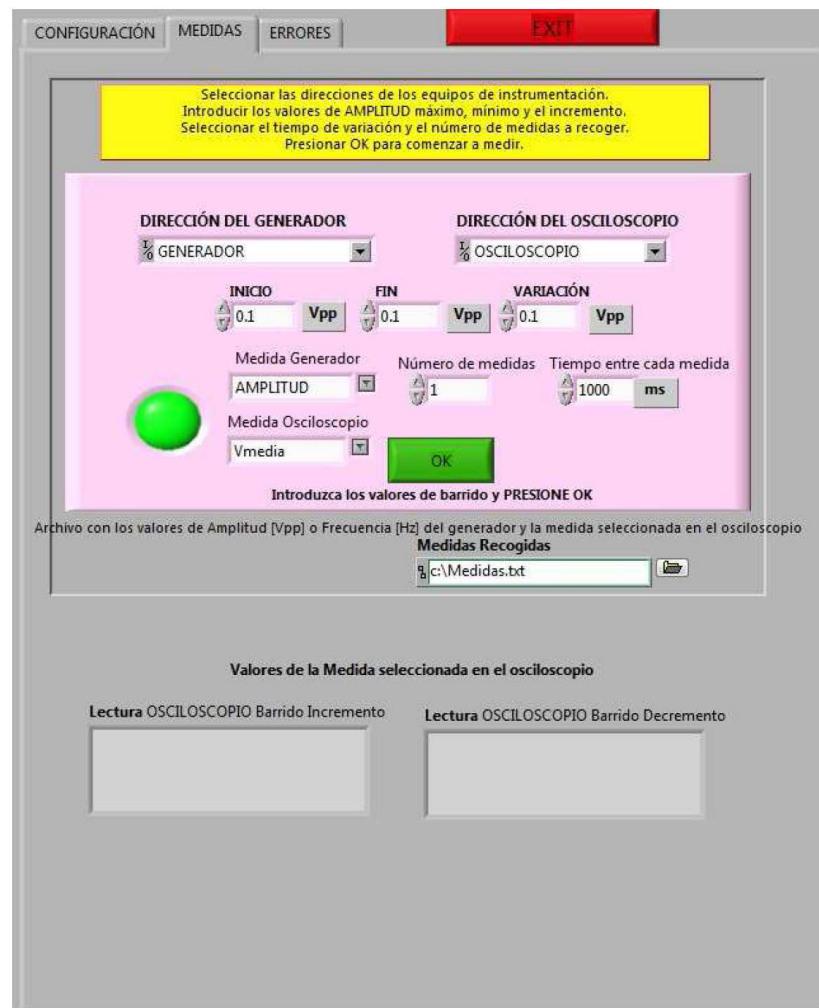


Figure VI-16: Window for configuring a split movement

Finally, Figure VI-16 depicts the window used for configuring movements step by step. Each actuator can be ordered independently. The movement from the beginning

to the end is performed in the number of steps indicated. In this type of movement, the measurements done with the multimeter in each point can be stored them in a text file. In manual set up, the program waits in each position until the user pushes the button for continuing. On the other hand, if automatic is selected, the software waits for a delay before performing the next movement.

As complement of the program previously described, other functions for controlling the wave generator and the oscilloscope have been implemented. Figure VI-17 shows the window of the implemented program. A voltage sweep can be configured for characterizing an optical device, the start and stop voltage and the increment in each step should be indicated for perform the sweep. It is possible measuring a voltage using the oscilloscope in each step. As occurs in the software described previously, the measure capture is stored in a text file.



**Figure VI-17:** Window of the function for controlling the wave generator and the oscilloscope

Further information, about how using the optical characterization bench can be seen in Appendix B.

## VI.6.- Test of the Optical Characterization Bench

Once the Optical Characterization Bench is introduced, is time for presenting some measurements done for probing its proper operation. The test has consisted on placing face-to-face two fibres and move one respect to the other in order to obtain the position with the maximum power transference. Two grin lenses have been placed between the fibres in order to collimate and focus light from the input fibre into the output one.

### VI.6.a.- Set-up Used for the Test

The input part has consisted of the input fibre and the two grin lenses and it has been placed in the three axes precision linear stage. The three axes precision linear stage has been equipped with three actuators CMA-25CCCL from Newport. The output part has been hold in a fixed post. The input system has been placed close to the output fibre and has been able to move around it in order to obtain the maximum power transference point. Figure VI-18 shows the set up used for the test.

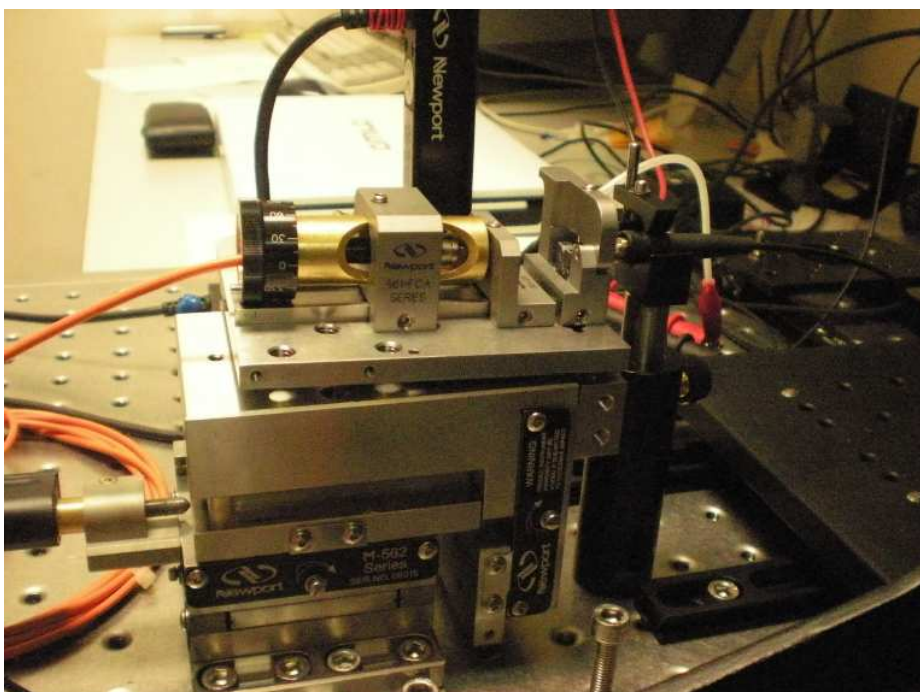


Figure VI-18: Set-up used for carrying out the test of the test.

The input fibre used for the test has been a two metres length multimode 62.5/125 $\mu$ m fibre. One of its edges has been connected to a 660nm LED from Ratioplast-Optoelectronic driven with 9V DC that has been used as optical source. The other edge has been placed in front of the grin lenses. The first lens collimates the light from the fibre and the second lens focuses the collimated light in the output fibre. The two grin lenses have their operation wavelength centred at 650nm.

Two different types of optical fibres have been used in the test: a 1mm diameter Polymer Optical Fibre (POF) stretch has been used in the first experiment, and a

62.5/125 $\mu\text{m}$  has been used in a second test. The optical power at the system output has been measured using an amplified photodetector PDA100A-EC from Thorlabs and the multimeter 1906 from Tti.

### VI.6.b.- Test using the 1mm Diameter Polymer Optical Fibre as Output Fibre

A 1mm diameter POF has been used as the output fibre used in the first experiment. The input has been moved in two axes for obtaining the maximum power transfer point. The axes origin is approximately configured in the centre of the output fibre. The displacement has been configured in 50 steps of 20 $\mu\text{m}$  each for travelling in the horizontal axis the diameter of the output fibre. The movement has started in the horizontal position -0.50mm (from the centre of the output fibre). Figure VI-19 shows the result obtained.



Figure VI-19: Optical power coupled between the fibres in the horizontal axis for the POF

The maximum has been obtained for a displacement of -0.16mm from de reference origin. Then, for analyzing the vertical axis, the horizontal actuator has been moved to the position where the maximum has been found. The same configuration used for the previous measurements has been used for characterizing the vertical axis. The movement has been started in the position -0.5mm and has been performed 50 steps of 20 $\mu\text{m}$  each. Figure VI-20 shows the result obtained for this experiment.

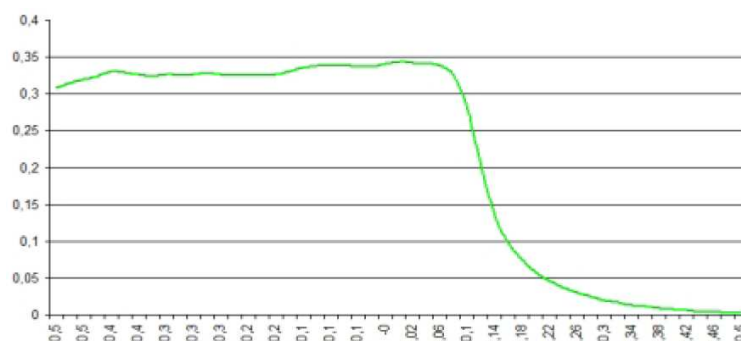


Figure VI-20: Optical power coupled between the fibres in the vertical axis for the POF

The maximum for this experiment is obtained for the position 0. It can be observed that the reference origin is not placed in the centre of the output fibre because the measurements do not represent the transition of the left part.

### VI.6.c.- Test using the 62.5/125 $\mu$ m Multimode Glass Fibre as Output Fibre

The experiment described in section VI.6.b has been carried again using a 62.5/125 $\mu$ m multimode fibre (MMF) instead of the POF fibre as the output fibre. The displacement has been configured in 65 steps of 0.96 $\mu$ m each, thus, the travel covers the core of the fibre, from -31.25 $\mu$ m to 31.25 $\mu$ m, fixing the reference origin in the centre of the output fibre. Figure VI-21 shows the results obtained for the horizontal displacement.

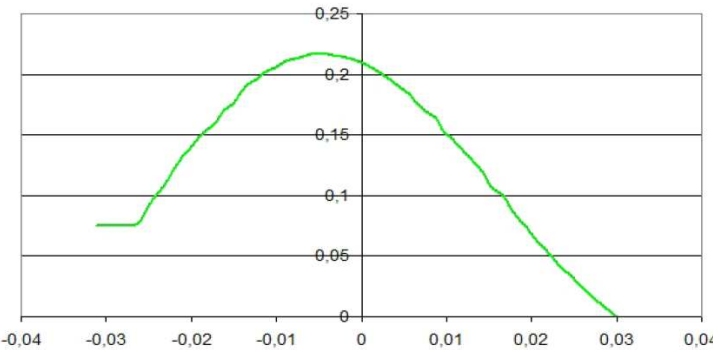


Figure VI-21: Optical power coupled between the fibres in the horizontal axis for the MMF

The maximum power transmission has been obtained at the position -5 $\mu$ m. The horizontal actuator is placed at the position where the maximum has been obtained for performing the vertical movement. This characterization has been configured in the same way than the horizontal travel. That is, 65 steps of 0.96 $\mu$ m each, from the position -31.25 $\mu$ m to the 31.25 $\mu$ m. Figure VI-22 shows optical power obtained at the fibre output for the vertical displacement.

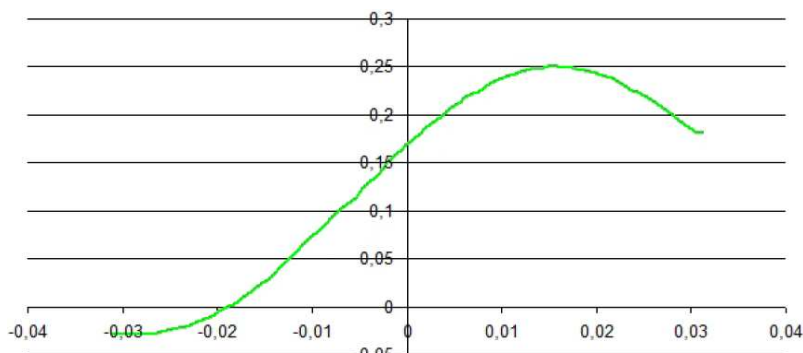


Figure VI-22: Optical power coupled between the fibres in the vertical axis for the MMF

The maximum for this experiment has been obtained for the position 15.4 $\mu$ m in the vertical axis of the output fibre.

## VI.7.- Summary and Conclusions

In this chapter, the implementation of an automated Optical Characterization Bench has been described. The proposed Optical Characterization Bench is versatile because distinct optical structures can be characterized using the same components in a different set-up. The user can configure the Optical Characterization Bench in accordance with his experiment requirements. The device under test is implemented in a separate aluminium base and can be removed from the Optical Characterization Bench when the experiment is finished without dismantling it.

Three actuators are available for automating up to three movements of the Optical Characterization Bench. These actuators are managed with the ESP 301 motion controller that allows remote control using a computer.

Automated movements up to 25mm when the linear translation stage is used and 13mm travel is available when the three axis precision linear stage it is used. The minimum incremental movement is  $0.2\mu\text{m}$  while the bidirectional repeatability is  $3\mu\text{m}$ . Additional movements are available by using manual actuators.

Software has been implemented in LabView for making easy the control of the Optical Characterization Bench. It allows the user to perform single movement of each actuator for positioning the axis in the correct place. Additionally, Split movement can be also executed for doing measurements in different positions. The software is complemented with some functions that allow controlling the wave generator and an oscilloscope if it is necessary for exciting the device under test.

Finally, two experiments have been carried out for testing the proper operation of the Optical Characterization Bench and the software developed. Both examples have consisted in searching the maximum transference point between two optical fibres. In the first test light from a Multimode Fibre, MMF, has been coupled in a Polymer Optical Fibre. In the second trial, coupling between two MMF have been carried out.

Each experiment has been performed in two set of measurements. First, the input fibre has been displaced respect to the output in the horizontal axis. Once the maximum in this axis has been obtained, the input is placed in the maximum and a vertical travel is performed for obtaining the maximum. Both phases have been carried out performing a split movement along the desired axis, while the optical power has been measured in each step.

The Optical Characterization Bench has work properly, the personal computer has handled the motion controller according to the configured sep-up have and the measurements have been captured from the multimeter and have been stored in a text file.



## **Chapter VII**

# **Conclusions and Future Work**

---

*In this chapter, the main conclusions extracted from the presented work are given. Different novel optical switches architectures based on fibres, integrated optics and liquid crystal have been proposed. Some of the presented schemes are able of working in WDM networks and advanced functions can be implemented by using the same device.*

*In addition, an optical characterization bench has been implemented for making easy the characterization of different optical devices, in particular, some of the devices proposed in the present work.*

*In the second part of this chapter, several issues related to the proposal reported in this work can be consider in further detail as future research.*



### **VII.1.- Conclusions**

In this work, several novel structures for being used as advanced devices in Wavelength Division Multiplexing (WDM) networks have been proposed. Different technologies have been utilized for their implementation. Some of them are based on liquid crystal cells and have been built with bulk elements, whereas others are based on integrated optics and have been simulated.

Those devices implemented with Liquid Crystal cells are suitable for being used in Polymer Optical Fibre (POF) networks. These kind of networks are used in short range applications and operates in the visible and near infrared wavelength range: 450-650nm for automobile applications, and 650 for home broadband applications using POF or 850nm using standard multimode fibres. Moreover, graded index POF works in the 850-1300nm wavelength range being used in access networks.

Thus, two novel structures for implementing a multiplexer have been proposed in Chapter III. A broadband 3x1 optical multiplexer based on polarization management has been presented. The novel scheme, make use of the polarization diversity method in order to reduce its insertion losses. High numerical aperture fibres should be used for proper operation. The proposed scheme has been implemented with TN-LC cells, and it has been measured at a single wavelength. Insertion losses less than 4dB and crosstalk better than 23 dB at 650nm have been measured. In addition, 30ms and 15ms setup and rise times have been obtained.

The second structure proposed in Chapter IIII, corresponds to an optical multiplexer and VOA (VMUX) based on Polymer Dispersed Liquid Crystal (PDLC). A PDLC cell without any pixel has been used in the implementation of the optical switch. The input has been placed in different positions of the PDLC cell in order to check the device operation.

Static and dynamic characterization have been carried out. Complete switching has been obtained for driving voltages of 20Vrms in all the situations. Insertion losses have been less than 1.6dB at 532nm and 1dB at 650nm. Attenuation, extinction ratios of 39.5dB at 532nm and 31dB at 650nm, have been obtained. Grey scale have been achieved approximately from 10Vrms to 20Vrms. Rise time less than 2.6ms and decay time better than 12.4ms have been measured when a 1kHz frequency square wave has been applied.

A novel structure of an Advanced Multifunctional Optical Switch (AMOS) based on Twisted Nematic Liquid Crystal (TN-LC) cells has been introduced in Chapter IV. The proposed scheme comes from the 3x1 multiplexer presented in Chapter III. As it occurs with the previous 3x1 multiplexer, the proposed device is suitable for being used in POF network, where the output light can be easily coupled to the output port due to the POF high numerical aperture.

TN-LC cells have been selected for acting as the active element in the proposed structure because they are able of performing light switching in a wide wavelength range. Due to the large operation wavelength range required for the proposed device,

up to four different types of TN-LC cells have been designed and fabricated. Characterization of the manufactured TN-LC cells has been carried out in order to check that they work properly in the operation range.

The proposed device has been characterized at different wavelengths in order to obtain the most relevant parameters. High insertion losses have been obtained, this can be due to the non coated polarization beam splitters used, the divergence of the input light not fully collimated, and can be in part corrected by using fibre lenses in the output ports.

The obtained crosstalk, as defined in section II.5, have been better than 13dB for 650nm and 850nm. Transmission through the device can be modified by applying less voltage to the TN-LC cells, so, variable attenuation can be achieved from 3 to 4 Vrms.

Response times from 10ms to more than 100ms have been obtained for the optical switch. The proposed device is suitable for being used in applications where switching speed is not fundamental. Larger response times have been obtained for the whole optical device than when only one LC cell has been characterized. A reason for that can be that the optical paths followed for each polarization are slightly different and makes the pulse wider. In addition, more liquid crystal has to be switched in order to commute the device.

Larger times are related to Liquid Crystal relaxation times. It is usual that relaxation times are larger than excitation times in this type of cells. In addition, larger times have been obtained for wider cells, because the equivalent capacitor is higher in this case.

Through different characterizations it has been tested the device performance in a 900nm range, so for operation in broadband access and home networks.

The proposed scheme is scalable. The main restrictions come from the output lens, which is in charge of focusing all the output light in the output port. The angle of the focused beams should be smaller than the acceptance angle of the output fibre. The lens used in the implementation is 50mm diameter and has a focal length of 75mm, this makes to the output lens fulfill the requirements of the numerical aperture of the output POF.

On the other hand, the divergence of the input beams cause that the output light is not focused properly into the output fibre. More light can be collected if a fibre lens is used in the output port. Due to the numerical aperture of POF, collimation in this kind of fibres makes greater divergences, In that case, the pixel size should be enlarged for covering the beam spot that comes from the input port.

Taking into account these restrictions, using the same lenses in the output ports, up to 6 input ports could be implemented in POF applications, and up to 18 for GI-POF or standard silica multimode fibre applications.

The proposed device in Chapter IV has been defined as Advanced Multifunctional Optical Switch because it can perform different functionalities without hardware changes, only by selecting the proper input and output ports and control electronics.

Thus the device can act as a 3x1 Optical Multiplexer/Combiner, Dual 3x1 Optical Multiplexer/Combiner or 2x2 Optical Switch. Moreover, by applying a variable voltage to the TN-LC cells, a Variable Optical Attenuator and a Variable Optical Power Splitter can be performed with the same device, and variable splitting or attenuation ratios are possible.

Comparing the proposed AMOS with the optical multiplexer presented in chapter III.2, better contrast is obtained for the optical multiplexer. This can be due to the use of cube Polarizing Beam Splitters (PBS) with Antirefringent Coating that exhibit more extinction ratio but in a reduced wavelength range. In addition, shorter response times are obtained for the multiplexer proposed in Chapter III.

In Chapter V, two kinds of optical switches based on Integrated Optics have been introduced. The first type of the proposed switches is formed by micro ring-resonators ( $\mu$ RR) combined with liquid crystals (LC), while the last type of the presented schemes makes use of a Mach-Zehnder Interferometer (MZI). Both types of devices have been described using integrated optic, and simulations of their behaviour have been carried out in order to determine their proper operation.

Different designs have been proposed for the optical switches base on  $\mu$ RR combined with LC. Simulations of the basic structure with distinct parameters: different RR lengths, coupling ratio or waveguides stretches with LC inside the loop, have been carried out in order to test the variation of the RR response.

All the parameters modified have changed the Free Spectral Range (FSR) of the structure. RR tuning has been possible by changing the state of the LC present in the waveguide. LC switch can be obtained by applying voltage to it.

Availability of RR with LC inside the loop in cross-grid has also been probed. Its behaviour is similar to the basic structure when same parameters have been used. Cross-grid scheme allows implementing compound structures. Thus, a reconfigurable three-channel wavelength selective switch comprised by two serial RR has been proposed. Reconfiguration has been done by modifying electrically the LC state.

The last optical switch proposed has been developed for implementing a Tap and Two Split (Ta2S) switch for being used in a multicast capable optical cross connect node architecture that features both tap-and-continue and tap-and-binary-split functionalities. By using this type of optical switch, the power efficiency of the light tree is increased, and less use of optical amplification is required.

An optical switch based on integrated optics has been designed for implementing the required functionalities. It is made of a 94:6 MMI splitter in combination with a reconfigurable MZI switch.

Simulations of the Ta2S switch have been done. Matlab has been used for simulating the behaviour of the switch described by the equations given in section V.4.b. These simulations have been carried out because it is important to know the losses induced by the optical switch, because it has to be taken into account for estimating the overall losses along the light tree, that determine the election of one or another lightpath.

The obtained refraction index variation necessary for switching a 100 $\mu\text{m}$  length waveguide MZI has been  $\Delta n = -7.75 \cdot 10^{-3}$ . Simulations have been made with a 6% tap, 0.1 dB extinction losses for each MMI, coupling ratios  $\kappa_1 = \kappa_2 = 0.5$ , 100 $\mu\text{m}$  waveguide length ( $L$ ), and 1.55  $\mu\text{m}$  vacuum wavelength. BPM software has been utilized in order to probe the preliminary results obtained in Matlab.

Finally, in Chapter VI, an automated Optical Characterization Bench has been implemented in order to make easy the measurement of different optical devices. In addition, it has been used for characterizing some of the devices proposed in this work.

The proposed Optical Characterization Bench is versatile because distinct optical structures can be characterized using the same components in a different set-up. The user can configure the Optical Characterization Bench in accordance with the experiment requirements. The device under test can be implemented in a separate aluminium base and can be removed from the Optical Characterization Bench, when the experiment is finished, without dismantling it.

Automated movements up to 25mm when the linear translation stage is used and 13mm travel is available when the three axis precision linear stage is used. The minimum incremental movement is 0.2 $\mu\text{m}$  while the bidirectional repeatability is 3 $\mu\text{m}$ . Additional movements are available by using manual actuators.

Software has been implemented in LabView for making easy the control of the Optical Characterization Bench. Two experiments have been carried out for testing the proper operation of the Optical Characterization Bench and the software developed. Both examples have consisted in searching the maximum transference point between two optical fibres. In the first test light from a Multimode Fibre, MMF, has been coupled in a Polymer Optical Fibre. In the second trial, coupling between two MMF have been carried out.

## VII.2.- Future Work

Finally, several issues related to the results reported in this work can be considered in further detail as future research. Some of them could be the following:

- Characterization of the optical switches based on bulk elements using grade index polymer optical fibre at the input port. By these measurements, characterization of the device in a GI-POF system would be carried out. In previous measurements, multimode silica fibre or lasers at different wavelengths have been used as input ports.
- Optimization of the light that comes from the POF input port. Fewer insertion losses can be obtained if the input light is well collimated. In that way, different collimation systems could be used for optimizing the optical switch behaviour. Also different collecting lenses at the output should be tested.

- Study and improvement of the output port of the optical switches based on bulk elements. If the light from the input ports is not collimated properly, the output lenses do not focus light well. In this case, coupling light into the output fibre can be improved by using a fibre lens in the output port.
- Related to the proposed multiplexer based on PDLC, The use of a PDLC with pixels should be implemented in order to characterize the optical device.
- Related to the Advanced Multifunctional Optical Switch (AMOS) based on Twisted Nematic Liquid Crystal cells, the optimization of the pixels in the used cells can reduce the size of the device and increase the number of available input ports.
- Study of the structure of the AMOS, trying to avoid reflections which can affect the device operation.
- Improvement of the excitation signal driven to the Liquid Crystal Cells, especially when the device is switching, in order to reduce the response times.
- The Polarization Dependent Losses in the proposed optical switches based on bulk elements should be characterized.
- Optimization of the AMOS structure in terms of LC orientation and driven voltages; in order to reduce asymmetries such as polarization dependent loss and different polarization delays.
- Different strategies to reduce AMOS size should be developed.
- Selective injection in multimode fibres as fundamental part of broadband network using multimode fibres should be explored through experience acquired in AMOS characterization and using the implemented Optical Characterization Bench.
- Related to the optical switches based on integrated optics, manufacturing of the proposed structures and their characterization could be interesting for checking their proper operation.



# Chapter VIII

## Resumen del Trabajo Realizado

---

*A lo largo de este capítulo se presenta un resumen en castellano del trabajo realizado. En la primera sección se muestra la motivación y objetivos del trabajo desarrollado. En el segundo apartado se realiza una introducción sobre redes ópticas y conmutadores ópticos.*

*En la tercera sección se describen los conmutadores ópticos basados en Cristal Líquido. Inicialmente se propone un multiplexor óptico basado en la gestión de la polarización utilizando Cristal Líquido Nemático. Posteriormente, se presenta un multiplexor y/o atenuador óptico variable fabricado con Crystal Líquido Disperso en Polímero. En la sección cuarta, se introduce un conmutador óptico multifunción avanzado hecho con Cristal Líquido.*

*En el quinto apartado se detallan varios conmutadores ópticos desarrollados en óptica integrada. Inicialmente se describen diferentes estructuras con anillos resonantes que incluyen cristal líquido, para finalmente presentar un conmutador óptico basado en un interferómetro Mach-Zehnder con una funcionalidad específica en redes ópticas transparentes. En la sexta sección se muestra el banco de caracterización óptica desarrollado para la realización de medidas. Finalmente, se indican las conclusiones obtenidas y las futuras líneas de investigación.*

---



### VIII.1.- Motivación y Objetivos

El incremento de ancho de banda requerido por los nuevos servicios de comunicaciones ofrecidos, hace necesario el uso de fibra óptica como medio de transmisión. La fibra óptica de sílice se ha empleado tradicionalmente en comunicaciones de larga distancia y ha provocado el desarrollo de diferentes elementos ópticos para su empleo en este tipo de redes, pero las tecnologías existentes son caras para su uso en los bucles de abonado.

Diversos sistemas han permitido aumentar el ancho de banda ofrecido por los bucles de abonado basados en el par trenzado, pero el incremento de banda requerido supera el ancho de banda que este sistema puede ofrecer.

Las fibras multimodo de núcleo grande, y elevada apertura numérica, de plástico o de sílice, permiten la realización de instalaciones menos costosas puesto que son menos restrictivas respecto a la falta de alineamiento en las interconexiones lo que permite el uso de conectores y equipos más baratos, a pesar de que el ancho de banda que presentan es menor. Por otro lado, la Fibra Óptica de Plástico (POF del inglés *Polymer Optical Fibre*), en distancias cortas, presenta diversas ventajas frente a la fibra óptica convencional. Es más ligera y flexible y permite un fácil acabado lo que reduce el tiempo de instalación. Por este motivo, la POF se está empleando en un número creciente de aplicaciones entre las que destacan la transmisión de video en equipos médicos o aplicaciones multimedia en aviación civil y coches de gama alta, además de redes en el hogar o redes de sensores entre otras.

Se puede obtener mayor ancho de banda con un tipo especial de POF, que es la fibra óptica de plástico de índice gradual perfluorinada (PF-GIPOF del inglés *Perfluorinated Graded Index POF*). Este tipo de fibra presenta menor atenuación en un amplio rango de longitudes de onda, desde 650nm hasta 1300nm. Por este motivo, se puede usar en redes en el edificio/hogar con distancias inferiores a 1km, permitiendo una tasa de transferencia de hasta 10Gbps en 100m y transmisión Ethernet de 1.25Gbps en 1km.

Por otro lado, multiplexores y combinadores son fundamentales en las redes ópticas que emplean multiplexación por división en longitud de onda (WDM del inglés *Wavelength Multiplexing Division*), pero todavía no se han desarrollado para este tipo de redes ópticas operando en un amplio rango de longitudes de onda y con fibras multimodo. Características adicionales en dichas redes ópticas pueden ser las bajas pérdidas y su capacidad de reconfiguración. También cabe mencionar que las redes reconfigurables para aplicaciones críticas demandan dispositivos de commutación con diversas funcionalidades. Por este motivo, el trabajo desarrollado se ha centrado en el desarrollo de diversos commutadores ópticos para varios tipos de redes ópticas.

Se emplean diversas tecnologías en la fabricación de commutadores ópticos. Los Cristales Líquidos se emplean con frecuencia en pantallas, aunque también se utilizan en telecomunicaciones. Otra tecnología disponible se basa en la óptica integrada. En este caso, la luz se transmite por una guía de onda en la que la commutación se realiza por la modificación de algunos de sus parámetros. También

se emplean los mecanismos micro-electromecánicos (MEMs del inglés *Micro-Electromechanical Mechanism*) que se basan en pequeños espejos móviles que cambian la dirección del haz de luz cuando es necesario.

### VIII.1.a.- Objetivos

El objetivo del presente trabajo consiste en proponer diversos conmutadores ópticos empleando diversas tecnologías dependiendo de la aplicación para la que se vayan a emplear. Algunas de las estructuras propuestas han sido implementadas y evaluadas experimentalmente, mientras que otras sólo han sido simuladas.

Algunos de los dispositivos presentados emplean células de cristal líquido y permiten la realización de diversas funcionalidades y pueden trabajar en un amplio rango de longitudes de onda. A tal respecto, se ha realizado un multiplexor/combinador y un conmutador óptico multifunción avanzado, todos ellos basados en la tecnología de Cristal Líquido Nemático. También se ha desarrollado un multiplexor/combinador basado en una célula de Cristal Líquido Disperso en Polímero (PDLC del inglés *Polymer Dispersed Liquid Crystal*).

El tercer tipo de conmutadores ópticos propuesto está basado en micro-anillos resonantes combinados con cristal líquido. La estructura del micro-anillo se compone de una guía de onda circular acoplada a una o dos guías de onda rectas que actúan como puertos de entrada/salida. La luz que pasa por la estructura se filtra de acuerdo a las características del anillo resonante: longitud, acople entre el anillo y las guías de onda rectas, pérdidas en el anillo... El uso de Cristal Líquido permite la variación de las características del anillo modificando su respuesta.

El último conmutador propuesto está basado en un Interferómetro Mach-Zehnder y realiza una función novedosa de monitorización y conmutación selectiva a 2 salidas, como parte de una matriz de interconexión de un nodo óptico. Este tipo de dispositivo emplea la tecnología de óptica integrada y la interferometría para realizar la conmutación. La variación de las propiedades ópticas que influyen en los dos haces de luz que interfieren se puede realizar básicamente por dos métodos: térmicamente o electrónicamente.

Finalmente, se ha implementado un banco de caracterización óptica automatizado que facilita la adquisición de medidas. Se compone de una plataforma de translación en tres ejes con tres actuadores, complementada con diversas plataformas de translación lineales y distintos soportes para elementos ópticos que permiten adaptar la estructura del banco al experimento.

## **VIII.2.- Tecnologías de Comutación para Redes Ópticas**

El desarrollo de los sistemas de comunicación ópticos ha permitido la implantación de nuevos servicios y aplicaciones para el usuario final. El ancho de banda requerido para la transmisión de dichos servicios se ha ido incrementando en los últimos años, mientras que a la vez, los usuarios demandan cada vez servicios que requieren una transferencia de datos mayor. Esto ha sido posible gracias al uso de las fibras ópticas como medio de transmisión y al empleo de dispositivos ópticos que realizan funciones que se desarrollaban anteriormente por circuitos electrónicos.

En relación con las fibras ópticas, el método esencial empleado para incrementar el ancho de banda ha sido el uso de multiplexación por división en longitud de onda (WDM del inglés *Wavelength Division Multiplexing*). Esta técnica consiste en transmitir diferentes longitudes de onda a través de la misma fibra óptica, cada longitud de onda lleva su propia información que no interfiere con la información transportada por el resto de longitudes de onda. Las longitudes de onda se separan en la etapa de recepción, y cada una es tratada por un receptor independiente.

### **VIII.2.a.- Tipos de Redes Ópticas**

La tecnología de la fibra óptica ha evolucionado incesantemente desde que en 1966 K. Kao se percató de que una guía de onda con una cubierta de material transparente con menor índice de refracción podía confinar la luz en su interior, además, si la diferencia entre los índices de refracción de la guía de onda y la cubierta eran pequeños, el diámetro del núcleo podría ser de unos pocos micrómetros y se guían transmitiendo únicamente un modo, lo que permitía su empleo en aplicaciones prácticas.

La reducción de la atenuación en las fibras ópticas, el uso de fibras multimodo, la aparición de los amplificadores ópticos, la introducción de sistemas WDM comerciales entre otras mejoras ha permitido la expansión del uso de la fibra óptica como medio preferente de transmisión.

Por otro lado, los diferentes tipos de redes ópticas que se han desplegado se pueden clasificar atendiendo al tipo de información que transmiten, así se puede tener: voz, vídeo o datos. La red telefónica nacional se ha encargado tradicionalmente de transmitir voz, mientras que el vídeo se ha emitido mediante radioenlaces o por medio de cable, finalmente, las redes de datos, se encargaban de transmitir datos entre computadores.

En la actualidad, la integración de tecnologías ha resultado en la transmisión de diferentes tipos de información a través del mismo medio. Por ello, resulta más interesante realizar una clasificación de las redes ópticas en función de su área de influencia. En ese sentido, pueden ser redes troncales, redes de área metropolitana (MAN del inglés *Metropolitan Area Networks*) o redes de acceso.

- **Redes Troncales (*Backbone Networks*)**

Este tipo de redes de comunicaciones se encargan de la transmisión de datos a largas distancias, conectan oficinas interregionales donde se concentran los datos de muchos usuarios. El flujo de datos de los usuarios se agregan en las MAN, que a su vez se interconectan con otras MANs por medio de las redes troncales.

El rango de aplicación de estas redes se extiende desde redes mundiales o submarinas hasta redes de menor ámbito como puedan ser las redes nacionales o regionales. Se emplea fibra óptica monomodo en combinación con WDM, lo que permite obtener un gran ancho de banda a grandes distancias.

Uno de los objetivos de este tipo de redes es su adaptación al tráfico demandado en cada instante de tiempo. Las matrices de interconexión, o *Cross-Connects*, se emplean para distribuir el ancho de banda en función de las demandas de tráfico. Por su parte, el ancho demandado se incrementa constantemente, lo que exige el empleo de matrices de interconexión ópticas, de esa forma la conmutación se realiza de una manera más rápida y eficiente que realizando la conversión al dominio eléctrico para ejecutar la conmutación. Únicamente aquellos tráficos que requieran conmutación IP se transfieren al dominio eléctrico.

Mediante el empleo de estas matrices de conmutación, las redes WDM pueden ser encaminadas por longitud de onda, permitiendo el cambio de destino según la longitud de onda. Las redes de protección y restablecimiento únicamente se deben encargar de modificar el camino cuando la ruta principal presente fallos.

Por otro lado, una característica de las matrices de interconexión es su posibilidad de realizar el envío a múltiples destinos o *Multicast*. De esta forma, se pueden implementar aplicaciones de distribución de datos a varios usuarios, como videoconferencias, juegos on-line o tele-enseñanza. La principal ventaja de las matrices de interconexión es su independencia del tipo de tráfico transmitido.

- **Redes de Área Metropolitana (MAN)**

Este tipo de redes están encargadas de unir las redes de acceso con las redes troncales. Debido a la diversidad del tipo de tráfico soportado, que depende de las singularidades de cada cliente, el uso de WDM permite aumentar el ancho de banda y el escalado de este tipo de redes.

En ese sentido, todas las ventajas descritas para las matrices de conmutación son aplicables a este tipo de redes. También es habitual el uso de multiplexores de inserción/extracción (ADM del inglés *Add Drop Multiplexers*) que permiten la extracción o adición de longitudes de onda de la red. También se hace uso del tráfico concentrado, en el que se empaquetan datos con diferentes tasas de transferencia formando una unidad que se transmite a alta velocidad, lo que reduce el número de conmutadores.

- **Redes de Acceso**

Estas redes son las encargadas de conectar a los usuarios con los proveedores de servicios. En telefonía se corresponde con el bucle de abonado y está basada en el par de cobre trenzado. Esta tecnología se emplea para la transmisión de voz a bajas frecuencias, por lo que soporta un ancho de banda pequeño. Diferentes técnicas como la Red de Servicios Integrados (ISDN del inglés *Integrated Service Digital Network*) o el bucle de abonado digital asimétrico (ADSL del inglés *Asymmetric Digital Subscriber Loop*) han permitido el incremento del ancho de banda ofrecido a los usuarios.

Los nuevos servicios demandados por los usuarios requieren mayor ancho de banda, por lo que el cambio hacia la fibra óptica en este tipo de redes es una de las soluciones. El problema de esta migración viene impuesta por el coste, por ello existen diferentes escenarios posibles dependiendo de la inversión permisible.

Las redes de acceso basadas en fibra óptica se pueden clasificar atendiendo al límite hasta donde se despliega la fibra, así se tienen: Fibra hasta el hogar (FTTH del inglés *Fibre to the Home*), fibra hasta el edificio (FTTB del inglés *Fibre to the Building*) o Fibra hasta el bordillo (FTTC del inglés *Fibre to the Curb*). Todas estas posibilidades se describen bajo las siglas FTTx. Otra posibilidad es el híbrido fibra coaxial (HFC del inglés *Hybrid Fibre Coax*) que hace uso de ambas tecnologías.

Tradicionalmente se emplean redes punto a punto en las que se despliega un cable por cada usuario. Por otro lado, las redes ópticas pasivas (PON del inglés *Passive Optical Networks*) en las que se emplean dispositivos como multiplexores o combinadores pasivos permiten el agrupamiento de tráfico, de forma que se reduce la cantidad de fibra desplegada y permite el ahorro de potencia.

### VIII.2.b.- Aplicaciones de la Fibra Óptica de Plástico

Otro tipo de fibra usado en las redes ópticas es la fibra óptica de plástico (POF del inglés *Polymer Optical Fibre*). Este tipo de fibra presenta un mayor tamaño de núcleo, es más ligera y flexible y segura en su tratamiento. Debido a estas características, es más sencilla de instalar lo que reduce considerablemente su coste. Al igual que ha ocurrido con las fibras ópticas de sílice, la atenuación en este tipo de fibras se ha ido reduciendo paulatinamente, y la aparición de las fibras de plástico de índice gradual (GI-POF del inglés *Graded Index POF*) han conseguido aumentar el ancho de banda que éstas presentan.

Existe un tipo especial de GI-POF que reduce su atenuación hasta el rango de longitudes de onda en el entorno de los 1300nm. Esta fibra se basa en la sustitución del hidrógeno presente en la moléculas de polímero por flúor, de ahí su nombre de GI-POF perfluorinadas. Con el empleo de este tipo de fibra, se ha demostrado una tasa de transmisión de hasta 10.7Gbps en una distancia de 220m [Lee-2007].

Dadas las razones expuestas previamente, la POF se emplea como sistema de transmisión para distancias pequeñas. En dichas aplicaciones, el cobre no ha sido sustituido puesto que es más barato que el uso de fibra óptica de sílice. En ese

sentido, POF es un buen candidato para la sustitución del cobre porque posee las siguientes características:

- Inmune frente interferencias electromagnéticas.
- Seguras, no hay riesgo de explosión en ambientes inflamables.
- Gran ancho de banda en distancias cortas, menos de cien metros
- Ligeras.
- Fáciles y baratas de producir
- Fáciles de manejar y conectar, lo que reduce el precio de instalación.
- Soporta radios de curvatura pequeños.
- Seguras en su manipulación, factible su uso por los clientes.

Por este motivo, POF se emplean en diferentes aplicaciones. A continuación se describen las más significativas:

- **Redes para el Automóvil**

Los servicios multimedia disponibles en el automóvil se han incrementado en los últimos años: reproductores de DVD (del inglés *Digital Video Disk*), sistemas GPS (del inglés *Global Positioning System*), manos libres... En 1998 se introdujo el bus doméstico digital (D2B del inglés *Digital Domestic Bus*), que fue la primera aplicación de transmisión de datos basada en POF en el automóvil, y permitía tasas de transferencia de hasta 5.6Mbps.

Uno de los estándares más empleados es el definido por el Sistema de Transporte Medio Orientado al Medio (MOST del inglés *Media Oriented System Transport*) que fue desarrollado bajo la participación de varios fabricantes y permite tasas de transferencia de hasta 25Mbps [Muyshondt-2005, Schönfeld-2000, Kibler-2004, Baierl-2001]. Su arquitectura está basada en un anillo unidireccional en el que cada dispositivo conectado a él funciona como un repetidor.

Los dispositivos de comunicación están separados en diferentes redes atendiendo al ancho de banda que precisan:

- Sistema de propulsión: incluye sistema anti-bloqueo de frenos (ABS del inglés *Anti-Block System*), sistema de control del motor (EMS del inglés *Engine Management System*), suspensión, caja de cambios...
- Electrónica del Habitáculo: panel de instrumentos, aire acondicionado, antirrobo, control del elevalunas, ajuste de los espejos o de los asientos...
- Sistemas del Chasis: dirección electrónica o freno electrónico.
- Sensores de entorno: acceso a los datos de diagnóstico, documentación del automóvil, manual de uso...
- Información y Entretenimiento: navegación, telefonía, audio y vídeo, multimedia.

Cada una de las redes cumple con la arquitectura ISO/OSI (del inglés *International Organization for Standardization/ Open System Interconnection*) de siete niveles. La longitud total de fibra en el coche es menor a 30m.

Existen otros sistemas desarrollados por otros fabricantes que también pueden emplear POF para su implementación en automóviles.

- **Redes en el Hogar**

Las redes desplegadas en el hogar derivan de las redes implantadas en las oficinas basadas en par de trenzado de cobre (Cat5e o Cat6), o fibra multimodo de silice. En el hogar, las redes son una extensión de las redes de acceso de banda ancha. Un controlador de la comunicación del hogar (HCC del inglés *Home Communication Controller*) se encarga de agrupar toda la información procedente de las diferentes redes de acceso para distribuirla en todas las habitaciones.

Existen diferentes topologías de red. La más directa se basa en una topología punto a punto, en la que se tiende una fibra individual desde el HCC hasta cada habitación (Figura VIII-1(a)). Una estructura alternativa es emplear una arquitectura punto a multipunto. En una estructura en árbol, cada fibra de subida conecta el HCC con un divisor colocado en cada planta que distribuye la señal entre las habitaciones de dicho piso (Figura VIII-1 (b)). En lugar de este tipo, en una arquitectura en bus como la presentada en Figura VIII-1 (c), se emplea la misma fibra para distribuir la señal a cada una de las habitaciones del mismo piso. Finalmente, en una estructura multipunto a multipunto, una red en forma de estrella, cada nodo de una habitación está conectado a un acoplador en estrella situado cerca del HCC. Este esquema permite la comunicación entre diferentes nodos sin hacer uso del HCC.

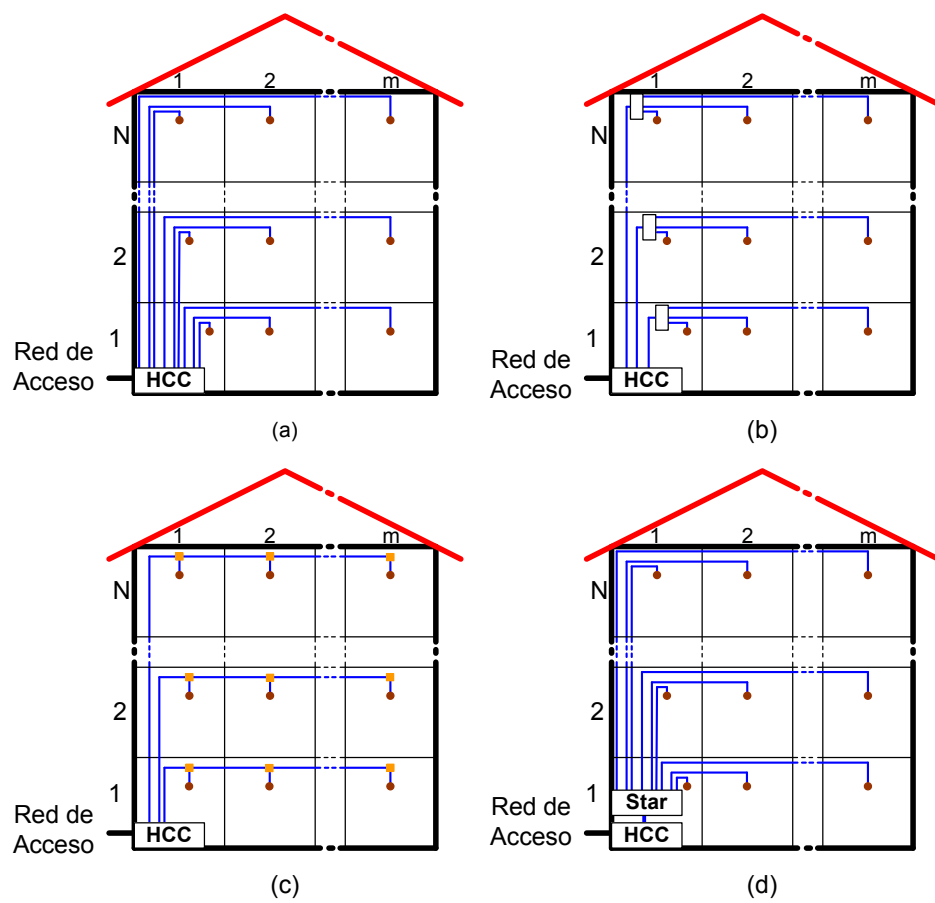


Figura VIII-1: Estructura de una Red en el Hogar:(a) Punto a Punto, (b) Árbol, (c) Bus, (d) Estrella.

Estas topologías se están utilizando también para distribuir las señales de radio dentro del hogar, considerando cada habitación como una pico-celda. Por otro lado, las arquitecturas propuestas pueden implementarse como todo ópticas, en tal caso no hay conversión a eléctrico, u opacas, en el que se realiza la conversión cuando se precisa.

En la Sección 4, se presenta un conmutador óptico multifunción avanzado basado en Cristal Líquido diseñado para ser empleado en redes POF capaz de operar en sistemas de radio sobre fibra (RoF del inglés *Radio over Fibre*) o como parte del HCC mostrado en esta sección.

#### • **Redes de Sensores**

La fibra óptica de plástico también se puede emplear en redes de sensores, bien como medio de transmisión de datos, bien actuando como el propio sensor. Mediante este tipo de redes, es posible la implementación de puntos de medida remotos. La medida es por tanto, transmitida por la fibra al punto de control para su evaluación.

En muchos sistemas de medida, la distancia entre el punto de medida y el centro de control es relativamente corta, y la medida no requiere de un gran ancho de banda. Además, la fibra óptica es segura por naturaleza, puesto que se puede emplear en ambientes inflamables sin que haya riesgo de explosión. En [Vázquez-2004] se muestra un sensor de nivel para tanques de aceite.

El uso de POF en combinación con conmutadores ópticos permite aumentar el número de puntos de medida, tal y como se muestra en [Vázquez-2003]. También se puede emplear como medida de seguridad, empleando otro sensor cuando falla el sensor principal.

Al igual que ocurre con las fibras de sílice, la POF también se puede emplear como sensor [Kalymnios-2004, Poisel-2005]. Los sensores de POF se pueden clasificar en diferentes grupos [Ziemann-2008], a continuación se dan algunos ejemplos:

*Sensores de Transmisión y Reflexión:* están basados en las propiedades de acople de las POFs. Presentan la ventaja del gran núcleo que poseen estas fibras y de la apertura numérica que favorece el acople de luz. La estructura consiste en una fibra que guía la luz hasta el punto de medida, de forma que la luz se acopla de nuevo, bien en la misma fibra de entrada o en otra de salida. La magnitud a medir modifica la cantidad de luz que regresa al centro de medida, por lo que son sensores extrínsecos. Algunos ejemplos de este tipo de sensores son [Vázquez-2004, Zubía-2007].

*Sensor con la Fibra como Elemento Sensible:* emplean la influencia de distintos parámetros cuando la luz se propaga a lo largo de una fibra óptica, por lo que se denominan sensores intrínsecos. La manera más normal de realizar este tipo de sensor es mediante el aumento de atenuación producido cuando la fibra se curva. Un ejemplo de este tipo de sensor se presenta en [Durana-2009].

*Sensores con Fibras de Superficie Modificada:* en algunas ocasiones, la sensibilidad obtenida con una fibra sin modificar es insuficiente, por ello se hacen modificaciones en la fibra para aumentar la sensibilidad de la fibra ante algunas perturbaciones. Las modificaciones realizadas pueden ser mecánicas, o mediante modificaciones químicas de los índices de refracción del núcleo o la cubierta. Algunos ejemplos de este tipo de sensores se muestran en [Miedreich-2004, Poisel-2005, Lomera-2007, Montero-2009]

*Sensores Químicos:* basados en la modificación de la transmisión de luz en una POF con un material sensible al elemento químico que se desea medir.

- **Redes de Control**

Otras aplicaciones en las que se emplea este tipo de fibra son en redes de control, como Byteflight, en redes para automatización, como Sercos, para realizar la interconexión de diferentes circuitos integrados, o en iluminación.

### VIII.2.c.- Parámetros de los Conmutadores Ópticos

Una vez se han descrito someramente los diferentes tipos de redes ópticas que se emplean, y antes de proceder a la descripción de las distintas tecnologías empleadas para realizar la conmutación óptica, se presentan los principales parámetros empleados para la caracterización de los conmutadores ópticos [Papadimitrou-2003, Chua-2010, Rivero-2008]. La definición de los parámetros se basa en la notación empleada en la Figura VIII-2.

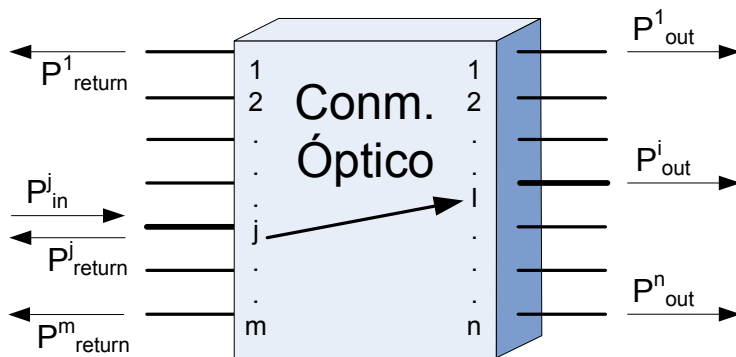


Figura VIII-2: Esquema de un Conmutador Óptico para la Definición de sus Parámetros.

*Pérdidas de Inserción (IL del inglés Insertion Loss):* se define como la fracción de la potencia de entrada que se pierde cuando la luz se transmite a un puerto de salida.

$$\text{IL} = -10 \cdot \log \left( \frac{P_{out}^j}{P_{in}^j} \right) > 0 \quad [\text{VIII-1}]$$

*Pérdidas en Exceso* (EL del inglés *Excess Loss*): es la relación entre la potencia total en todas las salidas respecto a la potencia de entrada.

$$EL = -10 \cdot \log \left( \frac{\sum_{k=1}^n P_{out}^k}{P_{in}^j} \right) > 0 \quad [\text{VIII-2}]$$

*Diáfonía* (CT del inglés *Crosstalk*): es la relación entre la potencia remanente en una salida no seleccionada, respecto de la potencia de entrada.

$$CT = 10 \cdot \log \left( \frac{P_{out}^n}{P_{in}^j} \right) < 0 \quad [\text{VIII-3}]$$

*Relación de Rechazo (Commutadores ON-OFF)*: es la relación entre la potencia de salida cuando el puerto correspondiente está en modo activo respecto de cuando se encuentra inactivo.

Tiempo de Comutación: es el tiempo que tarda en modificarse la salida desde el momento en el que se manda el comando que ordena el cambio.

Otras características de los conmutadores referidas a su funcionamiento son: las pérdidas de retorno, directividad, simetría, pérdidas dependientes de la polarización, dispersión por el modo de polarización, tasa de transferencia o la dependencia con la longitud de onda.

Además, otras características de los conmutadores están relacionadas con los requisitos de las redes en las que se emplean como enlaces multipunto, dimensión, escalabilidad... o también con los requisitos del sistema completo como consumo, coste, repetitividad...

### VIII.2.d.- Tipos de Conmutadores

La principal ventaja del uso de conmutadores ópticos es que no se necesita la conversión a señal eléctrica para realizar la conmutación. De esta forma se mejoran las características del sistema, reduciendo el número de elementos, incrementando la velocidad de transmisión y mejorando el consumo [Papadimitrou-2003, Ma-2003 and Rivero-2008].

Por el momento el uso de conmutadores ópticos había estado restringido debido a las limitaciones tecnológicas. Se han definido tres posibles escenarios para reemplazar la conmutación electrónica por conmutación óptica: conmutación de paquetes ópticos, protocolo múltiple generalizado de conmutación por etiquetas o conmutación óptica por ráfagas.

Dentro de las aplicaciones de los conmutadores ópticos, su uso depende del tipo de red en el que se empleen. Así, las matrices de conmutación se encargan de la interconexión de diferentes nodos de red empleando longitudes de onda dedicadas, creando caminos ópticos. De esta forma se permite la creación de comunicaciones

punto a punto [Ramaswami-2002]. Este tipo de conmutadores son transparentes al protocolo empleado y realizan el enrutamiento evitando la conversión al dominio eléctrico. Por otro lado, no permiten la realización de funciones de control ni la regeneración de la señal de entrada.

Los conmutadores de protección se encargan de recuperar la transmisión de información entre dos puntos cuando el enlace principal falla. Estos conmutadores deben ser robustos, mientras que el tiempo de conmutación no es crítico, puesto que las tareas a realizar al detectar el fallo y restablecer la comunicación son más complejas y tardarán más en realizarse.

Los multiplexores para la inserción/extracción de canales ópticos (OADMs del inglés *Optical Add/Drop Multiplexer*) permiten la extracción o introducción de información en el flujo de datos sin interferir con el resto de canales.

Los conmutadores para la monitorización óptica permiten la extracción de una pequeña porción de la potencia óptica disponible en la red WDM y permiten supervisar cada uno de los canales [Dugan-2001].

Finalmente, los conmutadores para el aprovisionamiento, permiten establecer nuevas rutas para los datos, o modificar las actuales existentes dentro de una red.

Por otro lado, los conmutadores ópticos se pueden clasificar en función de la tecnología empleada para realizar la conmutación. Así, se obtienen los siguientes grupos:

*Conmutadores Opto-mecánicos:* realizan la conmutación por medios mecánicos. Se emplean prismas, espejos y acopladores direccionales para realizar la conmutación. Poseen tiempos de respuesta del orden de milisegundos y se emplean como conmutadores de protección.

*Sistemas Micro-Electromecánicos:* a pesar de que pueden ser considerados como conmutadores opto-mecánicos, se han considerado aparte debido a su amplio desarrollo y gran interés. Están formados por pequeñas superficies reflectoras móviles que permiten modificar la dirección del haz incidente de acuerdo al destino seleccionado. Existen configuraciones en dos y tres dimensiones [Dobbelare-2002]. Este tipo de conmutadores se emplea en la implementación de OXC o OADM reconfigurables (ROADM del inglés *Reconfigurable Optical Add/Drop Multiplexer*) y también en monitorización o sistemas de protección.

Los MEMS en dos dimensiones poseen una limitación de 32 entradas y 32 salidas en el número de puertos, mientras que los basados en tres dimensiones pueden tener más de 1000 puertos de entrada y salida. El movimiento de los espejos se puede conseguir por medios electromagnéticos, electrostáticos o térmicos. Este tipo de conmutador se caracteriza por tener unos tiempos de respuesta pequeños, buena relación de acople fibra a fibra y bajo consumo de potencia.

*Conmutadores Termo-Ópticos:* realizan la conmutación por medio de la variación del índice de refracción de un material cuando se modifica su temperatura. Dentro de esta categoría los conmutadores se pueden agrupar en dos grupos, los

basados en los efectos termo-ópticos de los materiales y los conmutadores termo-ópticos, en los que la variación de temperatura se aplica a una guía de onda.

Ejemplos de conmutadores basados en los efectos termo-ópticos de los materiales son los conmutadores de burbuja [Fouquet-1998], por termo-capilaridad [Sakata-2001, Rivero-2008, Makihara-2000], resonadores de microesfera recubierta [Tapalian-2002].

Por el contrario, dentro del segundo tipo de conmutadores Termo-ópticos se encuentran entre otros los conmutadores interferométricos. Normalmente están basados en un interferómetro Mach-Zehnder, realizan la conmutación mediante la variación de las propiedades del interferómetro. Una versión generalizada de este tipo de conmutador consiste en la denominada zona de interferencia multimodo (MMI del inglés *Multi Mode Interference*). En este tipo de zona se cumple el principio de las auto-imágenes descrito en [Soldano-1995]. Si se modifica el índice de refracción dentro de la zona MMI, la potencia óptica puede ser guiada a la salida deseada. Un ejemplo de este tipo de conmutador se muestra en [Leuthold-2001].

Otro tipo de conmutadores interferométricos son aquellos basados en los anillos resonantes. Las condiciones de resonancia de dichos anillo se pueden modificar por diferentes métodos entre los que se encuentra la aplicación de calor al anillo. Otras tecnologías que permiten cambiar las propiedades del anillo son aplicando voltaje [Maune-2003], por efecto magneto-óptico [Tanushi-2005] o modificando el índice de refracción de la cubierta. En [Almeida-2004] se muestra el efecto de conmutación por el efecto de absorción de dos fotones.

*Conmutadores Acusto-Ópticos:* se basan en el efecto acusto-óptico que poseen ciertos materiales como la peratelurita ( $\text{TeO}_2$ ) [Sapriel-2002] o el Niobato de Litio ( $\text{LiNbO}_3$ ) [d'Alessandro-1993], por el cual, su índice de refracción se modula por medio de ondas acústicas. El fenómeno consiste en que una onda acústica que viaja por dicho medio causa una onda de presión periódica en dicho medio que altera su polarizabilidad modificando el índice de refracción del material.

*Conmutadores Todo-Ópticos:* realizan la conmutación por medio de efectos no lineales dependientes de la intensidad en las guías de onda, tales como el efecto de absorción de dos fotones, la auto-modulación de fase y el efecto Kerr que causa el fenómeno de mezcla de cuatro ondas (FWM del inglés *Four Wave Mixing*) y el fenómeno de modulación de fase cruzadas (XPM del inglés *Cross Phase Modulation*) [Ma-2003].

### **VIII.2.a.- Comparación entre Conmutadores Ópticos.**

Los conmutadores Opto-mecánicos fueron los primeros en desarrollarse. En general poseen menores velocidades de conmutación, pero están más extendidos. Presentan alto contraste, bajas pérdidas de inserción, y bajas pérdidas dependientes de la polarización. Por otro lado, muestran altos consumos de potencia.

Los MEMS, por su parte tienen bajas pérdidas de inserción, son independientes de la longitud de onda y de la polarización. Se emplean en los OXC que operan en las

redes troncales. En general precisan de altos voltajes para la conmutación, y presentan peores grados de estabilidad debido al uso de partes móviles.

La principal ventaja de los conmutadores termo-ópticos es su insensibilidad a la polarización y su velocidad de conmutación. Presentan bajos niveles de diafonía y medio-altos para la relación de rechazo. Sin embargo, los conmutadores interferométricos son dependientes de la longitud de onda, además de necesitar del control de la temperatura para su correcto funcionamiento.

En general, los conmutadores electro-ópticos presentan buenas características de velocidad, en el entorno de los picosegundos, son estables y poseen repetitividad, por ello son adecuados para la implementación de conmutación óptica de paquetes, y conmutación óptica por ráfagas. Por otro lado, estos conmutadores también requieren altas tensiones de excitación.

Los conmutadores acusto-ópticos presentan buena respuesta temporal, en el orden de los nanosegundos, y pueden operar con diversas longitudes de onda, que los hace adecuados para su uso en conmutadores selectivos en frecuencia. Con estos conmutadores se puede realizar conmutación a múltiples puntos, pero son caros.

Finalmente, los conmutadores todo-ópticos, permiten una rápida conmutación, son transparentes a los protocolos de red, poseen tasas de transferencia elevadas y permite un número elevado de canales.

Un resumen de las características más importantes de las diferentes tecnologías se muestra en la Tabla-II.1

### **VIII.3.- Conmutadores Basados en Cristal Líquido**

Como ya se ha comentado en el apartado anterior, hay diferentes tecnologías para la realización de conmutadores ópticos. En esta sección se van a presentar dos tipos de conmutadores novedosos basados en Cristal Líquido. En ambos casos, la fabricación se ha llevado a cabo empleando elementos discretos.

#### **VIII.3.a.- Multiplexor 3x1 Basado en el Tratamiento de la Polarización**

La estructura del multiplexor propuesto se muestra en la Figura VIII-3. Está compuesto por divisores polarizadores de haz (PBS del inglés *Polarizing Beam Splitters*), células de Cristal Líquido Nemático Torsionado (TN-LC del inglés *Twisted Nematic Liquid Crystal*), lentes, y polarizadores. Posee tres puertos de entrada y una salida.

El dispositivo está diseñado para su uso en redes de Fibra Óptica de Plástico (POF del inglés *Polymer Optical Fibre*). Se emplea la gran apertura numérica que ésta presenta para facilitar el acople de luz en el puerto de salida. También se puede emplear en redes de fibra de plástico de índice gradual que permiten un mayor rango de longitudes de onda de operación. En ese sentido, el uso de células de TN-LC

permite la operación del conmutador en un rango mayor de longitudes de onda en comparación con otras tecnologías y otros tipos de Cristal Líquido.

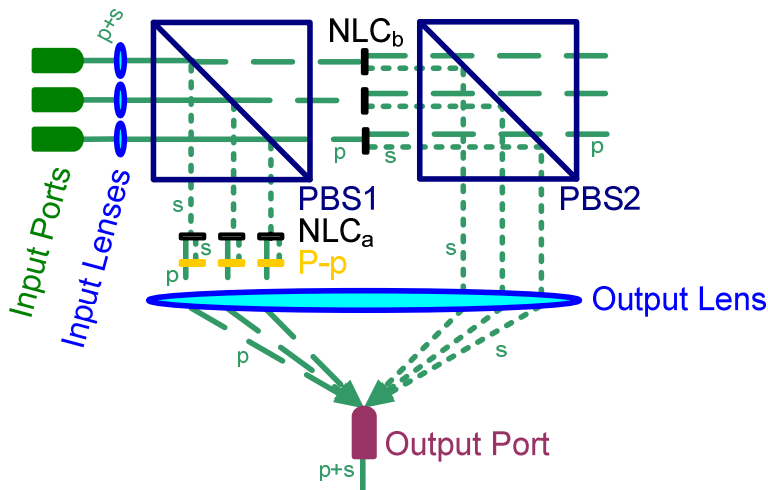


Figura VIII-3: Estructura del Multiplexor 3x1 Basada en el Tratamiento de la Polarización.

El esquema propuesto está basado en el tratamiento de la polarización, puesto que la conmutación se realiza a través de las células de TN-LC que actúan sobre la polarización de la luz que incide sobre ellas. En el caso de que no se aplique ningún campo eléctrico, las moléculas están ordenadas para que la polarización sea rotada 90°. Al aplicar un voltaje a la célula de TN-LC, las moléculas se reorientan en el sentido del campo, en esa situación la polarización de la luz incidente atraviesa la célula sin modificarse.

Por otro lado, el conmutador propuesto, es capaz de manejar ambas polarizaciones, haciendo uso del método de diversificación de la polarización. A pesar de que la estructura es más compleja, al transmitir las dos polarizaciones, el dispositivo tiene menos pérdidas.

El dispositivo se ha implementado y caracterizado. Se han llevado a cabo dos tipos de caracterizaciones, por un lado se ha medido la transmisión del conmutador para diferentes niveles de tensión aplicados a las células de TN-LC. También se ha realizado una caracterización dinámica del dispositivo para poder comprobar su comportamiento cuando se modifica su estado. Ambas caracterizaciones se han realizado a una longitud de onda de 650nm.

Del primer conjunto de medidas se ha comprobado que el dispositivo se encuentra completamente conmutado para tensiones superiores a 3Vrms. Para voltajes superiores a dicho valor, los puertos se encuentran en estado inactivo, es decir que no pasa luz de dicha entrada a la salida. Por otro lado, para tensiones inferiores a 1Vrms, no se ha inducido suficiente cambio en las células de cristal líquido, y la luz atraviesa el dispositivo hasta el puerto de salida. Las pérdidas de inserción son menores a 4dB, mientras que la diafonía medida es superior a 23dB.

Para facilitar el uso del dispositivo, se ha diseñado la electrónica de control que permite conmutar las células de TN-LC. Dicha electrónica puede comunicarse

mediante protocolo de comunicación serie RS232 con un ordenador para realizar el control remoto del dispositivo.

### VIII.3.b.- Multiplexor y Atenuador Óptico Variable Basado en Células de Cristal Líquido Disperso en Polímero

En la Figura VIII-2 se muestra otra novedosa estructura propuesta para funcionar como un multiplexor 3x1. El esquema presentado está formado básicamente por una célula de Cristal Líquido Disperso en Polímero (PDLC del inglés *Polymer Dispersed Liquid Crystal*). Al igual que sucede con el conmutador presentado previamente, este esquema está diseñado para trabajar en redes POF y GI-POF.

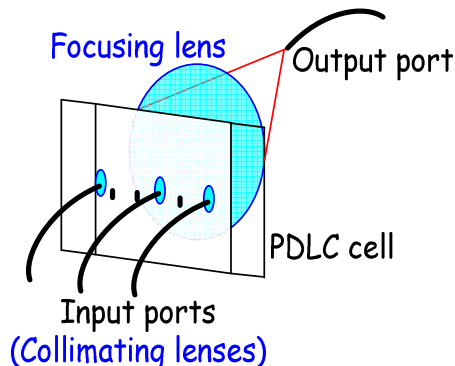


Figura VIII-4: Estructura del Multiplexor 3x1 Basada en el PDLC.

En este esquema también se emplea el cristal líquido como elemento activo, pero no hace uso del método de tratamiento de la polarización. Cuando no se aplica tensión a la célula de PDLC, las moléculas de cristal líquido que se encuentran en unas microbolas dentro de una matriz de polímero, se encuentran desordenadas, por lo que la luz incidente atraviesa una zona en la que el índice de refracción no es constante por lo que se dispersa.

Cuando se aplica un campo eléctrico a la célula de PDLC del conmutador, las células de Cristal Líquido se orientan en la dirección del campo, de forma que la luz incidente se encuentra con una zona donde el índice de refracción es constante, puesto que el índice extraordinario del cristal líquido coincide con el de la matriz polimérica, de forma que la luz atraviesa el dispositivo.

El dispositivo puede actuar como un atenuador óptico variable sobre cada uno de los puertos de entrada, porque la transmisión de las células de PDLC puede ser modificada mediante la tensión aplicada.

El dispositivo se ha implementado y se ha caracterizado, tanto estáticamente como dinámicamente. La caracterización se ha realizado a dos longitudes de onda diferentes. Puesto que la célula empleada para el montaje del dispositivo no tenía píxeles, se ha situado la entrada en diferentes posiciones para evaluar la capacidad del dispositivo como multiplexor.

La conmutación completa del dispositivo se produce para tensiones superiores a 20Vrms para todas las posiciones del puerto de entrada, y para las diferentes longitudes de onda empleadas. Las pérdidas de inserción obtenidas son menores a 1.6dB a 532nm y 1dB a 650nm. Se han obtenido valores de diafonía de 39.5dB a 532nm y 31dB a 650nm. La transmisión variable se obtiene para valores de tensión comprendidos entre 10Vrms y 20Vrms.

Respecto a la caracterización dinámica, en una primera caracterización se ha empleado una señal sinusoidal para excitar a la célula de cristal líquido. Se obtenía un rizado en la respuesta obtenida en la salida para esa situación. En una segunda caracterización se ha empleado una señal cuadrada. En los resultados obtenidos para el segundo grupo de medidas no se apreciaba la oscilación obtenida en las primeras medidas. Para las dos longitudes de onda medidas, el tiempo de subida es menor a 2.6ms mientras que el tiempo de bajada es mejor que 12.4ms. La diferencia entre ambos tiempos está en concordancia con las propiedades del cristal líquido nemático.

#### VIII.4.- Comutador Óptico Multifunción Avanzado Basado en Cristal Líquido

El Comutador Óptico Multifunción Avanzado está basado en el multiplexor 3x1 presentado en el apartado VIII-3.a. Al igual que dicho dispositivo, hace uso del método de tratamiento de la polarización y realiza el método de diversificación de la polaridad para reducir las pérdidas de inserción. El esquema del dispositivo propuesto se muestra en la Figura VIII-5. Se ha añadido un nuevo puerto de salida y un juego de puertos de entrada.

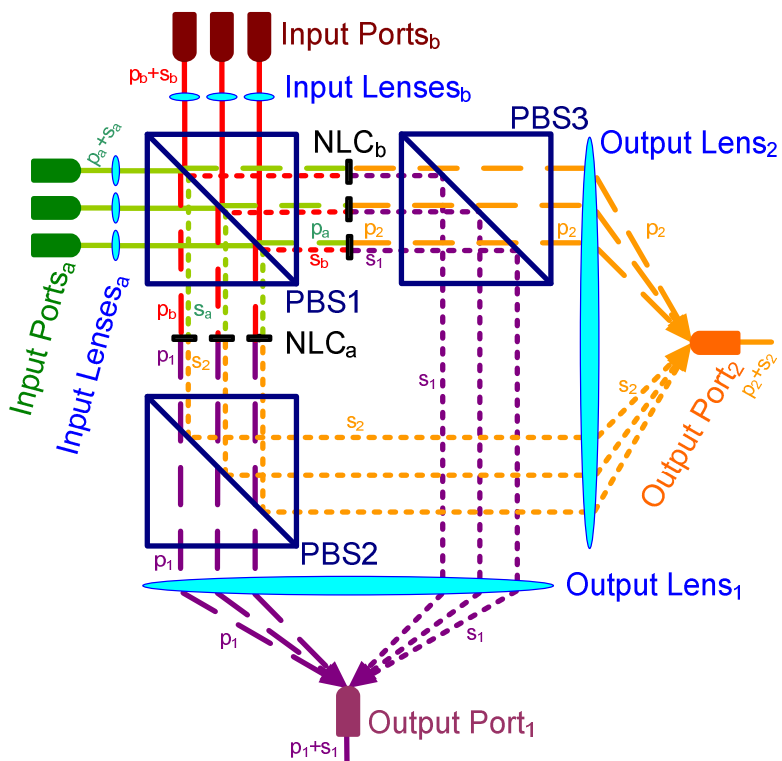


Figura VIII-5: Estructura del Comutador Óptico Multifunción Avanzado.

Los elementos añadidos hacen que la estructura sea más flexible, puesto que se pueden realizar más funciones seleccionando adecuadamente los puertos a emplear, y configurando las señales de control.

El funcionamiento del dispositivo es análogo al multiplexor descrito en la Sección VIII-3.a. Los cristales líquidos actúan sobre la polarización de la luz incidente dependiendo del voltaje que se les aplique. En el caso de que no se aplique voltaje, la estructura guía los puertos de entrada *Input Ports a* hacia la salida *Output Port 1*, y de forma análoga lo hace con los puertos complementarios de *Input Port b* hacia la salida *Output Port 2*.

Por el contrario, cuando se aplica suficiente tensión a la pareja de píxeles que tratan uno de los puertos de *Input Port a*, la estructura dirige la luz procedente del puerto correspondiente hacia la otra salida, es decir *Output Port 2*, mientras que el puerto asociado de *Input Port b* es guiado hacia *Output Port 1*.

Se pueden obtener valores de transmisión intermedios de potencia óptica en cada uno de los puertos de entrada, si se aplican un valor de tensión menor que el de conmutación a las células de TN-LC.

El uso de células de TN-LC permite el funcionamiento del dispositivo en un amplio rango de longitudes de onda. Debido al rango de operación esperado para el conmutador, se han diseñado y fabricado varias células de TN-LC con propiedades diferentes para que funcionen en diversos rangos de operación, en concreto aquellos para los que están diseñadas, es decir, poseen bajas pérdidas, las fibras POF y GI-POF.

De acuerdo con la información presentada previamente, el dispositivo permite implementar diferentes funcionalidades sin realizar modificaciones en el esquema, únicamente seleccionando los puertos de entrada y salida apropiados, y aplicando las señales de control a los píxeles adecuados.

El esquema propuesto es escalable. La principal restricción viene impuesta por las lentes de salida que se encargan de focalizar los haces de luz en el correspondiente puerto de salida. El ángulo con el que los haces son focalizados debe ser menor que el ángulo determinado por la apertura numérica asociada a la fibra de salida.

Por otro lado, la divergencia de los haces de entrada causa que la luz no se focaliza correctamente en el puerto de salida. Se puede mejorar el acople de luz en el puerto de salida empleando una lente de fibra en los puertos de salida. En ese mismo sentido, la gran apertura numérica que presentan las POF hace que la divergencia del haz de entrada sea mayor, por ello, los píxeles empleados en aplicaciones con POF han de tener un tamaño suficiente para cubrir todo el haz de salida.

Teniendo en cuenta estas consideraciones, se estima que para las lentes que utilizadas actualmente en el dispositivo, el mayor número de puertos de entrada para una aplicación con POF es de 6, mientras que para aplicaciones con GI-POF se puede llegar hasta 18 canales de entrada.

El dispositivo ha sido caracterizado con las distintas parejas de células para diferentes longitudes de onda. Se han obtenido pérdidas de inserción elevadas. Como

ya se ha comentado, esto se puede solucionar en parte empleando lentes de fibra en los puertos de salida y optimizando la colimación y la selección de las lentes.

La diafonía obtenida en todos los casos es mejor que 15dB en un rango de 900nm. Se pueden obtener valores de transmisión intermedios y controlados, aplicando voltajes menores a las células de TN-LC, entre 2Vrms y 3Vrms.

También se han medido los tiempos de respuesta. Se han obtenido valores entre 10ms y más de 100ms dependiendo de la célula de cristal líquido y los puertos empleados en la medida. Los tiempos mayores se corresponden con los tiempos de relajación del cristal líquido, además que para células con mayor espesor también se obtienen tiempos de respuesta mayores, como era de esperar.

Por otro lado, también se verifica que los tiempos del sistema completo exceden las medidas realizadas para los componentes individuales. Esto se puede deber a la diferencia de caminos físicos entre las dos polarizaciones y al hecho de que hay que conmutar una mayor cantidad de cristal líquido cuando se realiza la conmutación del sistema completo.

Finalmente, el dispositivo propuesto puede implementar varias funcionalidades con el mismo esquema, simplemente seleccionando los puertos adecuadamente y aplicando las señales de control a los píxeles adecuados. De esta forma, el conmutador puede funcionar como un Multiplexor/Combinador 3x1, un Multiplexor/Combinador 3x1 Dual, un Comutador 2x2. Además, si se aplican valores intermedios de tensión a las células de TN-LC, se puede obtener un Atenuador Óptico Variable o un Divisor de Potencia Óptica Variable.

El dispositivo se puede emplear en aplicaciones donde la velocidad de conmutación no sea crítica, tales como las descritas en la sección de aplicaciones.

### **VIII.5.- Conmutadores Basados en Óptica Integrada**

En esta sección se van a presentar los conmutadores basados en óptica integrada que se han desarrollado. Están basados en dos tipos de tecnologías, una en la que la conmutación se realiza mediante un anillo resonante en el que se introduce un tramo de cristal líquido para modificar sus propiedades, mientras que el último conmutador presentado es capaz de realizar *Tap and Two Split*, esto es, primero desvía una porción pequeña de la potencia de entrada hacia un puerto fijo y con la potencia óptica restante puede enviarla por las dos salidas en relaciones de potencia 100:0, 50:50 ó 0:100 y se basa en un interferómetro Mach-Zehnder (MZI del inglés *Mach-Zehnder Interferometer*).

#### **VIII.5.a.- Conmutadores y Filtros Sintonizables Basados en Anillos Resonantes y Cristal Líquido**

La estructura en anillo resonante posee una función de transferencia que puede ser empleada en filtros o conmutadores. Modificando las características del anillo

resonante, o también el acople con las guías de onda que actúan como puertos de entrada o salida, se puede variar la función de transferencia que esta estructura presenta.

En esta sección, se van a emplear tramos de cristal líquido dentro del anillo resonante para modificar sus características y obtener de esta forma filtros sintonizables o conmutadores.

En la Figura VIII-6 se muestra la estructura básica de un anillo resonante acoplado a dos guías de onda. La potencia de entrada se aplica a la entrada “*Input 1*” y se monitoriza la potencia óptica en las diferentes salidas. Para la realización de las simulaciones de esta estructura se ha empleado el programa Fullwave de Rsoft que hace uso del método de las Diferencias Finitas en el Dominio Temporal (FDTD del inglés *Finite Differences Time Domain*).

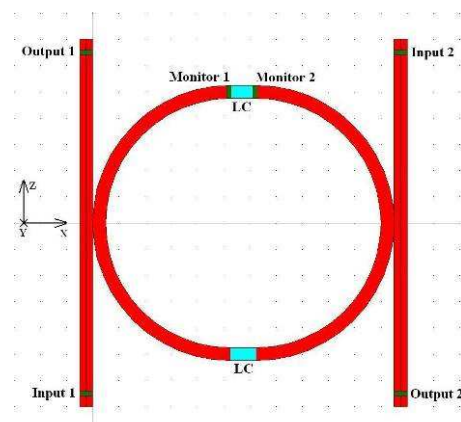


**Figura VIII-6:** Estructura del Conmutador Basado en Anillo Resonante con Cristal Líquido.

Las primeras simulaciones realizadas han servido para intentar optimizar los parámetros del anillo resonante, en especial la longitud de acople, el espacio entre las guías de onda en la zona de acople (*gap*) o la longitud del anillo resonante. En estas simulaciones previas, no se ha incluido ningún tramo con cristal líquido. Se ha obtenido un mejor resultado cuando el *gap* es nulo y para una longitud de acople de  $1.5\mu\text{m}$ .

En el siguiente grupo de simulaciones, se han introducido hasta dos tramos de cristal líquido dentro del anillo resonante. El cristal líquido permite modificar su índice de refracción aplicando un voltaje, de esta forma se puede modificar la respuesta del anillo resonante. De las simulaciones se desprende que se puede obtener un margen de variación de  $13\text{nm}$  que se corresponde con la mitad del Rango Espectral Libre, (FSR del inglés *Free Spectral Range*) cuando se emplea un tramo de cristal líquido de  $5\mu\text{m}$ , en un anillo con zonas de curvas de  $5\mu\text{m}$  de radio.

Para facilitar el diseño en estructuras más complejas, es interesante emplear la configuración en malla cruzada. En este tipo de dispositivo, la segunda guía de onda se sitúa en posición perpendicular a la guía de onda de entrada, con el anillo situado tangente a ambas guías de onda.

Comparando las simulaciones cuando se emplea la estructura convencional, y la estructura en malla cruzada, se obtienen resultados similares cuando se emplean los mismos parámetros.

Gracias a la estructura en malla cruzada, se pueden realizar estructuras compuestas como la mostrada en la Figura VIII-7

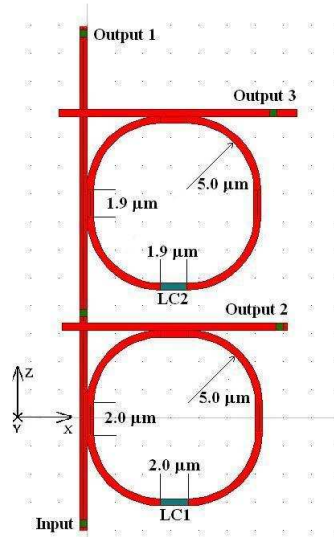


**Figura VIII-7:** Estructura Compuesta de un Comutador con dos Anillos Resonantes con Cristal Líquido.

La estructura propuesta permite realizar un conmutador 1 a 3 en el que la salida escogida viene determinada por el estado de los tramos de cristal líquido en los dos anillos resonantes.

### VIII.5.b.- Conmutador Óptico 2x2 Basado en un Interferómetro Mach - Zehnder

En esta sección se presenta un conmutador diseñado específicamente para su uso en matrices de conmutación capaces de realizar comunicaciones multipunto. El dispositivo se engloba dentro de una arquitectura de comunicaciones en la que una comunicación punto a multipunto se realiza sin conversión al dominio eléctrico.

En ese tipo de aplicaciones, se han propuesto diferentes arquitecturas para optimizar el número de enlaces y la potencia óptica necesaria para hacer llegar la información a los destinos deseados. La división en dos de la señal en cada nodo se ha demostrado como solución de compromiso porque posee las ventajas de las arquitecturas previamente propuestas y es eficiente en términos de potencia, además de ser su implementación menos complicada.

Por tanto, se precisa la implementación de un dispositivo capaz de monitorizar la señal de entrada para realizar una copia local de la información, con dos salidas adicionales que permiten la interconexión con otros dos nodos adyacentes, y que la potencia de salida se pueda distribuir únicamente por una salida o compartir al 50% entre las dos salidas.

De acuerdo con los requisitos de potencia previstos en el árbol de conmutación óptico, la potencia destinada al nodo local, *tap*, es el 6% de la potencia recibida. El resto de potencia óptica se puede direccionar a una salida, a la otra o a las dos a la vez en función del árbol de conmutación óptica a implementar.

En la Figura VIII-8 se muestra la arquitectura propuesta para el conmutador descrito. Está formado por un acoplador de Interferencia Multimodo (MMI del inglés *MultiMode Interference*) 94:6 que se encarga de realizar la copia de la información al nodo local. A continuación un conmutador 2x2 basado en un interferómetro Mach-Zehnder (MZI del inglés *Mach-Zehnder Interferometer*) permite seleccionar la salida por la que se transmite la potencia óptica.

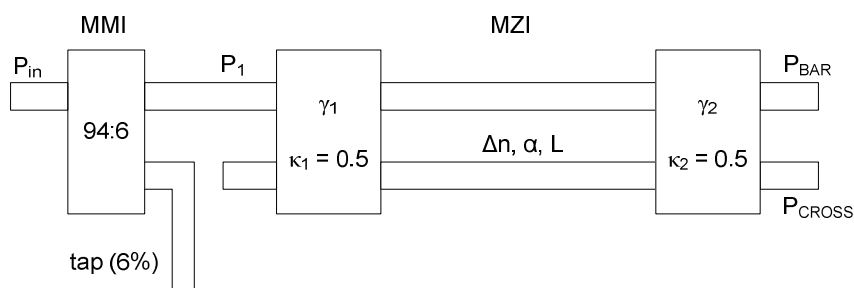


Figura VIII-8: Estructura del Conmutador Basado en Interferómetro Mach-Zehnder.

El conmutador propuesto se ha diseñado en óptica integrada para obtener un dispositivo más compacto. Se han simulado las ecuaciones del comportamiento del conmutador en Matlab, para comprobar el comportamiento correcto del dispositivo y poder estimar las pérdidas introducidas. Es importante cuantificar las pérdidas del conmutador para de esta forma poder realizar un cálculo más adecuado del árbol de conmutación óptico y seleccionar convenientemente los caminos ópticos más favorables.

La variación necesaria del índice de refracción para conmutar el interferómetro Mach-Zehnder que posee una guía de onda entre los acopladores de 100 $\mu\text{m}$  ha sido  $\Delta n = -7.75 \cdot 10^{-3}$ . Adicionalmente, se ha empleado el software BPM (*Beam Propagation Method*) para contrastar los resultados obtenidos empleando Matlab. Para ello se ha seleccionado un *tap* del 6%, unas pérdidas en exceso de 0.1dB en cada acoplador que forma parte del conmutador, y una longitud de la guía de onda del MZI de 100 $\mu\text{m}$ , todo ello para una longitud de onda en el vacío de 1.55  $\mu\text{m}$ .

### VIII.6.- Banco de Caracterización Óptica

Para la caracterización de algunos de los dispositivos presentados en el presente trabajo se ha desarrollado un Banco de Caracterización Óptica que facilite la toma de medidas.

Puesto que el banco diseñado se va a emplear en diferentes tipos de caracterización, se ha optado por que sea lo más versátil posible, facilitando al usuario que lo modifique de acuerdo al experimento que desea caracterizar. En la Figura VIII-9 se muestra la estructura propuesta para el banco.

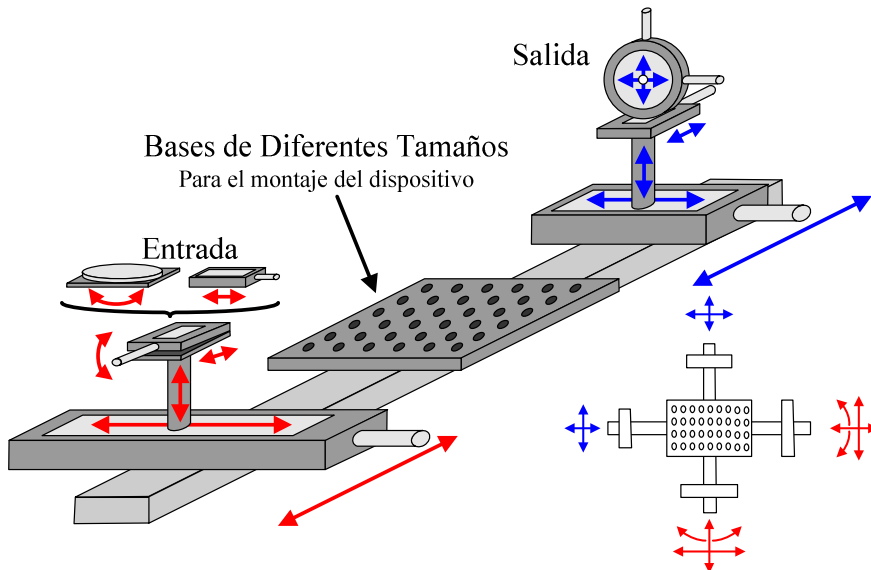


Figura VIII-9: Estructura del Banco de Caracterización Óptica

Adicionalmente, se ha dotado al banco con un sistema automatizado de movimientos en tres ejes que permite variar la posición de los componentes, dando más grados de libertad al usuario. También se han incluido los aparatos electrónicos de medida necesarios para la caracterización de diversos elementos optoelectrónicos.

En cuanto a la parte mecánica, el banco consta de una plataforma de translación de precisión en tres ejes, diversas plataformas de translación lineal, una plataforma rotatoria, bases y rieles.

El experimento se puede montar en una base que se sitúa sobre rieles de forma que permite su extracción del banco de prueba sin tener que desmontarlo.

Se ha desarrollado el software en LabView para la realización de movimientos automatizados, así como para la captura de medidas empleando el equipamiento disponible en el laboratorio.

Se han realizado dos experimentos para probar el sistema completo, incluyendo el software. Se han enfrentado dos fibras ópticas y se ha buscado el punto de máxima transferencia de potencia. En cada experimento se ha realizado el movimiento en un eje y se han tomado medidas para distintas posiciones.

En el primer experimento se ha realizado el acople entre una fibra monomodo de sílice y una fibra óptica de plástico, mientras que en el segundo experimento se han enfrentado dos fibras ópticas multimodo de sílice. El software ha funcionado correctamente, y las medidas se han almacenado en un fichero de texto. Este banco se ha utilizado para la caracterización del dispositivo multifunción conectado a fibras ópticas de entrada y salida.

### VIII.7.- Conclusiones y Trabajos Futuros

A lo largo de este trabajo se han propuesto diferentes estructuras novedosas para su uso en redes con Multiplexación en Longitud de Onda, (WDM del inglés *Wavelength Division Multiplexing*). Para su fabricación se han empleado diferentes tecnologías de conmutadores. Algunas de ellas están basadas en células de cristal líquido, y se han implementado con elementos discretos, mientras que otros dispositivos están basados en óptica integrada y se ha simulado su comportamiento.

Aquellos dispositivos basados en células de cristal líquido se pueden emplear en redes de fibra óptica multimodo como las Fibras Ópticas de Plástico (POF del inglés *Polymer Optical Fibre*). Ese tipo de dispositivos, tanto por sus características como por el tipo de fibras utilizado se pueden emplear en aplicaciones de corto alcance, y puede trabajar en longitudes de onda del rango visible e infrarrojo cercano: 450-650nm para aplicaciones en el automóvil, 650nm en redes dentro del hogar, o 850nm si se emplea con fibras multimodo. Además, pueden trabajar en el rango de 850-1300nm para redes de acceso.

Se han presentado dos estructuras novedosas para la implementación de un multiplexor óptico. En primer lugar, se ha descrito un multiplexor 3x1 de gran ancho de banda basado en el tratamiento de la polarización. El esquema hace uso del método de diversificación de la polarización, para reducir las pérdidas de inserción. El uso de fibras ópticas con gran apertura numérica mejora la operación de la estructura propuesta. El dispositivo descrito se ha fabricado mediante células de Cristal Líquido Nemático Torsionado (TN-LC del inglés *Twisted Nematic Liquid Crystal*). Se ha caracterizado a una longitud de onda, obteniéndose unas pérdidas de inserción, según se define en la sección VIII-2.c, menores a 4dB y una diafonía (definida en la sección VIII-2.c) mejor de 23dB a 650nm. También se ha obtenido un tiempo de establecimiento menor a 30ms, siendo el tiempo de subida mejor que 15ms.

La segunda estructura propuesta para la implementación del multiplexor se basa en el uso de una célula de Cristal Líquido Disperso en Polímero (PDLC del inglés *Polymer Dispersed Liquid Crystal*). El esquema propuesto para este conmutador permite combinar en un mismo dispositivo un multiplexor 3x1 junto con un atenuador óptico variable puesto que la transmisión se puede modificar entre los valores extremos simplemente modificando la tensión aplicada al cristal líquido.

Para la caracterización de este conmutador se ha empleado una célula de PDLC sin ningún pixel. La entrada se ha situado en diferentes posiciones respecto de la célula de PDLC y del puerto de salida para comprobar el funcionamiento del dispositivo. Se

ha realizado la caracterización tanto estática como dinámica. La conmutación completa se ha obtenido para valores de tensión superiores a 20Vrms en todas las posiciones. Las pérdidas de inserción son menores que 1.6dB a 532nm y que 1dB a 650nm. Se han medido relaciones de rechazo mayores que 39.5dB a 532nm y 31dB a 650nm. Se obtienen valores intermedios de transmisión se obtienen para tensiones de excitación entre 10Vrms y 20Vrms. Finalmente, se han medido tiempos de subida menores a 2.6ms y tiempos de bajada menores a 12.4ms al comutar la excitación de la célula de PDLC entre una onda cuadrada de 1kHz y cero voltios.

También se ha propuesto una estructura para la implementación de un dispositivo óptico multifunción avanzado basado también en células de TN-LC. El esquema propuesto deriva del multiplexor 3x1 propuesto anteriormente. Como se ha comentado con dicho multiplexor, el dispositivo propuesto permite su uso en redes POF debido a la gran apertura numérica que estas fibras presentan.

Se ha empleado TN-LC como elemento activo debido a que puede operar en un gran rango de longitudes de onda. Debido al rango de operación requerido para el dispositivo propuesto, se han diseñado y fabricado hasta cuatro tipos diferentes de células TN-LC. Dichas células también se han caracterizado para comprobar su rango de operación.

El dispositivo propuesto se ha caracterizado a diferentes longitudes de onda para obtener los parámetros más relevantes. Se han conseguido pérdidas de inserción superiores a lo esperado. Esto puede ser debido al uso de divisores polarizadores del haz (PBS del inglés *Polarizing Beam Splitters*) sin recubrimiento antireflejante, además de la divergencia que posee el haz de entrada que no está completamente colimado, y que en parte se puede corregir empleando lentes para fibra en los puertos de salida.

La diafonía obtenida, tal y como se define en la sección VIII-2.c, es mejor a 13dB para 650nm y 850nm. La transmisión a través del dispositivo se puede modificar con valores de excitación entre 3 y 4Vrms.

Los tiempos de respuesta medidos varían entre 10ms y más de 100ms. Estos tiempos del dispositivo completo son mayores que los obtenidos para las células de TN-LC debido en parte a la diferencia de caminos ópticos para las dos polarizaciones, lo que hace que se ensanche el pulso. Además de que se conmuta más cantidad de cristal líquido en el conmutador completo. El dispositivo se puede emplear en aplicaciones donde el tiempo de conmutación no sea fundamental.

Los mayores tiempos se corresponden con los tiempos de relajación del cristal líquido, puesto que estos tiempos superan a los tiempos de excitación para este tipo de células. También hay que destacar que se obtienen menores tiempos de conmutación para las células de menor espesor, debido a que el condensador equivalente es menor.

De la caracterización realizada, se puede decir, que el dispositivo es capaz de operar en un rango de 300nm, lo que permite su uso en redes de acceso de gran ancho de banda.

El esquema propuesto es escalable. Las principales restricciones vienen impuestas por la lente de salida, que se encarga de focalizar los haces de salida en el puerto de salida. El ángulo de los haces focalizados debe ser menor que el definido por la apertura numérica de la fibra óptica empleada a la salida. Puesto que la lente empleada tiene un diámetro de 50mm y una distancia focal de 75mm, no afecta a la restricción impuesta por la apertura numérica de la POF.

Por otro lado, la divergencia de los haces de entrada provoca que la luz no se focalice correctamente en el puerto de salida. Es posible acoplar más luz a la fibra de salida si se emplea una lente de fibra en dicho puerto. La gran apertura numérica que presenta la POF dificulta una correcta colimación de la luz, obteniendo haces con mayores divergencias. Para ese caso, el tamaño del píxel de la célula de TN-LC debe ser más grande para cubrir completamente el haz procedente de la fibra de entrada.

Teniendo en cuenta estas limitaciones y empleando la misma lente de salida, el número de puertos de entrada queda limitado en 6 para las aplicaciones con POF y 18 para aplicaciones con POF de índice gradual.

Por otro lado, el dispositivo presentado se ha descrito como multifunción. Esto es así, debido a que se pueden realizar diferentes funcionalidades con el mismo dispositivo, sin realizar cambios de hardware, únicamente seleccionando los puertos de entrada y salida adecuados, y aplicando las señales de control convenientes. De esta forma, se puede implementar un Multiplexor/Combinador 3x1, o un Multiplexor/Combinador 3x1 Dual, o un Conmutador Óptico 2x2. Además si se aplica un nivel de tensión intermedio a las células TN-LC se puede realizar un Atenuador Óptico Variable o un Divisor de Potencia Óptica Variable, con diferentes niveles de atenuación o división dependiendo del caso.

Adicionalmente a los conmutadores ópticos presentados hasta ahora, en el presente trabajo también se han propuesto dos estructuras de conmutación basadas en óptica integrada. En un primer diseño, se ha propuesto el empleo de micro-anillos resonantes combinados con cristal líquido. Se ha simulado la estructura básica con diferentes parámetros: longitudes del anillo, coeficientes de acople, tramos con cristal líquido dentro del anillo... para poder obtener la variación de la respuesta del anillo.

Todas las modificaciones afectan al Rango Espectral Libre (FSR del inglés *Free Spectral Range*) de la estructura, de forma que la modificación del estado del cristal líquido dentro del anillo resonante, modifica la respuesta del mismo. Esto se puede obtener aplicando un voltaje al cristal líquido que se encuentra dentro del anillo.

También se ha propuesto la aplicación del un tramo de cristal líquido dentro de un anillo resonante en configuración de rejilla cruzada, lo que permite la implementación de estructuras compuestas. Así, se ha propuesto un conmutador selectivo reconfigurable de tres canales formado por dos anillos situados en serie. La reconfiguración del dispositivo se puede realizar cambiando el estado del cristal líquido situado en cada uno de los anillos resonantes.

El último esquema propuesto para la implementación de un conmutador óptico está basado en un interferómetro Mach-Zehnder (MZI del inglés *Mach-Zehnder Interferometer*). El dispositivo es capaz de tomar una muestra de la potencia óptica a

la entrada (*Tap*) y si es necesario dividir el resto de la potencia remanente entre las dos salidas disponibles, o dejar que continúe hasta una de ellas. Este tipo de conmutador se puede emplear en nodos para arquitecturas de matrices de conexión que pueden realizar comunicaciones multipunto. Mediante el empleo del conmutador propuesto, se puede mejorar la eficiencia en potencia del árbol de comunicación empleado.

El conmutador óptico basado en óptica integrada ha sido específicamente diseñado para realizar las funcionalidades requeridas. Está compuesto por un divisor de potencia óptica 94:6 basado en una zona de interferencia multimodo (MMI del inglés *MultiMode Interference*), en combinación con un MZI reconfigurable.

Se han realizado simulaciones del dispositivo. Se ha empleado Matlab para simular el comportamiento del dispositivo mediante las ecuaciones presentadas en la sección V.4.b. Dichas simulaciones se han realizado puesto que es importante conocer las pérdidas inducidas por el dispositivo, dado que se han de tener en cuenta en la estimación de las pérdidas totales del sistema a lo largo del árbol para poder elegir un camino óptico u otro para realizar las comunicaciones.

La variación necesaria del índice de refracción para la conmutación del MZI con un brazo de  $100\mu\text{m}$  ha sido  $\Delta n = -7.75 \cdot 10^{-3}$ . Las simulaciones se han realizado con un *Tap* del 6%, 0.1dB de pérdidas por exceso para cada MMI que forman el interferómetro, constantes de acople de 0.5, para una longitud de onda en el vacío de  $1.55 \mu\text{m}$ . Se ha empleado el software BPM (*Beam Propagation Method*) para comprobar los resultados preliminares obtenidos con Matlab.

Finalmente, se ha diseñado y puesto a punto un Banco de Caracterización Óptica versátil que se ha empleado en la caracterización de varios de los dispositivos ópticos descritos. El usuario puede configurar el Banco Óptico de acuerdo con las restricciones de su experimento. El dispositivo a caracterizar se monta en una base independiente para facilitar su retirada cuando la caracterización haya acabado, sin necesidad de desmontarlo.

Se pueden realizar movimientos automatizados de hasta 25mm gracias a las plataformas de translación lineales. También está provisto de una plataforma de precisión con movimiento en 3 ejes de 13mm de recorrido. El mínimo recorrido incremental es de  $0.2\mu\text{m}$ , mientras que la repetitividad bidireccional es de  $3\mu\text{m}$ . Se pueden realizar movimientos adicionales empleando actuadores manuales. Además, se ha desarrollado un software mediante LabView para facilitar el control del banco de caracterización.

### **VIII.7.a.- Líneas de Trabajo Futuras**

Como posibles líneas de trabajo futuras relacionadas con los resultados obtenidos en el presente trabajo, se pueden considerar las siguientes:

- Caracterización de los dispositivos ópticos basados en elementos discretos empleando fibra óptica de plástico de índice gradual en el puerto de entrada. Con estas medidas, se puede llevar a cabo la caracterización de los dispositivos en un sistema de GI-POF. En las medidas realizadas, se ha empleado fibra multimodo de sílice o láseres a diferentes longitudes de onda como puertos de entrada.
- Optimización de la luz procedente de los puertos de entrada con POF. Se pueden obtener menores pérdidas de inserción si la entrada se colima correctamente. En ese sentido, se pueden usar diferentes sistemas de colimación para optimizar el comportamiento de los conmutadores ópticos. También se pueden emplear diferentes lentes para mejorar el acople en los puertos de salida.
- Estudio de la mejora de los puertos de salida en los conmutadores basados en elementos discretos. Si la luz procedente de la entrada no se colima correctamente, las lentes de salida no coliman la luz correctamente. En ese caso, el empleo de lentes de fibra puede mejorar el acople de luz en el puerto de salida, así como el uso de lentes con otras características.
- En relación al multiplexor propuesto, implementado con PDLC, se debe fabricar un PDLC con diferentes píxeles y caracterizar el dispositivo óptico completo con acople a fibras.
- En relación al Conmutador Óptico Multifunción Avanzado basado en células TN-LC, la optimización de los píxeles en las células empleadas puede reducir el tamaño del dispositivo e incrementar el número de puertos de entrada disponibles.
- Se debe realizar un estudio del AMOS para prevenir las reflexiones que puedan afectar al funcionamiento del dispositivo.
- Mejora de la señal de excitación de las células de Cristal Líquido, especialmente en la conmutación para reducir sus tiempos de respuesta.
- Se debe realizar la medida de las Pérdidas Dependientes de la Polarización en los conmutadores basados en elementos discretos.
- Optimización de la estructura del AMOS en términos de orientación de las células de Cristal Líquido y los voltajes aplicados para reducir las asimetrías como las relativas a las Pérdidas Dependientes de la Polarización y los retardos diferentes para cada polarización.
- Desarrollo de diferentes estrategias para reducir el tamaño del Conmutador Óptico Multifunción Avanzado.
- Se puede plantear el control de una inyección selectiva de modos en una fibra multimodo como parte fundamental de las redes de acceso de banda ancha. La

experiencia adquirida con la caracterización del Comutador Óptico Multifunción Avanzado, y el uso del Banco de Caracterización Óptico implementado se debe utilizar para avanzar en esta línea.

- Relacionado con los commutadores basados en óptica integrada, la fabricación y caracterización de las estructuras propuestas puede ser interesante para comprobar su funcionamiento.

### **VIII.8.- Publicaciones Obtenidas**

Véase Anexo A

## **Appendix A**

### **Publications Related to this Work**

---



### A.1.- Papers in International Journals and Books

**P. C. Lallana, C. Vázquez, B. Vinouze**

**"Advanced multifunctional optical switch for being used in polymer optical fiber networks"**

*Optical Engineering*, (under revision)

Co-author of the book: "*Optical Switches: Materials and Designs*"

**Chapter 8: "Liquid Crystal Optical Switches"**

C. Vázquez, I. Pérez, **P. C. Lallana**, B. Vinouze and B. Fracasso

Edited by :B. Li and S. J. Chua, Woodhead Publishing in Materials, Cambridge (2010)

G. M. Fernández, C. Vázquez, **P. C. Lallana** and D. Larrabeiti

**"Tap-and-2 Split Switch Design based on Integrated Optics for Light Routing in WDM Networks"**

*Journal of Lightwave Technology* 27(13), 2506 – 2517, July 2009

**P. C. Lallana, C. Vázquez, B. Vinouzé, K. Heggarty and D. S. Montero**

**"Multiplexer and Variable Optical Attenuator Based on PDLC for Polymer Optical Fiber Networks"**

*Molecular Crystals and Liquid Crystals* 502, 130 – 142, May 2009

**P. C. Lallana, C. Vázquez, J. M. S. Pena and R. Vergaz**

**"Reconfigurable Optical Multiplexer Based on Liquid Crystals for Polymer Optical Fiber Networks"**

*Opto-Electronics Review* 14(4), 311 - 318, April 2006

**C. Vázquez, J. Montalvo and P. C. Lallana**

**"Radio-Frequency Ring Resonators for Self-Referencing Fibre-Optic Intensity Sensors"**

*Optical Engineering Letters* 44(4), 040502-1 - 040502-2, April 2005

### A.2.- Contributions in International Conferences

**P. C. Lallana, C. Vázquez, D. S. Montero and B. Vinouzé**

**"Advanced Multifunction Optical Switch for Being Used in Polymer Optical Fiber Networks"**

*3rd International Workshop on Liquid Crystal for Photonics: LCP2010*

8 – 10 September 2010, Elche (Spain), Poster.

**G. M. Fernández, D. Larrabeiti, C. Vázquez, P. C. Lallana**

**"Power Cost-Effective Node Architecture for Light-Tree Routing in WDM Networks"**

*Global Telecommunications Conference, 2008. IEEE GLOBECOM 2008*

30 November – 4 December 2008, San Diego (USA), Poster

**P. C. Lallana, C. Vázquez, B. Vinouzé, K. Heggarty and D. S. Montero**

**"Multiplexer and Variable Optical Attenuator Based on PDLC for Polymer Optical Fiber Networks"**

*2nd International Workshop on Liquid Crystal for Photonics: LCP2008*

21 – 23 July 2008, Cambridge (UK), Poster

C. Vázquez, **P. C. Lallana**, D. S. Montero and J. Montalvo  
**"Self-reference intensity sensor techniques and advanced devices in WDM networks"**  
*VI symposium on Enabling Optical Networks (SEON 2008)*  
Porto (Portugal) (2008)

J. Montalvo, C. Vázquez and **P. C. Lallana**  
**"Ring Resonators with Sagnac Loops for Photonic Processing in DWDM Backbone Networks"**  
*IEEE International Symposium on Intelligent Signal Processing: WISP 2007*  
3 - 5 October 2007, Alcalá de Henares (Spain), Oral

**P. C. Lallana**, C. Vázquez, D. S. Montero, K. Heggarty and B. Vinouzé  
**"Dual 3x1 Multiplexer for POF Networks"**  
*XVI International Conference on Plastical Optical Fibers: POF conference 2007*  
10 - 12 September 2007, Turin (Italy), Oral

**P. C. Lallana** and C. Vázquez  
**"Plug and Play Connector for Automotive POF Networks"**  
*e-PhotoneONe/COST 291 Summer School*  
16 - 20 July 2007, Brest (France), Oral

C. Vázquez, J. Montalvo, D. S. Montero, **P. C. Lallana**  
**"Self-Referencing Technique in Photonics Sensors and Multiplexing"**  
*Microtechnologies for the New Millennium 2007*  
2 - 4 May 2007, Maspalomas (Spain), Oral

C. Vázquez, **P. C. Lallana**, J. Montalvo, J.M.S.Pena. A.d'Alesandro, D.Dionisi  
**"Switches and Tunable Filters Based on Ring Resonators and Liquid Crystals"**  
*Microtechnologies for the New Millennium 2007*  
2 - 4 May 2007, Maspalomas (2007), Oral

C. Vázquez, J. Montalvo, **P. C. Lallana**, D. S. Montero  
**"Self-Referencing Technique in Reflection Mode for Fibre-Optic Intensity Sensors Using Ring Resonators"**  
*Optical Fibre Sensors Conference: OFS-18*  
23 - 27 October 2006, Cancun (Mexico), Poster

**P. C. Lallana**, C. Vázquez, J. M. S. Pena, D. Sánchez  
**"Reconfigurable Optical Multiplexer Based on Liquid Crystal for Polymer Optical Fiber Networks"**  
*International Workshop on Liquid Crystal for Photonics*  
26 - 28 April 2006, Gent (Belgium), Oral

M. A. Jurado Pontes, Carmen Vázquez, J. M. Sánchez Pena, David Sánchez Montero, **P. C. Lallana**  
**"Variable Optical Attenuator for Perfluorinated Gradual Index Polymer Optical Fiber Using a Polymer Dispersed Liquid Crystal Cell"**  
*SPIE International Congress on Optics and Optoelectronics*  
28 August - 2 September 2005, Warsaw (Poland), Oral

J. Montalvo, **P. C. Lallana**, C. Vázquez

**"Self-Referencing Fibre-Optic Intensity Strain Sensors"**

*OFS'05: Optical Fibre Sensors Conference OFS-17*

23 – 27 May 2005, Bruges (Belgium), Poster

C. Vázquez, J. Montalvo, **P. C. Lallana**, J. M. S. Pena

**"Applications of Recirculating Optical Configurations on Filters and Lasers"**

*Microtechnologies for the New Millennium 2005*

9 – 11 May 2005, Seville (Spain), Oral

C. Vázquez, J. M. S. Pena, **P. C. Lallana**, M. A. Jurado Pontes

**"Development of a 2x2 Optical Switch for Plastic Optical Fiber Using Liquid Crystal Cells"**

*Microtechnologies for the New Millennium 2005*

9 – 11 May 2005, Seville (Spain), Oral

### A.3.- Contributions in National Conferences

D. S. Montero, C. Vázquez, **P. C. Lallana**, J. M. Baptista

**"Nueva Configuración Electro-Óptica Para Redes WDM de Sensores de Intensidad Óptica con Autoreferencia"**

*OPTOEL'09: VI Reunión Nacional de Optoelectrónica*

15 – 17 July 2009, Malaga (Spain), Poster

Carmen Vázquez, **P. C. Lallana**, D. S. Montero, J. M. Sánchez Pena, J.M: Otón

**"Optical Switch for Instrumentation Based on Liquid Crystals"**

*IV Reunión Española de Optoelectrónica: CDE'07*

31 January – 2 February 2007, El Escorial (Spain), Oral

C. Vázquez, **P. C. Lallana**, J. M. Sánchez Pena, M. A. Jurado Pontes

**"Multiplexor Óptico 3x1 para Fibra Óptica de Plástico Empleando Cristales Líquidos"**

*OPTOEL: IV Reunión Nacional de Optoelectrónica*

13- 15 July 2005, Elche (Spain), Poster

### A.4.- Research Stays

**November 2006 – January 2007 (3 months)**

Electronic Engineering Departemen La Sapienza University, Rome (Italy)

Funded by the V PM EU Network SAMPA program

Simulation and development of several integrated optics devices

**July 2007 (1 month)**

Optics Department, Telecom Bretagne, Brest (France)

Funded by: the Mobility Actions of University Carlos III de Madrid 2007

Bone Network of Excellence UE. IST FP7, grant ICT-216863

Manufacturing and characterization of Twisted Nematic Liquid Crystal Cells for broadband reconfigurable devices

**September 2008 – October 2007 (2 months)**

Optics Department, Telecom Bretagne, Brest (France)

Funded by the Mobility Actions of University Carlos III de Madrid 2008

Manufacturing and characterization of Twisted Nematic Liquid Crystal Cells for broadband reconfigurable devices

#### A.5.- Other Relevant Information

R. Vergaz, J. M. S. Pena, D. Barrios, C. Vázquez and **P. C. Lallana**

**“Modelling and Electrooptic Testing of Suspended Particle Devices”**

*Solar Energy Materials and Solar Cells* 92(11), 1483 - 1487, November 2008

Supervisor of the Master Thesis:

*“Implementación de herramienta software para la automatización de un banco de caracterización óptica”*

Author: José Joaquín Ferrer de la Cruz

Master in Advanced Electronic Systems, September 2010

Co-Supervisor of the Bachelor Project:

*“Desarrollo de Electrónica de Control para un Multiplexor Óptico 3 a 1 para Redes Ópticas con Fibra Óptica de Plástico”*

Author: Juan José Cañadas Rufo

Industrial Electronic Engineering, September 2006

## **Appendix B**

# **Optical Characterization Bench's User Manual**

---

*In this Appendix, a description of how to use the software developed for controlling the automated part of the Optical Characterization Bench is presented.*

*Two programs have been developed using LabView. The first one is in charge of controlling the automation part of the optical bench. It is capable of configuring the parameters of the actuators and performing single movements. Moreover, the software can make stepped displacements and capture the measurements in each position.*

*Additional functions have been implemented for controlling the wave generator and the oscilloscope.*



## B.1.- Software for Controlling the Motion Controller

A program implemented in LabView allows controlling the motion controller by means of a computer. The motion controller is connected to the computer thanks to a USB-GPIB converter from National Instruments. In addition, the software can also control a TTi 906 multimeter in order to capture the measurements.

The implemented software is able of configuring the motion controller parameters. Simple movements can be ordered using this program. Stepped displacements can also be configured by using this software. In this case, it is possible to capture a measurement in each position. The main window of the developed software is shown in Figure B-1.



Figure B-1: Main Window of the Developed Software.

The information of the actuators is in the left part of the window, while the right part of the window is dedicated to order the movements to the actuators.

### B.1.a. Configuration of the Communication Ports

Once the program is open, the communication ports where each equipment is connected has to be configured. In the top part of the Figure B-2 is the section for configuring purposes. Left channel will be used for handling the motion controller, while the channel placed on the right is used for configuring the multimeter.

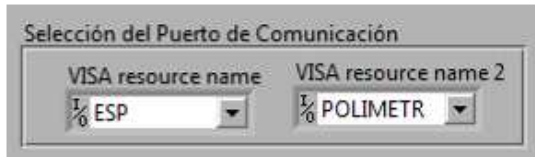


Figure B-2: Configuration of the Communication Ports.

The selected channel for the EPS 301 is *EPS*, while the channel selected for the multimeter TTi 906 is *POLIMETR*.

### B.1.b. Data File

The data captured and the position of the actuators when the data is measured can be stored in a file. The text file (“.txt”) has to be created in the desired destination folder before selecting it in the text box “*Archivo de Destino*”.

Each measurement is stored in a line with four columns separated by commas. The three first columns correspond with the position of the actuators when the data has been captured. The last column contains the voltage value measured with the multimeter.

The new captured data is written at the end of the file. It also happens when a new experiment is ordered, so old data are not overwritten.

### B.1.c. Parameters of the Actuators

The parameters related to the movement of the actuators are shown in the left side of the program window (see Figure B-3). These parameters are continuously updated.

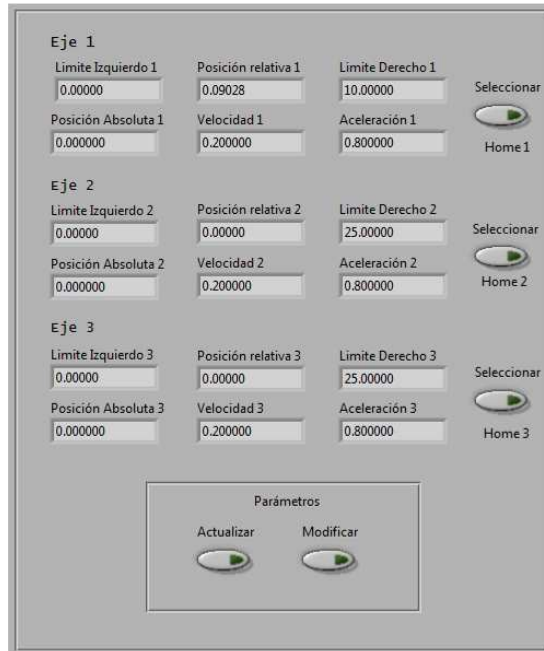


Figure B-3: Window Showing the Parameters of the Three Actuators.

For each axis, the parameters shown are:

- “*Posición Absoluta*”: This value indicates the real distance travelled by the actuator from its origin. In other words, it indicates the position in which the actuator is located.
- “*Posición Relativa*”: This value indicates the distance travelled from the position of reference that is known as *Home*. A positive value indicates that the travel is increasing the absolute position of the actuator, while a negative value denotes the travel is towards the origin of the actuator.
- “*Límite Izquierdo*”: Lower position allowed to the actuator. The relative position of the actuator is used for determining this limit. It is not configured by the absolute position of the actuators.
- “*Límite Derecho*”: Higher position allowed to the actuator. The relative position of the actuator is used for determining this limit. It is not configured by the absolute position of the actuators.
- “*Velocidad*”: Speed of the actuator.
- “*Aceleración*”: Acceleration of the actuator.

The *Home* position refers to the position saved as the reference for the relative movements. Initially, *Home* corresponds with the position of the actuator when the motion controller is switched on. A new value for the position of the *Home* can be stored by pressing the button labelled as “*Seleccionar Home*”.

The parameters that configure the movement of each actuator can be modified. The window for changing these parameters is shown in the Figure B-4. The default values of these parameters are configured until they are changed.



**Figure B-4:** Window for Configuring the Parameters of Each Actuator.

The parameters depend on the actuators used and the applications. In the present work, actuators CMA-25CCCL from Newport are used, so, the parameters stored in

the applications are those related to these actuators. The parameters the user can modify are:

- “*Velocidad*”: Set the speed for each actuator. For the actuators used in de Optical Characterization Bench, the speed can vary up to 0.4mm/s. By default, it is configured with 0.2mm/s.
- “*Accleración*”: Set the acceleration of the actuator. For the actuators used in the Optical Characterization Bench the acceleration is configures at 0.8mm/s<sup>2</sup>.
- “*Límite Izquierdo*” and “*Límite Derecho*”: Set the limits of the actuator’s movement at both edges. They should be used for stopping the actuator before obstacles. The reference position of the actuator is used for determining these limits. They are not configured by the absolute position of the actuators.

#### B.1.d. Actuator Enabling

The actuators can be enable or disabled. When they are disabled, they do not move. By pressing the button “*Habilitar/Deshabilitar Motores*” (see Figure B-5) the actuators can be enabled of disabled.

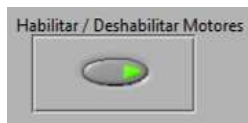


Figure B-5: Button for enabling/disabling the actuators

#### B.1.e. Single Movement of the Actuators

The actuators can be ordered to translate to the desired position. The movement can be ordered by indicating the position or the travel distance in the right part of the program window (see Figure B-6).

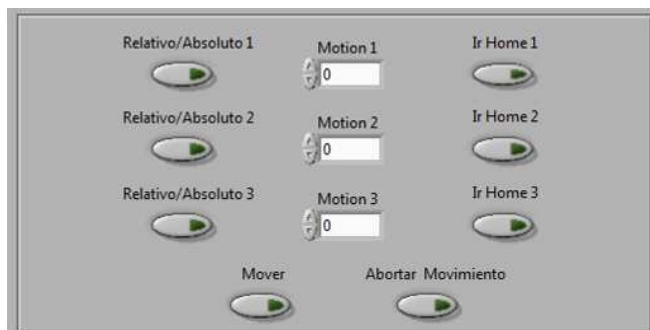


Figure B-6: Part of the Program’s Window where Order the Movement to the Actuators

The actuators have to be enabled of performing the movement. Relative and absolute movements is possible by selecting it in the “*Relativo/Absoluto*” button. In the absolute movement, the final position of the actuator is written in the “*Motion*” text

box. If “*Relativo*” is selected, then, the length of the movement is configured in the “*Motion*” text box. Once the movement for all the actuators is configured, it is performed by pressing the “*Mover*” button. The value used for ordering the travel of the actuators can have six decimals.

The three actuators move at the same time. An actuator does not perform the movement if zero is written in the “*Motion*” text box and a relative movement is selected.

It is possible to abort the movement of the actuators by pressing the “*Abortar*” button.

Absolute movements are useful for placing the actuators in a determined position, while the relative movements are used for applying a movement from the actual position of the actuators.

### B.1.f. Return to Home

By pressing the “*Ir Home*” button (see Figure B-6), the actuator moves to the position saved as the reference for the relative movements or “Home” position. This order is independent for each actuator.

### B.1.g. Stepped Movement of the Actuators

The developed software allows performing a travel in different steps in order to capture measurements in each intermediate position. The zone for configure this type of movement is on the left in the lower part of the program’s window (see Figure B-7).

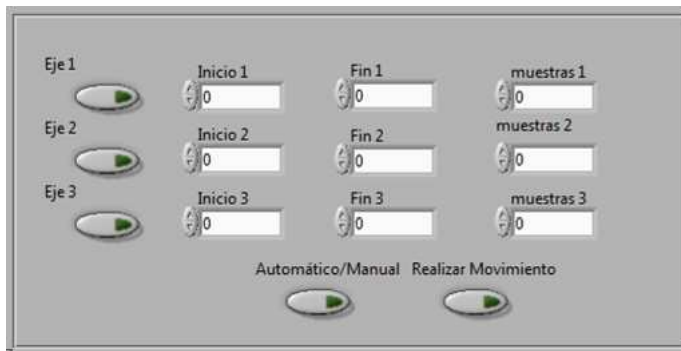


**Figure B-7:** Part of the Program’s Window where Order the Stepped Movement to the Actuators

The movement is performed by the selected axis using the “*Eje*” button on the right part of Figure B-7. The start and final positions are written in the “*Inicio*” and “*Fin*” text boxes respectively. The number of steps is configured in the “*Muestras*” text box. A warning message appears if the movement exceeds the limits configured for the actuators.

Two possibilities are available for continuing the movement after each step, manual and automatic configurations. In the automatic configuration, the translation of the actuators continue without the user confirmation, whereas, the manual configuration implies the user has to accept for continuing with the translation. This issue can be configured by pressing the “Automático/Manual” button.

The translation starts when the “Realizar Movimiento” button is pressed. Once the movement is started, it is not possible to abort it.

The measurements captured by the multimeter are stored in the text file indicated in “Archivo de Destino” with the structure indicated in section B-1.b.

### B.1.h. Voltage Measured with the Multimeter

By pressing the “Actualizar” button placed on the left of the “Valor Multimetro” text box (see Figure B-8), it is possible to visualize the voltage measured by the multimeter. The value is shown in “Valor Multimetro” text box.



Figure B-8: Measured Obtained with the Multimeter

## B.2.- Software for Controlling the Oscilloscope and the Wave Generator

Additional functions have been programmed in LabView for controlling the Oscilloscope TDS 1012 from Tektronix and the Wave Generator 33120A from Agilent. These functions operate independently of the motion controller and they can be used for characterizing the transmission response of several electro-optical elements such as the liquid crystal cells.

The program's window is organized in tabs; in order to reduce the information displayed at any time. In this way, the user watchs only the information required for the experiment he is carrying out.

The “Configuración” tab is used for configuring the equipment of the lab. Three possibilities are available. The “Medidas” tab is used for implementing amplitude swept in amplitude in the output signal of the wave generator. The “Error” tab contains all the error boxes related to each dialogue box programmed.

### B.2.a. “Configuración” Tab

The “Configuración” tab allows the user to configure the oscilloscope and the wave generator. Figure B-8 shows the information displayed in this tab. An additional

section allows the user to configure the equipment by using text commands. This section can also be used for configuring other equipment.

Each equipment addresses has to be selected in order to send and receive information to/from them.

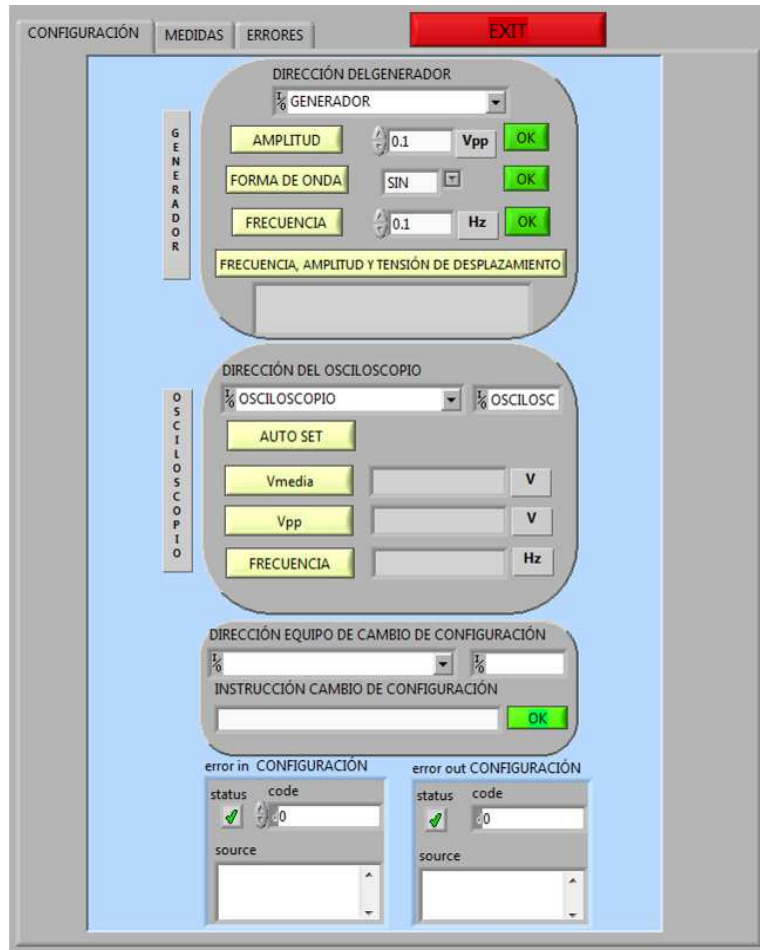


Figure B-9: Information Displayed in the “Configuración” Tab

The “*Generador*” section allows configuring the main parameters of the wave generator: amplitude, shape and frequency. An additional command allows obtaining the configuration from the wave generator.



Figure B-10: Detail of the Wave Generator Configuration Section

Once the configuration value is written in the text box, the parameter is applied by pressing the “OK” button.

The “Osciloscopio” section allows the user to obtain different measurements values from the oscilloscope (see Figure B-11)



Figure B-11: Detail of the Oscilloscope Configuration Section

The “Autoset” button makes the oscilloscope to perform a self-configuration order. In this way, the correct sensitivity values are obtained for the waves to measure.

By pressing other button: “Vmedia”, “Vpp” or “Frequency”, the average voltage, peak to peak voltage or the frequency of the channel number two are obtained. Correct values are obtained when the wave is properly display on the oscilloscope screen.

The additional section allows configuring some of the equipments using commands. This section only permits to send information to the equipment, it is not possible receiving information from the equipment.

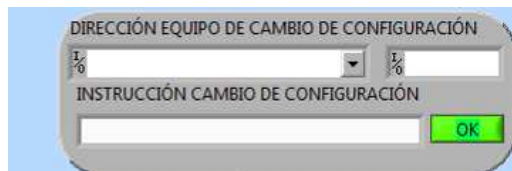


Figure B-12: Detail of the Additional Section

It is possible to configure another equipment by selecting the proper communication channel in the equipment address.

### B.2.b. “Medidas” Tab

The “Medidas” tab allows the user configuring amplitude swept of the signal provided by the wave generator. An image of the “Medidas” tab is shown in Figure B-13.

As it occurs in the “Configuración” tab, the addresses of each equipment has to be selected in order to send and receive the information properly.

The swept is configured by configuring the start value, the stop value and the increment in “*Inicio*”, “*Fin*” and “*Variación*” text boxes respectively. The amplitude values can increment or decrement.

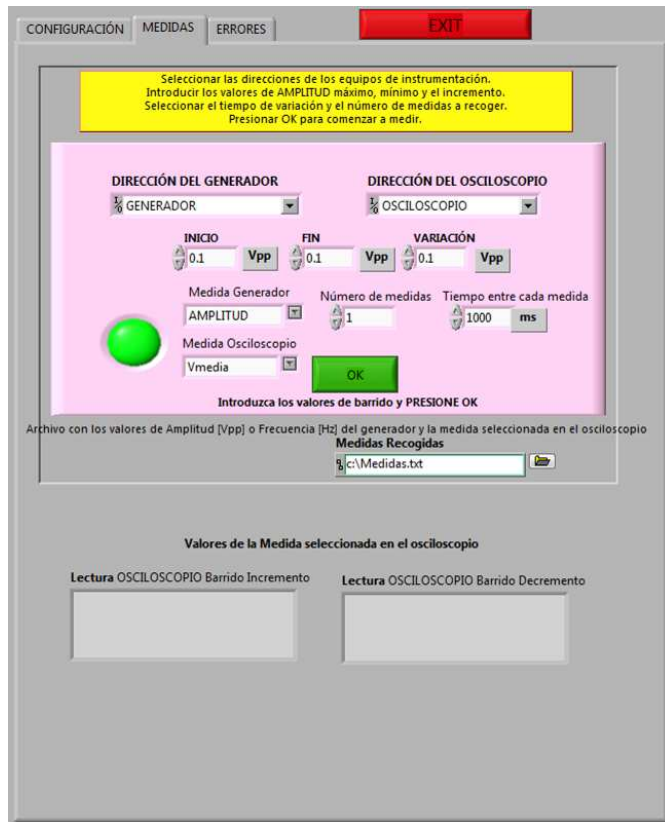


**Figure B-13:** Detail of the “*Medidas*” Tab

The information about the wave generator and the measurements obtained by the oscilloscope is saved in the file indicated by the “*Medidas Recogidas*” dialog box. The file is created if it does not exist, and the new measurements are saved at its end. The first column contains the information from the wave generator while the second one contains the measure obtained by the oscilloscope.

The number of measurements captured for each increment is configured in the “*Número de Medidas*” text box.

The delay between measurements is configured with the “*Tiempo entre cada medida*” text box.

The measurements captured by the oscilloscope are configured with the “*Medida Osciloscopio*” text box. The measurements obtained correspond with channel two.

The obtained measurements are displayed in the “*Lectura Osciloscopio*” text boxes. The one on the left is used when the amplitude is incremented while the one on the right shows the measurements when the amplitude swept is descendent.

The “*OK*” button is pressed in order to start the swept. Then, the green light switch to red until the measurement process is ended.



## Appendix C

# Software for the Simulation of Micro Ring-Resonators

---

*In this appendix, a brief introduction and some guidelines for using the software, Fullwave from RSoft, are given. This software is used in the simulations of the Ring Resonators of Chapter V.*

*Fullwave is a software based on the Finite Differences Time Domain method, which consists in calculating the Maxwell's equations in the nodes of a mesh at time intervals. In this way, light propagation in a waveguide is simulated. This method is used in those simulations where the beam propagation method is not possible, such as circular structures.*



### C.1.- Introduction

Fullwave is a general simulation package for computing the propagation of light waves in waveguides. The simulation is based on the Finite Differences Time Domain (FDTD) method. FDTD applies the solution of Maxwell's equations in the nodes of a mesh at time intervals. With this method, a propagation solution technique in integrated optics is used. It can be used when the Beam Propagation Method (BPM) is not adequate due to the structure geometry. FDTD is a direct solution of Maxwell's curl equations and therefore includes many effects than a solution of the monochromatic wave equation.

Physical and numerical parameters are required for performing the simulation. Apart from the physical parameters such as the refractive index distribution or the electromagnetic field excitation, other numerical parameters are required. For example, the computational domain that is the portion of structure simulated, the boundary conditions, or the spatial and temporal grids has to be observed in order to obtain a proper convergent solution.

### C.2.- Starting with the Simulation Software

Once the CAD Layout tool is opened, the start-up window, shown in Figure C-1, is displayed when a new simulation is selected.

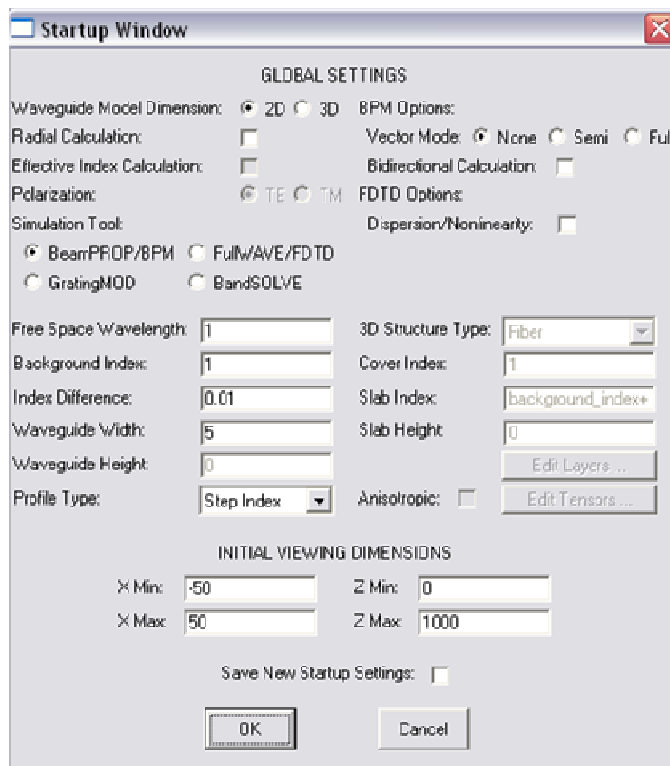


**Figure C-1:** Start-up Window Displays the Global Parameters of the Simulation

Global parameters of the simulations are selected in the Startup menu: the program used for the simulations, the number of dimensions, the refraction index of the waveguide or the background, the waveguide width. All this parameters configure the simulation of the software. The same window is used for BPM or other software used for simulating integrated optics.

The structure is depicted in the program window. Different utilities are available for accomplishing the design.

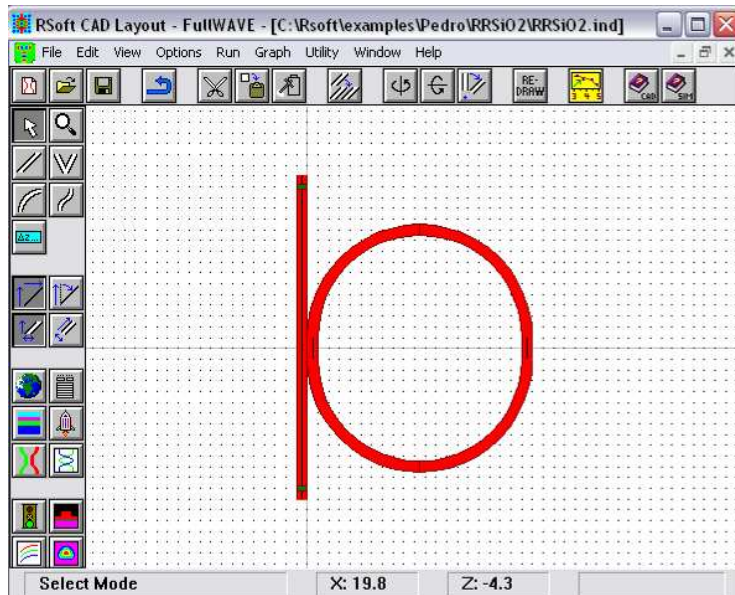


**Figure C-2:** Program Window with a Structure Drawn

The parameters of the segment depicted can be displayed by pressing with the right button of the mouse in the desired segment. The window with the parameters of the waveguide is shown in Figure C-3.

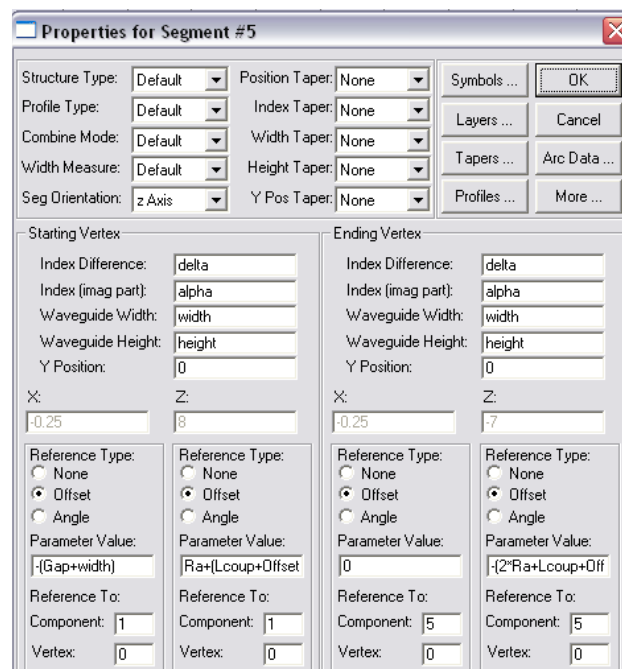


**Figure C-3:** Parameters of the Selected Waveguide

Different parameters of the waveguide are available like the start point and the end point, refraction index...

The use of variables makes easy the definition of the waveguide properties. Each label stores a value that can be applied to the properties of a waveguide. Then, changing the refraction index of all scheme can be done; by changing the value applied to the variable.

Some of the variables are created and used by the program; and others are created by the user. Figure C-4 shows the list of the variables available for the structure depicted in Figure C-2.

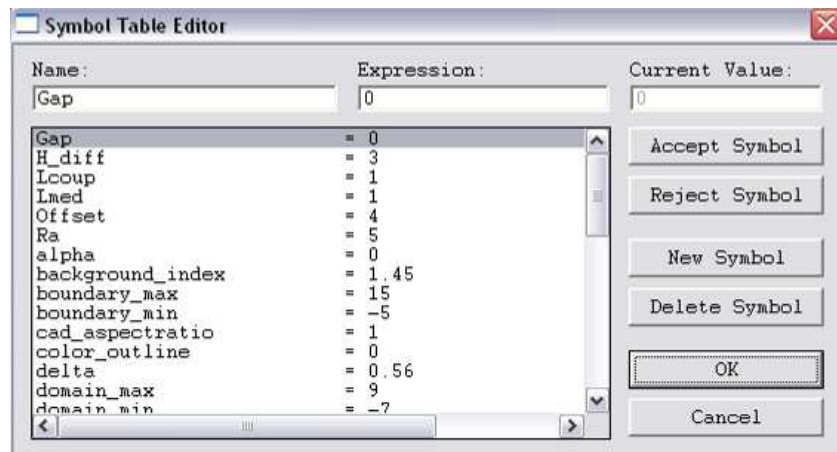


Figure C-4: List of the Variables of a Schematic.

Other things that have to be taken into account are the pathway that configures the waveguide where the input light is applied, as it is shown in Figure C-5.

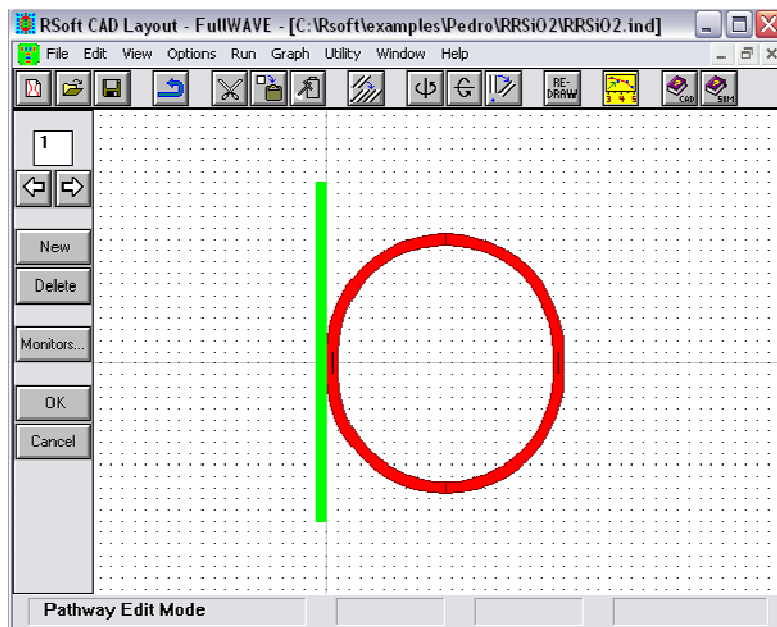


Figure C-5: Configuration of the Pathway

It is also important to place monitors in order to get the results. Different type of monitors are available, and different configurations can be applied to them in order

to obtain the desired result. Figure C-6 displays the menu for configuring the monitors.

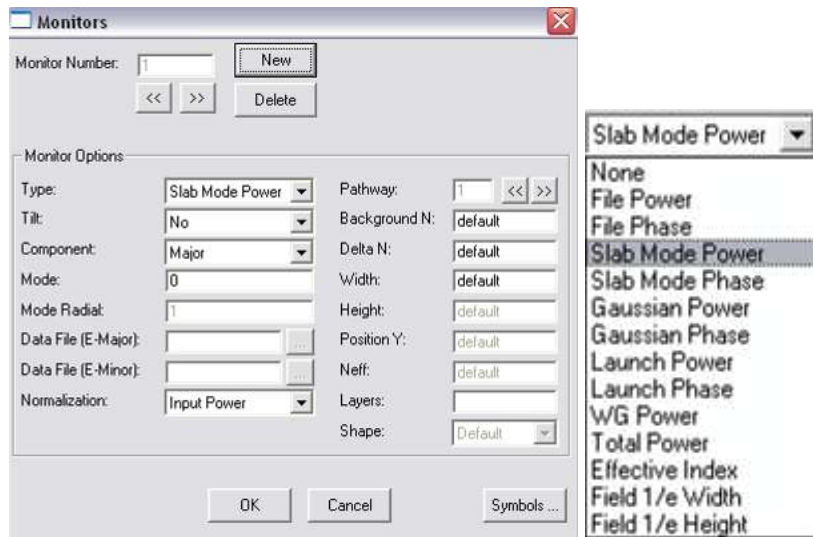


Figure C-6: Window for Configuring Parameters of Monitors

Once the structure is created, it is time of simulating it, in order to check its behavior.

### C.3.- Performing a Simulation

The light that is applied to the depicted structure is different, depending on the type of simulation required. The properties can be modified in the window of launch parameters (see Figure C-7).

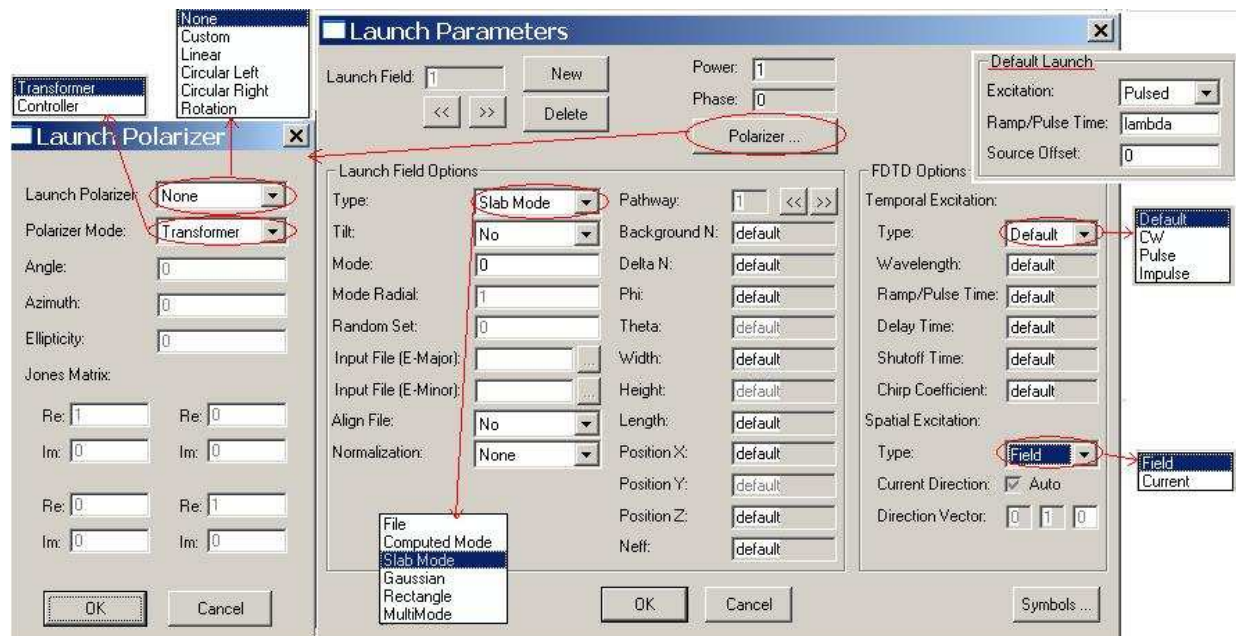
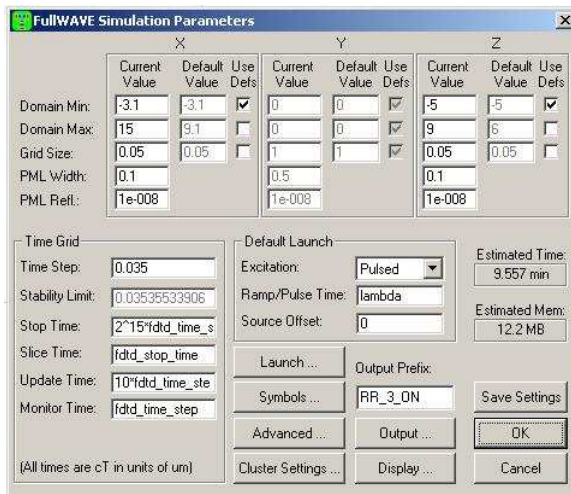


Figure C-7: Launch Parameters used in the Simulation.

Different types of excitations, both in the field options and in the temporal configuration can be applied to the scheme that is simulated. CW excitation is applied for watching the temporal behavior of the structure. On contrast, Pulse excitation is applied for obtaining the spectral response of the structure. In this case, posterior calculations are done for obtaining the results.

Once the excitation is configured, the window with the parameters of the simulations is displayed (see Figure C-8).



**Figure C-8:** Window with the Simulation Parameters

The program records different kinds of information depending on the configuration parameters and the excitation type. In a simulation with pulsed excitation the program saves the information in the .tmn file and calculates the FFT at the end generating the other files

The FDTD Output Options dialogue box (see Figure C-9) appears by pressing the Output button. You can use it for setting the data that you want the program saves. Depending on the selection, the program creates the different files.

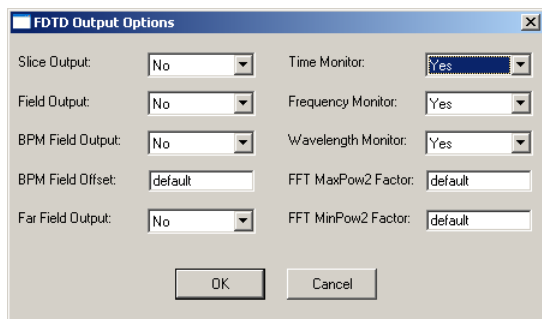


**Figure C-9:** Dialogue Box with the FDTD Output Options

Finally, when the simulation is running it appears in the window shown in Figure C-10.

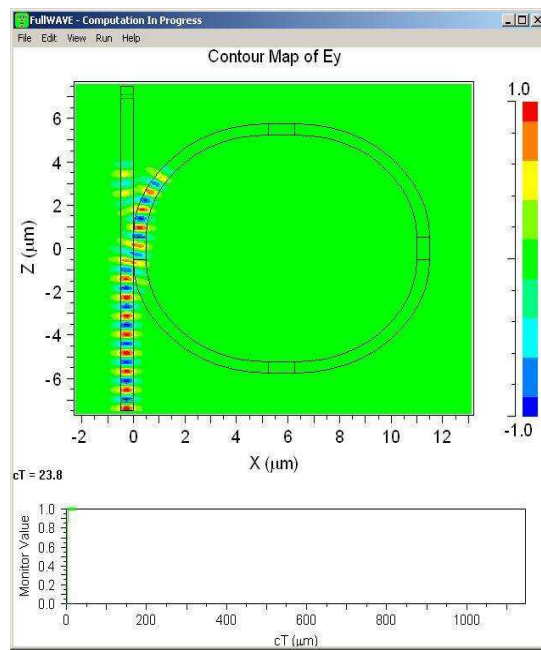


**Figure C-10:** Simulation Window

#### C.4.- Simulation Results

The obtained results can be plotted in the Winplot program that is also included in the software. The window of Winplot is shown in Figure C-11.

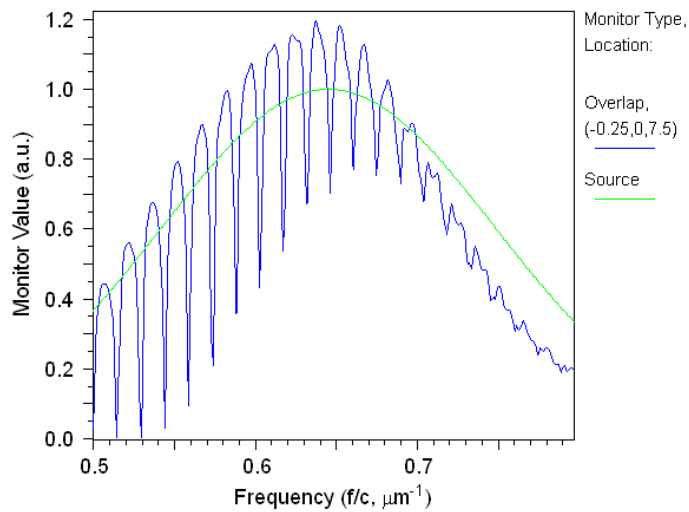


**Figure C-11:** Results Obtained for Simulation Displayed in Winplot Window

The files obtained for the simulations have different extensions, and their name is set using “Output Prefix” box, included in FullWave Simulation Parameters dialogue box. If any name is written in this box, the program only shows temporal information.

The extension of each file is added to the text of this box to get the final file name. The files obtained after the simulation have the following extensions:

- **.fmn:** contains spectral information of the monitors. The first column corresponds to the frequency and the others are related with the monitors, one column for each monitor.
- **.smn:** contains spectral information of the source used for the simulation. The first column corresponds to the frequency and the second to the values of the source for each frequency.
- **.tmn:** contains temporal information of the monitors. The first column corresponds to the time and the others are related to the monitors, one column for each monitor.
- **.wmn:** contains spectral information of the monitors. The first column corresponds to the wavelength and the others are related with the monitors, one column for each monitor.

The program generates other files for making possible to representation of the information using Winplot:

- **.pfm:** shows the power spectrum of the source and the monitors in the frequency domain.
- **.ptm:** shows the temporal representation of the source and the monitors.
- **.pwm:** shows the power spectrum of the monitors in the wavelength domain.

A program developed in Matlab capable of import data from a Fullwave file -.tmn (which contains temporal information about the simulation) is available. This program is used for importing data from a simulation with a pulsed excitation type, because in this way it is possible to make a spectral analysis of the simulation, as Fullwave does.

Matlab can calculate a FFT with more points than Fullwave do. Using the function FFT more points than the original signal can be obtained, by adding zeros at the end of the obtained results.

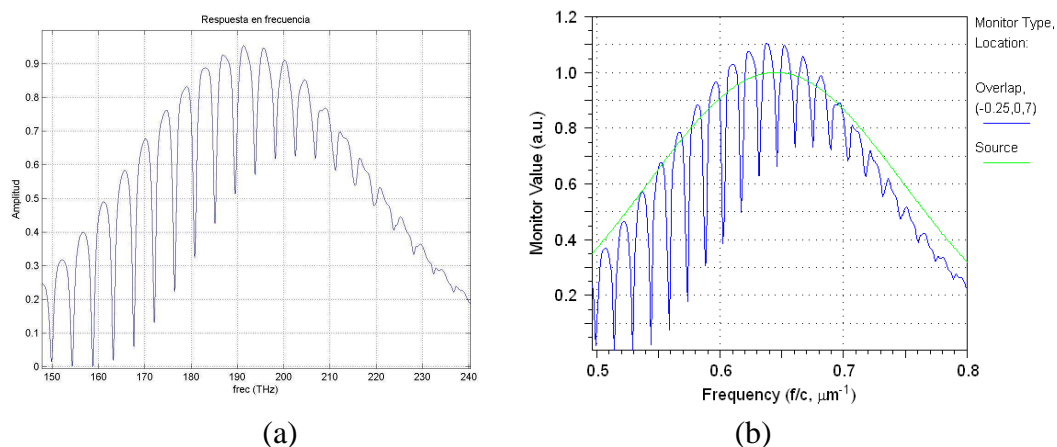


**Figure C-12:** Simulations Results Obtained for Simulation Displayed Using Matlab (a) and Winplot (b)

The program loads the file -.tmn in memory and gets two arrays uni-dimensional (if only one monitor is used). One of this arrays corresponds to the time and the other to

the signal values in the monitor. Then, the FFT with the desired samples is calculated and a plot is shown in a window. A comparison between results obtained with Matlab and Winplot is shown in Figure C-12.

# References

---

## A - F:

### **[Adamopoulos-2004]**

S. Adamopoulos, S. Konstantinou and D. Kalymnios.

“Variable POF attenuators”

*13<sup>th</sup> International Plastic Optical Fibres Conference 2004, Nürnberg, 567-573.*

### **[Agranat-1999]**

M. Ali and J. Deogun

“Electroholographic Wavelength Selective Crossconnect”

*Nanostructures and Quantum Dots/WDM Components/VCSELs and Microcavities/RF Photonics for CATV and HFC Systems* 1999, Dig. LEOS Summer Topical Mtgs., 61-62, 1999

### **[Ali-2000a]**

M. Ali and J. Deogun

“Power-efficient Design of Multicast Wavelength-Routed Networks”

*IEEE Journal on Selected Areas in Communications* 18 (10), 1852–1862, October 2000

### **[Ali-2000b]**

M. Ali and J. Deogun

“Cost-efficient Implementation of Multicasting in Wavelength-routed Networks”

*IEEE/OSA J. Lightwave Tech.* 18 (12), 1628–1638, December 2000

**[Almeida-2004]**

V. R. Almeida, C. A. Barrios, R. R. Panepucci and M. Lipson

“All-Optical Control of Light on a Silicon Chip”

*Nature*, 431, 1081–1084, October 2004.

**[Bahir-2005]**

T. Baher-Jones, M. Hochberg, G. Wang, R. Lawson, Y. Liao, P. A. Sullivan, L. Dalton, A. K.-Y. Jen and A. Scherer

“Optical modulation and Detection in Slotted Silicon Waveguides”

*Optic Express* 13 (14), 5216-5226, July 2005

**[Baierl-2001]**

W. Baierl

“Evolution of automotive Networks”

*10<sup>th</sup> Intern. Conf. POF*, 161-168, Amsterdam, September 2001

**[Bates-1992]**

R. J. S. Bates

“Equalization an Mode Partition Noise in All-Plastic Optical Fiber Data Links”

*IEEE Photon. Technol. Lett.* 4 (10), 1154-1157, October 1992

**[Bell-1991]**

J. Bell and C. N. Ironside

“Channel Optical Wavewuides Directly Written in Glass with an Electron Beam”

*Electronic Letters*, 27 (5), 448-450, February 1991

**[Beaugeois-2007]**

M. Beaugeois, B. Pinchemel, M. Bouazaoui, M. Lesecq, S. Maricot, and J. P. Vilcot

“All-optical tunability of InGaAsP/InP microdisk resonator by infrared light irradiation”

*Opt. Lett.* 32(1), 35-37, January 2007

**[Bogaerts-2010]**

W. Bogaerts, S. Selvaraja, P. Dumon, J. Brouckaert, K. De Vos, D. Van Thourhout and R. Baets

“Silicon-on-Insulator Spectral Filters Fabricated with CMOS Technology”

*J. Sel. Top. Quantum Electron.*, 16 (1), 33-44, January 2010

**[Bosc-1996]**

D. Bosc, C. Trubert, B. Vinouze and M. Guilbert

“Validation of a Scattering State Model for Liquid Crystal Polymer Composite”

*App. Phys. Lett.*, 68, 2489-2490, February 1996

**[Bregni-2001]**

S. Bregni, G. Guerra and A. Pattavina

“State of the art of Optical Switch Technology for All-Optical Networks”

*Communications World*, Rethymo Greece: WSES Press, 2001

**[Cao-2002]**

M. Cao, Q. Hu, Z. Wan and F. Luo

“A novel routing optical matrix switching method”

*Optics Communication*, 204, 163-175, April 2002

**[Cañas-2006]**

Juan José Cañas Rufo

“Desarrollo de la Electrónica de Control para un Multiplexor 3 a 1”

Bachelor Project, Universidad Carlos III de Madrid, September 2006

**[Chanclou-2003]**

P. Chanclou, B. Vinouze, M. Roy, C. Cornu and H. Ramanitra

“Phase-Shifting VOA with Polymer Dispersed Liquid Crystal”

*Journal of Lightwave Technology*, 21 (12), 3471-3476, December 2003

**[Chanclou-2005]**

P. Chanclou, B. Vinouze, M. Roy and C. Cornu

“Optical Fibered Variable Attenuator using Phase Shifting Polymer Dispersed Liquid Crystal”

*Optics Communication* 248, 167-172, April 2005

**[Chen-2006]**

R. Chen

“Polymer Offers Fabrication and Economic Advantages for Photonic Integrated Circuits”

SPIE OE magazine 24-26 Nov 2006

**[Chen-2008]**

Q.H. Chen, W. G. Wu, Z. Q. Wang, G. Z. Yan and Y. L. Hao

“Flexible Integration of Optical Switch with Optical Power Splitting and Attenuating Functions for Optical Fiber-Based Networking Applications”

*Optics Communications* 281, 5049-5057, June 2008

**[Chen-2010]**

Q.H. Chen, W. G. Wu, Z. Q. Wang, G. Z. Yan and Y. L. Hao

“Design and Performance of MEMS Multifunction Optical Device Using a Combined In-Plane and Out-of-Plane Motion of Dual-Slope Mirror”

*Journal of Lightwave Technology* 28(4), 3589-3598, December 2010

**[Chua-2010]**

S. J. Chua and B. Li

“Optical Switches: Materials and Design”

Woodhead Publishing Limited, UK, October 2010

**[Clark-1980]**

N.A. Clark and S.T. Lagerwall

“Submicrosecond bistable electro-optic switching in liquid crystals”

*Appl. Phys. Lett.* 36, 899-901, June 1980

**[Cornwell-2000]**

C. Cornwell and R. Albert

“Liquid-crystal devices promise high performance. *WDM solutions*”

*Suppl. Laser Focus World*, 35-39, February 2000

**[Crossland-2000]**

W. A Crossland, I. G. Manolis, M. M. Redmond, K. L. Tan, T. D. Wilkinson, M. J. Holmes, T. R. Parker, H H. Chu, J. Croucher, V. A. Handerek, S. T. Warr, B. Robertson, I. G. Bonas, G. Frankling, C. Satace, H. J. White, R. A. Woolley and G. Henshall

“Holographic optical switching; The “ROSES” demonstrator”

*Journal of Lightwave Technology* 18(12), 1845-1854, December 2000

**[d'Alessandro-1993]**

A. d'Alessandro, D. A Smith and J. E. Baran

“Polarisation-Independent Low Power Integrated Acousto-Optic Tunable Filter/Switch Using APE/Ti Polarisation Splitters on Lithium Niobate”

*Electronics Letters*, 29 (20), 1767-1769, September 1993

**[d'Alessandro-2006a]**

A. d'Alessandro, B. Bellini, I. G. Manolis, D. Donisi and R. Asquini

“Nematic Liquid Crystal Optical Channel Waveguides on Silicon”

*IEEE Journal of Quantum Electronics*, 42 (10), 1084-1090, October 2006

**[d'Alessandro-2006b]**

A. d'Alessandro, R. Beccherelli, B. Bellini, II. G. Manolis, R. Asquini and D. Donisi

“Integrated Optics Using Smectic and Nematic Liquid Crystals”

*Ferroelectrics*, 344, 247-254, November 2006

**[d'Alessandro-2008]**

A. d'Alessandro, D. Donisi, L. DE Sio, R. Beccherelli, R. Asquini, R. Caputo and C. Umeton

“Tunable Integrated Optical Filter Made of Glass Ion-Exchanged Waveguide and an Electro-Optic Composite Holographic Grating”

*Optic Express*, 16 (13), 9254-9260, June 2008.

**[DeCusatis-2008]**

C. DeCusatis

“Handbook of Fiber Optic Data Communication”

Academic Press/Elsevier 2008

**[Deri- 1991]**

R. J. Deri and E. Kapon

“Low-loss III-V semiconductor optical waveguides”

*IEEE J Quantum Electronics* 27(3), 626-640, March 1991

**[Desurvire-1998]**

Desurvire, C. R. Giles and J. R. Simpson

“Gain saturation effects in high-speed multichannel erbium-doped fibre amplifiers at  $\lambda=1.53\mu\text{m}$ ”

*Journal of Lightwave Technology* 7(12), 2095-2104, December 1989

**[Djordjev-2002a]**

K. Djordjev, S. Choi, S. Chou and P. Dapkus

“Microdisk tunable resonant filters and switches”

*IEEE Photonics Tech. Lett.*, 14 (6), 828-830, Agoust 2002

**[Djordjev, 2002b]**

K. Djordjev, S. Choi, S. Chou and P. Dapkus

"Vertically coupled InP Microdisk switches devices with electroabsorptive active regions"

*IEEE Photonics Tech. Lett.*, 14 (8), 1115-1117, November 2002

**[Djordjevich, 2003]**

A. Djordevich

"Alternative to Strain Measurement"

*Opt. Eng.* 42(7), 1888-1892, July 2003

**[Dobbelaere-2002]**

P. De Dobbelaere, K. Falta, L. Fan, S. Gloeckner and S. Patra

"Digital MEMS for Optical Switching"

*IEEE Commun. Mag.* 40(3), 88-95, March 2002

**[Doer-2005]**

C. R. Doer, M. Cappuzzo, L. Gómez, E. Chen, A. Wong-Foy, C. Ho, J. Lam and K. McGreer

"Planar Lightwave Circuit Eight-Channel CWDM Multiplexer with 3.9-dB insertion loss"

*J. Lightwave tech.*, 23 (1), 62-65, January 2005

**[Domash-1997]**

L. H. Domash, Y.-M. Chen, P. Haugsjaa and M. Oren

"Electronically Switchable Waveguide Bragg Gratings for WDM Routing"

*1997 Dig. IEEE/LEOS Summer Topical Mtgs.-WDM Components Tech.*, 34-35, August 1997

**[Donisi-2010]**

D. Donisi, B. Bellini, R. Beccherelli, R. Asquini, G. Giraldi, M. Trotta and A. d'Alessandro

"A switchable Liquid-Crystal Optical Channel Waveguide on Silicon"

*IEEE journal of Quantum Electronics*, 46 (5), 762-768, May 2010

**[Du-2004]**

F. Du, Y. Lu, H. Ren, S. Gauza and S. Wu

"Polymer-Stabilized Cholesteric Liquid Crystal for Polarization-Independent Variable Optical Attenuator"

*Japanese Journal of Applied Physics*, 43 (10), 7083-7086, October 2004

**[Dugan-2001]**

A. Dugan, I. Lightworks and J. C. Chiao

"The Optical Switching Spectrum: A primer on Wavelength Switching Technologies"

*Telecommunication Magazine*, May 2001.

**[Duport-1994]**

I. S. Duport, P. Benech and R Rimet

"New Integrated-Optics Interferometer in Planar Technology"

*Applied Optics*, 33 (25), 5954-5958, September 1994

**[Durana-2009]**

G. Durana, M. Kirchhof, M. Luber, I. S.-de Ocáriz, H. Poisel, J. Zubia, and C. Vázquez

"Use of a Novel Fiber Optical Strain Sensor for Monitoring the Vertical Deflection of an Aircraft Flap"

*IEEE Sensors Journal*, 9 (10), 1219-, October 2009

**[Eldada-2000]**

L. Eldada and L. W. Shacklette

"Advances in polymer integrated optics"

*IEEE J. selected topics in Quantum Electr.*, 6 (1), 54-68, January/February 2000

**[Feng-2007]**

J. Y Feng, T. S. Lay and T. Y. Chang

"Waveguide couplers with new power splitting ratios made possible by cascading of short multimode interference sections"

*Optics Express*, 15 (4) , 1588-1593, February 2007

**[Fernández-2009]**

G. M. Fernández, C. Vázquez, P. C. Lallana and D. Larrabeiti

"Tap-and-2 Split Switch Design Based on Integrated Optics for Light Routing in WDM Networks"

*Journal of Lightwave Technology* 27(13), 2506-2517, July 2009

**[Fernsener-2001]**

J. Fernsemer

"A Comparison of All-Optical Switching"

Stevens Institute of Technology, 2001

**[Ferrer-2010]**

José Joaquín Ferrer de la Cruz

"Implementación de Herramienta Software para la Automatización de un Banco de Caracterización Óptica"

Master Thesis, Universidad Carlos III de Madrid, September 2010

**[Fouquet-1998]**

J. E. Fouquet, S. Venkatesh, M. Troll, D. Chen, H. F. Wong and P. W. Barth

"A Compact, Scalable Cross-Connect Switch Using Total Internal Reflection Due to Thermally-Generated Bubbles"

*Lasers and Electro-Optics Society Annual Meeting (LEOS'98)* 2, 169-170, December 1998

**[Fracasso-2003]**

B. Fracasso, J.L. de Bougrenet de la Tocnaye, M. Razzak and C. Uche

"Design and Performance of a holographic Liquid Crystal Wavelength Selective Optical Switch"

*IEEE Journal of Lightwave Technology* 21(10), 2405-2411, October 2003

**[Fuji-1993]**

Y. Fujii

"Low-Crosstalk 2x2 Optical Switch Composed of Twisted Nematic Liquid Crystal Cells"

*Photonic Technology Letters*, 5 (6), 715-718, June 1993

G – L:

**[Gallep-2002]**

C. M. Gallep and E. Conforti

“Reduction of Semiconductor Optical Amplifier Switching Times by Preimpulse Step-Injected Current Technique”

*IEEE Photonics Tech. Lett.*, 14 (7), 902-904, July 2002.

**[Geuzebroek-2002]**

D. H. Geuzebroek, E. J. Klein, H. Kelderman, F. S. Tan, D. J. W. Klunder and A. Driessens

“Thermally Tunable, Wide FSR Switch based on Micro-ring Resonators”

*Proceedings Symposium IEEE/LEOS Benelux Chapter*, 155-158, 2002

**[Goh-1998]**

T. Goh, M. Yasu, K. Hattori, A. Himeno, M. Okuno and Y. Ohmori

“Low-Loss and High-Extinction-Ration Silica-Based Strictly Nonblocking 16x16 Thermooptic Matrix Switch”

*IEEE Phot. Tech. Lett.*, 10 (6), 810-812, June 1998

**[Gooch-1975]**

C. H. Gooch and H. A. Tarry

“The Optical Properties of Twisted Nematic Liquid Crystal Structures with Twist Angles  $\leq 90^\circ$ ”

*J. Physics D: Applied Physics* 8(13), 1575- 1584, May 1975

**[Grimes-1991]**

G. J. Grimes, L. L. Blyler, A. L. Larson and S. E. Farleigh

“A Plastic Optical Fiber Based Photonic Switch”

*Proceedings SPIE 1592, Polymer Optical Fiber*, 139-149, September 1991

**[Han-2009]**

Y.-T. Han, J.-U. Shin, S.-H. Park, S.-P. Han, Y. Baek, C.-H. Lee, Y.-O. Noh, H.-J. Lee and H.-H. Park

“Fabrication of 10-Channel Polymer Thermo-Optic Digital Switch Array”

*IEEE Phot. Tech. Lett.*, 21 (20), October 2009

**[Hardy-1999]**

S. Hardy

“Liquid-Crystal Technology Vies for Switching Applications”

*Lightwave* 16(13), 44 - 46, December 1999

**[Heaton-1999]**

J. M . Heaton and R. M. Jenkins

“General Matrix Theory of Self-Imaging in Multimode Interference (MMI) Couplers”

*IEEE Phot. Tech. Lett.*, 11 (2), 212-214, February 1999

**[Hecht-2004]**

J. Hecht

“*City of Light: The Story of Fiber Optics*”

Oxford University Press, 2004

**[Hecht-2006]**

J. Hecht

"*Understanding Fiber Optics*"

Pearson/Prentice Hall 2006

**[Heebner-1999]**

J. E. Heebner and R. W. Boyd

"Enhanced all-optical switching by use of a nonlinear fiber ring resonator"

*Opt. Lett.* 24 (12), 847-849, June 1999

**[Higuma-2001]**

K. Higuma, S. Oikawa, Y. Hashimoto, H. Nagata and M. Izutsu

"X-cut lithium niobate optical single sideband modulator"

*Electron. Lett.* 37(8), 515-516, April 2001

**[Hirabayashi-2001]**

K. Hirabayashi, M. Wada and C. Amano

"Compact Optical-Fiber Variable Attenuator arrays with Polymer-Network Liquid Crystals"

*Applied Optics*, 40 (21), 3509-3517, July 2001

**[Hu-1998]**

W. S. Hu. and Q. J. Zeng

"Multicasting Optical Cross Connects Employing Splitter-and-Delivery Switch"

*IEEE Photonics Tech. Lett.*, 10(7), 970-972, July 1998

**[IEEE-2006]**

IEEE, Institute of Electrical and Electronics Engineers, 2006

<http://www.ieee802.org/3/aq>, (Accessed 18 March 2011)

**[Ilyas-2003]**

M. Ilyas and H. T. Mouftah

"*The Handbook of Optical Communication Networks*"

CRC Press, 2003

**[Ishigure-1994]**

T. Ishigure, E. Nihei and Y. Koike

"Graded-Index Polymer Optical Fiber for High Speed Data Communication"

*Appl. Opt.*, 33 (19), 4261-4266, July 1994

**[Jiang-]**

H. Jiang, Y. K. Zou, Q. Chen, K .K. Li, R. Zhang and Y. Wang

"Transparent Electro-optics Ceramics and Devices"

Boston Applied Technologies, Inc., Woburn, MA, 01801, USA

**[Jurado-2005]**

M. A. Jurado Pontes, Carmen Vázquez, J. M. Sánchez Pena, David Sánchez Montero, P. C. Lallana

"Variable Optical Attenuator for Perfluorinated Gradual Index Polymer Optical Fiber Using a Polymer Dispersed Liquid Crystal Cell"

*SPIE International Congress on Optics and Optoelectronics*, Warsaw (Poland), September 2005

**[Kalymnios-2004]**

D. Kalymnios, P. Scully, J. Zubia and H. Poisel

“POF Sensor Overview”

*13<sup>th</sup> International Plastic Optical Fibres Conference POF2004, 237-244, Nürnberg, 2004*

**[Kao-1966]**

K. C. Kao and G. A. Hockham

“Dielectric-Fibre Surface Waveguide for Optical Frequencies”

*Proceedings IEEE 113, 1151-1158, July 1966*

**[Kapron-1970]**

R. P. Kapron, D. B. Keck and R. D. Maurer

“Radiation Losses in Glass Optical Waveguides”

*Applied Physics Letters, 17 (10), 423-425, November 1970*

**[Kaminow-2008a]**

I. P Kaminow, T. Li and A. E. Willner

“Optical Fiber Telecommunications IV A – Components and Subsystems”

Academic Press, Elsevier, 2008

**[Kaminow-2008b]**

I. P. Kaminow, T. Li and A. E. Willner

“Optical Fiber Telecommunications IV B – Systems and Networks”

Academic Press, Elsevier, 2008

**[Kawachi-1990]**

M. Kawachi

“Silica Waveguides on Silicon and Their Application to Integrated-Optic Components”

*Optical and Quantum Electronics 22(5), 391-416, 1990*

**[Keil-1996]**

H. Keil, H. H. Yao and C. Zawadki

“2x2 Digital Optical Switch Realized by Low Cost Polymer Waveguide Technology”

*Electron Lett. 32(16), 1470-1471, August 1996*

**[Kibler-2004]**

T. Kibler, S. Poferl, G. Böck, H.-P. Huber and E. Zeeb

“Optical Data Buses for Automotive Applications”

*J. Lightwave Technol. 22 (9), 2184-2199, September 2004*

**[Kodl-2003]**

G. Kodl

“Large Area Optical Pressure Detecting Sensor Based on Evanescent Field”

*Conference Proceedings POF'2003, Seattle, 64-67, September 2003.*

**[Koike-1991]**

Y. Koike

“Optical Resin Material with Distributed Refractive Index, Process for Producing the Materials, and Optical Conductors Using the Materials”

*JP Patent 333292: US Patent 5,541,247: EU Patent 0566744: KR: Patent 170358: CA Patent 2098604, 1991*

**[Koike-1994]**

Y. Koike and M. Naritomi

"Graded-Refractive-Index Optical Plastic Material and Method for its Production"

*JP Patent 3719733: US Patent 5.783.636: EU Patent 0710855: KR Patent 375581: CN Patent ZL951903152: TW090942, 1994*

**[Kokubun-2005]**

Y. Kokubun

"Photonics Based on Wavelength Integration and Manipulation"

*IPAP Books 2, 303–316, February 2005*

**[Koonath-2006]**

P. Koonath, T. Indukuri, and B. Jalali

"Monolithic 3-D Silicon Photonics"

*J. Light. Tech. Lett. 24(4), 1796-1804, April 2006*

**[Krähenbül-2002]**

R. Krähenbül, M. N. Howerton, J. Dubinger and A. S. Greenblatt

"Performance and Modelling of Advanced Ti:LiNbO<sub>3</sub> Digital Optical Switch"

*J. Lightwave Tech. 20(1), 92-99, January 2002*

**[Ksendzov-2005]**

A. Ksendzov and Y. Lin

"Integrated Optics Ring-Resonator Sensor for Protein Detection"

*Optics Letters, 30 (24), 3344-3349, December 2005*

**[Lallana-2006]**

P. C. Lallana, C. Vázquez, J. M. S. Pena and R. Vergaz

"Reconfigurable Optical Multiplexer Based on Liquid Crystals for Polymer Optical Fiber Networks"

*Opto-Electronics Review 14(4), 311 – 318, December 2006*

**[Lallana-2007]**

P. C. Lallana and C. Vázquez

"Plug and Play Connector for Automotive POF Networks"

*e-PhotoneONe/COST 291 Summer School, Brest (France), July 2007*

**[Lallana-2008]**

P. C. Lallana, C. Vázquez, B. Vinouze, K. Heggarty and D. S. Montero

"Multiplexer and Variable Optical Attenuator based on PDLC for Polymer Optical Fiber networks"

*Molecular Crystals and Liquid Crystals 502, 130 – 142, May 2009*

**[Lallana-2011]**

P. C. Lallana, C. Vázquez, B. Vinouze

"Advanced multifunctional optical switch for being used in polymer optical fiber networks"

*Optical Engineering, (In revision), 2011*

**[Layadi-1998]**

A. Layadi, A. Vonsovici, R. Orobtchouck, D. Pascal and A. Koster

"Low-Loss Optical Waveguide on Standard SOI/SIMOX Substrate"

*Optical Communications. 146, 31-33, January 1988*

**[Lee-2002]**

M. H. Lee, Y. H. Min, S. Park, J. J. Ju, J. Y. Do and S. K. Park  
“Fully Packaged Polymeric Four Arrayed 2x2 Digital Optical Switch”  
*IEEE Phot.Tech. Lett.* 14(5), 615-617, May 2002

**[Lee-2004]**

C. Lee and Y. S. Lin  
“A new Micromechanism for Transformation of Small Displacements to Large Rotations for a VOA”  
*IEEE Sensors Journal* 4 (4), 503-509, August 2004

**[Lee-2007]**

C. J. Lee, F. Breyer, S. Randel, B. Spinnler, I. L. Lobato Polo, D. Van Den Borne, J. Zeng, E. De Man, H. P. A. Van Den Boom, and A. M. J. Koonen  
“10.7 Gbit/s transmission over 220 m polymer optical fiber using maximum likelihood sequence estimation”  
*Optical Fiber Communication and the National Fiber Optic Engineers Conference 2007 OFC/NFOEC 2007*, 2007

**[Leuthold-2001]**

J. Leuthold and C. H. Joyner  
“Multimode Interference Couplers with Tunable Power Splitting Ratios”  
*IEEE/OSA J. Lightwave Tech.* 19 (5), 700–706, May 2001

**[Levy-2006]**

U. Levy, K. Campbell, A. Groisman, S. Mookherjea and Y. Fainman  
“On-chip microfluidic tuning of an optical microring resonator”  
*Appl. Phys. Lett.* 88, 111107 – 111107-3, March 2006

**[Li-2010]**

B. Li and S. J. Chua  
“Optical Switches: Materials and Designs”  
Woodhead Publishing in Materials, Cambridge (2010)

**[Little-1998a]**

B. E. Little, H. A. Haus, J. S. Foresi, L. C. Kimerling, E. P. Ippen, and D. J. Ripin  
“Wavelength Switching and Routing Using Absorption and Resonance”  
*IEEE Photonics Tech. Lett.*, 10 (6), 816-818, June 1998

**[Little-1998b]**

B. E. Little, J. S. Foresi, G. Steinmeyer, E. R. Thoen, S. T. Chu, H. A. Haus, E. P. Ippen, L. C. Kimerling, and W. Greene  
“Ultra-Compact Si-SiO Microring Resonator Optical Channel Dropping Filters”  
*IEEE Photonics Tech. Lett.*, 10 (4), 549-551, April 1998

**[Little-2004]**

B. E. Little, S. T. Chu, P. P. Absil, J. V. Hryniewicz, F. G. Johnson, F. Seiferth, D. Gill, V. Van, O. King and M. Trakalo  
“Very High-Order Microring Resonator Filters for WDM Applications”  
*IEEE Photonics Tech. Lett.*, 16 (10), 2263-2265, October 2004

**[Liu-2004a]**

A. Liu, J. Richard, L. Ling, D. Samara-Rubio, D Rubin, O. Cohen, R. Nicolaescu and M. Paniccia  
“A High-Speed Silicon Optical Modulator based on Metal-Oxide Semiconductor Capacitor”  
*Nature*, 427 (6975), 615-618, February 2004

**[Liu-2004b]**

C.-Y. Liu and L.-W. Chen  
“Tunable Photonic Crystal Waveguide Coupler With Nematic Liquid Crystals”  
*IEEE Photonics Technology Letters* 16(8), 1849-1851, August 2004

**[Liu-2005]**

Y. J. Liu, X. W. Sun, J. H. Liu, H. T. Dai and K. S. Xu  
“A Polarization Insensitive 2x2 Optical Switch Fabricated by Liquid Crystal-Polymer Composite”  
*Applied Physics Letters* 86, 041115-1 – 041115-3, January 2005

**[Liu-2007]**

A. Liu, L. Liao, D. Rubin, H. Nguyen, B. Ciftcioglu, Y. Chetrit, N. Izhaky and M. Paniccia  
“High Speed Optical Modulation Based on Carrier Depletion in a Silicon Waveguide”  
*Optic Express* 15(2) 660-668, January 2007

**[Liua-2006]**

Y. Liua, E. Tangdiongcaa, Z. Lia, S. Zhangaa, M.T. Hilla, J.H.C. van Zantvoorta, F.M. Huijskensa, H. de Waardta, M.K. Smithb, A.M.J. Koonena, G.D. Khoea and H.J.S. Dorrenaa  
“Ultra-Fast All-Optical Signal Processing: Towards Optical Packet Switching”  
[Invited] *Optical Transmission, Switching, and Subsystems IV Proc. of SPIE* Vol. 6353 635312-1

**[Losert-2004]**

W. Losert, G. Bauer, O. Zieman and H. Poisel  
“POF Variable Optical Attenuators – Status and New Concepts”  
13<sup>th</sup> *International Plastic Optical Fibres Conference 2004*, Nürnberg, 546-551

**[Lomera-2007]**

M. Lomera, J. Arrue, C. Jauregui, P. Aiestaran, J. Zubia, J. M. López-Higuera  
“Lateral Polishing of Bends in Plastic Optical Fibres Applied to a Multipoint Liquid-Level Measurement Sensor”  
*Sensors and Actuators A* , 137, 68–73, June 2007

**M – R:**

**[Ma-2003]**

X. Ma and G. S. Kuo  
“Optical Switching Technology Comparison: Optical MEMS vs Other Technologies”  
*IEEE Optical Communications*, 41 (11), S16 - S23, November 2003

**[Maalouf 2006]**

A. Maalouf, D. Bosc, F. Henrio, S. Haesaert, P. Grosso, I. Hardy and M. Gadonna  
“Polymer Optical Circuits Technology for Large-Scale Integration of Passive Functions”  
*Integrated Optics, Silicon Photonics, and Photonic Integrated Circuits*, edited by Giancarlo C. Righini, *Proc. of SPIE* Vol. 6183, 61831H, 2006

**[MacDonald-2000]**

R. MacDonald, L.-P. Chen, C.-X. Shi and B. Faer  
"Requirements of Optical Layer Network Restoration"  
*Proc. Optical Fiber Communications Conference Vol. 3, 68 - 70, Baltimor, March 2000*

**[Madamopoulos-1998]**

N. Madamopoulos and N. A. Riza  
"Polarization Sensitive Hologram-based Photonic delay lines"  
*Opticas Communications 157, 225-237, December 1998*

**[Madsen-1999]**

C. K. Madsen and J. H. Zhao  
"Optical Filter Design and Analysis, a Signal Procesing Approach"  
John Wiley & Sons, 1999

**[Makihara-2000]**

M. Makihara  
"Microelectromechanical Intersecting Waveguide Optical Switch Based on Thermo-Capillarity"  
*IEEE/LEOS International Conference on Optical MEMS, 33-34, August 2000*

**[Martin-1975]**

W. E. Martin  
"A New Waveguide Switch/Modulator for Integrated Optics"  
*Applied Physic Letters 26(10), 562-564, May 1975*

**[Maune, 2003]**

B. Maune, R. Lawson, C. Gunn, A. Scherer and L. Dalton  
"Electrically Tunable Ring Resonators Incorporating Nematic Liquid Cystals as Cladding Layers"  
*Applied Physics Letters 83(23), 4689-4691, December 2003*

**[McAdams-1990a]**

L. R. McAdams and J. W. Goodman  
"Liquid Crystal 1xN Optical Switch"  
*Optic Letters 15(20), 1150-1152, October 1990*

**[McAdams-1990b]**

L. R. McAdams, R. N. McRuer and J. W. Goodman  
"Liquid Crystal Optical Routing Switch"  
*Applied Optics 29(9), 1304-1307, March 1990*

**[Mears-1987]**

R. J. Mears, L. Reekie, I. M. Jauncy and D. N. Payne  
"Low-Noise Erbium-Doped Fiber Amplifier Operating at  $1.54\mu\text{m}$ "  
*Electron. Lett. 23(19), 479-480, September 1987*

**[Méndez-2007]**

A. Méndez and T. F. Morse  
"Specialty Optical Fibers Handbook"  
Academic Press, 2007

**[Miedreich-2004]**

M. Miedreich, and B. L'Henoret.

"Fiber Optical Sensor for Pedestrian Protection"

*Conference Proceedings POF'2004, Nürnberg, 386-392, September 2004*

**[Miya-1979]**

T. Miya, Y. Terunume, T. Hosaka and T. Miyashita

"An Ultimate Low-Loss Single-Mode Fiber at 1.55 $\mu$ m"

*Electron. Lett., 15, 106-108, 1979*

**[Mizuno-2005]**

T. Mizuno, H. Takahashi, T. Kitoh, M. Oguma, T. Kominato and T. Shibata

"Mach-Zehnder Interferometer Switch with a High Extinction Ratio Over a Wide Wavelength Range"

*Optics Letters 30(3), 251 - 253, February 2005*

**[Moddel-1989]**

G. Moddel, K. M. Johnson, W. Li, R. A. Rice, L. A. Pagano-Stauffer, and M. A. Handschy

"High-speed Binary Optically Addressed Spatial Light Modulators"

*Appl. Phys. Lett. 55, 537-639, August 1989*

**[Montalvo-2008]**

Julio Montalvo García

"Applications of Ring Resonators and Fiber Delay Lines for Sensors and WDM Networks"

PhD Thesis, Universidad Carlos III de Madrid, February 2008

**[Montero-2009]**

D. S. Montero, C. Vázquez, I. Möllers, J. Arrúe and D. Jäger

"A Self-Referencing Intensity Based Polymer Optical Fiber Sensor for Liquid Detection"

*Sensors 9(8), 6446-6455, August 2009*

**[Montero-2011]**

David Sánchez Montero

"Multimode Fibre Broadband Access and Self Referencing Sensor Networks"

PhD Thesis, Universidad Carlos III de Madrid, March 2011

**[Morand-2006]**

A. Morand, Y.Zhang, B.Martin, K.P. Huy, D. Amans, P., Benech, J. Verbert, E. Hadji and J.-M. Fédeli

"Ultra-Compact Microdisk Resonator Filters on SOI Substrate"

*Optics Express 14(26), 12814-12821, December 2006*

**[Muyshondt-2005]**

H. Muyshondt.

*Automotive LAN seminar, Tokyo, 2005*

**[Nashimoto-2001]**

K. Nashimoto, H. Moriyama, S. Nakamura, M. Watanabe, T. Morikawa, E. Osakabe and K. Haga

"PLZT Electro-Optic Waveguides and Switches"

*Optical Fiber Communication Conference and Exhibit OFC 2001, Vol. 4, PD10-1 PD10-3, 2001*

**[Noguchi-1991]**

"A rearrangeable Multichannel Free-Space Optical Switch Based on Multistage Network Configuration"

K. Noguchi, T. Sakano and T. Matsumoto

*Journal of Lightwave Technology* 9(12), 1726-1732, December 1991

**[Noguchi-1998]**

K. Noguchi

"Optical Free-Space Multichannel Switches Composed of Liquid Crystal Light Modulator Arrays and Birrefringent Crystals"

*Journal of Lightwave Technology*, 16 (8), 1473-1481, August 1998

**[Noh-2006]**

Y. O. Noh, H.-J. Lee, Y.-H. Won and M.-C. Oh

"Polymer Waveguide Thermo Optic Switches with -70dB Optical Crosstalk"

*Opt Comm.* 258, 18-22, February 2006

**[Ohtsuka-1976]**

Y. Ohtsuka and Y. Hatanaka

"Preparation of Light-Focusing Plastic Fiber by Heat-Drawing Process"

*Appl. Phys. Lett.* 29(11), 735- 737, December 1976

**[Ohtsuka-1990]**

Y. Ohtsuka, E. Nihei and Y. Koike

"Graded-Index Optical Fibers of Methyl Methacrylate-Vinyl Benzoate Copolymer with Low Loss and High Bandwidth"

*Appl. Phys. Lett.* 57(2), 120-122, July 1990

**[Okuno-2003]**

M. Okuno, T. Goh, S. Sohma and T. Shibata

"Recent Advances in Optical Switches Using Silica Based PLC Technology"

*NTT Technical Review* 1(7), 20-30, October 2003

**[Ollier-2006]**

E. Ollier

"Optical MEMS Devices Based on Moving Waveguides"

*IEEE J. Sel. Topics Quantum Elect.* 8(1), 155-162, January/February 2006

**[Pal-2006]**

B. P. Pal

"Guided Wave Optical Components and Devices"

Elsevier Academic Press, 2006

**[Papadimitriou-2003]**

G. I. Papadimitriou, C. Papazoglou and A. S. Pomportis

"Optical Switching: Switch Fabrics, Techniques and Architectures"

*Journal of Lightwave Technology*, 21(2), 384-405, February 2003

**[Patel-1995]**

J. S. Patel and Y. Silberberg

"Liquid crystal and grating-based multiple-wavelength cross-connect switch"

*IEEE Phot. Tech. Lett.* 7(5), 514-516, May 1995

**[Payne-1975]**

D. N. Payne and W. A. Gambling

"Zero Material Dispersion in Optical Fibers"

*Electron. Lett.* 11(8), 176-178, April 1975

**[Pena-2002]**

J .M. S. Pena, C. Vázquez, I. Pérez, I. Rodríguez and J. M. Otón

"Electro-optic System for Online Light Transmission Control of Polymer-Dispersed Liquid Crystal Windows"

*Optical Engineering* 41(7) 1-4. July 2002

**[Pena-2003]**

J. M. Pena, I. Rodríguez, C. Vázquez, I. Pérez and J.M. Otón

"Spatial Distribution of the Electric Field in Liquid Crystal Dispersions Devices by using a Finite-Element Method"

*Journal of Molecular Liquids* 108 (1-3), 107 - 117, November 2003

**[Pereda-2004]**

J. A. Martín Pereda

"Sistemas y Redes Ópticas de Comunicaciones"

Prentice Hall, 2004

**[Peter-2002]**

Y.-A. Peter, F. Gonté, H. P. Herzig and R. Dändliker

"Micro-Optical Fiber Switch for a Large Number of Interconnects Using a Deformable Mirror"

*IEEE Photonics Tech. Lett.* 14(3), 301-303, March 2002

**[Pickavet-2008]**

M. Pickavet, R. Tucker

"Energy Footprint of ICT: Big Picture - Introduction"

<http://www.ecoc2008.org/programme.asp#tutorials> (accesed 15 March 2011)

*European Conference on Optical Communication - ECOC 2008*, Brussels, September 2008

**[Poisel-2005]**

H. Poisel, M. Luber and O. Ziemann

"POF Sensors for Automotive and Industrial Use Come of Age"

[InvitedPaper] *Conference Proceedings POF2005*, 285-289, Hong Kong, September 2005

**[Popovic-2006]**

M. A. Popovic, T. Barwicz, M. R. Watts, P. T. Rakich, L. Socci, E. P. Ippen, F. X. Kärtner and H. I. Smith

"Multistage High-Order Microring-Resonator Add-Drop Filters"

*Opt. Lett.* 31(17), 2571-2573, September 2006

**[Porzi-2010]**

C. Porzi, L. Ma, M. Yao, L. Potí and A. Bogoni

"All-Optical Low-Power 2x2 Cross/Bar Switch with a Single Semiconductor Optical Amplifier"

*IEEE Photonics Technology Letters* 22(17), 13271329, September 2010

**[Potasek-2002]**

M. J. Potasek and Y. Yang

“Multiterabit-per-Second All-Optical Switching in a Nonlinear Directional Coupler”

*IEEE J. Sel. Topics on Quantum Elect.*, 8 (3), 714-721, May/June 2002

**[Quintard-2009]**

V. Quintard, A. Pérennou and J. Aboujeib

“Characterization of a 2x2 Optical Switch Based on a Multitranstducers Acousto-Optic Deflector”

*IEEE Photonics Technology Letters* 21(24), 1825-1827, December 2009

**[Ramanitra-2003]**

H. Ramanitra, P. Chanclou, B. Vinouze and L. Dupont

“Application of Polymer Dispersed Liquid Crystal (PDLC) Nematic: Optical-Fiber Variable Attenuator”

*Mol. Cryst. Liq. Cryst.* 404, 57-73, July 2003

**[Ramaswami-2002]**

R. Ramaswami and K. N. Sivarajan

“Optical Networks: a practical perspective” (II edition)

Morgan Kaufmann, 2002

**[Ramaswamy-1988]**

R. V. Ramaswamy and R. Srivastava

“Ion-Exchanged Glass Waveguides: a Review”

*J. Light. Techn.*, 6 (6), 984-1002, June 1988

**[Ramos-]**

F. Ramos Pascual

“Técnicas de Demultiplexación y Comutación Ópticas”

Conectrónica, 59

**[Ramos-2009]**

F. Ramos Pascual

“Interferómetros Mach-Zehnder Activos: Conversores de Medio para Fibra Óptica”

<http://www.conectronica.com/conversores-de-medio/interferometros-mach-zehnder-activos>  
(último acceso: 7 de abril de 2011),

**[Rivero-2008]**

Diego Rivero Hernández

“Diseño y Simulación de un Enrutador Óptico con Dispositivos de Comutación Basados en Resonadores en Anillo”

Bachelor Project, Universidad Carlos III de Madrid, December 2008

**[Riza-1998a]**

N. A. Riza and S. Yuan

“Low Optical Interchannel Crosstalk, Fast Switching Speed, Polarization Independent 2x2 Fiber Optic Switch using Ferroelectric Liquid Crystals”

*Electr. Lett.*, 34 (13), 1341-1342, June 1998

**[Riza-1998b]**

N. A. Riza and N. Madamopoulos

"Photonic Delay Line Using Electrically Switched Gratings in Polymer Dispersed Liquid Crystals"

*Optical Engineering* 37(11), 3061 – 3065, November 1998

**[Riza- 1999]**

N. A. Riza and S. Yuan

"Reconfigurable Wavelength Add-Drop Filtering Based on a Bayan Network Topology and Ferroelectric Liquid Crystal Fiber-Optic Switch",

*Journal of Lightwave Technology* 17(9), 1575-1584, September 1999

**[Riza-2005]**

N. A. Riza and N. Madamopoulos

"Compact Switched-Retroreflection-Based 2x2 Optical Switching Fabric for WDM Applications"

*Journal of Lightwave Technology* 23(1), 247-259, January 2005

**[Riza-2007]**

N. A. Riza and S. A. Reza

"Smart value-added fiber-optic modules spatially multiplexed processing"

*Applied Optics* 46(18), 3800-3810, June 2007

**[Rogozinski-2005]**

R. Rogozinski and P. Karasinski

"Optical Waveguides Produced in Ion Exchange Process from the Solutions of AgNO<sub>3</sub>-NaNO<sub>3</sub> for Planar Chemical Amplitude Sensors"

*Opto-Electronics Review*, 13 (3), 229-238, 2005

S – Z:

**[Sahasrabuddhe-1999]**

L. H. Sahasrabuddhe and B. Mukherjee

"Light-Trees: Optical Multicasting for Improved Performance in Wavelength-Routed Networks"

*IEEE Communications Magazine* 37(2), 67-73, February. 1999

**[Sakano-1995]**

T. Sakano, K. Kimura, K. Noguchi and N. Naito

"256x256 Turnover-Type Free-Space Multichannel Optical Switch Based on Polarization Control Using Liquid-Crystal Spatial Light Modulators"

*Applied Optics* 34(14), 2581-2589, May 1995

**[Sakata-2001]**

T. Sakata, H. Togo, M. Makihara, F. Shimokawa and K. Kaneko

"Improvement of Switching Time in Thermocapillarity Optical Switch"

*J. Light. Techn.* 19(7), 1023-1027, July 2001

**[Sakuma-2001]**

K. Sakuma, H. Ogawa, D. Fujita and H. Hosoya

"Polymer Y-Branching Thermo-Optic Switch for Optical Fiber Communication System"

*8<sup>th</sup> Microoptics Conf. (MOF'01)*, Osaka, (Japan), 24-26, October 2001

**[Sapriel-2002]**

J. Sapriel, D. Charissoux, V. Voloshinov and V. Molchanov  
“Tunable Acoustooptic Filters and Equalizers for WDM Applications”  
*J. Lightwave Technology*, 20 (5), 892-899, May 2002

**[Schöndfel-2000]**

O. Schönfeld  
“MOST Transceiver Components”  
[http://www.mostcooperation.com/news\\_and\\_events/events\\_archive/articles/166665/index.html?do=download&id=167422](http://www.mostcooperation.com/news_and_events/events_archive/articles/166665/index.html?do=download&id=167422) (Available 18 March 2011)  
Presented at the MOST All Members Meeting, June 2000

**[Shankar-1990]**

N. K. Shankar, J. A. Morris, C. P. Yakymyshyn and C. R. Pollock  
“A 2x2 Fiber Optic Switch Using Chiral Liquid Crystals”  
*Photonics Technology Letters*, 2 (2), 147-149, February 1990

**[Shizhuo-1999]**

Y. Shizhuo  
“Lithium Niobate Fibers and Waveguides: Fabrication and Applications”  
*Proceedings of IEEE 87, 1962-1974*, November 1999

**[Soldano-1995]**

L. B. Soldano and E. C. M. Pennings  
“Optical Multi-Mode Interference Devices Based on Self-Imagin: Principles and Applications”  
*J. Light. Tech.*, 13 (4), 615-627, April 1995

**[Soref-1981]**

R. A. Soref  
“Low-Cross-Talk 2x2 Optical Switch”  
*Optics Letters*, 6 (6), 275-277, June 1981

**[Soref-1982]**

R. A. Soref and D. H. McMahon  
“Calcite 2x2 Optical Bypass Switch Controlled by Liquid-Crystal cells”  
*Optics Letters*, 7 (4), 186-188, April 1982

**[Soref-1986]**

R. A. Soref and J. P. Lorenzo  
“All-Silicon Active and Passive Guided-Waveguide Components for Lambda=1.3 and 1.6  $\mu\text{m}$ ”  
*IEEE J. Quantum Electron*, 22, 873-879, June 1986

**[Sumriddetchkajorn-2000]**

S. Sumriddetchkajorn and N. A. Riza  
“Fiber-Connectorized Multiwavelength 2x2 Switch Structure Using a Fiber Loop Mirror”  
*Opt. Comm.* 175(1-3), 89-95, February 2000

**[Sun-2004]**

Y. Sun and X. Fan

"Analysis of Ring Resonators for Chemical Vapor Sensor Development"

*Optics Express*, 16(14), 10254 - 10268, July 2008

**[Sun-2005]**

D. G. Sun, Z. Liu, Y. Zha, W. Deng, Y. Zhang and X. Li

"Thermo-Optic Waveguide Digital Optical Switch"

*Optics Express*, 13 (14), 5463 - 5471, June 2005

**[Suzuki-2004]**

K. Suzuki, T. Mizuno, M. Oguma, T. Shibata, H. Takahashi, Y. Hibino and A. Himeo

"Low Loss Fully Reconfigurable Wavelength-Selective Optical 1xN Switch Based on Transversal Filter Configuration Using Silica Based Planar Lightwave Circuit"

*IEEE Phot Tech Lett* 16(6), 1480-1482, June 2004

**[Syms-2004]**

R.R.A. Syms, H. Zou, J. Stagg and H. Veladi

"Sliding-Blade MEMS Iris and Variable Optical Attenuator"

*Journal of Micromech. and Microeng.* 14, 1700-1710, September 2004

**[Takatoh-2005]**

K. Takatoh, M. Hasagawa, M. Koden, N. Itoh, R. Hasegawa and M. Sakamoto

"Alignment Technologies and Applications of Liquid Crystal Devices"

Taylor & Francis, May 2005

**[Tan-2008]**

Y. Tan F. Chen, M. Stepic, V. Shandarov and D. Kip

"Reconfigurable Optical Channel Waveguides in Lithium Niobate Crystals Produced by Combination of Low-Dose O<sub>3</sub><sup>+</sup> ion Implantation and Selective White Light Illumination"

*Opt. Exp.* 16(14), 10465-10470, July 2008

**[Tanushi-2005]**

Y. Tanushi and S. Yokoyama

"High Speed and Low Voltage Ring Resonator Optical Switches Using Electro-and Magneto-Optic Materials"

*2<sup>nd</sup> IEEE International Conference on Group IV Photonics*, 165-167, September 2005

**[Tapalian-2002]**

H. C. Tapalian, J.-P. Laine and P. A. Lane

"Thermo-optical Switch Using Coated Microsphere Resonators"

*IEEE Photonics Technology Letters* 14(8), 1118-1120, August 2002

**[Tarek-2006]**

S. Tarek

"Optical Switching"

Springer, USA, 2006

**[Thomson-2010]**

D. J. Thomson, Y. Hu, G. T. Reed and J.-M. Fedeli

"Low Loss MMI Couplers for High Performance MZI Modulators"

*IEEE Phot.Tech. Lett.* 22(20), 1485-1487, October 2010

**[Tsao-1995]**

S. L. Tsao, H. W. Tsao and Y. H. Lee

"Design of a Self-Routing Frequency Division Multiple Access (SR-FDMA) Network Using an Optical Ring Filter with or without Gain as a Router"

*J. Light. Tech.* 13(11), 2168-2182, November 1995

**[Uebbing-2006]**

J. J. Uebbing, S. Hengstler, D. Schroeder, S. Venkatesh and R. Haven

"Heat and Fluid Flow in an Optical Switch Bubble"

*J. Microelectromechanical Systems*, 15 (6), 1528-1539, December 2006

**[Vargas-2003]**

Salvador Vargas Palma

"Contribución al Diseño de Filtros Ópticos para Redes con Multiplexación en Longitud de Onda"

PhD Thesis, Universidad Carlos III de Madrid, 2003

**[Vargas-2010]**

S. Vargas and C. Vázquez

"Synthesis of Optical Filters Using Microring Resonators with Ultra-large FSR"

*Optics Express* 18(25), 25936 – 25949, December 2010

**[Vázquez-1995]**

C. Vázquez, F. J. Mustieles and J. F. Hernández Gil

"Three-Dimensional Method for Simulation of Multimode Interference Couplers"

*Journal of Lightwave Technology* 13(11), 2296-2299, November 1995

**[Vázquez-2000]**

C. Vázquez, S. Vargas and J. M. S. Pena

"Design and Tolerance Analysis of a Router using an Amplified Ring Resonator and Bragg Gratings"

*Applied Optics* 39(12), 1934-1940, April 2000

**[Vázquez-2003]**

C. Vázquez, J. M. S. Pena, A. L. Aranda

"Broadband 1x2 Polymer Optical Fiber Switch using Nematic Liquid Crystals"

*Opt. Commun.* 224(1-3), 57-62, 2003

**[Vázquez-2004]**

C. Vázquez, A. B. Gonzalo, S. Vargas and J. Montalvo

"Multi-Sensor System Using Plastic Optical Fibers for Intrinsically Safe Level Measurements"

*Sensors and Actuators A* 116(1), 22-32, October 2004

**[Vázquez-2005a]**

C. Vázquez, J. Montalvo and P. C. Lallana

"Radio-Frequency Ring Resonators for Self-Referencing Fiber-Optic Intensity Sensors"

*Optical Engineering Letters* 44(4), 040502-1 - 040502-2, April 2005

**[Vázquez-2005b]**

C. Vázquez, J. M. S. Pena, P. C. Lallana, M. A. Jurado Pontes  
"Development of a 2x2 Optical Switch for Plastic Optical Fiber Using Liquid Crystal Cells"  
*Microtechnologies for the New Millennium 2005*, Seville (Spain), May 2005

**[Vázquez-2005c]**

C. Vázquez, S. Vargas and J. M. S. Pena  
"Sagnac Loop in Ring Resonators for Tunable Optical Filters"  
*J. Light. Tech.* 23(8), 2555-2567, August 2005

**[Vázquez-2007]**

C. Vázquez, P. C. Lallana, J. Montalvo, J. M. S. Pena, A. d'Alessandro and D. Donisi  
"Switches and Tuneable Filters Based on Ring Resonator and Liquid Crystals"  
*Proceedings Microtechnologies for the New Millennium*, Maspalomas (Spain), May 2007

**[Vázquez-2008]**

C. Vázquez, P. C. Lallana, D. S. Montero and J. Montalvo,  
"Self-reference intensity sensor techniques and advanced devices in WDM networks"  
*VI symposium on Enabling Optical Networks (SEON 2008)*, Porto (Portugal), 2008

**[Viens-1999]**

J. F. Viens, C. L. Callender, J. P. Noad, L. A. Eldada and R. A. Norwood  
"Polymer-Based Waveguide Devices for WDM Applications"  
Proc SPIE vol 3799C, October 1999

**[Wagner-1980]**

R. E. Wagner and J. Cheng  
"Electrically Controlled Optical Switch for Multimode Fiber Applications"  
*Applied Optics* 19(17), 2921-2925, September 1980

**[Ward-1999]**

M. Ward and F. Briamonte  
"Lucent's New All-Optical Router Uses Bell Labs Microscopic Mirrors"  
<http://www.bell-labs.com/news/1999/november/10/1.html>, November 1999.  
(Accessed 18 November 2010)

**[Whinnery-1977]**

J. R. Whinnery, C. Hu and Y. S. Kwon  
"Liquid-Crystal Waveguides for Integrated Optics"  
*IEEE J. Quantum Electronics*, 13 (4), 262-267, April 1977

**[Wu-2006]**

Q. Wu P. L. Chu, H. P. Chan and B. P. Pal  
"A Y-Junction Polymer Optical Waveguide Interleaver"  
Opt. Comm 267(2), 373-378, November 2006

**[Yamada-1981]**

J. I. Yamada, S. Machida and T. Kimura  
"2Gb/s Optical Transmission Experiments at 1.3μm with 44km Single Mode Fiber"  
*Electron Lett.* 17(13), 479 - 480, June 1981

**[Yang-2008a]**

J. Yang, X. Su, X. Liu, X. He and J. Lan

“Design of Polarisation-Independent Bidirectional 2x2 Optical Switch”

*Journal of Modern Optics* 55 (7), 1051-1063, April 2008

**[Yang-2008b]**

J. Yang and X. Su

“Optical Implementation of a Polarization-Independent Bidirectional 3x3 Optical Switch”

*Photonic Networks Communications*, 15, 153-158, April 2008

**[Yasuda-2005]**

T. Yasuda, Y. Tsuji and M. Koshiba

“Tunable Light Propagation in Photonic Crystal Coupler Filled With Liquid Crystal”

*IEEE Photonics Technology Letters* 17(1), 55 -57, January 2005

**[Yujie-2009]**

X. Yujie

“Design and Fabrication of Liquid Crystal (LC) based on Electro-Optical Waveguide Device”

City University of Hong Kong, June 2009

**[Zheng-2011]**

C.-T. Zheng, C. -S. Ma, X. Yan, Z. -C. Cui and D.-M. Zhang

“Manufacture Tolerance Analysis and Control for a Polymer-on-Silicon Mach-Zehnder Interferometer Based Electro-optic Switch”

*Optoelectronics Letters* 7(2), 0101-0104, March 2011

**[Zhou-2005]**

Y. Zhou and G. S. Poo

“Optical Multicast over Wavelength-Routed WDM Networks: A Survey”

*Optical Switching and Networking*, 2, 176-197, November 2005

**[Ziemann-2005]**

O. Ziemann, J. Krauser, P. E. Zamzow and W. Daum

“POF Handbook: Optical Short Range Transmission Systems”

Springer, 2008

**[Zubia-2002]**

J. Zubia, G. Durana, J. Arrue and I. Garcés

“Design and Performance of Active Coupler for Plastic Optical Fibres”

*Electronic Letters*, 38 (2), 65-67, January 2002

**[Zubia-2007]**

J. Zubia, O. Aresti, J. Arrúe, J. Miskowicz and M. López-Amo

“Barrier Sensor Based on Plastic Optical Fibre to Determine the Wind Speed at a Wind Generator”

*IEEE Journ. on Sel. Top in Quant. Electr.*, 6 (5), 773-779, 2000